

NATIONAL BUREAU OF STANDARDS

Technical Note 101

ISSUED May 7, 1965

REVISED May 1, 1966

REVISED January 1, 1967

TRANSMISSION LOSS PREDICTIONS FOR TROPOSPHERIC COMMUNICATION CIRCUITS

VOLUME II

P. L. Rice, A. G. Longley, K. A. Norton, and A. P. Barsis
Institute for Telecommunication Sciences and Aeronomy*
Environmental Science Services Administration
Boulder, Colorado

NBS Technical Notes are designed to supplement the Bureau's regular publications program. They provide a means for making available scientific data that are of transient or limited interest. Technical Notes may be listed or referred to in the open literature.

**Formerly the Central Radio Propagation Laboratory of the National Bureau of Standards.
ESSA will use the NBS publication series until establishment of their ESSA counterparts.*

For sale by the Superintendent of Documents, U. S. Government Printing Office
Washington, D.C. 20402
Price: \$1.00

FOREWORD

A short history of the development of the prediction methods in this Technical Note will permit the reader to compare them with earlier procedures. Some of these methods were first reported by Norton, Rice and Vogler [1955]. Further development of forward scatter predictions and a better understanding of the refractive index structure of the atmosphere led to changes reported in an early unpublished NBS report and in NBS Technical Note 15 [Rice, Longley and Norton, 1959]. The methods of Technical Note 15 served as a basis for part of another unpublished NBS report which was incorporated in Air Force Technical Order T. O. 31Z-10-1 in 1961. A preliminary draft of the current technical note was submitted as a U. S. Study Group V contribution to the CCIR in 1962.

Technical Note 101 uses the metric system throughout. For most computations both a graphical method and formulas suitable for a digital computer are presented. These include simple and comprehensive formulas for computing diffraction over smooth earth and over irregular terrain, as well as methods for estimating diffraction over an isolated rounded obstacle. New empirical graphs are included for estimating long-term variability for several climatic regions, based on data that have been made available.

For paths in a continental temperate climate, these predictions are practically the same as those published in 1961. The reader will find a number of graphs have been simplified and that many of the calculations are more readily adaptable to computer programming. The new material on time availability and service probability in several climatic regions should prove valuable for areas other than the U. S. A.

Changes in this revision concern mainly sections 2 and 10 of volume 1 and annexes I, II and V of volume 2, and certain changes in notation and symbols. The latter changes make the notation more consistent with statistical practice.

Section 10, Long-Term Power Fading contains additional material on the effects of atmospheric stratification.

For convenience in using volume 2, those symbols which are found only in an annex are listed and explained at the end of the appropriate annex. Section 12 of volume 1 lists and explains only those symbols used in volume 1.

Note: This Technical Note consists of two volumes as indicated in the Table of Contents.

TABLE OF CONTENTS

Volume 1

	<u>PAGE NO.</u>
1. INTRODUCTION	1-1
2. THE CONCEPTS OF SYSTEM LOSS, TRANSMISSION LOSS, PATH ANTENNA GAIN, AND PATH ANTENNA POWER GAIN	2-1
2.1 System Loss and Transmission Loss.	2-1
2.2 Antenna Directive Gain and Power Gain	2-3
2.3 Polarization Coupling Loss and Multipath Coupling Loss	2-5
2.4 Path Loss, Basic Transmission Loss, Path Antenna Gain, and Attenuation Relative to Free Space	2-7
3. ATMOSPHERIC ABSORPTION.	3-1
3.1 Absorption by Water Vapor and Oxygen	3-1
3.2 Sky-Noise Temperature.	3-3
3.3 Attenuation by Rain	3-4
3.4 Attenuation in Clouds	3-6
4. DETERMINATION OF AN EFFECTIVE EARTH'S RADIUS	4-1
5. TRANSMISSION LOSS PREDICTION METHODS FOR WITHIN-THE-HORIZON PATHS	5-1
5.1 Line-of-Sight Propagation Over Irregular Terrain.	5-1
5.2 Line-of-Sight Propagation Over a Smooth or Uniformly Rough Spherical Earth	5-3
5.2.1 A curve-fit to terrain	5-8
5.2.2 The terrain roughness factor, σ_h	5-9
5.3 Some Effects of Cluttered Terrain	5-10
5.4 Examples of Line-of-Sight Predictions.	5-11
6. DETERMINATION OF ANGULAR DISTANCE FOR TRANSHORIZON PATHS.	6-1
6.1 Plotting a Great Circle Path	6-1
6.2 Plotting a Terrain Profile and Determining the Location of Radio Horizon Obstacles	6-3
6.3 Calculation of Effective Antenna Heights for Transhorizon Paths.	6-4
6.4 Calculation of the Angular Distance, θ	6-5
7. DIFFRACTION OVER A SINGLE ISOLATED OBSTACLE.	7-1
7.1 Single Knife Edge, No Ground Reflections	7-1
7.2 Single Knife Edge with Ground Reflections	7-3
7.3 Isolated Rounded Obstacle, No Ground Reflections	7-4
7.4 Isolated Rounded Obstacle with Ground Reflections	7-6
7.5 An Example of Transmission Loss Prediction for a Rounded Isolated Obstacle.	7-7

	<u>PAGE NO.</u>
8. DIFFRACTION OVER SMOOTH EARTH AND OVER IRREGULAR TERRAIN	8-1
8.1 Diffraction attenuation Over a Smooth Earth	8-1
8.2 Diffraction Over Irregular Terrain.	8-3
8.2.1 Diffraction over paths where $d_{st} \cong d_{sr}$	8-4
8.2.2 For horizontal polarization	8-4
8.3 Single-Horizon Paths, Obstacle not Isolated	8-5
9. FORWARD SCATTER.	9-1
9.1 The Attenuation Function, $F(\theta d)$	9-2
9.2 The Frequency Gain Function, H_o	9-3
9.3 The Scattering Efficiency Correction, F_o	9-5
9.4 Expected Values of Forward Scatter Multipath Coupling Loss	9-6
9.5 Combination of Diffraction and Scatter Transmission Loss	9-7
9.6 An Example of Transmission Loss Predictions for a Transhorizon Path	9-8
10. LONG-TERM POWER FADING	10-1
10.1 Effects of Atmospheric Stratification	10-4
10.2 Climatic Regions	10-6
10.3 The Effective Distance, d_e	10-8
10.4 The Functions $V(0.5, d_e)$ and $Y(q, d_e)$	10-9
10.5 Continental Temperate Climate	10-10
10.6 Maritime Temperate Climate	10-12
10.7 Other Climates	10-13
10.8 Variability for Knife-Edge Diffraction Paths	10-13
11. REFERENCES	11-1
12. LIST OF SYMBOLS AND ABBREVIATIONS	12-1

TABLE OF CONTENTS

Volume 2

	<u>PAGE NO.</u>
ANNEX I: AVAILABLE DATA, STANDARD CURVES, AND A SIMPLE PRE- DICATION MODEL	I-1
I. 1 Available Data as a Function of Path Length	I-1
I. 2 Standard Point-to-Point Transmission Loss Curves	I-2
I. 3 Preliminary Reference Values of Attenuation Relative to Free Space A_{cr}	I-29
I. 3. 1 Introduction	I-29
I. 3. 2 The Terrain Roughness Factor Δh	I-29
I. 3. 3 The Diffraction Attenuation, A_d	I-30
I. 3. 4 The Forward Scatter Attenuation, A_s	I-31
I. 3. 5 Radio Line-of-Sight Paths	I-32
I. 3. 6 Ranges of the Prediction Parameters	I-34
I. 3. 7 Sample Calculations	I-35
ANNEX II: AVAILABLE POWER, FIELD STRENGTH, AND MULTIPATH COUPLING LOSS	II-1
II. 1 Available Power from the Receiving Antenna	II-1
II. 2 Propagation Loss and Field Strength	II-4
II. 3 Beam Orientation, Polarization, and Multipath Coupling Loss	II-9
II. 3. 1 Representation of Complex Vector Fields	II-9
II. 3. 2 Principal and Cross-Polarization Components	II-12
II. 3. 3 Unit Complex Polarization Vectors	II-14
II. 3. 4 Power Flux Densities	II-16
II. 3. 5 Polarization Efficiency	II-18
II. 3. 6 Multipath Coupling Loss	II-20
II. 3. 7 Idealized Theoretical Antenna Patterns	II-23
II. 3. 8 Conclusions	II-31
II. 4 List of Special Symbols Used in Annex II	II-34
ANNEX III: SUPPLEMENTARY INFORMATION AND FORMULAS USEFUL FOR PROGRAMMING	III-1
III. 1 Line-of-Sight	III-2
III. 2 Diffraction Over a Single Isolated Obstacle	III-15
III. 3 Diffraction Over a Single Isolated Obstacle with Ground Reflections	III-17
III. 4 Parameters K and b° for Smooth Earth Diffraction	III-23
III. 5 Forward Scatter	III-24
III. 6 Transmission Loss with Antenna Beams Elevated or Directed Out of the Great Circle Plane	III-37

	<u>PAGE NO.</u>
III. 7	Long-Term Power Fading III-44
III. 7. 1	Diurnal and seasonal variability in a continental temperate climate III-45
III. 7. 2	To mix distributions III-54
III. 8	List of Special Symbols Used in Annex III. III-73
ANNEX IV:	FORWARD SCATTER IV-1
IV. 1	General Discussion. IV-1
IV. 2	Models for Forward Scattering IV-2
IV. 3	List of Special Symbols Used in Annex IV. IV-11
ANNEX V:	PHASE INTERFERENCE FADING AND SERVICE PROBABILITY . . V-1
V. 1	The Two Components of Fading V-3
V. 2	The Nakagami-Rice Distribution. V-5
V. 3	Noise-Limited Service V-13
V. 4	Interference-Limited Service V-15
V. 5	The Joint Effect of Several Sources of Interference Present Simultaneously V-19
V. 6	The System Equation for Noise-Limited Service V-20
V. 7	The Time Availability of Interference-Limited Service. V-22
V. 8	The Estimation of Prediction Error. V-23
V. 9	The Calculation of Service Probability Q for a Given Time Availability q V-25
V. 10	Optimum Use of the Radio Frequency Spectrum. V-31
V. 11	List of Special Symbols Used in Annex V V-35

Annex I

AVAILABLE DATA, STANDARD CURVES, AND A SIMPLE PREDICTION MODEL

The simplest way to predict long-term median transmission loss values would be to use a best-fit curve drawn through measured data (represented by their overall median values) plotted as a function of path length. Such a method ignores essentially all of our understanding of the physics of tropospheric propagation, is subject to especially large errors over rough terrain, and such empirical curves represent only the conditions for which data are available.

Curves that may be useful for establishing preliminary allocation plans are presented in section I.2 of this annex. These "standard" curves were prepared for a fixed combination of antenna heights and assume propagation over a smooth earth. The curves are not suitable for use on particular point-to-point paths, since they make no allowance for the wide range of propagation path profiles or atmospheric conditions that may be encountered over particular paths.

A method for computing preliminary reference values of transmission loss is described in section I.3. This method is based on a simple model, may readily be programmed, and is especially useful when little is known of the details of terrain.

I.1 Available Data as a Function of Path Length

Period-of-record median values of attenuation relative to free space are plotted vs. distance in figures I.1 to I.4 for a total of 750 radio paths, separating the frequency ranges 40-150 MHz, 150-600 MHz, 600-1000 MHz, and 1-10 GHz. Major sources of data other than those referenced by Herbstreit and Rice [1959] are either unpublished or are given by Bray, Hopkins, Kitchen, and Saxton [1955], Bullington [1955], duCastel [1957b], Crysedale [1958], Crysedale, Day, Cook, Psutka, and Robillard [1957], Dolukhanov [1957], Grosskopf [1956], Hirai [1961a, b], Josephson and Carlson [1958], Jowett [1958], Joy [1958a, b], Kitchen and Richmond [1957], Kitchen, Richards, and Richmond [1958], Millington and Isted [1950], Newton and Rogers [1953], Onoe, Hirai, and Niwa [1958], Rowden, Tagholm, and Stark [1958], Saxton [1951], Ugai [1961], and Vvedenskii and Sokolov [1957].

Three straight lines were determined for each of the data plots shown in figures I.1 to I.4. Near the transmitting antenna, $A = 0$ on the average. Data for intermediate distances, where the average rate of diffraction attenuation is approximately $0.09 f^{\frac{1}{3}}$ db per kilometer, determine a second straight line. Data for the greater distances, where the level of forward scatter fields is reached, determine the level of a straight line with a slope varying from 1/18 to 1/14 db per kilometer, depending on the frequency.

The dashed curves of figures I.1-I.3 show averages of broadcast signals recorded at 2500 random locations in six different areas of the United States. The data were normalized to 10-meter and 300-meter antenna heights, and to frequencies of 90, 230, and 750 MHz.

For this data sample [TASO 1959], average fields are low mainly because the receiver locations were not carefully selected, as they were for most other paths for which data are shown.

The extremely large variance of long-term median transmission loss values recorded over irregular terrain is due mainly to differences in terrain profiles and effective antenna heights. For a given distance and given antenna heights a wide range of angular distances is possible, particularly over short diffraction and extra-diffraction paths. Angular distance, the angle between radio horizon rays from each antenna in the great circle plane containing the antennas, is a very important parameter for transmission loss calculations, (see section 6). Figure I. 5 shows for a number of paths the variability of angular distance relative to its value over a smooth spherical earth as a function of path distance and antenna heights.

Most of the "scatter" of the experimental long-term medians shown in figures I. 1 - I. 4 is due to path-to-path differences. A small part of this variation is due to the lengths of the recording periods. For all data plotted in the figures the recording period exceeded two weeks, for 630 paths it exceeded one month, and for 90 paths recordings were made for more than a year.

An evaluation of the differences between predicted and measured transmission loss values is discussed briefly in annex V. In evaluating a prediction method by its variance from observed data, it is important to remember that this variance is strongly influenced by the particular data sample available for comparison. Thus it is most important that these data samples be as representative as possible of the wide range of propagation path conditions likely to be encountered in the various types of service and in various parts of the world.

To aid in deciding whether it is worthwhile to use the point-to-point prediction method outlined in sections 4 - 10, instead of simpler methods, figure I. 6 shows the cumulative distribution of deviations of predicted from observed long-term median values. The dash-dotted curve shows the cumulative distribution of deviations from the lines drawn in figures I. 1 - I. 4 for all available data. The solid and dashed curves compare predictions based on these figures with ones using the point-to-point method for the same paths. Note that the detailed point-to-point method could not be used in many cases because of the lack of terrain profiles.

Figure I. 6 shows a much greater variance of data from the "empirical" curves of figures I. 1 - I. 4 for the sample of 750 paths than for the smaller sample of 217 paths for which terrain profiles are available. The wide scatter of data illustrated in figure I. 4 for the frequency range 1 - 10 GHz appears to be mainly responsible for this. Figure I. 4 appears to show that propagation is much more sensitive to differences in terrain profiles at these higher frequencies, as might be expected. The point-to-point prediction methods, depending on a number of parameters besides distance and frequency, are also empirical, since they are made to agree with available data, but estimates of their reliability over a period of years have not varied a great deal with the size of the sample of data made available for comparison with them.

1.2 Standard Point-to-Point Transmission Loss Curves

A set of standard curves of basic transmission loss versus distance is presented in figures I.7 to I.26. Such curves may be useful for establishing preliminary allocation plans but they are clearly not suitable for use on particular point-to-point paths, since they make no allowance for the wide range of propagation path terrain profiles or atmospheric conditions which may be encountered. Similar curves developed by the CCIR [1963g; 1963h] are subject to the same limitation.

The standard curves show predicted levels of basic transmission loss versus path distance for 0.01 to 99.99 percent of all hours. These curves were obtained using the point-to-point predictions for a smooth earth, $N_s = 301$, antenna heights of 30 meters, and estimates of oxygen, water vapor, and rain absorption described in section 3. Cumulative distributions of hourly median transmission loss for terrestrial links may be read from figures I.7 to I.17 for distances from 0 to 1000 kilometers and for 0.1, 0.2, 0.5, 1, 2, 5, 10, 22, 32.5, 60 and 100 GHz. The same information may be obtained from figures I.18 to I.20.

For earth-space links, it is important to know the attenuation relative to free space, A , between the earth station and space station as a function of distance, frequency, and the angle of elevation, θ_h , of the space station relative to the horizontal at the earth station [CCIR 1963i; 1963j]. Using the CCIR basic reference atmosphere*, [CCIR Report 231, 1963e] standard propagation curves providing this information for 2, 5, 10, 22, 32.5, 60 and 100 GHz, for 0.01 to 99.99 percent of all hours, and for $\theta_h = 0, 0.03, 0.1, 0.3, 1.0,$ and $\pi/2$ radians are shown in figures I.21-I.26, where A is plotted against the straight-line distance r_o between antennas. The relationship between A and L_b is given by

$$L_b = A + L_{bf} = A + 32.45 + 20 \log f + 20 \log r \quad \text{db} \quad (\text{I.1})$$

where f is the radio frequency in megahertz and r is the straight-line distance between antennas, expressed in kilometers.

The curves in figures I.7-I.26 provide long-term cumulative distributions of hourly median values. Such standard propagation curves are primarily useful only for general qualitative analyses and clearly do not take account of particular terrain profiles or particular climatic effects. For example, the transmission loss at the 0.1% and 0.1% levels will be substantially smaller in maritime climates where ducting conditions are more common.

* The transmission loss predictions for this atmosphere are essentially the same as predictions for $N_s = 301$.

PERIOD OF RECORD MEDIANS VERSUS DISTANCE
FREQUENCY RANGE: 40-150 MHz; MEDIAN FREQUENCY: 90 MHz
343 PATHS

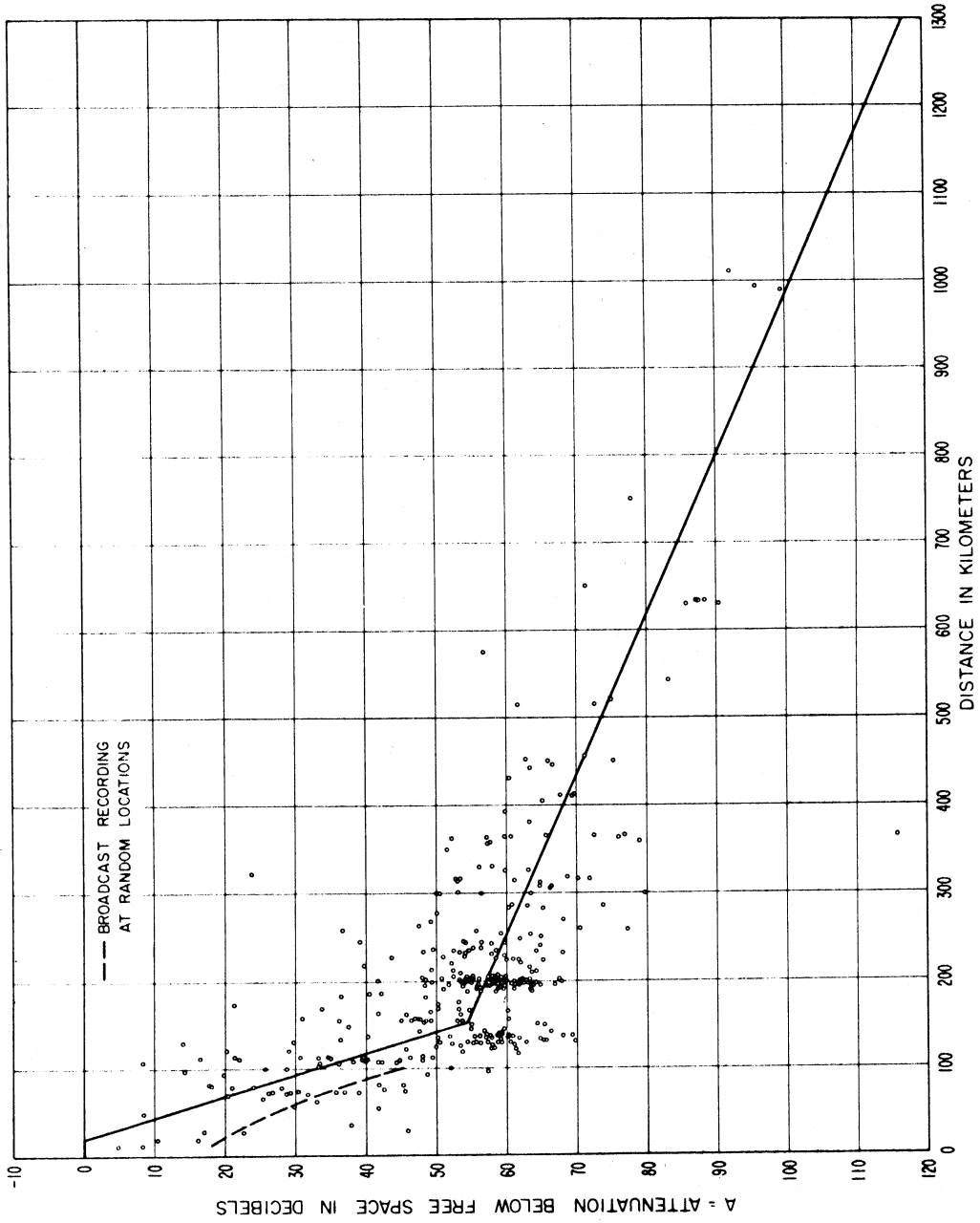


Figure 1.1

PERIOD OF RECORD MEDIANS VERSUS DISTANCE
FREQUENCY RANGE : 150-600MHz; MEDIAN FREQUENCY : 230MHz
183 PATHS

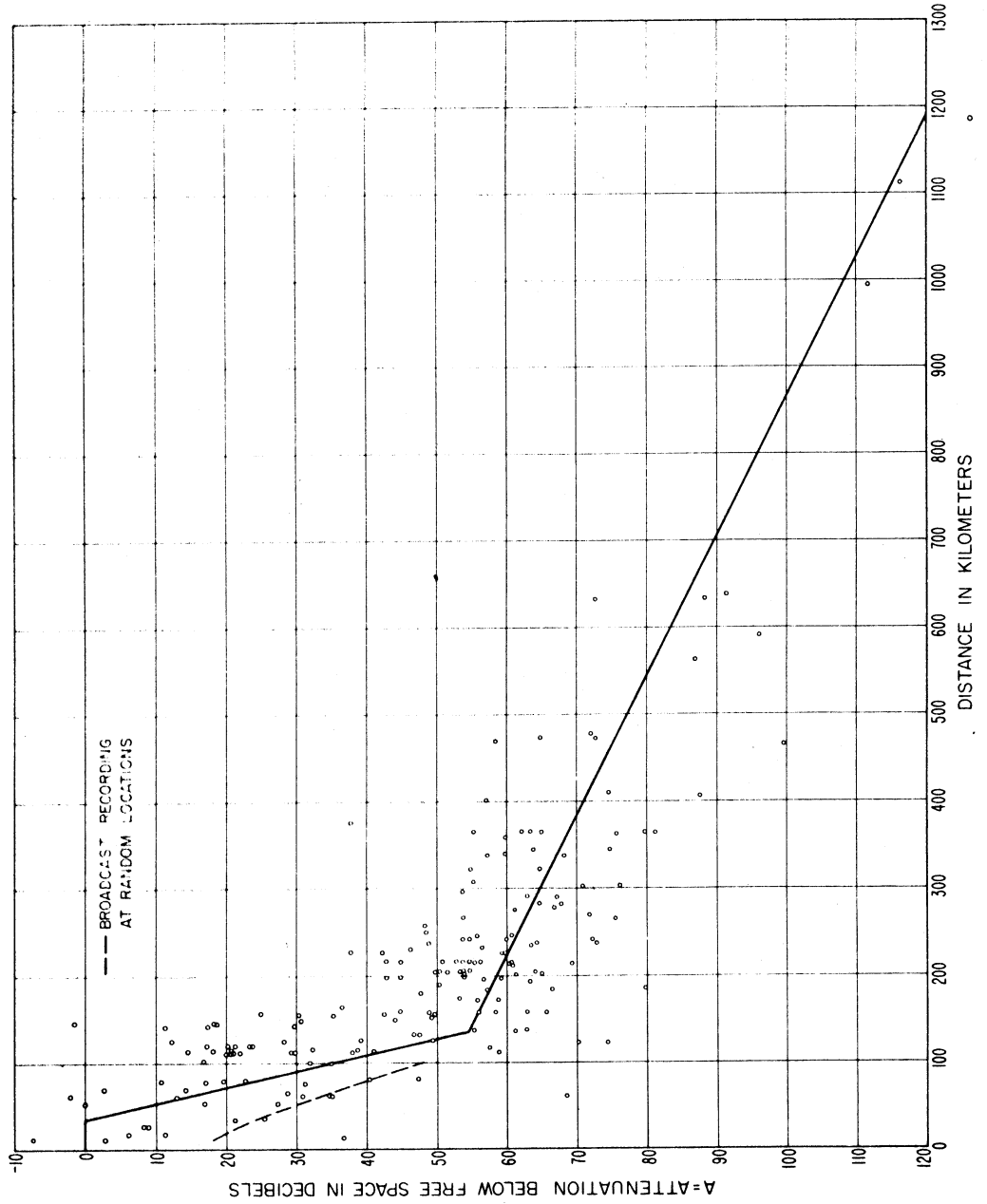


Figure 1.2

PERIOD OF RECORD MEDIANS VERSUS DISTANCE
 FREQUENCY RANGE: 600-1000MHZ; MEDIAN FREQUENCY: 750MHZ
 108 PATHS

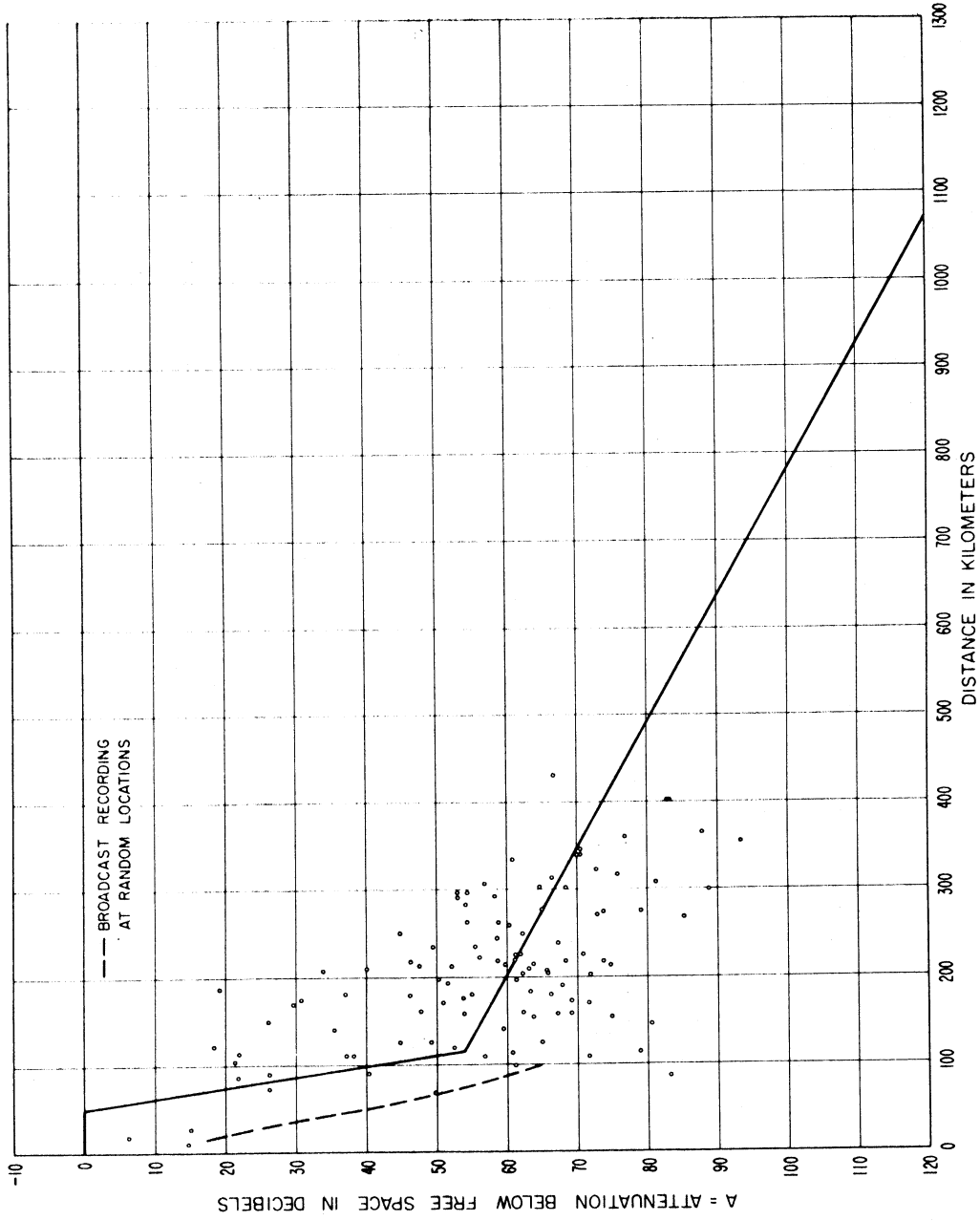


Figure 1.3

PERIOD OF RECORD MEDIANS VERSUS DISTANCE
 FREQUENCY RANGE: 1000-10,000 MHz, MEDIAN FREQUENCY: 3500 MHz
 110 PATHS

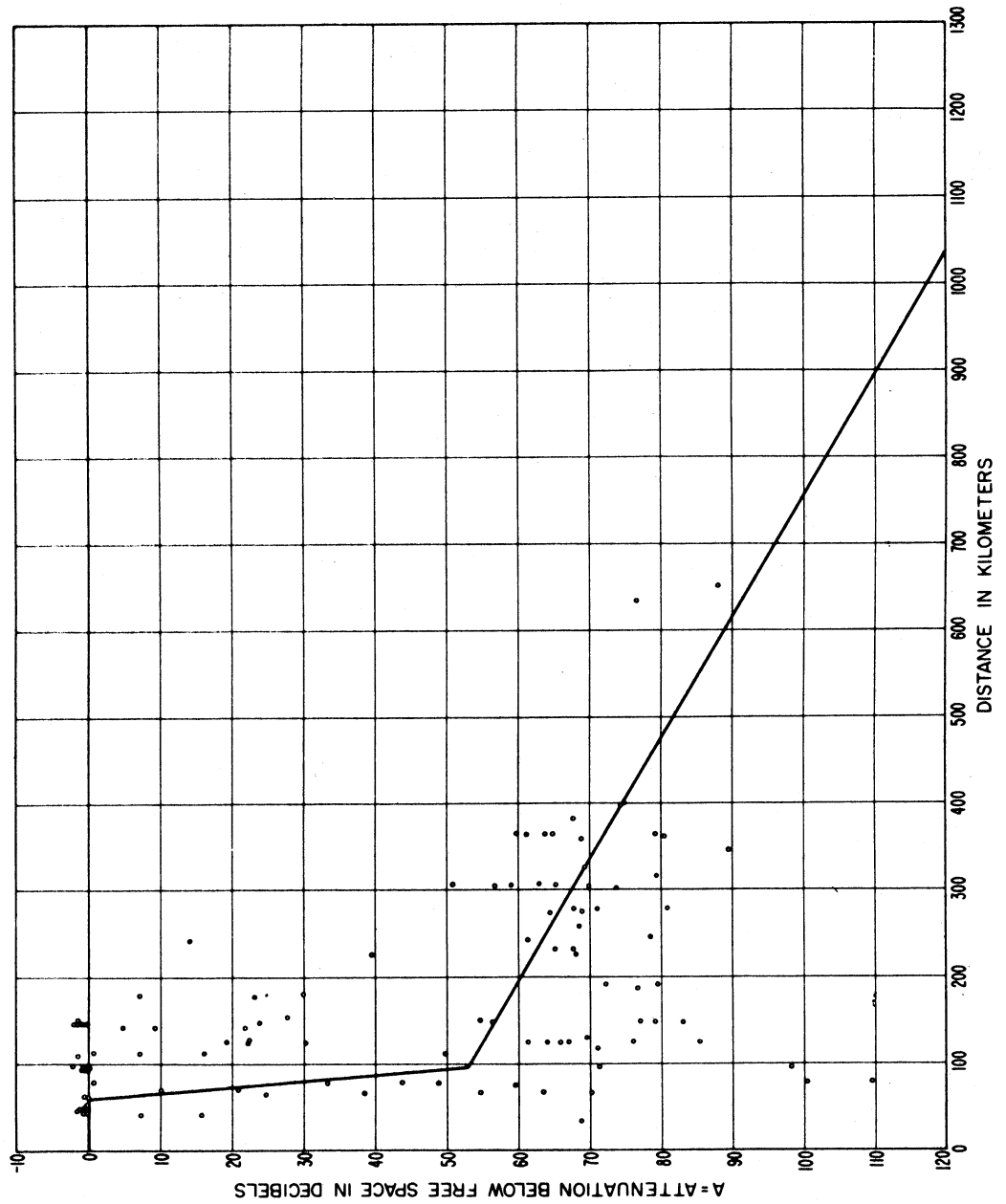


Figure I.4

ANGULAR DISTANCE VERSUS DISTANCE FOR THE 290 PATHS FOR WHICH
TERRAIN PROFILES ARE AVAILABLE

THE CURVES SHOW ANGULAR DISTANCE, θ , AS A FUNCTION OF DISTANCE
OVER A SMOOTH EARTH OF EFFECTIVE RADIUS = 9000 KILOMETERS

THE WIDE SCATTER OF THE DATA ON THIS FIGURE ARISES ALMOST ENTIRELY
FROM DIFFERENCES IN TERRAIN PROFILES, AND ILLUSTRATES THE
IMPORTANCE OF ANGULAR DISTANCE AS A PREDICTION PARAMETER

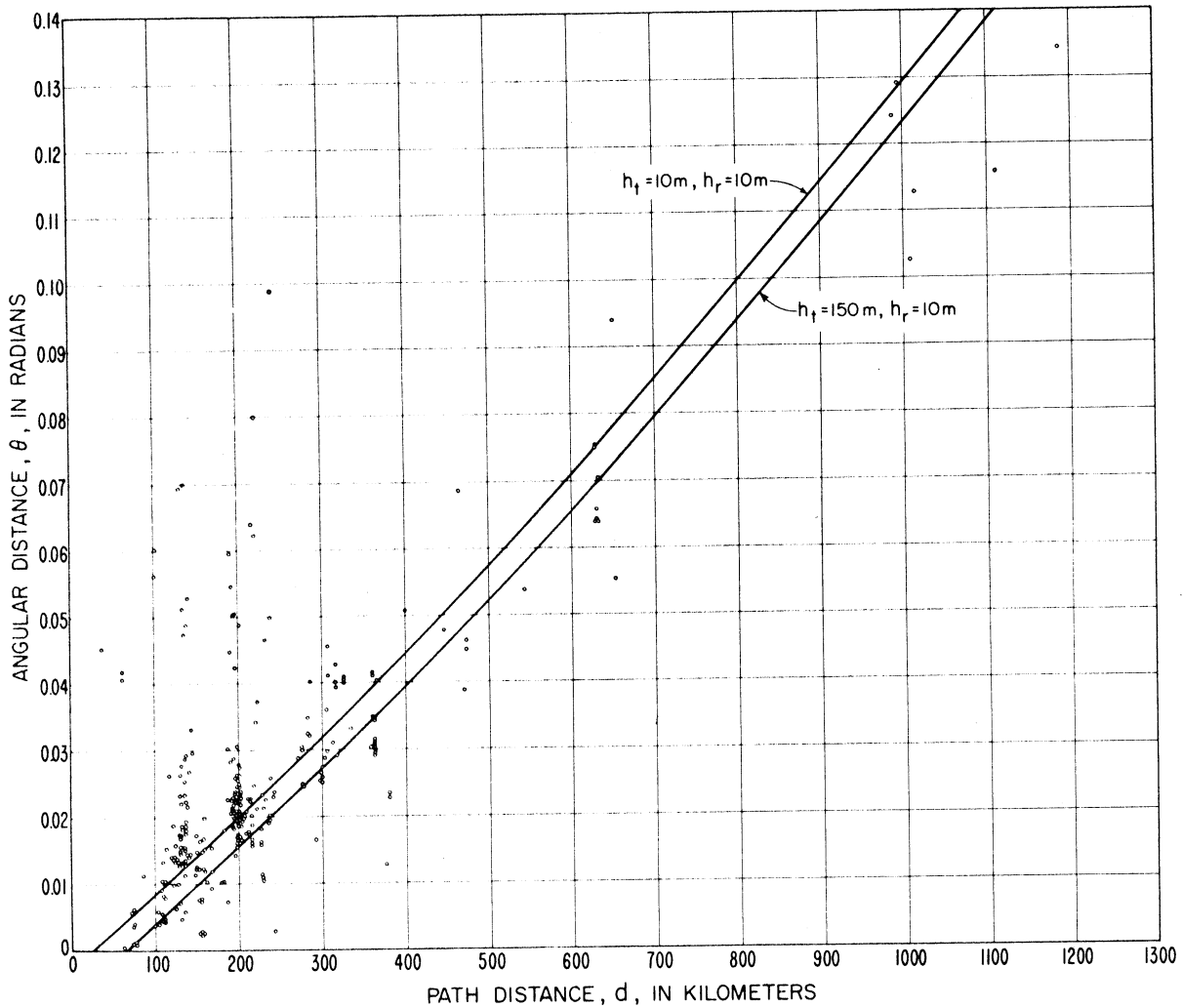


Figure 1.5

CUMULATIVE DISTRIBUTION OF DEVIATIONS OF OBSERVED
FROM PREDICTED VALUES OF TRANSMISSION LOSS

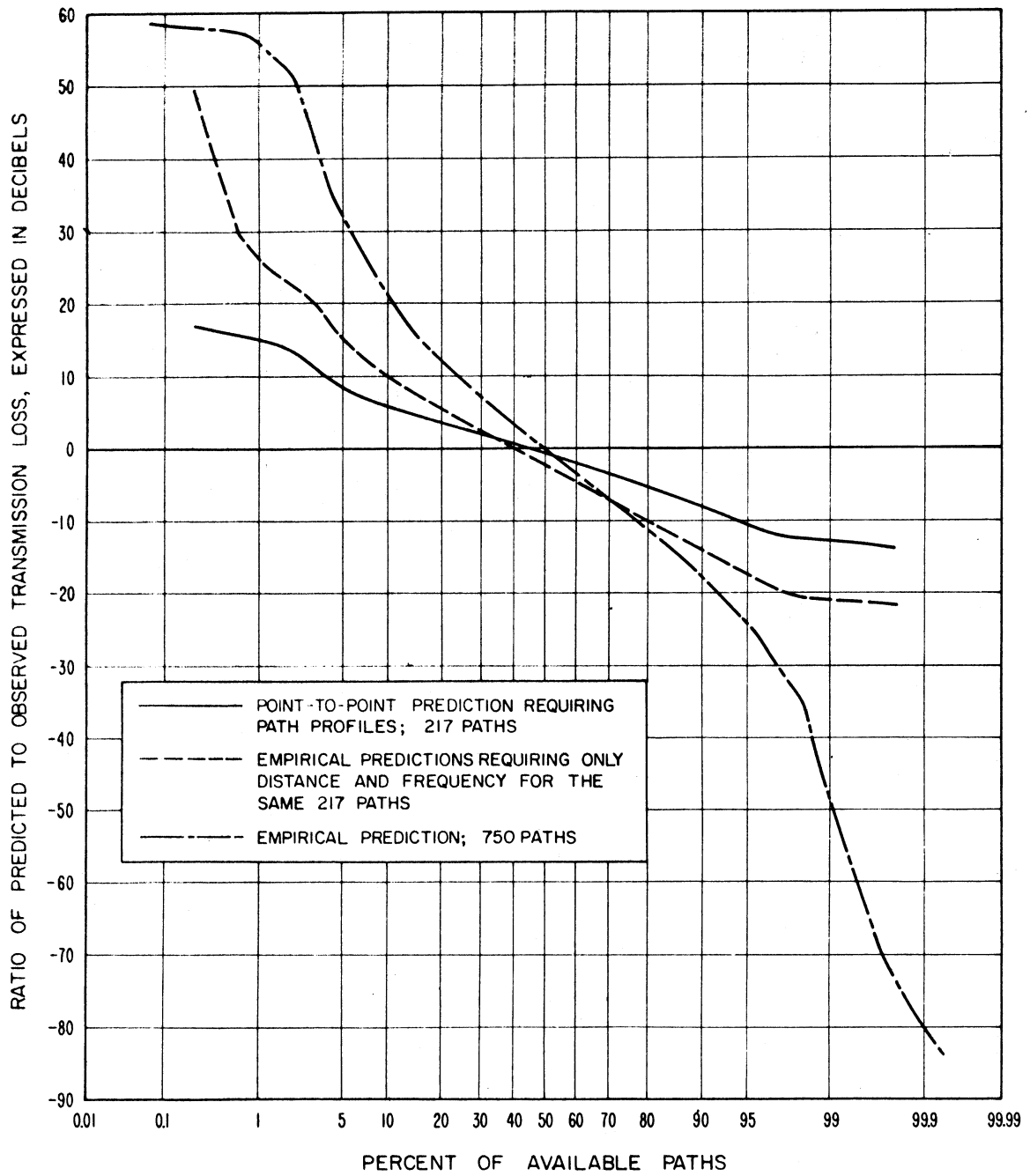


Figure I.6

STANDARD PROPAGATION CURVES
 HOURLY MEDIAN BASIC TRANSMISSION LOSS
 VERSUS DISTANCE AND TIME AVAILABILITY
 FREQUENCY 0.1 GHz $h_{re} = h_{re} = 30$ m

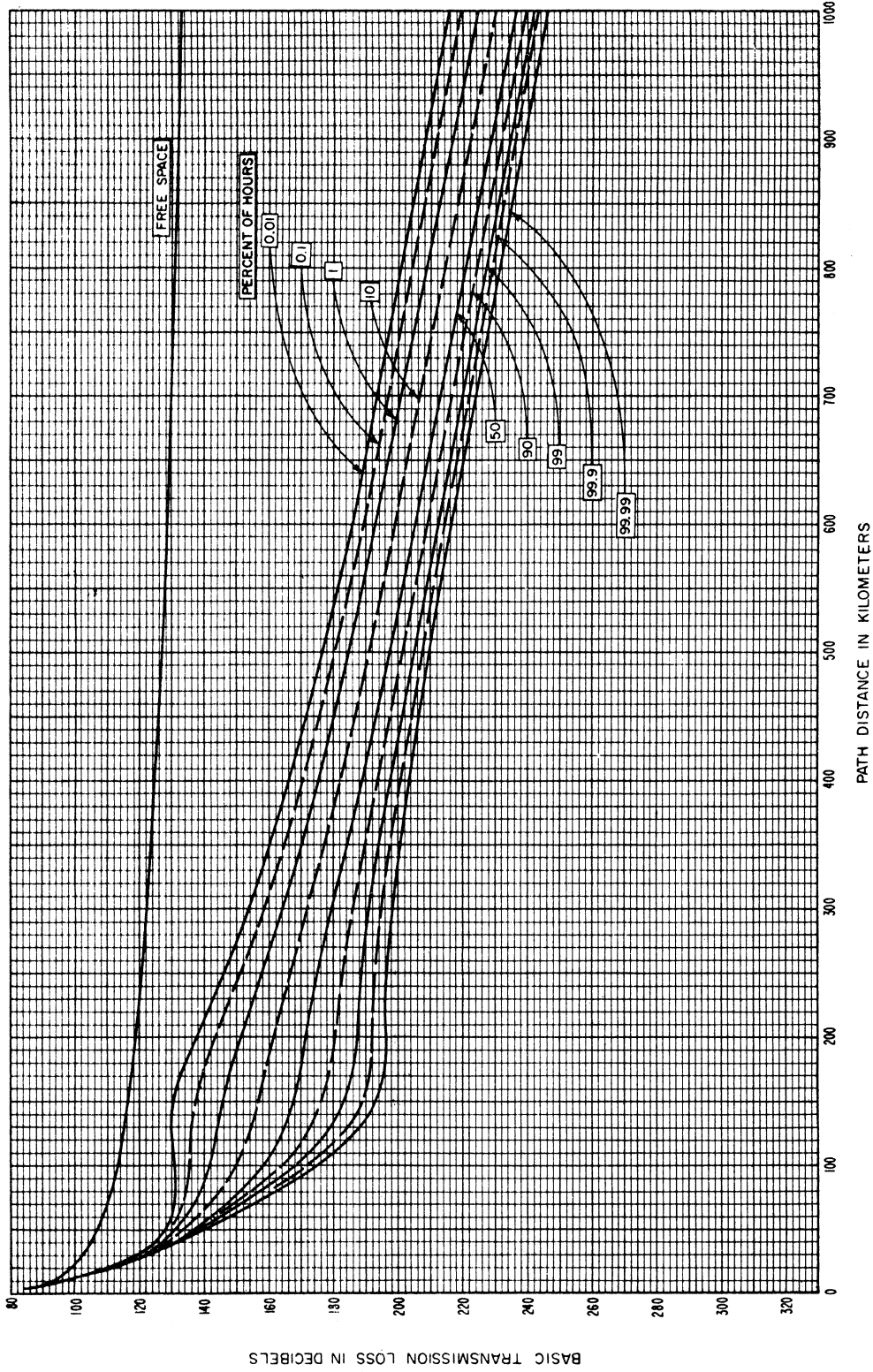


Figure I.7

STANDARD PROPAGATION CURVES
 HOURLY MEDIAN BASIC TRANSMISSION LOSS
 VERSUS DISTANCE AND TIME AVAILABILITY
 FREQUENCY 0.2 GHz $n_{fs} = n_{rs} = 3.0$

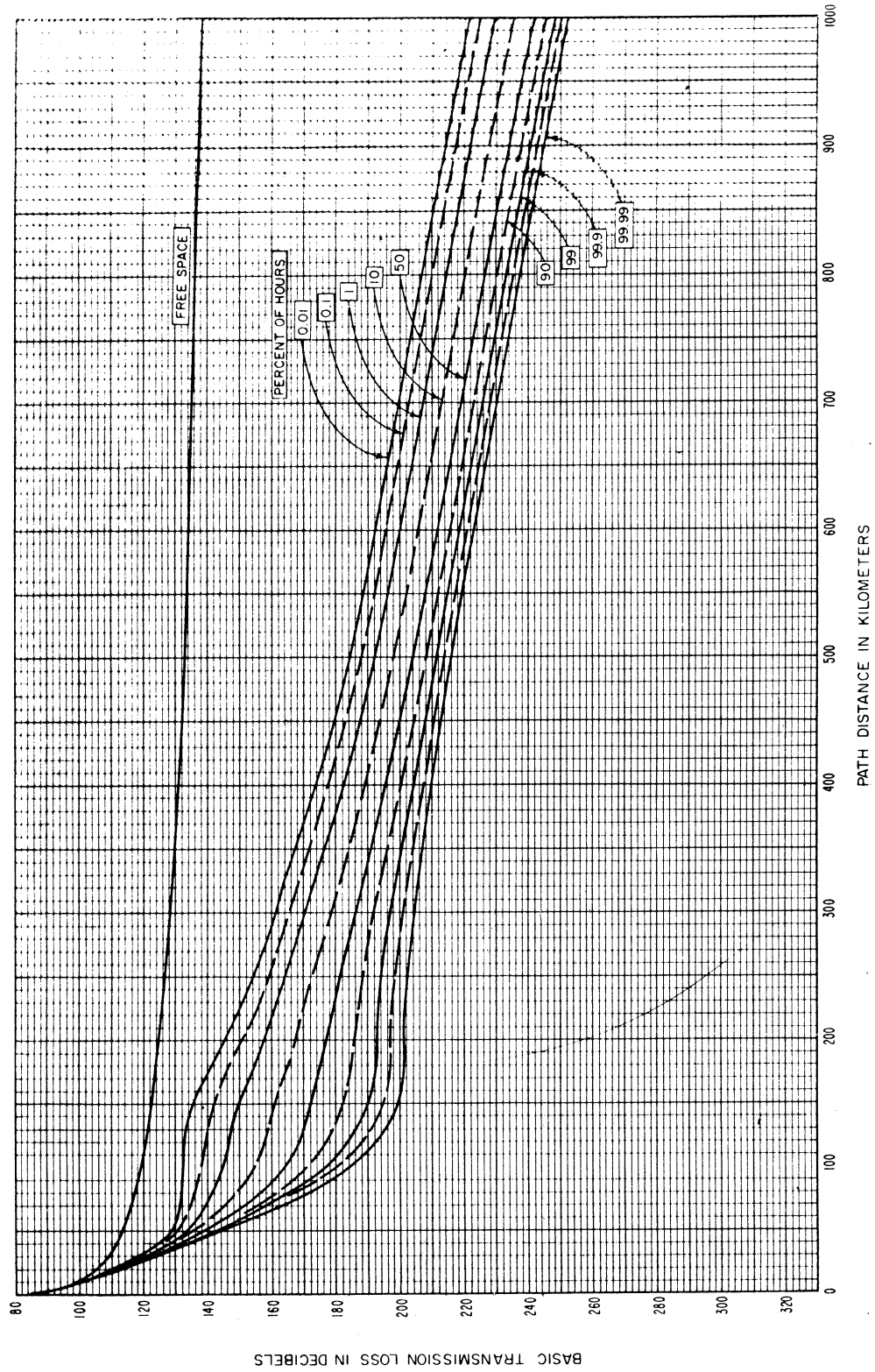


Figure I.8

STANDARD PROPAGATION CURVES
 HOURLY MEDIAN BASIC TRANSMISSION LOSS
 VERSUS DISTANCE AND TIME AVAILABILITY
 FREQUENCY 0.5 GHz $h_{te} = h_{re} = 30$ m

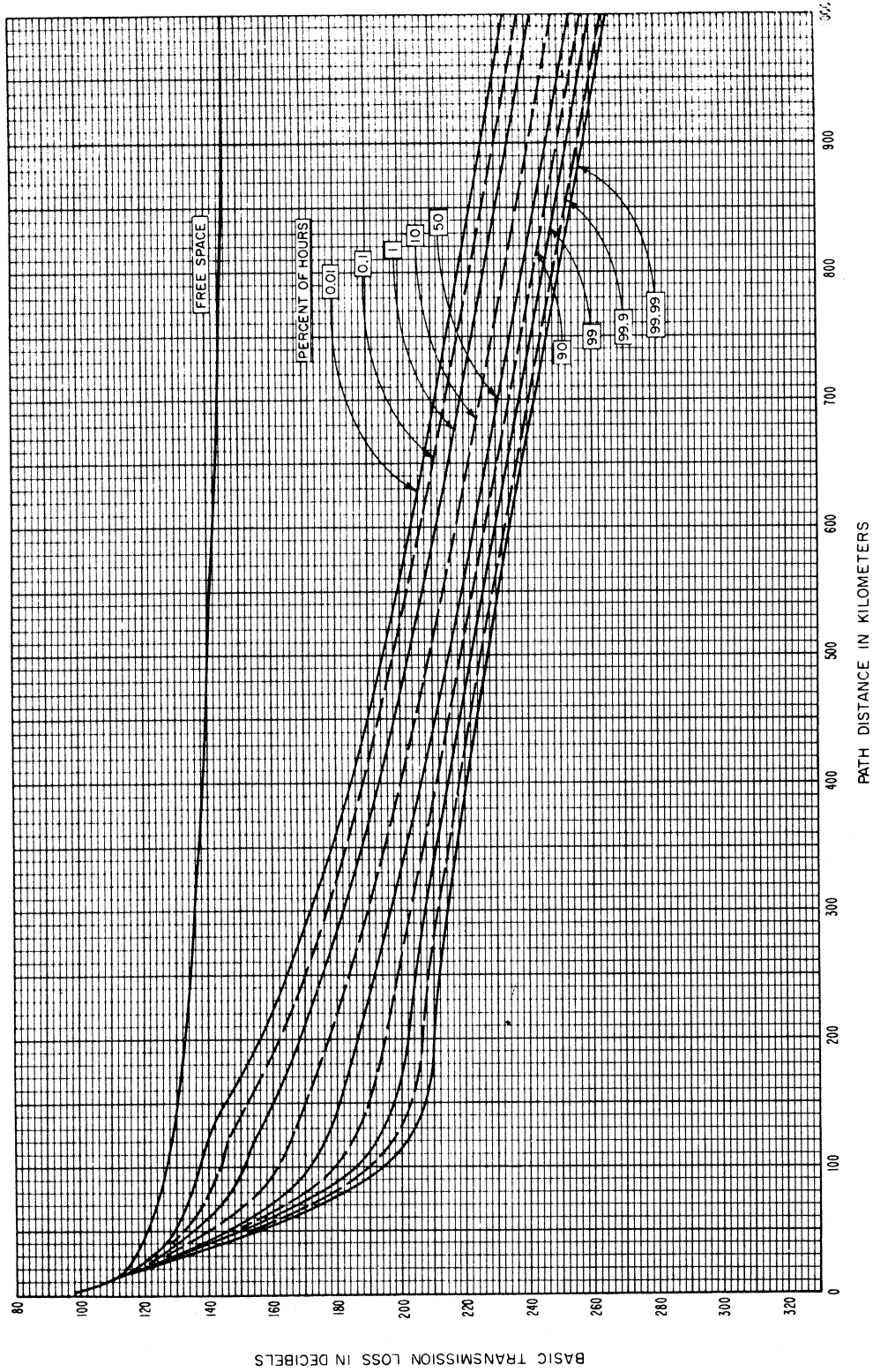


Figure 1.9

STANDARD PROPAGATION CURVES
 HOURLY MEDIAN BASIC TRANSMISSION LOSS
 VERSUS DISTANCE AND TIME AVAILABILITY
 FREQUENCY 1 GHz $h_{t_e} = h_{r_e} = 30$ m



Figure I.10

STANDARD PROPAGATION CURVES
 HOURLY MEDIAN BASIC TRANSMISSION LOSS
 VERSUS DISTANCE AND TIME AVAILABILITY
 FREQUENCY 2 GHz $n_{re} = n_{re} = 30m$

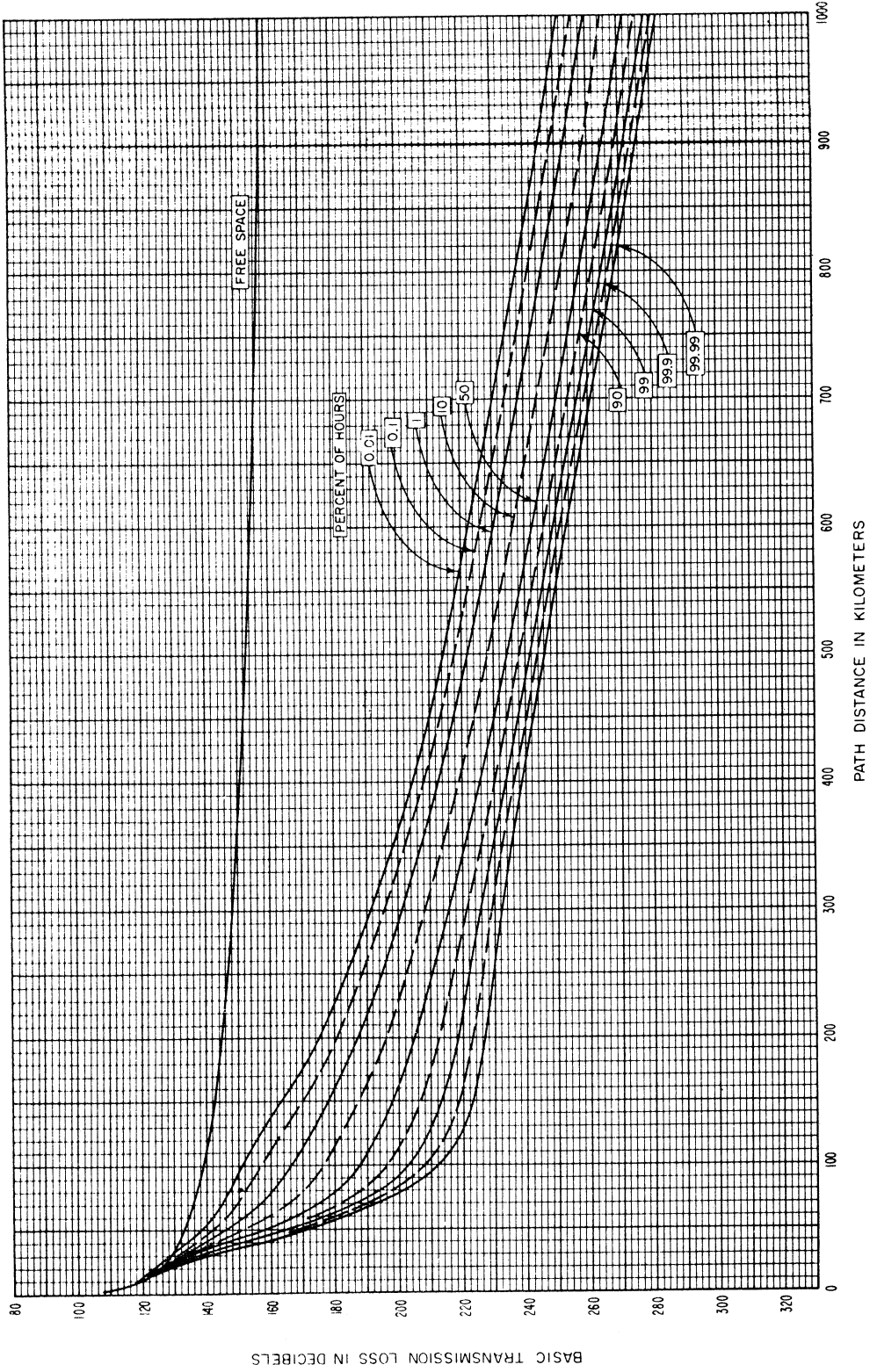


Figure I.11

STANDARD PROPAGATION CURVES
 HOURLY MEDIAN BASIC TRANSMISSION LOSS
 VERSUS DISTANCE AND TIME AVAILABILITY
 FREQUENCY 5 GHz $h_{t,e} = h_{r,e} = 30\text{m}$

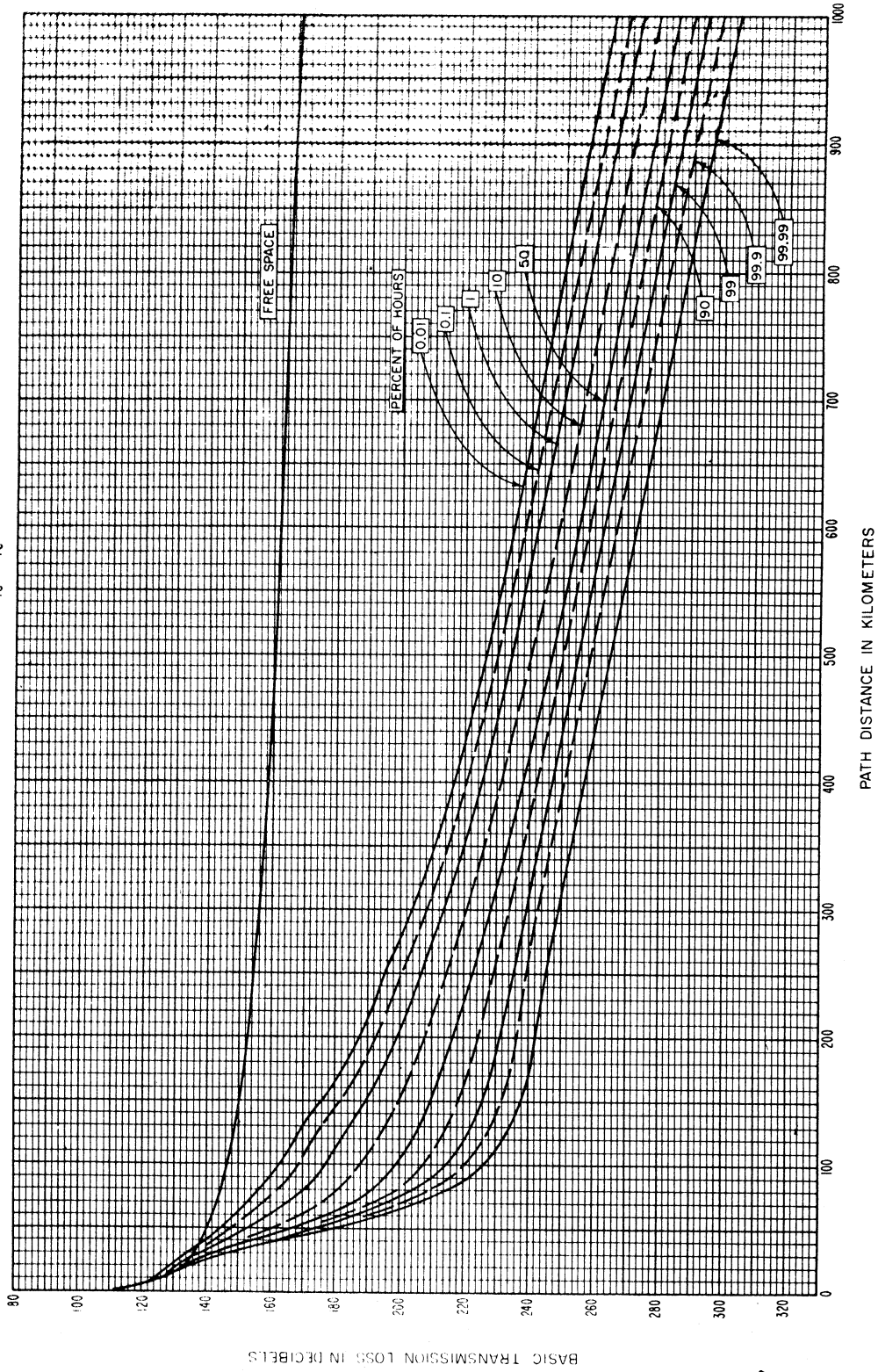


Figure I.12

STANDARD PROPAGATION CURVES
 HOURLY MEDIAN BASIC TRANSMISSION LOSS
 VERSUS DISTANCE AND TIME AVAILABILITY
 FREQUENCY 10 GHz $h_{te} = h_{re} = 30\text{ m}$

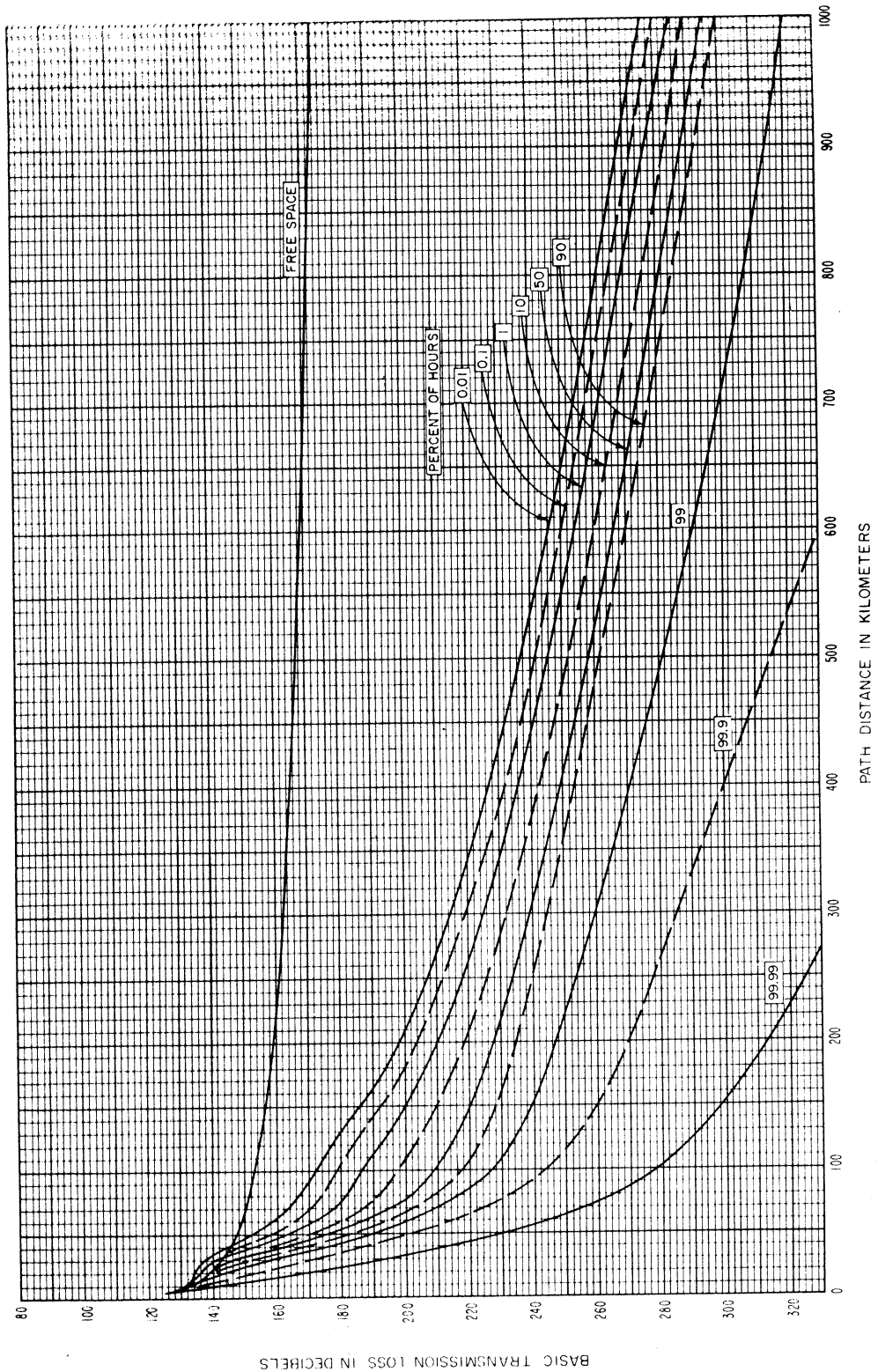


Figure 1.13

STANDARD PROPAGATION CURVES
 HOURLY MEDIAN BASIC TRANSMISSION LOSS
 VERSUS DISTANCE AND TIME AVAILABILITY
 FREQUENCY 22.2 GHz $n_{fe} = n_{re} = 3.0$

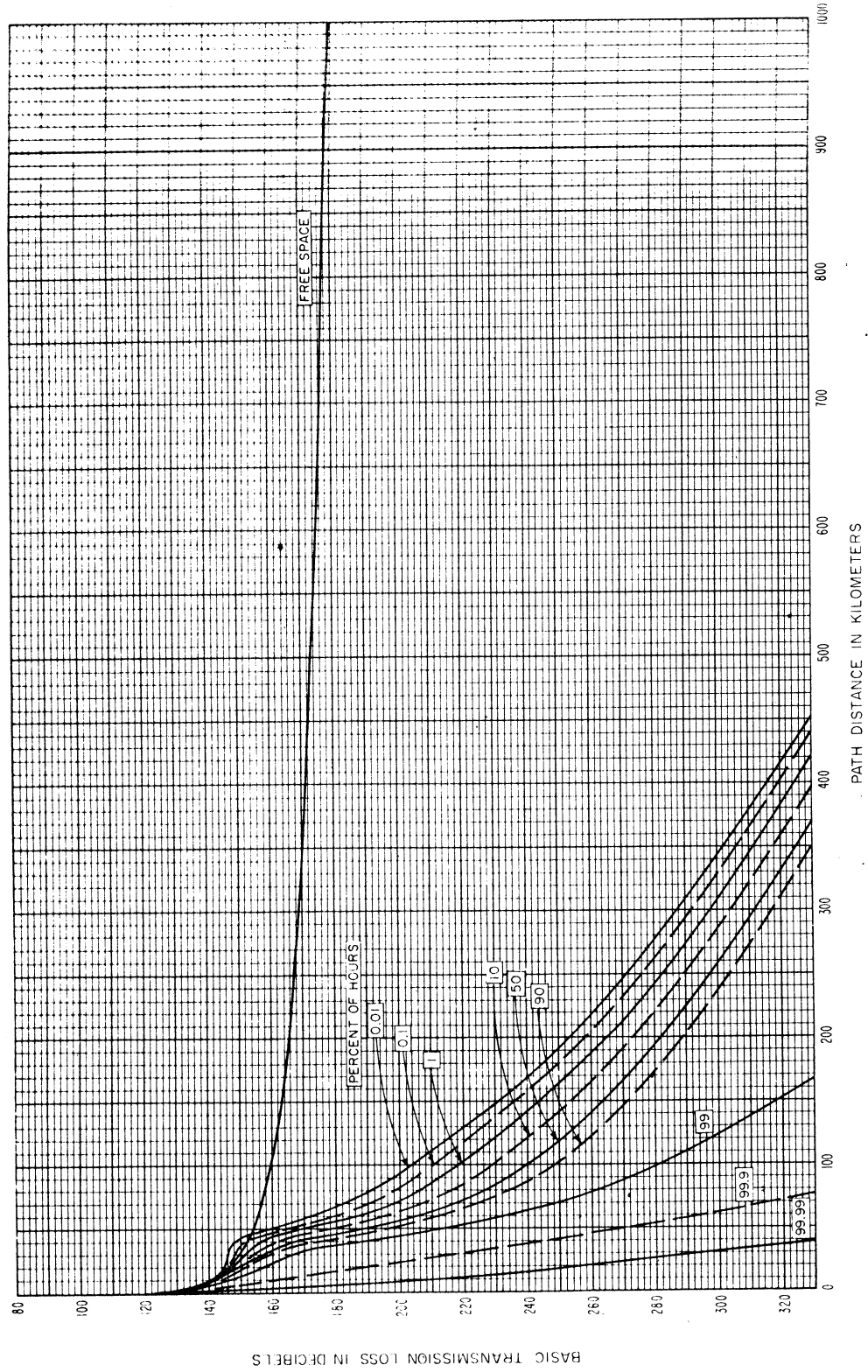


Figure I.14

STANDARD PROPAGATION CURVES
 HOURLY MEDIAN BASIC TRANSMISSION LOSS
 VERSUS DISTANCE AND TIME AVAILABILITY
 FREQUENCY 32.5 GHz $r_{re} = h_{re} = 30$ m

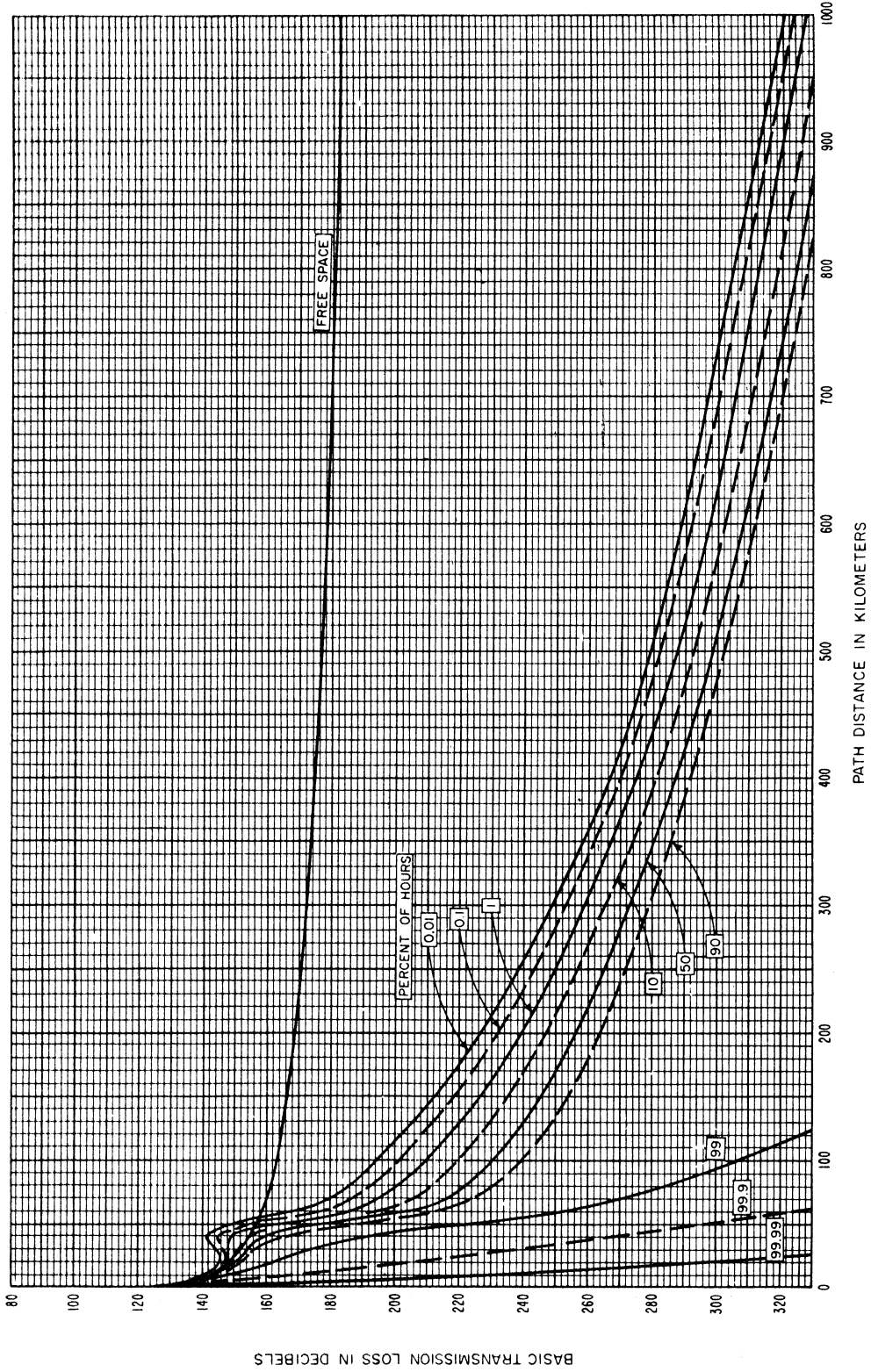


Figure I.15

STANDARD PROPAGATION CURVES
 HOURLY MEDIAN BASIC TRANSMISSION LOSS
 VERSUS DISTANCE AND TIME AVAILABILITY
 $h_{te} = h_{re} = 30\text{ m}$

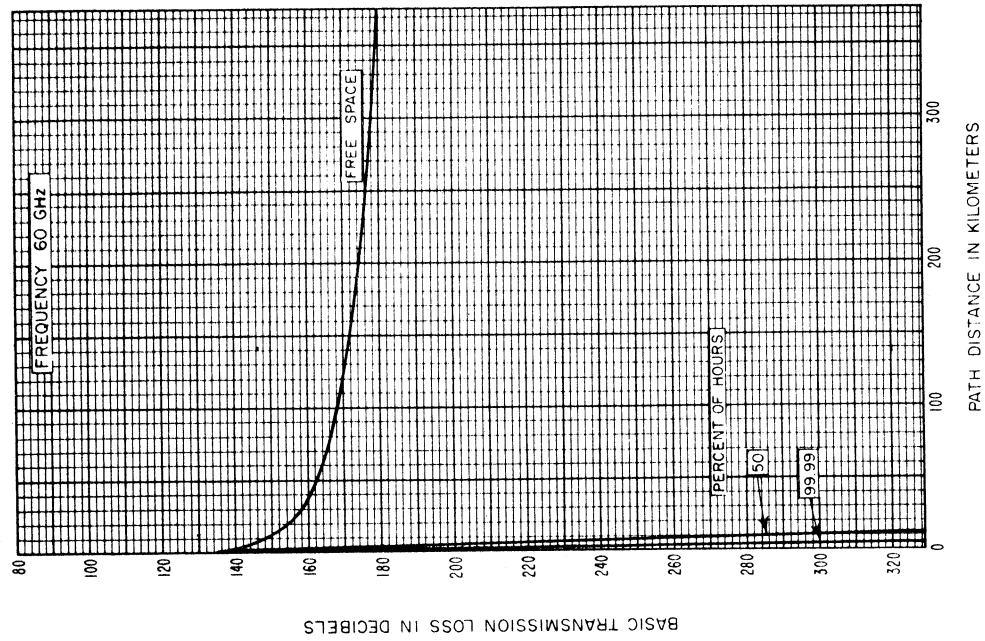


Figure I.16

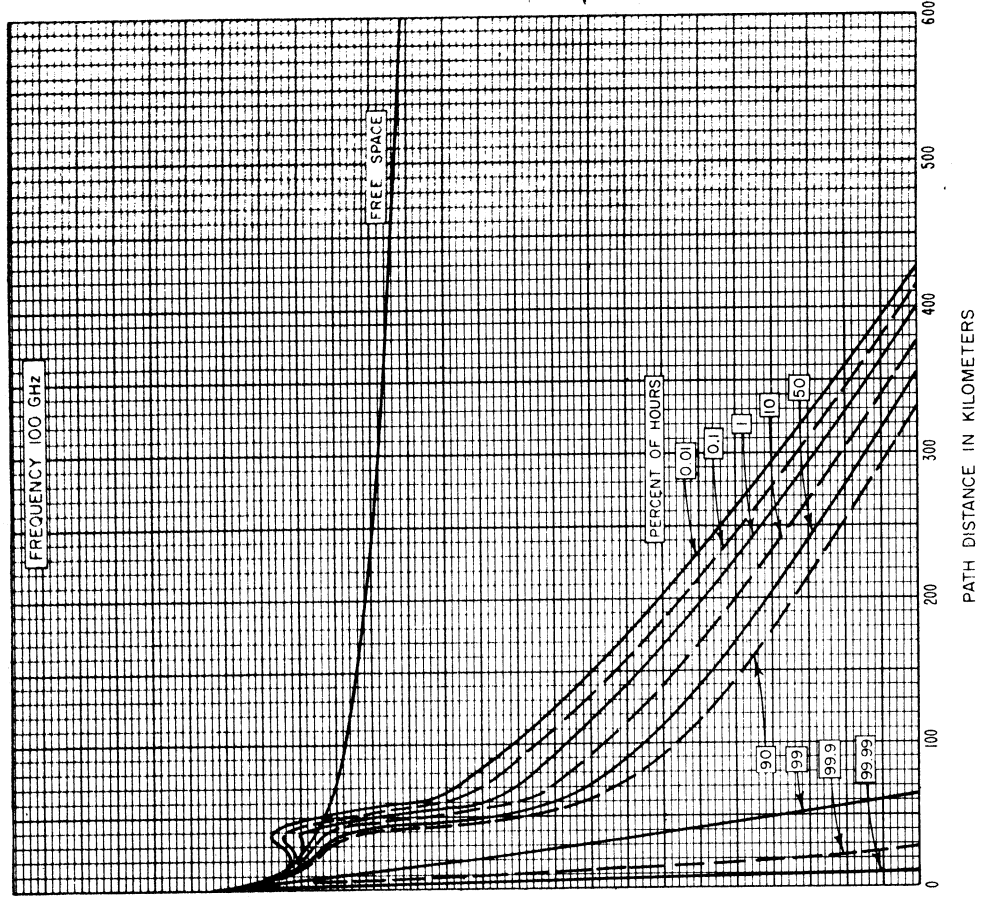


Figure I.17

STANDARD PROPAGATION CURVES
 PREDICTED MEDIAN LEVELS OF BASIC TRANSMISSION LOSS
 FOR FREQUENCIES FROM 0.1 TO 100 GHz

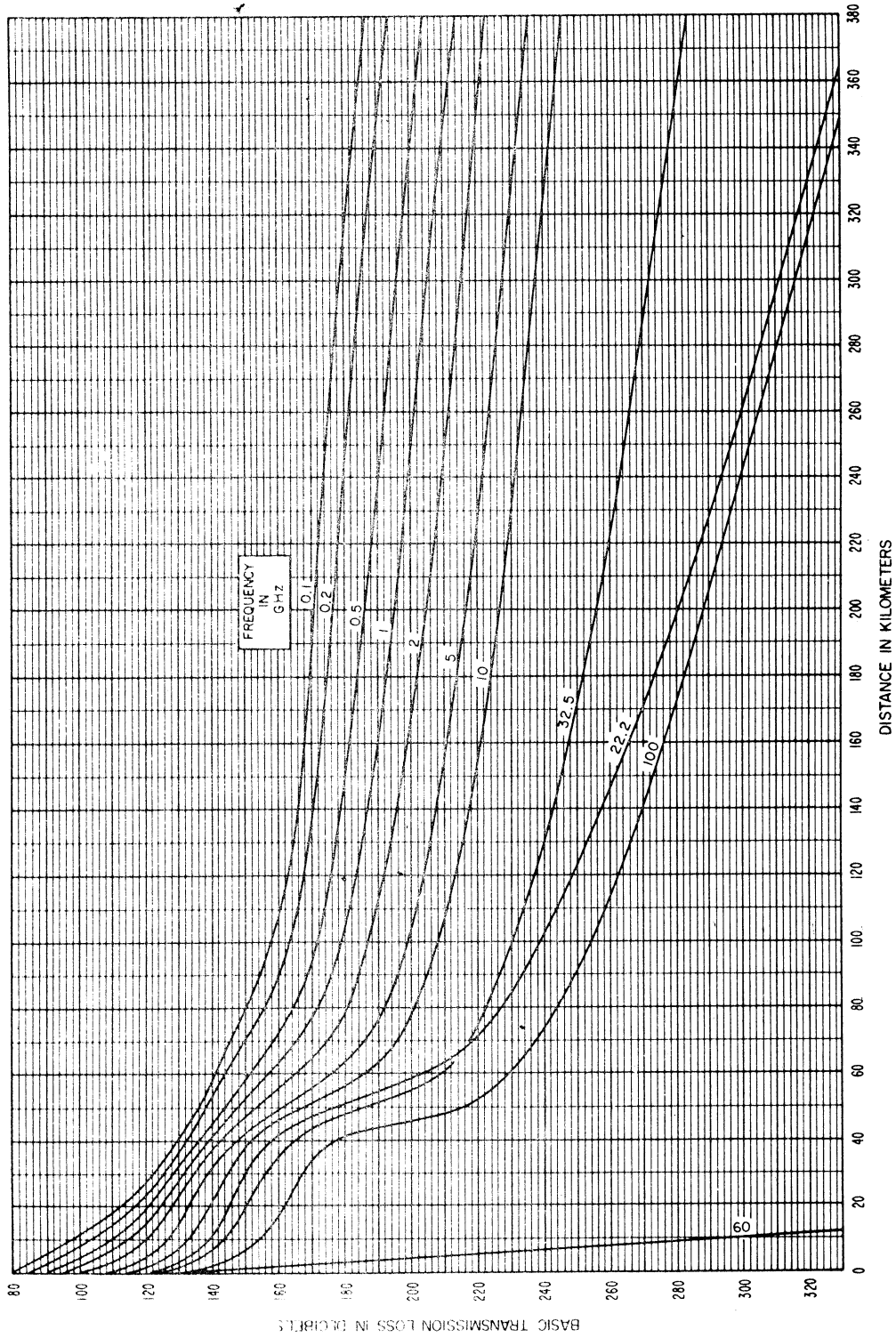


Figure 1.18

STANDARD PROPAGATION CURVES
 CUMULATIVE DISTRIBUTION OF HOURLY MEDIAN BASIC TRANSMISSION LOSS
 RELATIVE TO THE LONG-TERM MEDIAN

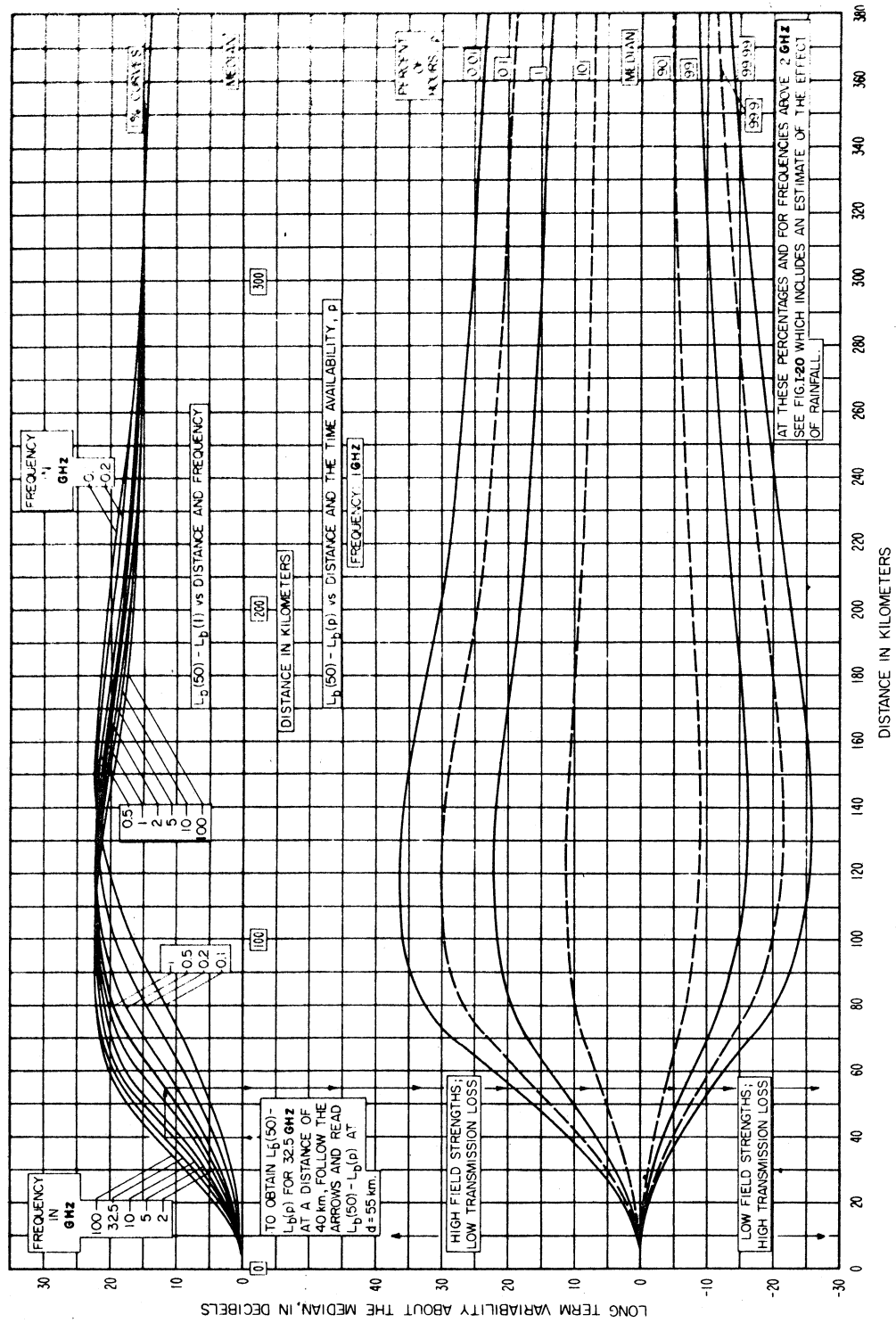


Figure I.19

STANDARD PROPAGATION CURVES

BASIC TRANSMISSION LOSS NOT EXCEEDED FOR 99 AND 99.99 PERCENT OF ALL HOURS INCLUDING AN ESTIMATE OF ABSORPTION BY RAIN, ASSUMING 100 cm TOTAL ANNUAL RAINFALL. THE CURVES ARE DRAWN FOR FREQUENCIES BETWEEN 5 AND 100 GHz

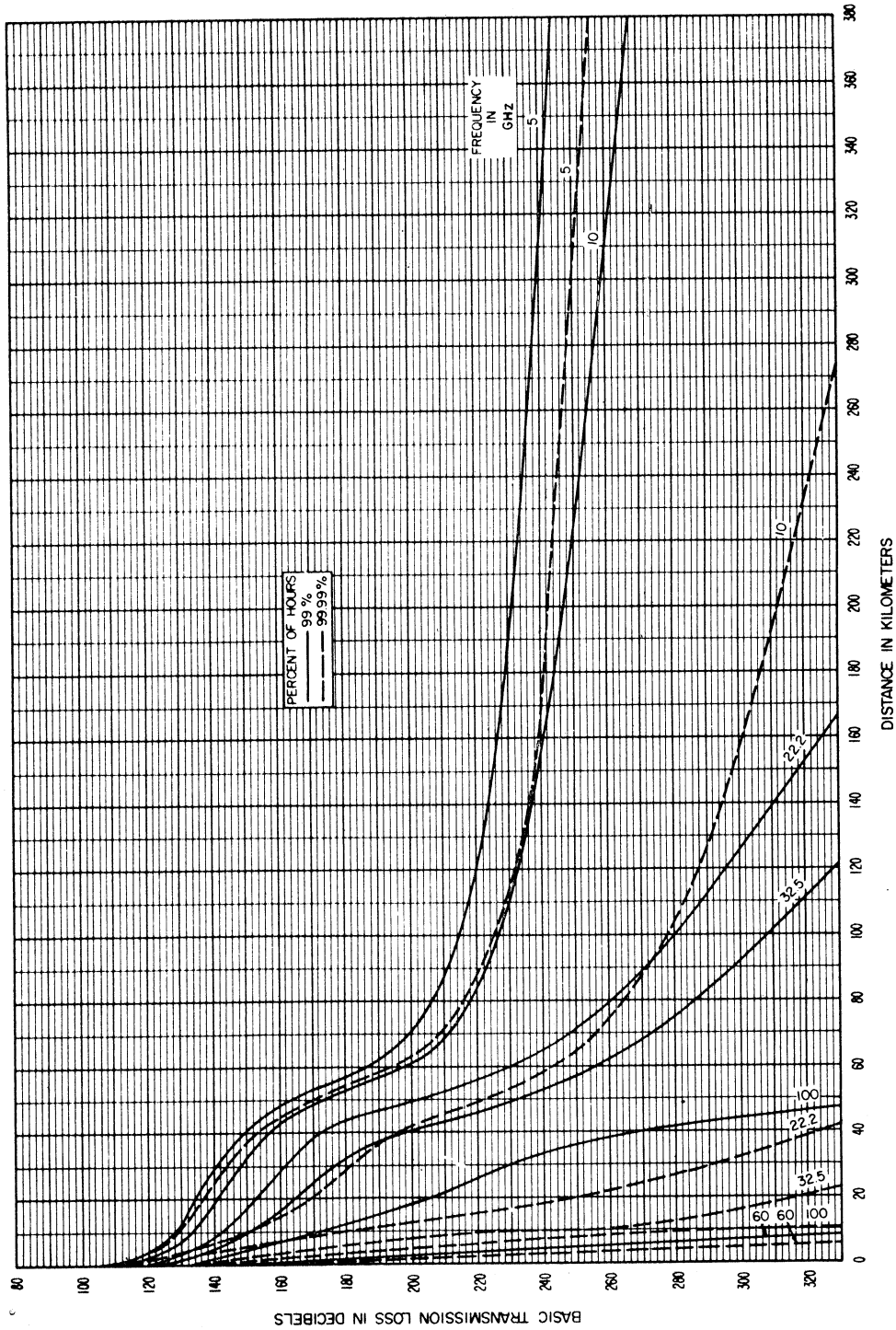


Figure 1.20

STANDARD PROPAGATION CURVES FOR EARTH-SPACE LINKS
 $\theta_0 = 0$ RADIANS
 NO ALLOWANCE HAS BEEN MADE FOR GROUND REFLECTION

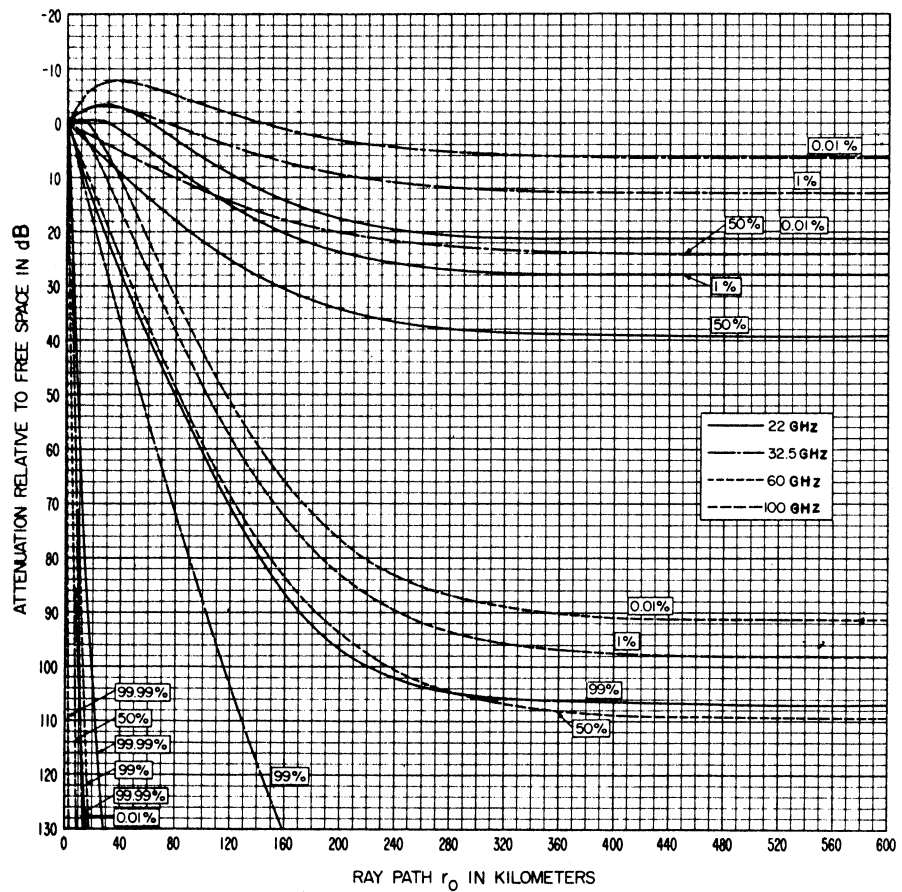
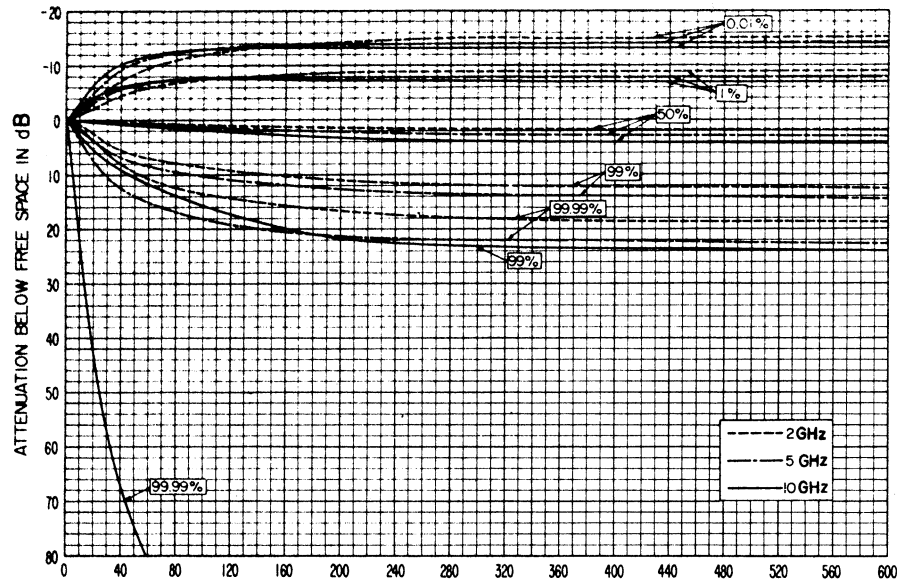


Figure I.21

STANDARD PROPAGATION CURVES FOR EARTH SPACE LINKS
 $\theta_0 = 0.03$ RADIANS

NO ALLOWANCE HAS BEEN MADE FOR GROUND REFLECTION

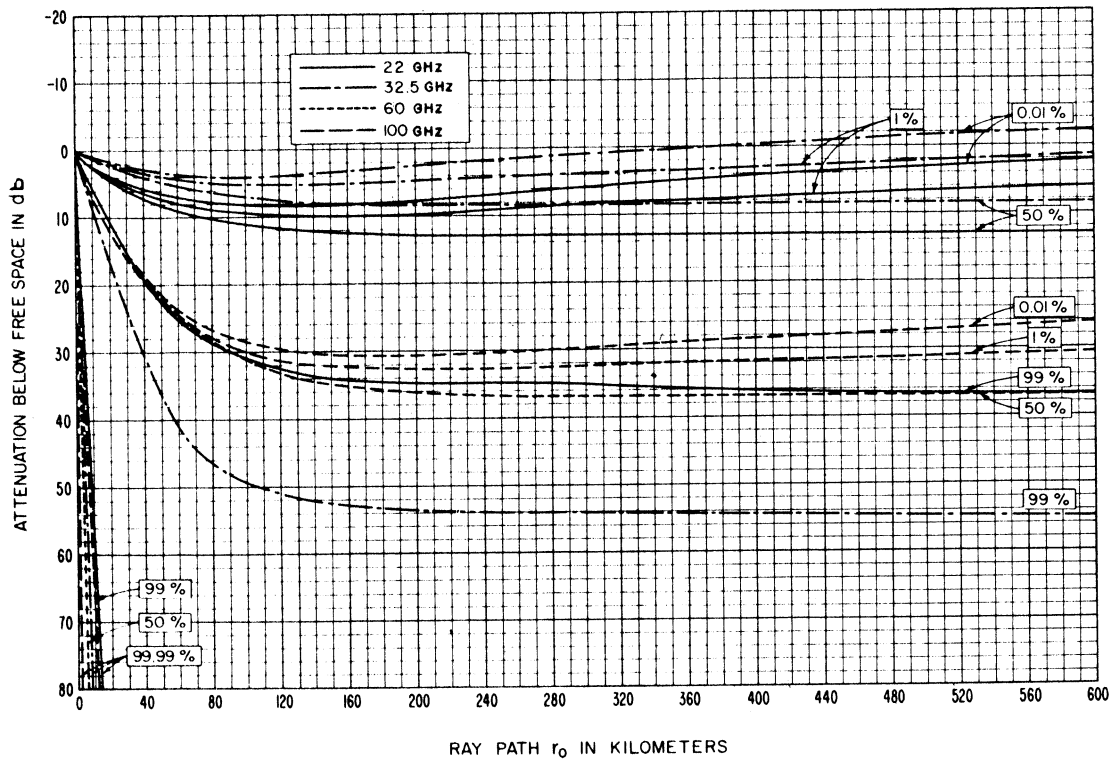
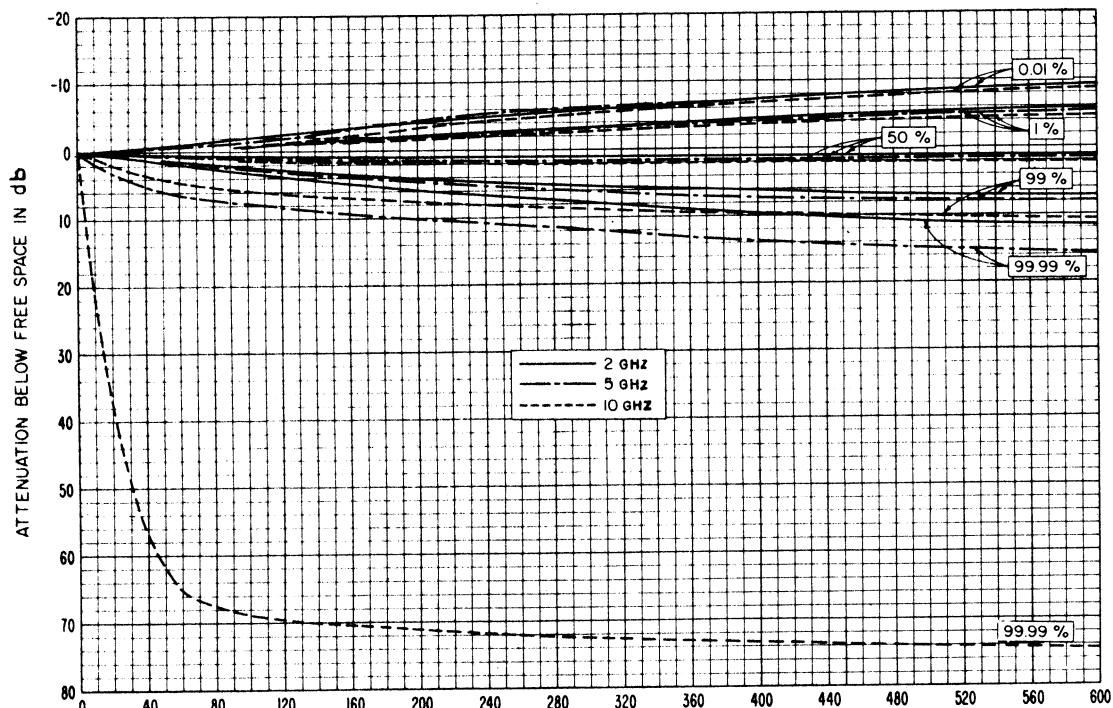


Figure I.22

STANDARD PROPAGATION CURVES FOR EARTH-SPACE LINKS
 $\theta_0 = 0.1$ RADIANS
 NO ALLOWANCE HAS BEEN MADE FOR GROUND REFLECTION

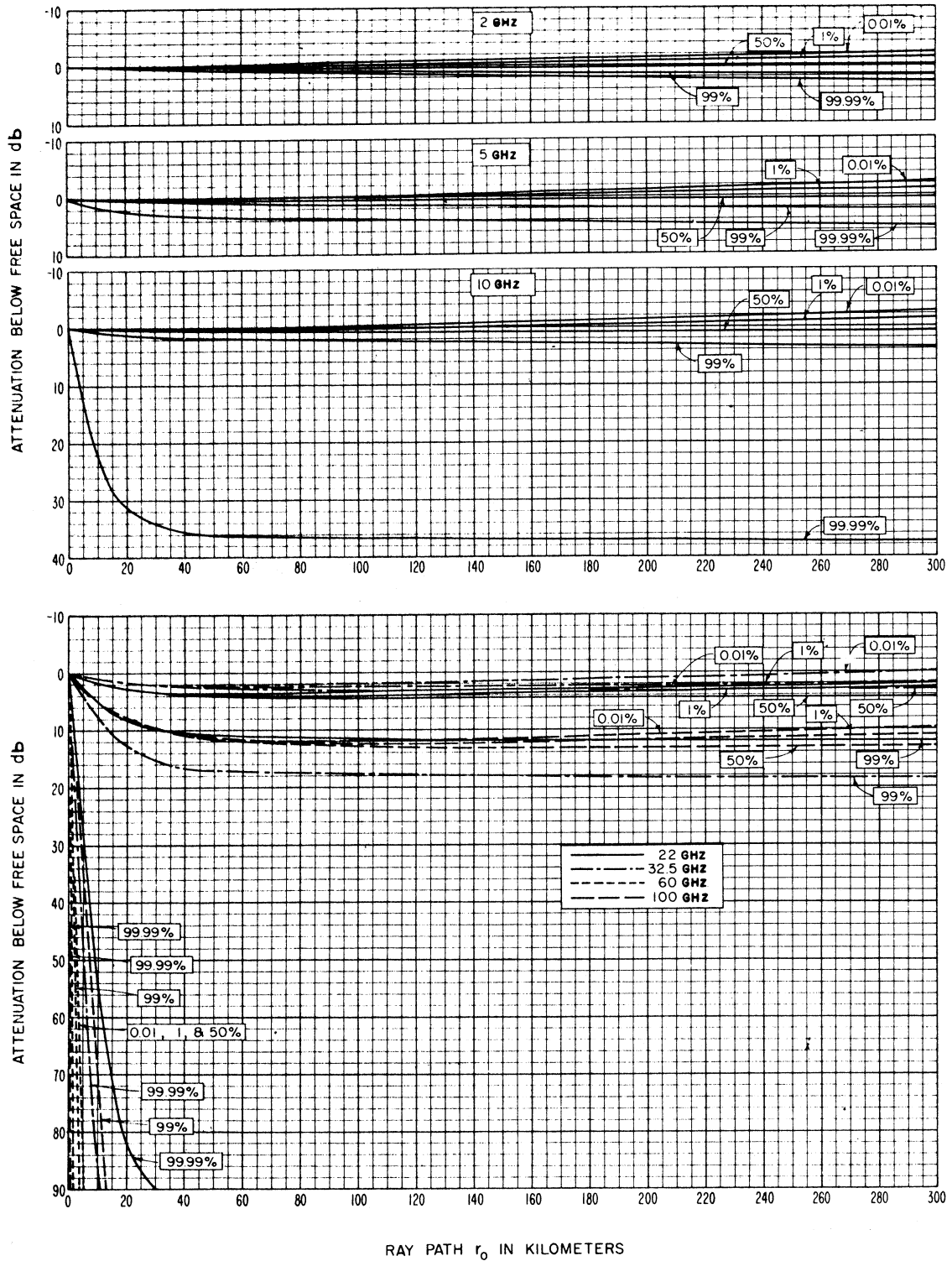


Figure 1.23

STANDARD PROPAGATION CURVES FOR EARTH-SPACE LINKS
 $\theta_0 = 0.3$ RADIANS

NO ALLOWANCE HAS BEEN MADE FOR GROUND REFLECTION

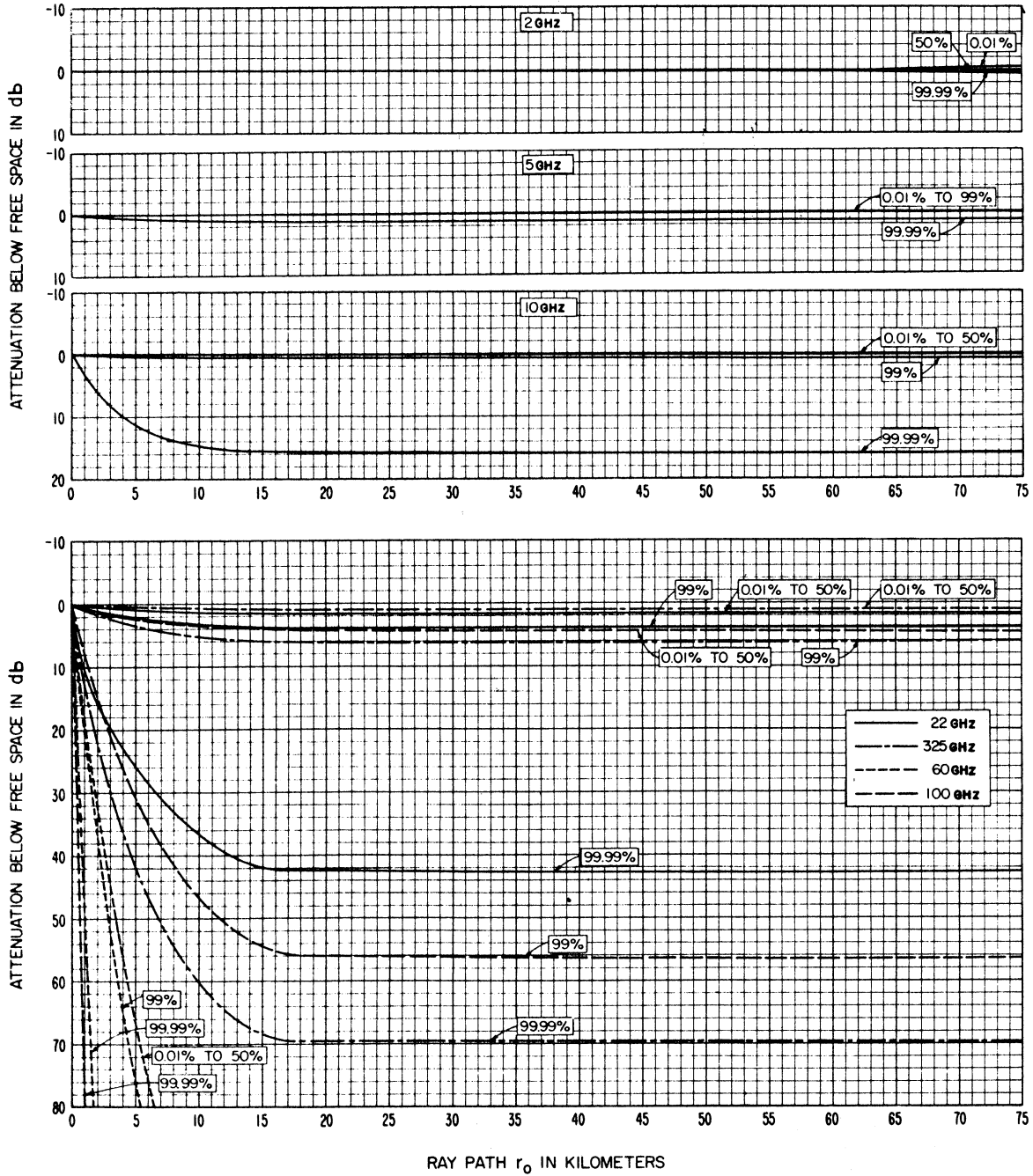


Figure I.24

STANDARD PROPAGATION CURVES FOR EARTH-SPACE LINKS

$\theta_0 = 1.0$ RADIAN

NO ALLOWANCE HAS BEEN MADE FOR GROUND REFLECTION

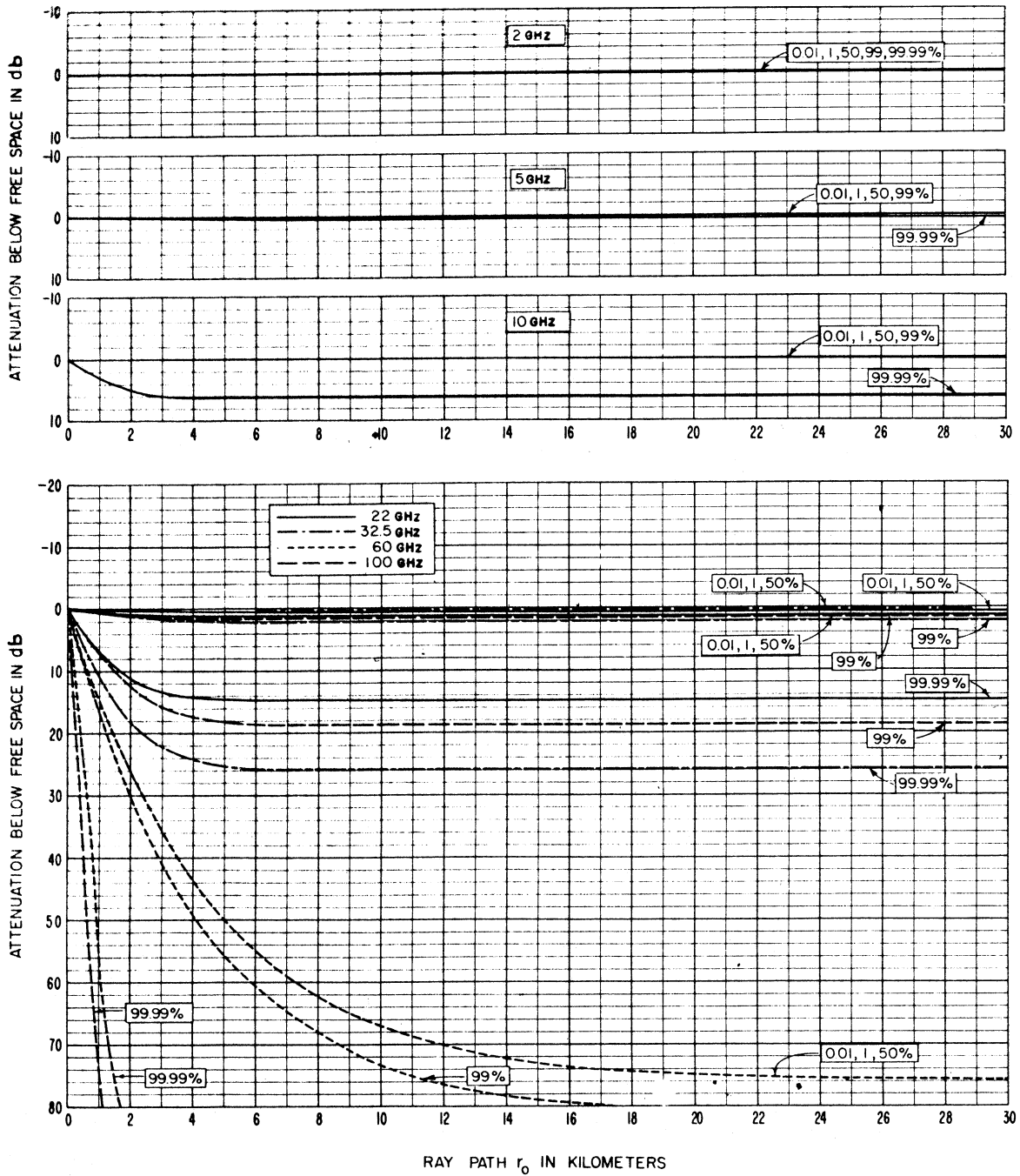


Figure I.25

STANDARD PROPAGATION CURVES FOR EARTH-SPACE LINKS

$$\theta_0 = \pi/2$$

NO ALLOWANCE HAS BEEN MADE FOR GROUND REFLECTION

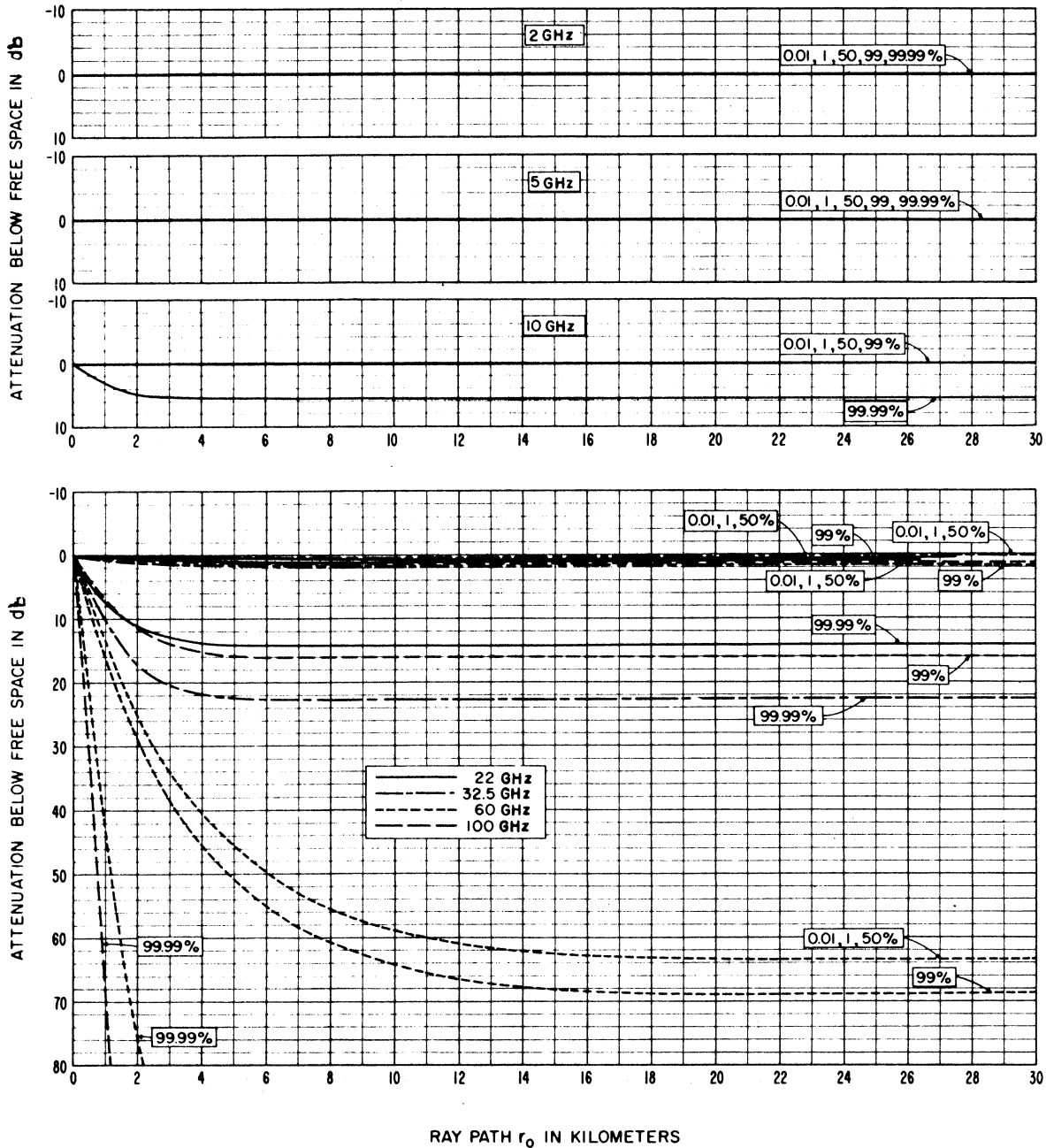


Figure I.26

1.3 Preliminary Reference Values of Attenuation Relative
to Free Space, A_{cr}

1.3.1 Introduction

Three main elements of the problem of prediction are the intended application, the characteristics of available data, and the basis of relevant propagation models. The theoretical basis of the model proposed here is simple, and its advantages and limitations are easily demonstrated. Preliminary comparisons with data indicate standard errors of prediction considerably greater than those associated with the specific methods described in volume 1, which are designed for particular applications. However, the method described below is especially useful when little is known of the details of terrain; it may readily be programmed for a digital computer; and it is adequate for most applications where a preliminary calculated reference value A_{cr} of attenuation relative to free space is desired. The minimum prediction parameters required are frequency, path distance, and effective antenna heights. For the other parameters mentioned typical values are suggested for situations where accurate values are not known.

For radio line-of-sight paths the calculated reference value A_{cr} is either a "foreground attenuation" A_f or an extrapolated value of diffraction attenuation A_d , whichever is greater. For transhorizon paths, A_{cr} is either equal to A_d or to a forward scatter attenuation A_s , whichever is smaller.

1.3.2 The Terrain Roughness Factor Δh

Different types of terrain are distinguished according to the value of a terrain roughness factor Δh . This is the interdecile range of terrain heights in meters above and below a straight line fitted to the average slope of the terrain. When terrain profiles are available Δh is obtained by plotting terrain heights above sea level, fitting a straight line by least squares to define the average slope and obtaining a cumulative distribution of deviations of terrain heights from the straight line. Ordinarily Δh will increase with distance to an asymptotic value. This is the value to be used in these computations.

When terrain profiles are not available estimates of Δh may be obtained from the following table:

TABLE I. 1

<u>Type of Terrain</u>	<u>Δh (meters)</u>
Water or very smooth terrain	0-1
Smooth terrain	10-20
Slightly rolling terrain	40-60
Hilly terrain	80-150
Rugged mountains	200-500

I.3.3 The Diffraction Attenuation A_d

If the earth is smooth $A_d = R$ is computed using the method described in section 8 of volume 1. If the terrain is very irregular, the path is considered as though it were two simple knife edges: a) transmitter-first ridge-second ridge, and b) first ridge-second ridge-receiver. The total diffraction attenuation K is then the sum of the losses over each knife-edge.

$$K = A(v_1, 0) + A(v_2, 0) \quad (I.1)$$

These functions are defined by (I.7) to (I.12).

The main features of a transhorizon propagation path are the radio horizon obstacles, the radio horizon rays and the path distance d , which is greater than the sum d_L of the distances d_{Lt} and d_{Lr} to the radio horizons of the antennas. The diffraction attenuation A_d depends on d , d_{Lt} , d_{Lr} , the minimum monthly mean surface refractivity N_s , the radio frequency f in MHz, the terrain roughness factor Δh , and the sum θ_e of the elevations θ_{et} and θ_{er} of horizon rays above the horizontal at each antenna. The latter parameters may be measured, or may be calculated using (6.15) of volume 1.

In general, the diffraction attenuation A_d is a weighted average of K and R plus an allowance A_{bs} for absorption and scattering by oxygen, water vapor, precipitation, and terrain clutter:

$$A_d = (1 - \Lambda) K + \Lambda R + A_{bs} \quad (I.2)$$

where Λ is an empirical weighting factor:

$$\Lambda = \left[1 + 0.045 \left(\frac{\Delta h}{\lambda} \right)^{\frac{1}{2}} \left(\frac{a \theta + d_L}{d} \right)^{\frac{1}{2}} \right]^{-1} \quad (I.3)$$

$$d_L = d_{Lt} + d_{Lr} \quad \text{km} \quad (I.4)$$

$$\theta = \theta_e + d/a \quad \text{radians,} \quad (I.5)$$

$$a = 6370 / [1 - 0.04665 \exp(0.005577 N_s)] \quad (I.6)$$

The angular distance θ is in radians and the wavelength λ is expressed in meters. The parameter $(a\theta + d_L)/d$ in (I.5) is unity for a smooth earth, where $\Delta h/\lambda$ is small and $\Lambda \cong 1$. For very irregular terrain, both $\Delta h/\lambda$ and $(a\theta + d_L)/d$ tend to be large so that $\Lambda \cong 0$.

The following set of formulas used to calculate K and R are consistent with sections 7 and 8, volume 1.

$$v_{1,2} = 1.2915 \theta \left[f d_{Lt,r} (d-d_L)/(d-d_L + d_{Lt,r}) \right]^{\frac{1}{2}} \quad (\text{I.7})$$

$$A(v, \theta) = \begin{cases} 6.02 + 9.11 v - 1.27 v^2 & \text{for } 0 < v \leq 2.4 \\ 12.953 + 20 \log v & \text{for } v > 2.4 \end{cases} \quad (\text{I.8})$$

$$R = G(x_0) - F(x_1) - F(x_2) - C_1(K_{1,2}) \quad (\text{I.9})$$

$$x_1 = B_{01} d_{Lt}, x_2 = B_{02} d_{Lr}, x_0 = B_{0s} D_s + x_1 + x_2 \quad (\text{I.10})$$

$$B_{01} = f^{\frac{1}{3}} C_{01}^2 B_1 \quad B_{02} = f^{\frac{1}{3}} C_{02}^2 B_2 \quad B_{0s} = f^{\frac{1}{3}} C_{0s}^2 B_s$$

$$C_{01} = (8497/a_1)^{\frac{1}{3}} \quad C_{02} = (8497/a_2)^{\frac{1}{3}} \quad C_{0s} = (8497/a_s)^{\frac{1}{3}} \quad (\text{I.11})$$

$$a_1 = d_{Lt}^2/(2 h_{te}) \quad a_2 = d_{Lr}^2/(2 h_{re}) \quad a_s = D_s/\theta \quad (\text{I.12})$$

If the path distance d is less than d_3 as given by (I.13), it is advisable to calculate A_d for larger distances d_3 and d_4 and to extrapolate a straight line through the points (A_{d_3}, d_3) and (A_{d_4}, d_4) back to the desired value (A, d) . The following is suggested for d_3 and d_4 :

$$d_3 = d_L + 0.5 (a^2/f)^{\frac{1}{3}} \text{ km}, \quad d_4 = d_3 + (a^2/f)^{\frac{1}{3}} \text{ km} \quad (\text{I.13})$$

I.3.4 The Forward Scatter Attenuation, A_s

The scatter attenuation A_s for a transhorizon path depends on the parameters $d, N_s, f, \theta_e, h_{te}, h_{re}$ and A_{bs} . If the product θd of the angular distance θ and the distance d is

greater than 0.5, the forward scatter attenuation A_s is calculated for comparison with A_d :

$$A_s = \begin{cases} S + 103.4 + 0.332 \theta d - 10 \log(\theta d) & \text{for } 0.5 < \theta d \leq 10 \\ S + 97.1 + 0.212 \theta d - 2.5 \log(\theta d) & \text{for } 10 \leq \theta d \leq 70 \\ S + 86.8 + 0.157 \theta d + 5 \log(\theta d) & \text{for } \theta d \geq 70 \end{cases} \quad (\text{I.14})$$

$$S = H_o + 10 \log(f \theta^4) - 0.1 (N_s - 301) \exp(-\theta d/40) + A_{bs} \quad (\text{I.15})$$

$$H_o = \left[\frac{1}{h_{te}} + \frac{1}{h_{re}} \right] / \left[\theta f | 0.007 - 0.058 \theta | \right] \text{ or}$$

$$H_o = 15 \text{ db, whichever is smaller.} \quad (\text{I.16})$$

The reference attenuation $A_{cr} = A_s$ if $A_s < A_d$.

I.3.5 Radio Line-of-Sight Paths

For line-of-sight paths the attenuation relative to free space increases abruptly as d approaches d_L , so an estimate of d_L is required in order to obtain A_{cr} . For sufficiently high antennas, or a sufficiently smooth earth, (see [I.18]), d_{Lt} and d_{Lr} are expected to equal the smooth earth values d_{Lst} and d_{Lsr} :

$$d_{Lst} = \sqrt{0.002 a h_{te}} \text{ km, } d_{Lsr} = \sqrt{0.002 a h_{re}} \text{ km} \quad (\text{I.17})$$

where a is the effective earth's radius in kilometers and h_{te} , h_{re} are heights in meters above a single reflecting plane which is assumed to represent the dominant effect of the terrain between the antennas or between each antenna and its radio horizon. The effective reflecting plane is usually determined by inspection of the portion of terrain which is visible to both antennas.

For a "typical" or "median" path and a given type of terrain d_{Lt} and d_{Lr} may be estimated as

$$d_{Lt} = d_{Lst} [1 \pm 0.9 \exp(-1.5 \sqrt{h_{te}/h})] \text{ km} \quad (\text{I.18a})$$

$$d_{Lr} = d_{Lsr} [1 \pm 0.9 \exp(-1.5 \sqrt{h_{re}/h})] \text{ km.} \quad (\text{I.18b})$$

If for a median path an antenna is located on a hilltop, the plus sign in the corresponding square bracket in (I.18a) or (I.18b) is used, and if the antenna is behind a hill, the minus sign is used. If $d_L = d_{Lt} + d_{Lr}$ is less than a known line-of-sight path distance d , the estimates (I.18a) and (I.18b) are each increased by the ratio (d/d_L) so that $d_L = d$.

For example, in a broadcasting situation with $h_{te} = 150$ meters, $h_{re} = 10$ meters, and $\Delta h = 50$ meters, (I. 18) using minus signs indicates that $d_{Lt} = 0.97 d_{Lst}$ and $d_{Lr} = 0.63 d_{Lsr}$.

For small grazing angles, (5. 6) and (5. 9) of volume 1 may be combined to describe line-of-sight propagation over a perfectly-conducting smooth plane earth:

$$A = 20 \log \left[\frac{\lambda d \cdot 10^3}{4\pi h_{te} h_{re}} \right] \text{ db} \quad (\text{I. 19})$$

where d is in kilometers and h_{te} , h_{re} , and the radio wavelength λ are in meters. This formula is not applicable for small values of $\lambda d / (h_{te} h_{re})$, where the median value of A is expected to be zero. It is proposed therefore to add unity to the argument of the logarithm in (I. 19).

The expression (I. 19) is most useful when d is large and nearly equal to d_L . Better agreement with data is obtained if d is replaced by d_L and the constant $10^3 / (4\pi)$ is replaced by $\Delta h / \lambda$, the terrain roughness factor expressed in wavelengths. Accordingly, the foreground attenuation factor A_f can be written as

$$A_f = 20 \log \left[1 + d_L \Delta h / (h_{te} h_{re}) \right] + A_{bs} \text{ db.} \quad (\text{I. 20})$$

The absorption A_{bs} defined following (I. 2) is discussed in sections 3 and 5 of volume 1. For frequencies less than 10,000 MHz the major component of A_{bs} is usually due to terrain clutter such as vegetation, buildings, bridges, and power lines.

For distances small enough so that A_f is greater than the diffraction attenuation extrapolated into the line-of-sight region, the calculated attenuation relative to free space A_{cr} is given by (I. 20) and depends only on h_{te} , h_{re} , Δh , A_{bs} and an estimate of d_L . For long line-of-sight paths, the foreground attenuation given by (I. 20) is less than the extrapolated diffraction attenuation A_d , so $A_{cr} = A_d$.

If d_{Lt} , d_{Lr} , and θ_e are known, these values are used to calculate A_d . Otherwise, (I. 18) may be used to estimate d_{Lt} and d_{Lr} , and θ_e is calculated as the sum of a weighted average of estimates of θ_{et} and θ_{er} for smooth and rough earth. For a smooth earth,

$$\theta_{et,r} = -0.002 h_{te,re} / d_{Lt,r} \text{ radians,}$$

and for extremely irregular terrain it has been found that median values are nearly

$$\theta_{et,r} = (\Delta h / 2) / (d_{Lt,r} \cdot 10^3) \text{ radians.}$$

Using $d_{Lt,r} / d_{Lst,r}$ and $(1 - d_{Lt,r} / d_{Lst,r})$ respectively as weights, the following formula is suggested for estimating $\theta_{et,r}$ when this parameter is unknown:

$$\theta_{et,r} = \frac{0.0005}{d_{Lst,r}} \left[\left(\frac{d_{Lst,r}}{d_{Lt,r}} - 1 \right) \Delta h - 4 h_{te,re} \right] \text{ radians} \quad (\text{I. 21a})$$

$$\theta_e = \theta_{et} + \theta_{er} \text{ or } \theta_e = -d_L/a, \text{ whichever is larger algebraically,} \quad (\text{I. 21b})$$

As explained following (I. 12), the formulas for A_d require a path distance d greater than d_3 . For a line-of-sight path d is always less than d_L , so A_d is calculated for the distances d_3 and d_4 given by (I. 13) and a straight line through the points (A_3, d_3) and (A_4, d_4) is extrapolated back to the desired value (A, d) . This straight line has the formula

$$A_d = A_e + M d \text{ db} \quad (\text{I. 22})$$

where

$$M = (A_{d4} - A_{d3}) / (d_4 - d_3) \text{ db/km} \quad (\text{I. 23})$$

$$A_e = A_{d4} - M d_4 \text{ db.} \quad (\text{I. 24})$$

The straight line given by (I. 22) intersects the level A_f where the path distance is

$$d_f = (A_f - A_e) / M \text{ km.} \quad (\text{I. 25})$$

$$\text{For } d \leq d_f, \quad A_{cr} = A_f. \quad (\text{I. 26a})$$

$$\text{For } d > d_f, \quad A_{cr} = A_d. \quad (\text{I. 26b})$$

I. 3. 6 Ranges of the Prediction Parameters

These estimates of A_{cr} are intended for the following ranges of the basic parameters:

TABLE I. 2

$20 \leq f \leq 40,000 \text{ MHz}$	$1 \leq d \leq 2000 \text{ km}$
$\lambda/2 \leq h_{te,re} \leq 10,000 \text{ m}$	$250 \leq N_s \leq 400$
$-d_L/a \leq \theta_e \leq 0.2 \text{ radians}$	$0 \leq A_{bs} \leq 50 \text{ db}$
$0.1 d_{Lst} \leq d_{Lt} \leq 3 d_{Lst}$	$0.1 d_{Lsr} \leq d_{Lr} \leq 3 d_{Lsr}$
$0 \leq \Delta h \leq 500 \text{ m}$	

I. 3. 7 Sample Calculations

Table I. 3 lists a set of sample calculations referring to the example introduced after Table I. 1. Values for the following independent parameters are assumed: $h_{te} = 150$ m, $h_{re} = 10$ m, $\Delta h = 50$ m, $N_s = 301$, $f = 700$ MHz. $d_{Lt} = 49.0$ km, $d_{Lr} = 8.2$ km, $\theta_e = -0.00634$ radians, $A_{bs} = 0$ db. An appropriate equation number is listed in parentheses after each of the calculated parameters in Table I. 3. For these calculations the arbitrary distance d_3 was set equal to $d_L + 1$ instead of $d_L + 0.3(a^2/f)^{1/3}$

TABLE I. 3

$d_L = 57.2$ km	(I. 4)	$a = 8493$ km	(I. 6)
$\Delta h/\lambda = 116.8$		$A_f = 9.3$ db	(I. 20)
$d_3 = 58.2$ km		$d_4 = 105.1$ km	(I. 13)
$\theta_3 = 0.000514$ rad.		$\theta_4 = 0.00603$ rad.	(I. 5)
$v_3 = 0.096$		$v_4 = 1.95$	(I. 7)
$v_{13} = 0.0174$		$v_{14} = 1.014$	(I. 8)
$v_{23} = 0.0166$		$v_{24} = 0.546$	(I. 8)
$v_3 \rho_3 = 0.10$		$v_4 \rho_4 = 1.87$	(I. 9)
$\rho_3 = 1.04$		$\rho_4 = 0.96$	(I. 9)
$A(v_3, 0) = 6.9$ db		$A(v_4, 0) = 18.9$ db	(I. 10)
$A(v_{13}, 0) = 6.2$ db		$A(v_{14}, 0) = 14.0$ db	(I. 10)
$A(v_{23}, 0) = 6.2$ db		$A(v_{24}, 0) = 10.6$ db	(I. 10)
$A(0, \rho_3) = 16.0$ db		$A(0, \rho_4) = 14.7$ db	(I. 11)
$U(v_3, \rho_3) = -.9$ db		$U(v_4, \rho_4) = 14.7$ db	(I. 12)
$K_3 = 12.4$ db		$K_4 = 24.6$ db	(I. 6)
$R_3 = 18.1$ dB		$R_4 = 55.3$ db	(I. 5)
$\frac{a \theta_3 + d_L}{d_3} = 1.058$		$\frac{a \theta_4 + d_L}{d_4} = 1.032$	
$\Lambda_3 = 0.667$		$\Lambda_4 = 0.669$	(I. 3b)
$A_{d_3} = 29.5$ db		$A_{d_4} = 58.5$ db	(I. 3a)
$d_3 \theta_3 = 0.0299$		$d_4 \theta_4 = 0.634$	
		$H_{04} = 3.8$ db	(I. 16)
		$S_4 = -56.5$ db	(I. 15)
		$A_{S4} = 49.1$ db	(I. 14)
$A_{cr3} = 29.5$ db		$A_{cr4} = 49.1$ db	

For this example, $M = 0.619$ db/km, $A_e = -6.49$ db, and $d_f = 25.5$ km. The corresponding basic transmission loss L_{bcr} and field strength E_{bcr} for distances less than d_f are $98.65 - 20 \log d$ db and $97.62 - 20 \log d$ db, respectively, corresponding to a constant value $A_{cr} = A_f = 9.3$ db. In general:

$$L_{\text{bcr}} = 32.45 + 20 \log d + 20 \log f + A_{\text{cr}} \text{ db} \quad (\text{I.27})$$

$$E_{\text{bcr}} = 106.92 - 20 \log d - A_{\text{cr}} \text{ db} \quad (\text{I.28})$$

For the example given above, $L_{\text{bcr}_3} = 154.2 \text{ db}$, $L_{\text{bcr}_4} = 178.9 \text{ db}$, $E_{\text{bcr}_3} = 42.1 \text{ db}$, and $E_{\text{bcr}_4} = 17.4 \text{ db}$.

Annex II

AVAILABLE POWER, FIELD STRENGTH AND MULTIPATH COUPLING LOSS

II.1 Available Power from the Receiving Antenna

The definitions of **system loss** and **transmission loss** in volume 1 depend on the concept of available power, the power that would be delivered to the receiving antenna load if its impedance were conjugately matched to the receiving antenna impedance. For a given radio frequency ν in hertz, let $z_{l\nu}$, z'_ν , and z_ν represent the impedances of the load, the actual lossy antenna in its actual environment, and an equivalent loss-free antenna, respectively:

$$z_{l\nu} = r_{l\nu} + ix_{l\nu} \quad (\text{II. 1a})$$

$$z'_\nu = r'_\nu + ix'_\nu \quad (\text{II. 1b})$$

$$z_\nu = r_\nu + ix_\nu \quad (\text{II. 1c})$$

where r and x represent resistance and reactance, respectively. Let $w_{l\nu}$ represent the power delivered to the receiving antenna load and write $w'_{a\nu}$ and $w_{a\nu}$, respectively, for the available power at the terminals of the actual receiving antenna and at the terminals of the equivalent loss-free receiving antenna. If v'_ν is the actual open-circuit r.m.s. voltage at the antenna terminals, then

$$w_{l\nu} = \frac{v'^2_\nu r_{l\nu}}{|z'_\nu + z_{l\nu}|^2} \quad (\text{II. 2})$$

When the load impedance conjugately matches the antenna impedance, so that $z_{l\nu} = z'^*_\nu$ or $r_{l\nu} = r'_\nu$ and $x_{l\nu} = -x'_\nu$, (II. 2) shows that the power $w_{l\nu}$ delivered to the load is equal to the power $w'_{a\nu}$ available from the actual antenna:

$$w'_{a\nu} \equiv \frac{v'^2_\nu}{4 r'_\nu} \quad (\text{II. 3})$$

Note that the available power from an antenna depends only upon the characteristics of the antenna, its open-circuit voltage v'_ν , and the resistance r'_ν , and is independent of the load

impedance. Comparing (II.2) and (II.3), we define a mismatch loss factor

$$l_{mv} \equiv \frac{w'_{av}}{w'_{lv}} = \frac{(r'_v + r_{lv})^2 + (x'_v + x_{lv})^2}{4 r'_v r_{lv}} \quad (\text{II. 4})$$

such that the power delivered to a load equals w'_{av}/l_{mv} . When the load impedance conjugately matches the antenna impedance, l_{mv} has its minimum value of unity, and $w'_{lv} = w'_{av}$. For any other load impedance, somewhat less than the available power is delivered to the load. The power available from the equivalent loss-free antenna is

$$w_{av} = \frac{v_v^2}{4 r_v} \quad (\text{II. 5})$$

where v_v is the open circuit voltage for the equivalent loss-free antenna.

Comparing (II.3) and (II.5), it should be noted that the available power w'_{av} at the terminals of the actual lossy receiving antenna is less than the available power $w_{av} \equiv l_{erv} w'_{av}$ for a loss-free antenna at the same location as the actual antenna:

$$l_{erv} \equiv \frac{w_{av}}{w'_{av}} = \frac{r'_v v_v^2}{r_v v_v^2} \geq 1. \quad (\text{II. 6})$$

The open circuit voltage v'_v for the actual lossy antenna will often be the same as the open circuit voltage v_v for the equivalent loss-free antenna, but each receiving antenna circuit must be considered individually.

Similarly, for the transmitting antenna, the ratio of the total power w'_{tv} delivered to the antenna at a frequency ν is l_{etv} times the total power w_{tv} radiated at the frequency ν :

$$l_{etv} \equiv w'_{tv}/w_{tv}. \quad (\text{II. 7})$$

The concept of available power from a transmitter is not a useful one, and l_{etv} for the transmitting antenna is best defined as the above ratio. However, the magnitude of this ratio can be obtained by calculation or measurement by treating the transmitting antenna as a receiving antenna and then determining l_{etv} to be the ratio of the available received powers from the equivalent loss-free and the actual antennas, respectively.

General discussions of l_{erv} are given by Crichlow et al. [1955] and in a report prepared under CCIR Resolution No. 1 [Geneva 1963c]. The loss factor l_{erv} was successfully

determined in one case by measuring the power w_{tv} radiated from a loss-free target transmitting antenna and calculating the transmission loss between the target transmitting antenna and the receiving antenna. There appears to be no way of directly measuring either l_{erv} or l_{etv} without calculating some quantity such as the radiation resistance or the transmission loss. In the case of reception with a unidirectional rhombic terminated in its characteristic impedance, l_{erv} could theoretically be greater than 2 [Harper, 1941], since nearly half the received power is dissipated in the terminating impedance and some is dissipated in the ground. Measurements were made by Christiansen [1947] on single and multiple wire units and arrays of rhombics. The ratio of power lost in the termination to the input power varied with frequency and was typically less than 3 db.

For the frequency band ν_l to ν_m it is convenient to define the effective loss factors L_{er} and L_{et} as follows:

$$L_{er} = 10 \log \frac{\int_{\nu_l}^{\nu_m} (d w_{av}/d\nu) d\nu}{\int_{\nu_l}^{\nu_m} (d w'_{av}/d\nu) d\nu} \text{ db} \quad (\text{II. 8})$$

$$L_{et} = 10 \log \frac{\int_{\nu_l}^{\nu_m} (d w'_{tv}/d\nu) d\nu}{\int_{\nu_l}^{\nu_m} (d w_{tv}/d\nu) d\nu} \text{ db} \quad (\text{II. 9})$$

The limits ν_l and ν_m on the integrals (II. 8) and (II. 9) are chosen to include essentially all of the wanted signal modulation side bands, but ν_l is chosen to be sufficiently large and ν_m sufficiently small to exclude any appreciable harmonic or other unwanted radiation emanating from the wanted signal transmitting antenna.

II.2 Propagation Loss and Field Strength

This subsection defines terms that are most useful at radio frequencies lower than those where tropospheric propagation effects are dominant.

Repeating the definitions of r and r' used in subsection II.1, and introducing the new parameter r_f :

- $r_{t,r}$ = antenna radiation resistance,
- $r'_{t,r}$ = resistance component of antenna input impedance,
- r_{ft}, r_{fr} = antenna radiation resistance in free space,

where subscripts t and r refer to the transmitting antenna and receiving antenna, respectively. Next define

$$L_{et} = 10 \log (r'_{t,t}/r_{t,t}), \quad L_{er} = 10 \log (r'_{r,r}/r_{r,r}) \quad (\text{II.10})$$

$$L_{ft} = 10 \log (r'_{t,ft}/r_{t,ft}), \quad L_{fr} = 10 \log (r'_{r,fr}/r_{r,fr}) \quad (\text{II.11})$$

$$L_{rt} = 10 \log (r_{t,ft}/r_{t,t}) = L_{ft} - L_{et} \quad (\text{II.12})$$

$$L_{rr} = 10 \log (r_{r,fr}/r_{r,r}) = L_{fr} - L_{er} \quad (\text{II.13})$$

[Actually, (II.8) and (II.9) define L_{et} and L_{er} while (II.10) defined $r_{t,t}$ and $r_{r,r}$, given $r'_{t,t}$ and $r'_{r,r}$].

Propagation loss first defined by Wait [1959] is defined by the CCIR [1963a] as

$$L_p = L_s - L_{ft} - L_{fr} = L - L_{rt} - L_{rr} \text{ db.} \quad (\text{II.14})$$

Basic propagation loss is

$$L_{pb} = L_p + G_p. \quad (\text{II.15})$$

Basic propagation loss in free space is the same as the basic transmission loss in free space, L_{bf} , defined by (II.74).

The system loss L_s defined by (2.1) is a measurable quantity, while transmission loss L , path loss L_o , basic transmission loss L_b , attenuation relative to free space A , propagation loss L_p , and the field strength E are derived quantities, which in general require a theoretical calculation of $L_{et, er}$ and/or $L_{ft, fr}$ as well as a theoretical estimate of the loss in path antenna gain L_{gp} .

The following paragraphs explain why the concepts of effective power, and an equivalent plane wave field strength are not recommended for reporting propagation data.

A half-wave antenna radiating a total of w_t watts produces a free space field intensity equal to

$$s_o = 1.64 w_t / (4\pi r^2) \text{ watts/km}^2 \quad (\text{II. 16})$$

at a distance r kilometers in its equatorial plane, where the directive gain is equal to its maximum value 1.64, or 2.15 db. The field is linearly polarized in the direction of the antenna. In general, the field intensity s_p at a point \vec{r} in free space and associated with the principal polarization for an antenna is

$$s_p(\vec{r}) = w_t g_p(\hat{r}) / (4\pi r^2) \text{ watts/km}^2 \quad (\text{II. 17})$$

as explained in a later subsection. In (II. 17), $\vec{r} = r \hat{r}$ and $g_p(\hat{r})$ is the principal polarization directive gain in the direction \hat{r} . A similar relation holds for the field intensity $s_c(\vec{r})$ associated with the cross-polarized component of the field.

Effective radiated power is associated with a prescribed polarization for a test antenna and is determined by comparing s_o as calculated using a field intensity meter or standard signal source with s_p as measured using the test antenna:

$$\text{Effective Radiated Power} = W_t + 10 \log(s_p/s_o) = W_t + G_{pt}(\hat{r}_1) - 2.15 \text{ dbw} \quad (\text{II. 18})$$

where $G_{pt}(\hat{r}_1)$ is the principal polarization directive gain relative to a half-wave dipole in the direction \hat{r}_1 towards the receiving antenna in free space, and in general is the initial direction of the most important propagation path to the receiver.

These difficulties in definition, together with those which sometimes arise in attempting to separate characteristics of an antenna from those of its environment, make the effective radiated power an inferior parameter, compared with the total radiated power W_t , which can be more readily measured. The following equation, with W_t determined from (II. 18), may be used to convert reported values of Effective Radiated Power to estimates of the transmitter power output W_{lt} when transmission line and mismatch losses L_{lt} and the power radiation efficiency $1/l_{et}$ are known:

$$W_{lt} = W_t + L_{lt} = W_t + L_{et} + L_{lt} \text{ dbw} \quad (\text{II. 19})$$

The electromagnetic field is a complex vector function in space and time, and information about amplitude, polarization, and phase is required to describe it. A real antenna responds to the total field surrounding it, rather than to E , which corresponds to the r. m. s. amplitude of the usual "equivalent" electromagnetic field, defined at a single point and for a specified polarization.

Consider the power averaged over each half cycle as the "instantaneous" available signal power, w_{π}

$$w_{\pi} = v^2/R_v \text{ watts}$$

where v is the r.m.s. signal voltage and R_v is the real part of the impedance of the receiving antenna, expressed in ohms. The signal power w_{π} available from an actual receiving antenna is a directly measurable quantity.

The field strength and power flux density, on the other hand, cannot be measured directly, and both depend on the environment. In certain idealized situations the relationship of field strength e , and power flux density, s , to the available power may be expressed as

$$s = e^2/z = w_{\pi} 4\pi/(g\lambda^2) \text{ watts/m}^2$$

where e is the r.m.s. electric field strength in volts/m, z is the impedance in free space in ohms, λ is the free space wavelength in meters and g is the maximum gain of the receiving antenna.

The common practice of carefully calibrating a field strength measuring system in an idealized environment and then using it in some other environment may lead to appreciable errors, especially when high gain receiving antennas are used.

For converting reported values of E in dbu to estimates of W_{ft} or estimates of the available power W_{lr} at the input to a receiver, the following relationships may be useful:

$$W_{ft} = E + L_{ft} + L_{ft} - G_t + L_{pb} - 20 \log f - 107.22 \text{ dbw} \quad (\text{II. 20})$$

$$W_{lr} = E - L_{lr} - L_{fr} + G_r - L_{gp} - 20 \log f - 107.22 \text{ dbw} \quad (\text{II. 21})$$

$$W_{lr} = W'_a - L_{lr} = W_a - L_{er} - L_{lr} \text{ dbw} \quad (\text{II. 22})$$

In terms of reported values of field strength E_{1kw} in dbu per kilowatt of effective radiated power, estimates of the system loss, L_s , basic propagation loss L_{pb} , or basic transmission loss L_b may be derived from the following equations,

$$L_s = 139.37 + L_{et} + L_{fr} - G_p + G_t - G_{pt}(\hat{r}_1) + 20 \log f - E_{1kw} \text{ db} \quad (\text{II. 23})$$

$$L_{pb} = 139.37 - L_{rt} + G_t - G_{pt}(\hat{r}_1) + 20 \log f - E_{1kw} \text{ db} \quad (\text{II. 24})$$

$$L_b = 139.37 + L_{rr} + G_t - G_{pt}(\hat{r}_1) + 20 \log f - E_{1kw} \text{ db} \quad (\text{II. 25})$$

provided that estimates are available for all of the terms in these equations.

For an antenna whose radiation resistance is unaffected by the proximity of its environment, $L_{rt} = L_{rr} = 0$ db, $L_{ft} = L_{et}$, and $L_{fr} = L_{er}$. In other cases, especially important for frequencies less than 30 MHz with antenna heights commonly used, it is often assumed that $L_{rt} = L_{rr} = 3.01$ db, $L_{ft} = L_{et} + 3.01$ db, and $L_{fr} = L_{er} + 3.01$ db, corresponding to the assumption of short vertical electric dipoles above a perfectly-conducting infinite plane. At low and very low frequencies, L_{et} , L_{er} , L_{ft} , and L_{fr} may be very large. Propagation curves at HF and lower frequencies may be given in terms of L_p or L_{pb} so that it is not necessary to specify L_{et} and L_{er} .

Naturally, it is better to measure L_s directly than to calculate it using (II. 23). It may be seen that the careful definition of L_s , L_p , L , or L_o is simpler and more direct than the definition of L_b , L_{pb} , A , or E .

The equivalent free-space field strength E_o in dbu for one kilowatt of effective radiated power is obtained by substituting $W_{ft} = W_t = \text{Effective Radiated Power} = 30$ dbw, $G_{pt}(\hat{r}_1) = G_t = 2.15$ db, $L_{ft} = L_{er} = 0$ db, and $L_{pb} = L_{bf}$ in (II.18) - (II.20), where L_{bf} is given by (2.16):

$$E_o = 106.92 - 20 \log d \quad \text{dbu/kw} \quad (\text{II. 26})$$

where r in (2.16) has been replaced by d in (II.26). Thus e_o is 222 millivolts per meter at one kilometer or 138 millivolts per meter at one mile. In free space, the "equivalent inverse distance field strength", E_I , is the same as E_o . If the antenna radiation resistances r_t and r_r are equal to the free space radiation resistances r_{ft} and r_{fr} , then (II. 25) provides the following relationship between E_{1kw} and L_b with $G_{pt}(\hat{r}_1) = G_t$:

$$E_{1kw} = 139.37 + 20 \log f - L_b \quad \text{dbu/kw} \quad (\text{II. 27})$$

Consider a short vertical electric dipole above a perfectly-conducting infinite plane, with an effective radiated power = 30 dbw, $G_t = 1.76$ db, and $L_{rr} = 3.01$ db. From (II.18) $W_t = 30.39$ dbw, since $G_{pt}(\hat{r}_1) = 1.76$ db. Then from (II. 26) the equivalent inverse distance field is

$$E_I = E_o + L_{rt} + L_{rr} = 109.54 - 20 \log d \quad \text{dbu/kw} \quad (\text{II. 28})$$

corresponding to $e_I = 300$ mv/m at one kilometer, or $e_I = 186.4$ mv/m at one mile. In this situation, the relationship between E_{1kw} and L_b is given by (II. 25) as

$$E_{1kw} = 142.38 + 20 \log f - L_b \quad \text{dbu/kw} \quad (\text{II. 29})$$

The foregoing suggests the following general expressions for the equivalent free space field strength E_o and the equivalent inverse distance field E_I :

$$E_o = (W_t - L_{rt} + G_t) - 20 \log d + 74.77 \quad \text{dbu} \quad (\text{II. 30})$$

$$E_I = E_o + L_{rt} + L_{rr} \quad \text{dbu} \quad (\text{II. 31})$$

Note that L_{rt} in (II. 30) is not zero unless the radiation resistance of the transmitting antenna in its actual environment is equal to its free space radiation resistance. The definition of "attenuation relative to free space" given by (2.20) as the basic transmission loss relative to that in free space, may be restated as

$$A = L_b - L_{bf} = L - L_f = E_I - E \quad \text{db} \quad (\text{II. 32})$$

Alternatively, attenuation relative to free space, A_t , might have been defined (as it sometimes is) as basic propagation loss relative to that in free space:

$$A_t = L_{pb} - L_{bf} = A - L_{rt} - L_{rr} = E_o - E \quad \text{db} \quad (\text{II. 33})$$

For frequencies and antenna heights where these definitions differ by as much as 6 db, caution should be used in reporting data. For most paths using frequencies above 50 MHz, $L_{rt} + L_{rr}$ is negligible, but caution should again be used if the loss in path antenna gain L_{gp} is not negligible. It is then important not to confuse the "equivalent" free space loss L_f given by (2.19) with the loss in free space given by (2.18).

II.3 MULTIPATH COUPLING LOSS

Ordinarily, to minimize the transmission loss between two antennas, they are oriented to take advantage of maximum directive gains (directivity) and the polarizations are matched. This maximizes the path antenna gain. With a single uniform plane wave incident upon a receiving antenna, there will be a reduction in the power transferred if the antenna beam is not oriented for maximum free space gain. If the polarization of the receiving antenna is matched to that of the incident wave, this loss in path antenna gain is due to "orientation coupling loss", and if there is a polarization mismatch, there will be an additional "polarization coupling loss". In general, more than one plane wave will be incident upon a receiving antenna from a single source because of reflection, diffraction, or scattering by terrain or atmospheric inhomogeneities. Mismatch between the relative phases of these waves and the relative phases of the receiving antenna response in different directions will contribute to a "multipath coupling loss" which will include orientation, polarization, and phase mismatch effects. If multipath propagation involves non-uniform waves whose amplitudes, polarizations, and phases can only be described statistically, the corresponding loss in path antenna gain will include "antenna-to-medium coupling loss", a statistical average of phase incoherence effects.

This part of the annex indicates how multipath coupling loss may be calculated when incident waves are plane and uniform with known phases, and when the directivity, polarization, and phase response of the receiving antenna are known for every direction. It is assumed that the radiation resistance of the receiving antenna is unaffected by its environment, and that the electric and magnetic field vectors of every incident wave are perpendicular to each other and perpendicular to the direction of propagation.

II.3.1 Representation of Complex Vector Fields

Studying the response of a receiving antenna to coherently phased plane waves with several different directions of arrival, it is convenient to locate the receiving antenna at the center of a coordinate system. A radio ray traveling a distance r from a transmitter to the receiver may be refracted or reflected so that its initial and final directions are different. If $-\hat{f}$ is the direction of propagation at the receiver, $\vec{r} = \hat{f} r$ is the vector distance from the receiver to the transmitter if the ray path is a straight line, but not otherwise.

A paper by Kales [1951] shows how the amplitude, phase, and polarization of a uniform, monochromatic, elliptically polarized and locally plane wave may be expressed with the aid of complex vectors. For instance, such a wave may be expressed as the real part of the sum of two linearly polarized complex plane waves $\sqrt{2} \vec{e}_r \exp(i\tau)$ and $i\sqrt{2} \vec{e}_i \exp(i\tau)$. These components are in time phase quadrature and travel in the same direction $-\hat{f}$, where $i = \sqrt{-1}$ and \vec{e}_r and \vec{e}_i are real vectors perpendicular to \hat{f} . The vector $\vec{e}_r + i\vec{e}_i$ is then a complex vector. Field strengths are denoted in volts/km (10^3 microvolts per meter) and field intensities in watts/km² (10^{-3} milliwatts per square meter), since all lengths are in kilometers.

The time-varying phase

$$\tau = k(ct - r) \quad (\text{II. 34})$$

is a function of the free-space wavelength λ , the propagation constant $k = 2\pi/\lambda$, the free-space velocity of radio waves $c = 299792.5 \pm 0.3$ km/sec, the time t at the radio source, and the length of a radio ray between the receiver and the source.

Figure II-1 illustrates three sets of coordinates which are useful in studying the phase and polarization characteristics associated with the radiation pattern or response pattern of an antenna. Let $\vec{r} = fr$ represent the vector distance between the antenna and a distant point, specified either in terms of a right-handed cartesian unit vector coordinate system $\hat{x}_0, \hat{x}_1, \hat{x}_2$ or in terms of polar coordinates r, θ, ϕ :

$$\vec{r} = fr = \hat{x}_0 x_0 + \hat{x}_1 x_1 + \hat{x}_2 x_2, \quad r^2 = x_0^2 + x_1^2 + x_2^2 \quad (\text{II. 35a})$$

$$x_0 = r \cos \theta, \quad x_1 = r \sin \theta \cos \phi, \quad x_2 = r \sin \theta \sin \phi \quad (\text{II. 35b})$$

$$\hat{f} = f(\theta, \phi) = \hat{x}_0 \cos \theta + (\hat{x}_1 \cos \phi + \hat{x}_2 \sin \phi) \sin \theta. \quad (\text{II. 35c})$$

As a general rule, either of two antennas separated by a distance r is in the far field or radiation field of the other antenna if $r > 2D^2/\lambda$, where D is the largest linear dimension of either antenna.

The amplitude and polarization of electric field vectors \vec{e}_θ and \vec{e}_ϕ , perpendicular to each other and to \hat{f} , is often calculated or measured to correspond to the right-handed cartesian unit vector coordinate system $\hat{f}, \hat{e}_\theta, \hat{e}_\phi$ illustrated in figure II-1. The unit vector \hat{e}_ϕ is perpendicular to \hat{f} and \hat{x}_0 , and \hat{e}_θ is perpendicular to \hat{e}_ϕ and \hat{f} . In terms of vector cross-products:

$$\hat{e}_\phi = (\hat{f} \times \hat{x}_0) / \sin \theta = \hat{x}_1 \sin \phi - \hat{x}_2 \cos \phi \quad (\text{II. 36a})$$

$$\hat{e}_\theta = \hat{e}_\phi \times \hat{f} = (\hat{x}_0 - \hat{f} \cos \theta) / \sin \theta. \quad (\text{II. 36b})$$

The directive gain g , a scalar, may be expressed as the sum of directive gains g_θ and g_ϕ associated with polarization components $\vec{e}_\theta \equiv \hat{e}_\theta e_\theta$ and $\vec{e}_\phi \equiv \hat{e}_\phi e_\phi$, where the coefficients e_θ and e_ϕ are expressed in volts/km:

$$g = g_\theta + g_\phi. \quad (\text{II. 37})$$

Subscripts t and r are used to refer to the gains g_t and g_r of transmitting and receiving antennas, while g is the ratio of the available mean power flux density and e_0^2/η_0 , where

e_o as defined by (II.38) is the free space field strength at a distance r in kilometers from an isotropic antenna radiating w_t watts:

$$e_o = [\eta_o w_t / (4\pi r^2)]^{1/2} \text{ volts/km.} \quad (\text{II. 38})$$

Here, $\eta_o = 4\pi c \cdot 10^{-7} = 376.7304 \pm 0.0004$ ohms is the characteristic impedance of free space. The maximum amplitudes of the θ and ϕ components of a radiated or incident field are $|\vec{e}_\theta| \sqrt{Z}$ and $|\vec{e}_\phi| \sqrt{Z}$, where

$$|\vec{e}_\theta| = e_\theta = e_o g_\theta^{1/2} \text{ volts/km,} \quad |\vec{e}_\phi| = e_\phi = e_o g_\phi^{1/2} \text{ volts/km,} \quad (\text{II. 39})$$

If phases τ_θ and τ_ϕ are associated with the electric field components \vec{e}_θ and \vec{e}_ϕ , which are in phase quadrature in space but not necessarily in time, the total complex wave at any point \vec{r} is

$$\sqrt{Z} (\vec{e}_r + i\vec{e}_i) \exp(i\tau) = \sqrt{Z} [\vec{e}_\theta \exp(i\tau_\theta) + \vec{e}_\phi \exp(i\tau_\phi)] \exp(i\tau). \quad (\text{II. 40})$$

From this expression and a knowledge of $\vec{e}_{\theta, \phi}$, $\tau_{\theta, \phi}$, we may determine the real and imaginary components \vec{e}_r and \vec{e}_i , which are in phase quadrature in time but not necessarily in space:

$$\vec{e}_r \equiv \hat{e}_r e_r = \vec{e}_\theta \cos \tau_\theta + \vec{e}_\phi \cos \tau_\phi \quad (\text{II. 41a})$$

$$\vec{e}_i \equiv \hat{e}_i e_i = \vec{e}_\theta \sin \tau_\theta + \vec{e}_\phi \sin \tau_\phi, \quad (\text{II. 41b})$$

The next section of this annex introduces components of this wave which are in phase quadrature in both time and space.

II. 3.2 Principal and Cross-Polarization Components

Principal and cross-polarization components of an incident complex wave $\sqrt{2} (\vec{e}_r + i\vec{e}_i) \exp(i\tau)$ may be defined in terms of a time-independent phase τ_1 which is a function of \vec{r} [Kales, 1951]. If we write

$$\vec{e}_r + i\vec{e}_i = (\vec{e}_1 + i\vec{e}_2) \exp(i\tau_1) \quad (\text{II. 42})$$

and solve for the real and imaginary components of the complex vector $\vec{e}_1 + i\vec{e}_2$, we find that

$$\vec{e}_1 = \hat{e}_1 e_1 = \vec{e}_r \cos \tau_1 + \vec{e}_i \sin \tau_1 \quad (\text{II. 43a})$$

$$\vec{e}_2 = \hat{e}_2 e_2 = \vec{e}_i \cos \tau_1 - \vec{e}_r \sin \tau_1. \quad (\text{II. 43b})$$

Whichever of these vectors has the greater magnitude is the principal polarization component \vec{e}_p , and the other is the orthogonal cross-polarization component \vec{e}_c :

$$e_1^2 = e_r^2 \cos^2 \tau_1 + e_i^2 \sin^2 \tau_1 + \vec{e}_r \cdot \vec{e}_i \sin(2\tau_1) \quad (\text{II. 44a})$$

$$e_2^2 = e_r^2 \sin^2 \tau_1 + e_i^2 \cos^2 \tau_1 - \vec{e}_r \cdot \vec{e}_i \sin(2\tau_1). \quad (\text{II. 44b})$$

The phase angle τ_1 is determined from the condition that $\vec{e}_1 \cdot \vec{e}_2 = 0$:

$$\tan(2\tau_1) = 2\vec{e}_r \cdot \vec{e}_i / (e_r^2 - e_i^2). \quad (\text{II. 45})$$

Any incident plane wave, traveling in a direction $-\hat{f}$ is then represented as the real part of the complex wave given by

$$\sqrt{2} \vec{e} \exp[i(\tau + \tau_1)] \equiv \sqrt{2} (\vec{e}_p + i\vec{e}_c) \exp[i(\tau + \tau_1)]. \quad (\text{II. 46})$$

The principal and cross-polarization directions \hat{e}_p and \hat{e}_c are chosen so that their vector product is a unit vector in the direction of propagation:

$$\hat{e}_p \times \hat{e}_c = -\hat{f}. \quad (\text{II. 47})$$

A bar is used under the symbol for the complex vector $\bar{e} \equiv \bar{e}_p + i\bar{e}_c$ in (II.46) to distinguish it from real vectors such as \bar{e}_θ , \bar{e}_ϕ , \bar{e}_r , \bar{e}_i , \bar{e}_p , and \bar{e}_c . The absolute values of the vector coefficients e_p and e_c may be found using (II.44).

As the time t at the transmitter or the time τ at the receiver increases, the real vector component of (II.46), or "polarization vector",

$$\sqrt{2} [\bar{e}_p \cos(\tau + \tau_1) - \bar{e}_c \sin(\tau + \tau_1)]$$

describes an ellipse in the plane of the orthogonal unit vectors $\hat{e}_p = \bar{e}_p / e_p$ and $\hat{e}_c = \bar{e}_c / e_c$. Looking in the direction of propagation $-r(\theta, \phi)$ with e_p and e_c both positive or both negative, we see a clockwise rotation of the polarization vector as τ increases.

Right-handed polarization is defined by the IRE or IEEE and in CCIR Report 321 [1963m] to correspond to a clockwise rotation of a polarization ellipse, looking in the direction of propagation with r fixed and t or τ increasing. This is opposite to the definition used in classical physics.

The "axial ratio" e_c / e_p of the polarization ellipse of an incident plane wave $\sqrt{2} \bar{e} \exp[i(\tau + \tau_0)]$ is denoted here as

$$a_x \equiv e_c / e_p \quad (\text{II.48})$$

and may be either positive or negative depending on whether the polarization of the incident wave is right-handed or left-handed. The range of possible values for a_x is -1 to $+1$.

II. 3. 3 Unit Complex Polarization Vectors

If the receiving antenna were a point source of radio waves, it would produce a plane wave $\sqrt{Z} \vec{e}_r \exp[i(\tau + \tau_r)]$ at a point \vec{r} in free space. The receiving pattern of such an antenna as it responds to an incident plane wave $\sqrt{Z} \vec{e} \exp[i(\tau + \tau_i)]$ traveling in the opposite direction $-\hat{f}$ is proportional to the complex conjugate of $\vec{e}_r \exp(i\tau_r)$ [S. A. Schelkunoff and H. T. Friis, 1952]:

$$[\vec{e}_r \exp(i\tau_r)]^* = (\vec{e}_{pr} - i\vec{e}_{cr}) \exp(-i\tau_r). \quad (\text{II. 49})$$

The axial ratio e_{cr}/e_{pr} of the type of wave that would be radiated by a receiving antenna is defined for propagation in the direction \hat{f} . An incident plane wave, however, is propagating in the direction $-\hat{f}$, and by definition the sense of polarization of an antenna used for reception is opposite to the sense of polarization when the antenna is used as a radiator. The polarization associated with a receiving pattern is right-handed or left-handed depending on whether a_{xr} is positive or negative, where

$$a_{xr} \equiv -e_{cr}/e_{pr}, \quad e_{cr} = -e_{pr} a_{xr}. \quad (\text{II. 50})$$

The amplitudes $|e_{pr}|$ and $|e_{cr}|$ of the principal and cross-polarization field components \vec{e}_{pr} and \vec{e}_{cr} are proportional to the square roots of principal and cross-polarization directive gains g_{pr} and g_{cr} , respectively. It is convenient to define a unit complex polarization vector $\hat{\underline{f}}_r$ which contains all the information about the polarization response associated with a receiving pattern:

$$\hat{\underline{f}}_r = (\hat{e}_{pr} + i\hat{e}_{cr} a_{xr}) (1 + a_{xr}^2)^{-1/2} \quad (\text{II. 51})$$

$$a_{xr}^2 = g_{cr}/g_{pr}. \quad (\text{II. 52})$$

The directions \hat{e}_{pr} and \hat{e}_{cr} are chosen so that

$$\hat{e}_{pr} \times \hat{e}_{cr} = \hat{f}. \quad (\text{II. 53})$$

In a similar fashion, the axial ratio a_x defined by (II. 48) and the orientations \hat{e}_p and \hat{e}_c of the principal and cross-polarization axes of the polarization ellipse completely describe the state of polarization of an incident wave $\sqrt{Z} \vec{e} \exp[i(\tau + \tau_i)]$, and its direction of propagation $-\hat{f} = \hat{e}_p \times \hat{e}_c$. The unit complex polarization vector for the incident wave is

$$\hat{p} = \vec{e} / |\vec{e}| = (\hat{e}_p + i\hat{e}_c a_x) (1 + a_x^2)^{-1/2}. \quad (\text{II. 54})$$

The magnitude of a complex vector $\vec{e} = \vec{e}_p + i\vec{e}_c$ is the square root of the product of \vec{e} and its complex conjugate $\vec{e}_p - i\vec{e}_c$:

$$|\vec{e}| = (\vec{e} \cdot \vec{e}^*)^{1/2} = (e_p^2 + e_c^2)^{1/2} \quad \text{volts/km.} \quad (\text{II. 55})$$

II. 3.4 Power Flux Densities

The coefficients e_p and e_c of the unit vectors \hat{e}_p and \hat{e}_c are chosen to be r.m.s. values of field strength, expressed in volts/km, and the mean power flux densities s_p and s_c associated with these components are

$$s_p = e_p^2 / \eta_0 \quad \text{watts/km}^2, \quad s_c = e_c^2 / \eta_0 \quad \text{watts/km}^2, \quad (\text{II. 56})$$

The corresponding principal and cross-polarization directive gains g_p and g_c are

$$g_p = 4\pi r^2 s_p / w_t, \quad g_c = 4\pi r^2 s_c / w_t \quad (\text{II. 57})$$

where w_t is the total power radiated from the transmitting antenna. This is the same relation as that expressed by (II. 39) between the gains g_θ , g_ϕ , and the orthogonal polarization components \vec{e}_θ and \vec{e}_ϕ .

The total mean power flux density s at any point where \vec{e} is known to be in the radiation field of the transmitting antenna and any reradiating sources is

$$\begin{aligned} s &= |\vec{e}|^2 / \eta_0 = g e_o^2 / \eta_0 = s_p + s_c = (e_p^2 + e_c^2) / \eta_0 \\ &= (e_r^2 + e_i^2) / \eta_0 = (e_\theta^2 + e_\phi^2) / \eta_0 \quad \text{watts/km}^2 \end{aligned} \quad (\text{II. 58a})$$

$$g = g_p + g_c = g_\theta + g_\phi = 4\pi r^2 s / p_t = s \eta_0 / e_o^2 \quad (\text{II. 58b})$$

where e_o is given by (II. 38). The power flux density s is proportional to the transmitting antenna gain g_t , but in general g is not equal to g_t as there may be a fraction a_p of energy absorbed along a ray path or scattered out of the path. We therefore write

$$g \equiv g_p (1 + a_x^2) = a_p g_{pt} (1 + a_x^2) = a_p g_t. \quad (\text{II. 59})$$

The path absorption factor a_p can also be useful in approximating propagation mechanisms which are more readily described as a sum of modes than by using geometric optics. For instance, in the case of tropospheric ducting a single dominant TEM mode may correspond theoretically to an infinite number of ray paths, and yet be satisfactorily approximated by a single great-circle ray path if a_p is appropriately defined. In such a case, a_p will occasionally be greater than unity rather than less.

Orienting a receiving dipole for maximum reception to determine s_p and for minimum reception to determine s_c will also determine \hat{e}_p and \hat{e}_c , except in the case of circular polarization, where the direction of \hat{e}_p in the plane normal to \vec{r} is arbitrary. In the general case where $|a_x| < 1$, either of two opposite directions along the line of principal polarization is equally suitable for \hat{e}_p .

Reception with a dipole will not show the sense of polarization. Right-handed and left-handed circularly polarized receiving antennas will in theory furnish this information, since \vec{e} may also be written to correspond to the difference of right-handed and left-handed circularly polarized waves which are in phase quadrature in time and space:

$$\vec{e} \equiv (\hat{e}_p + i\hat{e}_c) \left(\frac{e_p + e_c}{2} \right) - i(\hat{e}_c - i\hat{e}_p) \left(\frac{e_p - e_c}{2} \right). \quad (\text{II. 60})$$

The mean power flux densities s_r and s_l associated with right-handed and left-handed polarizations are

$$s_r = (e_p + e_c)^2 / (2\eta_0) \text{ watts/km}^2 \quad (\text{II. 61a})$$

$$s_l = (e_p - e_c)^2 / (2\eta_0) \text{ watts/km}^2 \quad (\text{II. 61b})$$

so the sense of polarization may be determined by whether s_r/s_l is greater than or less than unity. The flux densities s_r and s_l are equal only for linear polarization, where $e_c = 0$.

II. 3. 5 Polarization Efficiency

The polarization efficiency for a transfer of energy from a single plane wave to the terminals of a receiving antenna at a given radio frequency may be expressed as a function of the unit complex polarization vectors defined by (II.51) and (II.54) and the angle ψ_p between principal polarization directions associated with \vec{e}_x and \vec{e}_{xr} . This polarization efficiency is

$$|\hat{p}_x \cdot \hat{p}_{xr}|^2 = \frac{\cos^2 \psi_p (a_x a_{xr} + 1)^2 + \sin^2 \psi_p (a_x + a_{xr})^2}{(a_x^2 + 1)(a_{xr}^2 + 1)} \quad (\text{II.62})$$

where

$$\hat{e}_p \cdot \hat{e}_{pr} = -\hat{e}_c \cdot \hat{e}_{cr} = \cos \psi_p, \quad \hat{e}_p \cdot \hat{e}_{cr} = \hat{e}_{pr} \cdot \hat{e}_c = \sin \psi_p. \quad (\text{II.63})$$

As noted in section 2 following (2.11), any receiving antenna is completely "blind" to an incoming plane wave $\sqrt{2} \vec{e} \exp[i(\tau + \tau_1)]$ which has a sense of polarization opposite to that of the receiving antenna if the eccentricities of the polarization ellipses are the same ($|a_x| = |a_{xr}|$) and if the principal polarization direction \hat{e}_p of the incident wave is perpendicular to \hat{e}_{pr} . In such a case, $\cos \psi_p = 0$, $a_x = -a_{xr}$, and (II.62) shows that the polarization efficiency $|\hat{p}_x \cdot \hat{p}_{xr}|^2$ is zero. As an interesting special case, reflection of a circularly polarized wave incident normally on a perfectly conducting sheet will change the sense of polarization so that the antenna which radiates such a wave cannot receive the reflected wave. In such a case $a_x = -a_{xr} = \pm 1$, so that $|\hat{p}_x \cdot \hat{p}_{xr}|^2 = 0$ for any value of ψ_p .

On the other hand, the polarization efficiency given by (II.62) is unity and a maximum transfer of power will occur if $a_x = a_{xr}$ and $\psi_p = 0$, that is, if the sense, eccentricity, and principal polarization direction of the receiving antenna match the sense, eccentricity, and principal polarization direction of the incident wave.

For transmission in free space, antenna radiation efficiencies, their directive gains, and the polarization coupling efficiency are independent quantities, and all five must be maximized for a maximum transfer of power between the antennas. A reduction in either one of the directive gains $g(-f)$ and $g_r(f)$ or a reduction in the polarization efficiency $|\hat{p}_x \cdot \hat{p}_{xr}|^2$ will reduce the transfer of power between two antennas.

With each plane wave incident on the receiving antenna there is associated a ray of length r from the transmitter, an initial direction of radiation, and the radiated wave $\vec{e}_t \exp[i(\tau + \tau_t)]$ which would be found in free space at this distance and in this direction. When it is practical to separate antenna characteristics from environmental and path characteristics, it is assumed that the antenna phase response τ_t , like τ_r , is a characteristic of the antenna and its environment and that

$$\tau_i = \tau_t + \tau_p$$

(II. 64)

where τ_p is a function of the ray path and includes allowances for path length differences and diffraction or reflection phase shifts.

Random phase changes in either antenna, absorption and reradiation by the environment, or random fluctuations of refractive index in the atmosphere will all tend to fill in any sharp nulls in a theoretical free-space radiation pattern \vec{e} or \vec{e}_r . Also, it is not possible to have a complex vector pattern \vec{e}/r which is independent of r in the vicinity of antenna nulls unless the radiation field, proportional to $1/r$, dominates over the induction field, which is approximately proportional to $1/r^2$.

II. 3.6 Multipath Coupling Loss

Coherently phased multipath components from a single source may arrive at a receiving antenna from directions sufficiently different so that τ_i and τ_r vary significantly. It is then important to be able to add complex signal voltages at the antenna terminals. Let $n = 1, 2, \dots, N$ and assume N discrete plane waves incident on an antenna from a single source. The following expressions represent the complex open-circuit r.m.s. signal voltage v_n corresponding to a radio frequency ν cycles per second, a single incident plane wave $\sqrt{2} \vec{e}_{-n} \exp[i(\tau + \tau_{in})]$, a loss-free receiving antenna with a directivity gain g_{rn} and an effective absorbing area a_{en} , matched antenna and load impedances, and an input resistance r_ν which is the same for the antenna and its load:

$$v_n = (4r_\nu s_n a_{en})^{1/2} (\hat{p}_n \cdot \hat{p}_{rn}) \exp[i(\tau + \tau_{pn} + \tau_{tn} - \tau_{rn})] \text{ volts} \quad (\text{II. 65})$$

$$s_n = \left| \frac{\vec{e}_{-n}}{r_n} \right|^2 / \eta_0 = w_r a_{pn} g_{tn} / (4\pi r_n^2) \text{ watts/km}^2 \quad (\text{II. 66})$$

$$a_{en} = g_{rn} \lambda^2 / (4\pi) \text{ km}^2 \quad (\text{II. 67})$$

$$\hat{p}_n \cdot \hat{p}_{rn} = [(1 + a_{xn}^2)(1 + a_{xrn}^2)]^{-1/2} [(1 + a_{xn} a_{xrn}) \cos \psi_{pn} + i(a_{xn} + a_{xrn}) \sin \psi_{pn}]. \quad (\text{II. 68})$$

If the polarization of the receiving antenna is matched to that of the incident plane wave, then $a_{xn} = a_{xrn}$, $\psi_{pn} = 0$, $\hat{p}_n \cdot \hat{p}_{rn} = 1$, and

$$v_n = [4r_\nu w_r a_{pn} g_{tn} g_{rn} \lambda^2 / (4\pi r_n^2)]^{1/2} \exp[i(\tau + \tau_{pn} + \tau_{tn} - \tau_{rn})] \text{ volts.} \quad (\text{II. 69})$$

If the coefficient of the phasor in (II. 69) has the same value for two incident plane waves, but the values of $\tau_{in} - \tau_{rn}$ differ by π radians, the sum of the corresponding complex voltages is zero. This shows that the multipath coupling efficiency can theoretically be zero even when the beam orientation and polarization coupling are maximized. Adjacent lobes in a receiving antenna directivity pattern, for instance, may be 180° out of phase and thus cancel two discrete in-phase plane-wave components.

Equation (II. 3) shows the relation between the total open-circuit r.m.s. voltage

$$v_\nu = \left[\sum_{n=1}^N \sum_{m=1}^N v_n v_m^* \right]^{1/2} \text{ volts} \quad (\text{II. 70})$$

and the power w_a available at the terminals of a loss-free receiving antenna:

$$w_a = v_v^2 / (4 r_v) \text{ watts} . \quad (\text{II. 71})$$

In writing w_a for w_{av} in (II. 71), the subscript v has been suppressed, as with almost all of the symbols in this annex. Studying (II. 65) - (II. 68), (II. 70), and (II. 71), it is seen that the expression for w_a is symmetrical in the antenna gains g_p , g_{pr} , and $g_c = a_x^2 g_p$, $g_{cr} = a_{xr}^2 g_{pr}$, and that w_a is a linear function of these parameters, though v_v is not. From this follows a theorem of reciprocity, that the transmission loss $L = -10 \log (w_a / w_t)$ is the same if the roles of the transmitting and receiving antennas are reversed.

The basic transmission loss L_b is the system loss that would be expected if the actual antennas were replaced at the same locations by hypothetical antennas which are:

- (a) loss-free, so that $L_{ct} = L_{cr} = 0$ db. See (2.3).
- (b) isotropic, so that $g_t = g_r = 1$ in every direction important to propagation between the actual antennas.
- (c) free of polarization coupling loss, so that $|\hat{p} \cdot \hat{p}_r|^2 = 1$ for every locally plane wave incident at the receiving antenna.
- (d) isotropic in their phase response, so that $\tau_t = \tau_r = 0$ in every direction.

The available power w_{ab} corresponding to propagation between hypothetical isotropic antennas is then

$$w_{ab} = \frac{w_t \lambda^2}{(4\pi)^2} \sum_{\substack{n=1 \\ m=1}}^N \frac{(a_{pn} a_{pm})^{1/2} \cos(\tau_{pn} - \tau_{pm})}{r_n r_m} \quad (\text{II. 72})$$

The basic transmission loss L_b corresponding to these assumptions is

$$L_b = -10 \log (w_{ab} / w_t) = W_t - W_{ab} \text{ db} \quad (\text{II. 73})$$

The basic transmission loss in free space, L_{bf} , corresponds to $N = 1$, $a_{p1} = 1$, $\tau_{p1} = 0$, $r_1 = r$:

$$L_{bf} = -10 \log [\lambda / (4\pi r)]^2 = 32.45 + 20 \log f + 20 \log r \text{ db} \quad (\text{II. 74})$$

where f is in megacycles per second and r is in kilometers. Compare with (2.16).

As may be seen from the above relations, only a fraction s_e of the total flux density s_n per unit radiated power w_t contributes to the available received power w_a from N plane waves. While s_n is expressed in watts/km², s_e is expressed in watts/km² for each watt

of the power w_t radiated by a single source:

$$s_e = 4\pi w_a / (\lambda^2 w_t) \quad (\text{II. 75})$$

For each plane wave from a given source, $\vec{e}_n \exp(i\tau_{in})$ or $\hat{p}_{rn} \exp(-i\tau_{rn})$ may sometimes be regarded as a statistical variable chosen at random from a uniform distribution, with all phases from $-\pi$ to π equally likely. Then real power proportional to $|\vec{e}_n \cdot \vec{e}_{rn}^*|^2$ may be added at the antenna terminals, rather than the complex voltages defined by (II. 65)-(II. 68). For this case, the statistical "expected value" $\langle s_e \rangle$ of s_e is

$$\langle s_e \rangle = \sum_{n=1}^N a_{pn} g_{tn} g_{rn} |\hat{p}_n \cdot \hat{p}_{rn}|^2 / (4\pi r_n^2). \quad (\text{II. 76})$$

In terms of s_e , the transmission loss L is

$$L = 21.46 + 20 \log f - 10 \log s_e \quad \text{db.} \quad (\text{II. 77})$$

Substituting $\langle s_e \rangle$ for s_e in (II. 77), we would not in general obtain the statistical expected value $\langle L \rangle$ of L , since $\langle L \rangle$ is an ensemble average of logarithms, which may be quite different from the logarithm of the corresponding ensemble average $\langle s_e \rangle$. For this reason, median values are often a more practical measure of central tendency than "expected" values. With w_t and λ fixed, median values of s_e and L always obey the relation (II. 77), while average values of s_e and L often do not.

The remainder of this annex is concerned with a few artificial problems designed to show how these formulas are used and to demonstrate some of the properties of radiation and response patterns. In general, information is needed about antenna patterns only in the few directions which are important in determining the amplitude and fading of a tropospheric signal. Although section II. 3. 7 shows how a complex vector radiation or reception pattern may be derived from an integral over all directions, it is proposed that the power radiation efficiencies and the gains $g_r(\hat{f})$ or $g_t(-\hat{f})$ for actual antennas should be determined by measurements in a few critical directions using standard methods and a minimum of calculations.

II. 3. 7 Idealized Theoretical Antenna Patterns

Consider a point source of plane waves, represented by complex dipole moments in three mutually perpendicular directions, \hat{x}_0 , \hat{x}_1 , and \hat{x}_2 . These three unit vectors, illustrated in figure II. 1, define a right-handed system, and it is assumed that the corresponding elementary dipoles support r. m. s. currents of I_0 , I_1 , and I_2 amperes, respectively. The corresponding peak scalar current dipole moments are $\sqrt{2} I_m \ell$ ampere-kilometers, where $m = 0, 1, 2$, and the sum of the complex vector dipole moments $\hat{x}_m \sqrt{2} I_m \ell \exp(i \tau_m)$ may be expressed as follows:

$$\vec{a} = \vec{a}_1 + i \vec{a}_2 \quad (\text{II. 78a})$$

$$\vec{a}_1 = \sqrt{2} \ell (\hat{x}_0 c_0 + \hat{x}_1 c_1 + \hat{x}_2 c_2), \quad \vec{a}_2 = \sqrt{2} \ell (\hat{x}_0 s_0 + \hat{x}_1 s_1 + \hat{x}_2 s_2) \quad (\text{II. 78b})$$

$$I^2 = I_0^2 + I_1^2 + I_2^2, \quad c_m = (I_m / I) \cos \tau_m, \quad s_m = (I_m / I) \sin \tau_m, \quad m = 0, 1, 2. \quad (\text{II. 79})$$

Here, τ_0 , τ_1 , and τ_2 represent initial phases of the currents supported by the elementary dipoles. The time phase factor is assumed to be $\exp(ikct)$.

Using the same unit vector coordinate system to represent the vector distance \vec{r} from this idealized point source to a distant point:

$$\vec{r} = \hat{x}_0 x_0 + \hat{x}_1 x_1 + \hat{x}_2 x_2 = \hat{f} r \quad (\text{II. 80})$$

where x_0 , x_1 , and x_2 are given by (II. 35b) as functions of r , θ , ϕ . The complex wave at \vec{r} due to any one of the elementary dipoles is polarized in a direction

$$\hat{r} \times (\hat{x}_m \times \hat{f}) = \hat{x}_m - \hat{f} x_m / r \quad (\text{II. 81})$$

which is perpendicular to the propagation direction \hat{f} and in the plane of \hat{x}_m and \hat{f} . The total complex wave at \vec{r} may be represented in the form given by (II. 41):

$$\begin{aligned} \sqrt{2} \vec{e}(\vec{r}) \exp(i \tau) &= \sqrt{2} (\vec{e}_r + i \vec{e}_i) \exp(i \tau) = \sqrt{2} (\vec{e}_p + i \vec{e}_c) \exp[i(\tau + \tau_t)] \\ &= [\hat{f} \times (\vec{a} \times \hat{f})] [\eta_0 / (2\lambda r)] \exp(i \tau) \end{aligned} \quad (\text{II. 82})$$

$$\tau = k(ct - r) + \pi/4 \quad (\text{II. 83})$$

$$\sqrt{2} \vec{e}_r = [\vec{a}_1 - \hat{f}(\vec{a}_1 \cdot \hat{f})] \eta_0 / (2\lambda r) \text{ volts/km} \quad (\text{II. 84a})$$

$$\sqrt{2} \vec{e}_i = [\vec{a}_2 - \hat{r}(\vec{a}_2 \cdot \hat{r})] \eta_0 / (2\lambda r) \text{ volts/km.} \quad (\text{II. 84b})$$

The total mean power flux density $s(\vec{r})$ at \vec{r} is given by (II. 58a):

$$\begin{aligned} s(\vec{r}) &= (e_r^2 + e_i^2) / \eta_0 = [a_1^2 - (\vec{a}_1 \cdot \hat{r})^2 + a_2^2 - (\vec{a}_2 \cdot \hat{r})^2] / \eta_0 \\ &= \frac{\eta_0 (Il)^2}{4\lambda^2 r^2} \left[1 - (I_0^2 x_0^2 + I_1^2 x_1^2 + I_2^2 x_2^2) / (Ir)^2 - 2(c_{01} x_0 x_1 + c_{02} x_0 x_2 + c_{12} x_1 x_2) / r^2 \right] \end{aligned} \quad (\text{II. 85})$$

$$c_{mn} = (I_m I_n / I^2) \cos(\tau_m - \tau_n). \quad (\text{II. 86})$$

The total radiated power w_t is obtained by integrating $s(r)$ over the surface of a sphere of radius r , using the spherical coordinates r, θ, ϕ illustrated in figure II. 1:

$$w_t = \int_0^{2\pi} d\phi \int_0^\pi d\theta r^2 s(\vec{r}) \sin\theta = \frac{2\pi \eta_0 (Il)^2}{3\lambda^2} \text{ watts.} \quad (\text{II. 87})$$

From (II. 87) it is seen that the peak scalar dipole moment $\sqrt{2}Il$ used to define \vec{a}_1 and \vec{a}_2 in (II. 78) may be expressed in terms of the total radiated power:

$$\sqrt{2}Il = \lambda \sqrt{3w_t / (\pi \eta_0)} \text{ ampere-kilometers.} \quad (\text{II. 88})$$

The directive gain $g(\hat{r})$ is

$$\begin{aligned} g(\hat{r}) &= 4\pi r^2 s(\vec{r}) / w_t = \frac{3}{2} \left[1 - \left(\frac{I_0}{I}\right)^2 \cos^2\theta - \left(\frac{I_1}{I}\right)^2 \sin^2\theta \cos^2\phi \right. \\ &\quad \left. - \left(\frac{I_2}{I}\right)^2 \sin^2\theta \sin^2\phi - (c_{01} \cos\phi + c_{02} \sin\phi) \sin(2\theta) - c_{12} \sin^2\theta \sin(2\phi) \right]. \end{aligned} \quad (\text{II. 89})$$

This is the most general expression possible for the directive gain of any combination of elementary electric dipoles centered at a point. Studying (II. 89), it may be shown that no combination of values for $I_0, I_1, I_2, \tau_0, \tau_1, \tau_2$ will provide an isotropic radiator. As defined in this annex, an isotropic antenna radiates or receives waves of any phase and polarization equally in every direction.

For the special case where $I_0 = I_1 = I_2 = I/\sqrt{3}$, $\tau_0 = \pi/2$, $\tau_1 = 0$, and $\tau_2 = \pi$, (II.89) shows that

$$g(\hat{r}) = 1 + \sin^2 \theta \sin \phi \cos \phi. \quad (\text{II.90})$$

With these specifications, (II.78) shows that $c_0 = 0$, $c_1 = -c_2 = 1/\sqrt{3}$, $s_0 = 1/\sqrt{3}$, $s_1 = s_2 = 0$, and (II.78) with (II.88) shows that

$$\vec{a}_1 = (\hat{x}_1 - \hat{x}_2) b, \quad \vec{a}_2 = \hat{x}_0 b \quad (\text{II.91a})$$

$$b = \lambda \left[w_r / (\pi \eta_0) \right]^{1/2}. \quad (\text{II.91b})$$

Substituting next in (II.84) with the aid of (II.2):

$$\sqrt{2} \vec{c}_r = c_0 (\hat{x}_1 - \hat{x}_2 - \hat{r} b_2), \quad \sqrt{2} \vec{c}_i = c_0 (\hat{x}_0 - \hat{r} \cos \theta) \quad (\text{II.92})$$

$$c_0 = \left[\eta_0 w_t / (4\pi r^2) \right]^{1/2}, \quad b_2 = \sin \theta (\cos \phi - \sin \phi). \quad (\text{II.93})$$

The principal and cross-polarization gains determined using (II.57) and (II.58) are

$$g_p(\hat{r}) = 1 + \sin^2 \theta (\sin \phi \cos \phi - 1/2), \quad g_c(\hat{r}) = 1/2 \sin^2 \theta. \quad (\text{II.94})$$

The subscripts p and c in (II.94) should be reversed whenever $g(\theta, \phi)$ is less than $\sin^2 \theta$. Minimum and maximum values of g are $1/2$ and $3/2$ while g_p ranges from $1/3$ to 1 and g_c from 0 to $1/2$.

The importance of phases to multipath coupling is more readily demonstrated using a somewhat more complicated antenna. The following paragraphs derive an expression for a wave which is approximately plane at a distance r exceeding 200 wavelengths, radiated by an antenna composed of two three-dimensional complex dipoles located at $-5 \lambda \hat{x}_0$ and $+5 \lambda \hat{x}_0$ and thus spaced 10 wavelengths apart. When the radiation pattern has been determined, it will be assumed that this is the receiving antenna. Its response to known plane waves from two given directions will then be calculated.

With the radiated power w_t divided equally between two three-dimensional complex dipoles, \vec{a} is redefined as

$$\vec{a} = (b/\sqrt{2}) \vec{a}_0, \quad \vec{a}_0 = \hat{x}_1 - \hat{x}_2 + i\hat{x}_0. \quad (\text{II.95})$$

Since 5λ is negligible compared to r except in phase factors critically depending on $r_1 - r_2$, the exact expressions

$$\vec{r}_1 = \vec{r} - 5\lambda \hat{x}_o, \quad \vec{r}_2 = \vec{r} + 5\lambda \hat{x}_o \quad (\text{II. 96})$$

lead to the following approximations and definitions:

$$r_1 = r(1 - \epsilon), \quad r_2 = r(1 + \epsilon), \quad \epsilon = 5(\lambda/r) \cos \theta \quad (\text{II. 97})$$

$$\hat{r}_1 = \hat{r}(1 + \epsilon) - \hat{x}_o \epsilon \sec \theta, \quad \hat{r}_2 = \hat{r}(1 - \epsilon) + \hat{x}_o \epsilon \sec \theta \quad (\text{II. 98})$$

$$\hat{r} = \hat{x}_o \cos \theta + (\hat{x}_1 \cos \phi + \hat{x}_2 \sin \phi) \sin \theta. \quad (\text{II. 99})$$

For distances r exceeding 200 wavelengths, $|\epsilon| < 0.025$ and ϵ^2 is neglected entirely, so that

$$\hat{r}_1 r_1 = \vec{r} - 5\lambda \hat{x}_o, \quad \hat{r}_2 r_2 = \vec{r} + 5\lambda \hat{x}_o. \quad (\text{II. 100})$$

At a point \vec{r} , the complex wave radiated by this antenna is approximately plane and may be represented as

$$\sqrt{Z} \left(\vec{e}_r + i \vec{e}_i \right) \exp(i\tau) = \sqrt{Z} \left[\vec{e}_1 \exp(i\tau_1) + \vec{e}_2 \exp(i\tau_2) \right] \quad (\text{II. 101})$$

where

$$\tau = k(ct - r) + \pi/4 \quad (\text{II. 102})$$

$$\tau_1 = \tau + \tau_a, \quad \tau_2 = \tau - \tau_a, \quad \tau_a = 10\pi \cos \theta. \quad (\text{II. 103})$$

As in (II. 82), the waves radiated by the two main elements of this antenna are represented in (II. 101) as the product of phasors $\exp(i\tau_1)$ and $\exp(i\tau_2)$ multiplied by the complex vectors $\sqrt{Z} \vec{e}_1$ and $\sqrt{Z} \vec{e}_2$, respectively:

$$\sqrt{Z} \vec{e}_1 = \left[\hat{r}_1 \times \left(\vec{a} \times \hat{r}_1 \right) \right] \eta_o / (2\lambda r) = (e_o/2) \left[\vec{a}_o - \hat{r}_1 \left(\vec{a}_o \cdot \hat{r}_1 \right) \right] \quad (\text{II. 104a})$$

$$\sqrt{Z} \vec{e}_2 = \left[\hat{r}_2 \times \left(\vec{a} \times \hat{r}_2 \right) \right] \eta_o / (2\lambda r) = (e_o/2) \left[\vec{a}_o - \hat{r}_2 \left(\vec{a}_o \cdot \hat{r}_2 \right) \right] \quad (\text{II. 104b})$$

Evaluating $\vec{a}_0 \cdot \hat{r}_1$, $\vec{a}_0 \cdot \hat{r}_2$, \vec{e}_1 , and \vec{e}_2 with the aid of (II.95), (II.98), (II.99) and (II.104):

$$\vec{a}_0 \cdot \hat{r}_1 = b_2(1+\epsilon) + i \left[\cos \theta - \epsilon(\sec \theta - \cos \theta) \right] \quad (\text{II.105a})$$

$$\vec{a}_0 \cdot \hat{r}_2 = b_2(1-\epsilon) + i \left[\cos \theta + \epsilon(\sec \theta - \cos \theta) \right] \quad (\text{II.105b})$$

$$\begin{aligned} \vec{e}_1 = (e_0/2) \left\{ \left[\hat{x}_1 - \hat{x}_2 - \hat{r} b_2(1+2\epsilon) + \hat{x}_0 b_2 \epsilon \sec \theta \right] \right. \\ \left. + i \left[\hat{x}_0(1+\epsilon) - \hat{r} \cos \theta + \hat{r} \epsilon(\sec \theta - 2 \cos \theta) \right] \right\} \end{aligned} \quad (\text{II.106a})$$

$$\begin{aligned} \vec{e}_2 = (e_0/2) \left\{ \left[\hat{x}_1 - \hat{x}_2 - \hat{r} b_2(1-2\epsilon) - \hat{x}_0 b_2 \epsilon \sec \theta \right] \right. \\ \left. + i \left[\hat{x}_0(1-\epsilon) - \hat{r} \cos \theta - \hat{r} \epsilon(\sec \theta - 2 \cos \theta) \right] \right\} . \end{aligned} \quad (\text{II.106b})$$

Since the sum and difference of $\exp(i\tau_1)$ and $\exp(i\tau_2)$ are $2 \cos \tau_a \exp(i\tau)$ and $2i \sin \tau_a \exp(i\tau)$, respectively, \vec{e}_r and \vec{e}_i as defined by (II.101) are

$$\vec{e}_r = e_0 \left\{ \left[\hat{x}_1 - \hat{x}_2 - \hat{r} b_2 \right] \cos \tau_a - \epsilon \left[\hat{x}_0 + \hat{r}(\sec \theta - 2 \cos \theta) \right] \sin \tau_a \right\} \quad (\text{II.107a})$$

$$\vec{e}_i = e_0 \left\{ \left[\hat{x}_0 - \hat{r} \cos \theta \right] \cos \tau_a - b_2 \left[2\hat{r} - \hat{x}_0 \sec \theta \right] \sin \tau_a \right\} . \quad (\text{II.107b})$$

The complex wave $\sqrt{2}(\vec{e}_r + i\vec{e}_i)$ is a plane wave only when \vec{e}_r and \vec{e}_i are both perpendicular to the direction of propagation, \hat{r} , or when

$$\hat{r} \cdot (\vec{e}_r + i\vec{e}_i) = \epsilon \sin \tau_a \left[(\cos \theta - \sec \theta) + i \sin \theta (\cos \phi - \sin \phi) \right] = 0 \quad (\text{II.108})$$

which requires that $\epsilon = 0$, $\sin \tau_a = 0$, or $\theta = 0$. If ϵ is negligible, the total mean power flux density in terms of the directive gain $g(\hat{r})$ is given by

$$s(\vec{r}) = (e_r^2 + e_i^2) / \eta_0 = g(\hat{r}) e_0^2 / \eta_0 \quad (\text{II.109})$$

$$g(\hat{r}) = 2(1 + \sin^2 \theta \sin \phi \cos \phi) \cos^2 \tau_a . \quad (\text{II.110})$$

That w_t is the corresponding total radiated power may be verified by substituting (II.108) and (II.110) in (II.87), with the aid of (II.93) and (II.103).

Now let this antenna be a receiving antenna, and suppose that direct and ground-reflected waves arrive from directions $\hat{r}(\theta, \phi)$ equal to

$$\hat{r}_1(0.32, \pi/4) = 0.9492 \hat{x}_0 + 0.2224(\hat{x}_1 + \hat{x}_2) \quad (\text{II.111a})$$

$$\hat{r}_2(0.28, 0.75) = 0.9611 \hat{x}_0 + 0.1430 \hat{x}_1 + 0.1332 \hat{x}_2 . \quad (\text{II.111b})$$

Note that \hat{r}_1 and \hat{r}_2 in (II.111) are not related to \hat{r}_1 and \hat{r}_2 in (II.98) but are two particular values of \hat{r} . Corresponding values of τ_a , $\cos \tau_a$, and $\sin \tau_a$ are

$$\tau_{a1} = 29.82111 , \quad \cos \tau_{a1} = -0.0240 , \quad \sin \tau_{a1} = -0.9997 \quad (\text{II.112a})$$

$$\tau_{a2} = 30.19245 , \quad \cos \tau_{a2} = 0.3404 , \quad \sin \tau_{a2} = -0.9403 . \quad (\text{II.112b})$$

The incoming waves in the two directions \hat{r}_1 and \hat{r}_2 are assumed to be plane, and the distances r_1 and r_2 to their source are assumed large enough so that $\epsilon_1 \sin \tau_{a1}$ and $\epsilon_2 \sin \tau_{a2}$ are negligible compared to $\cos \tau_{a1}$ and $\cos \tau_{a2}$, respectively. The plane wave response of the receiving antenna in these directions may be expressed in terms of the complex vectors associated with \hat{r}_1 and \hat{r}_2 :

$$\vec{e}_{r1} + i\vec{e}_{i1} = -0.024 e_o \left[(\hat{x}_1 - \hat{x}_2) + i(0.099 \hat{x}_0 - 0.211 \hat{x}_1 - 0.211 \hat{x}_2) \right] \quad (\text{II.113a})$$

$$\vec{e}_{r2} + i\vec{e}_{i2} = 0.340 e_o \left[(-0.013 \hat{x}_0 + 0.998 \hat{x}_1 - 1.002 \hat{x}_2) + i(0.076 \hat{x}_0 - 0.137 \hat{x}_1 - 0.128 \hat{x}_2) \right] . \quad (\text{II.113b})$$

Since $\vec{e}_{r1} \cdot \vec{e}_{r2} = 0$, (II.44) with (II.42) and (II.43) shows that $\tau_{r1} = 0$, so that \vec{e}_{r1} and \vec{e}_{i1} are principal and cross-polarization components of the complex vector receiving pattern:

$$\vec{e}_{pr1} + i\vec{e}_{cr1} = \vec{e}_{r1} + i\vec{e}_{i1} . \quad (\text{II.114a})$$

These same equations show that $\tau_{r_2} = -0.005$ and that

$$\vec{e}_{pr2} + i\vec{e}_{cr2} = 0.340 e_o \left[(-0.013 \hat{x}_o + 0.999 \hat{x}_1 - 1.001 \hat{x}_2) + i(0.076 \hat{x}_o - 0.132 \hat{x}_1 - 0.113 \hat{x}_2) \right] \quad (\text{II. 114b})$$

differing only slightly from (II. 113b), since τ_{r_2} is almost zero.

The axial ratios of the two polarization ellipses, defined by (II. 50), are

$$a_{xr1} = -0.222, \quad a_{xr2} = -0.143 \quad (\text{II. 115})$$

and the unit complex polarization vectors \hat{p}_{r1} and \hat{p}_{r2} defined by (II. 51) are therefore

$$\hat{p}_{r1} = 0.674(\hat{x}_1 - \hat{x}_2) + i(0.067 \hat{x}_o - 0.142 \hat{x}_1 - 0.142 \hat{x}_2) \quad (\text{II. 116a})$$

$$\hat{p}_{r2} = (-0.009 \hat{x}_o + 0.692 \hat{x}_1 - 0.694 \hat{x}_2) + i(0.053 \hat{x}_o - 0.095 \hat{x}_1 - 0.089 \hat{x}_2). \quad (\text{II. 116b})$$

The antenna gains $g_r(\hat{r}_1)$ and $g_r(\hat{r}_2)$ are given by (II. 110):

$$g_r(\hat{r}_1) = 0.0021, \quad g_r(\hat{r}_2) = 0.241 \quad (\text{II. 117})$$

which shows that the gain $G_r(\hat{r}_1) = 10 \log g_r(\hat{r}_1)$ associated with the direct ray is 29.2 db below that of an isotropic antenna, while the gain $G_r(\hat{r}_2)$ associated with the ground-reflected ray is -6.2 db. It might be expected that only the incident wave propagating in the direction $-\hat{r}_2$ would need to be considered in determining the complex voltage at the receiving antenna terminals. Suppose, however, that the ground-reflected ray has been attenuated considerably more than the direct ray, so that the path attenuation factor a_{p2} is 0.01, while $a_{p1} = 1$. Suppose further that the transmitting antenna gain associated with the ground-reflected ray is 6 db less than that associated with the direct ray. Then the mean incident flux density s_2 associated with the ground-reflected ray will be 26 db less than the flux density s_1 associated with the direct ray.

In order to calculate the complex received voltage v given by (II. 70) then, the following is assumed:

$$r_v = 52 \text{ ohms}, \quad s_1 = 1 \text{ watt/km}^2 (= -30 \text{ dbm/m}^2)$$

$$s_2 = 0.0025 \text{ watts/km}^2, \quad \lambda = 0.0003 \text{ km} (f = 1000 \text{ MHz})$$

$$a_{x_1} = 0.2, \quad a_{x_2} = 0.4, \quad \psi_{p_1} = \pi/2, \quad \psi_{p_2} = 1.5$$

$$\tau_{i_1} = \tau_{p_1} + \tau_{t_1} = 0, \quad \tau_{i_2} = \tau_{p_2} + \tau_{t_2} = \pi, \quad (\text{II. 118})$$

It will be seen that these assumptions imply a more nearly complete polarization coupling loss between the direct wave and the receiving antenna than between the ground-reflected wave and the receiving antenna. The effective absorbing area of the receiving antenna for each wave, as given by (II. 67) is

$$a_{e_1} = 1.504 \times 10^{-11} \text{ km}^2, \quad a_{e_2} = 1.726 \times 10^{-9} \text{ km}^2. \quad (\text{II. 119})$$

The polarization factors are

$$(\hat{p}_1 \cdot \hat{p}_{r_1}) = -0.021 i, \quad (\hat{p}_2 \cdot \hat{p}_{r_2}) = 0.062 + 0.236 i \quad (\text{II. 120})$$

and the phase factors are $\exp(i\tau)$ and $\exp[i(\tau + 3.137)]$, respectively. Substituting these values in (II. 65), the complex voltages are

$$v_1 = -1.175(10^{-6})i \exp(i\tau), \quad v_2 = -(1.887 + 7.071i)(10^{-6}) \exp(i\tau). \quad (\text{II. 121})$$

The real voltage at the antenna terminals, as given by (II. 70) is

$$v_v = (v_1 + v_2)(v_1 + v_2)^* = 8.33 \times 10^{-6} \text{ volts} = 8.33 \text{ microvolts} \quad (\text{II. 122})$$

and the corresponding power w_a available at the terminals of the loss-free receiving antenna is

$$w_a = 0.334 \times 10^{-12} \text{ watts}, \quad W_a = -125 \text{ dbw} = -95 \text{ dbm} \quad (\text{II. 123})$$

as given by (II. 71).

II.3.8 Conclusions

The foregoing exercise demonstrates that:

(1) Even small changes in antenna beam orientation, transmission loss, polarization coupling, and multipath phasing may have a visible effect on the available power at the terminals of a receiving antenna.

(2) If the formulation of the general relationships for a completely polarized wave is programmed for a digital computer, it may be feasible to estimate the complete statistics of a received signal whenever reasonable assumptions can be made about the statistics of the parameters described in this annex.

(3) The measurement of antenna characteristics in a few critical directions will often be sufficient to provide valuable information to be used with the relationships given here. The measurement of Stokes' parameters, for instance, will provide information about a_{xr} , g_r , ψ_p , and both the polarized field intensity s_r and the unpolarized field intensity s_o . These parameters [Stokes, 1922] are

$$s_r + s_o = \text{total mean field intensity} \quad (\text{II. 124})$$

$$Q = s_r \cos(2\beta) \cos(2\psi_p) \quad (\text{II. 125})$$

$$U = s_r \cos(2\beta) \sin(2\psi_p) \quad (\text{II. 126})$$

$$V = s_r \sin(2\beta) \quad (\text{II. 127})$$

where

$$\beta = \tan^{-1} a_{xr} \quad (\text{II. 128})$$

The unpolarized or randomly polarized field intensity s_o is determined from (II. 124) and the identity

$$s_r = (Q^2 + U^2 + V^2)^{1/2} \quad (\text{II. 129})$$

Using standard sources and antenna model ranges, the gain g_r may be determined from

$$g_r = s_r / (e_o^2 / \eta_o), \quad e_o^2 = \eta_o p_t / (4\pi r^2) \quad (\text{II. 130})$$

assuming, if e_o is measured, that any power reception efficiency $1/l_{er}$ less than unity will affect s_r and e_o^2 alike.

Finally, a method for measuring relative phase responses τ_r is also needed. In individual cases, multipath coupling loss may be insufficient to provide adequate unwanted signal rejection. Variations of τ_r may lead to phase interference fading of wanted signals, just as variations of a_p are associated with long-term power fading. Because of the complexity of these phenomena, they are usually described in terms of cumulative distributions of signal amplitudes or fade durations. Fortunately, even crude measurements or simple theories may then suffice to provide statistical information about τ_r .

COORDINATE SYSTEMS FOR STUDYING ANTENNA PATTERNS

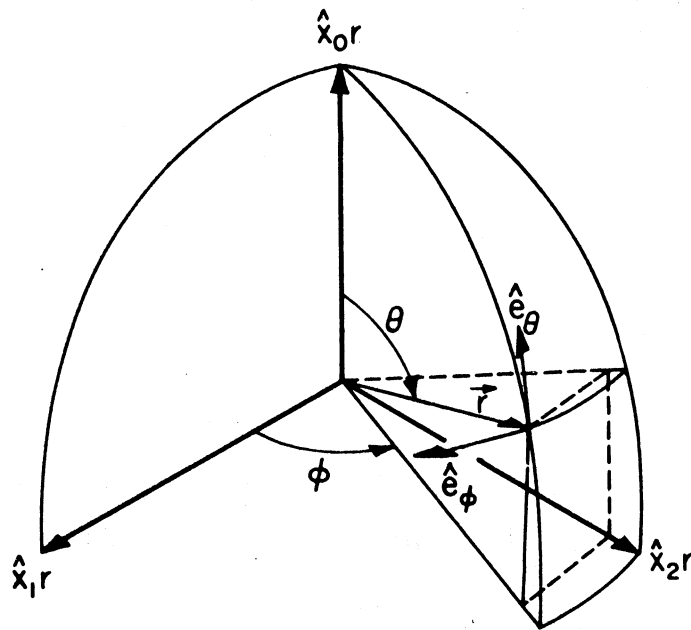


Figure II.1

II.4 List of Special Symbols Used in Annex II

- a_{en}, a_{e1}, a_{e2} The effective absorbing area for the n^{th} discrete plane wave incident on an antenna from a single source, (II. 67), and for each of two waves (II. 119).
- a_p, a_{pm}, a_{pn} The fraction of energy absorbed along a ray path, or scattered out of it, (II. 59), and the fraction of energy, a_p , for the m^{th} and n^{th} multipath components from a single source, where m and n take on integral values from 1 to N , (II. 72)
- a_{xn}, a_{x1}, a_{x2} Axial ratios of the polarization ellipse of the n^{th} , first, and second plane wave from a single source, (II. 68) and (II. 118).
- $a_{xrn}, a_{xr1}, a_{xr2}$ Axial ratios of the polarization ellipse associated with the receiving pattern for the n^{th} , first, and second plane wave from a single source, (II. 68) and (II. 115).
- a_1, a_2 Positive or negative amplitudes of real and imaginary components of a complex vector: $\vec{a} = \vec{a}_1 + i\vec{a}_2$, $a^2 = a_1^2 + a_2^2$, (II. 78).
- \vec{a}, \hat{a} The real vector $a = a\hat{a}$, where \hat{a} is a unit vector.
- \vec{a}_1, \vec{a}_2 Real vectors defining real and imaginary components of a complex vector: $\vec{a} = \vec{a}_1 + i\vec{a}_2$, (II. 78).
- \vec{a} A complex vector: $\vec{a} = \vec{a}_1 + ia_2$, (II. 78).
- \vec{a}_0 A complex vector defined in terms of the unit vector system $\hat{x}_0, \hat{x}_1, \hat{x}_2$, (II. 95).
- e_{cr} The positive or negative amplitude of the cross-polarized vector component \vec{e}_{cr} of a receiving antenna response pattern, (II. 50).
- e_i The positive or negative amplitude of the real vector \vec{e}_i associated with a complex plane wave $\sqrt{2}(\vec{e}_r + i\vec{e}_i)\exp(i\tau)$, where \vec{e}_r and \vec{e}_i are time-invariant and $\exp(i\tau)$ is a time phasor, (II. 41b).
- e_{pr} The positive or negative amplitude of the principal polarization component \vec{e}_p of a receiving antenna response pattern, (II. 50).
- e_r The positive or negative amplitude of the real vector component \vec{e}_r associated with a complex plane wave $\sqrt{2}(\vec{e}_r + i\vec{e}_i)\exp(i\tau)$, where \vec{e}_r and \vec{e}_i are time invariant and $\exp(i\tau)$ is a time phasor, (II. 41a).
- e_o Equivalent free space field strength, (II. 38).
- e_1, e_2 The positive or negative real amplitudes of real and imaginary components of the complex polarization vector \vec{e} , (II. 43).
- e_θ, e_ϕ The positive amplitudes of real vectors \vec{e}_θ and \vec{e}_ϕ associated with the θ and ϕ components of a complex plane wave, (II. 4) figure II. 1.
- \vec{e}_c, \vec{e}_p Real vectors associated with cross and principal polarization components of a uniform elliptically polarized plane wave, annex II, section II. 3. 2.
- \hat{e}_c, \hat{e}_p Directions of cross and principal polarization, chosen so that their vector product $\hat{e}_p \times \hat{e}_c$ is a unit vector in the direction of propagation, (II. 47).

$\vec{e}_{cr}, \vec{e}_{pr}$	Cross and principal polarization field components of a receiving antenna response pattern, (II. 49).
$\hat{e}_{cr}, \hat{e}_{pr}$	Directions of cross and principal polarization components of a receiving antenna response pattern, (II. 51), (II. 53).
\vec{e}_i	The real vector associated with the imaginary component of the time-invariant part of a complex plane wave $\sqrt{2} (\vec{e}_r + i\vec{e}_i) \exp(i\tau)$, (II. 41b).
\vec{e}_r	The real vector associated with the real component of the time-invariant part of a complex plane wave $\sqrt{2} (\vec{e}_r + i\vec{e}_i) \exp(i\tau)$, (II. 41a).
\vec{e}_1, \vec{e}_2	Real vector components of a complex polarization vector \vec{e} which has been resolved into components which are orthogonal in both space and time, (II. 43).
$\vec{e}_\theta, \vec{e}_\phi$	Real vectors associated with the θ and ϕ components of a complex plane wave $\sqrt{2} [\vec{e}_\theta \exp(i\tau_\theta) + \vec{e}_\phi \exp(i\tau_\phi)] \exp(i\tau)$, where only the phasor $\exp(i\tau)$ depends on time, (II. 40) figure II.1.
\hat{e}_θ	A unit vector $\hat{e}_\theta \times \hat{r}$ perpendicular to \hat{e}_ϕ and \hat{r} , (II.36b) figure II.1.
\hat{e}_ϕ	A unit vector $(\hat{r} \times \hat{x}_o) / \sin \theta$ perpendicular to \hat{r} and \hat{x}_o , (II. 36a) figure II.1.
$\underline{\vec{e}}, \underline{\vec{e}}_r$	A bar is used under the symbol to indicate a complex vector: $\underline{\vec{e}} = \vec{e}_p + i\vec{e}_c$, $\underline{\vec{e}}_r = \vec{e}_{pr} + i\vec{e}_{cr}$, (II. 46).
\vec{e}^*	The complex conjugate of $\underline{\vec{e}}$: $\underline{\vec{e}}^* = \vec{e}_p - i\vec{e}_c$.
$ \underline{\vec{e}} , \underline{\vec{e}}_r $	The magnitudes of the complex vectors $\underline{\vec{e}}$ and $\underline{\vec{e}}_r$, (II. 55).
$ e_c , e_{cr} , e_p , e_{pr} $	The amplitudes of the cross and principal polarization components $\vec{e}_c, \vec{e}_{cr}, \vec{e}_p$, and \vec{e}_{pr} , section II. 3.3.
E	Field strength in dbu, (II. 20).
E_o	The equivalent free space field strength in dbu, (II. 26).
E_I	The equivalent inverse distance field, (II. 28).
E_{1kw}	Field strength in dBu per kilowatt effective radiated power, (II. 23) -(II. 25).
g	Maximum free space directive gain, or directivity, Section II. 3.4.
g_c	The cross-polarization component of the directive gain, (II. 57).
g_{cr}	The cross-polarization component of the directive gain of a receiver, (II. 51).
g_p	Principal polarization directive gain, (II. 57).
g_{pr}, g_{pt}	Principal polarization directive gains for the receiving and transmitting antennas, respectively, (II. 59).
g_{rn}, g_{tn}	The directive gains g_r and g_t for the n^{th} of a series of plane waves, (II. 66) and (II. 67).
g_θ, g_ϕ	Directive gains associated with the field components $\vec{e}_\theta, \vec{e}_\phi$, (II. 37).
$g(\hat{r})$	Directive gain in the direction \hat{r} , (II. 89).
$g_c(\hat{r}), g_p(\hat{r})$	Cross polarization and principal polarization directive gains in the direction \hat{r} , (II. 94).
$g_r(\hat{r}_1), g_r(\hat{r}_2)$	Directive gains associated with direct and ground-reflected rays, respectively, (II. 117).

$G_{pt}(\hat{r}_1)$	Principal polarization directive gain of the transmitter in the direction \hat{r}_1 , which is the initial direction of the most important propagation path to the receiver, (II.18) and (II.23) to (II.25).
i	$i = \sqrt{-1}$.
I_m	Current in r. m. s. amperes where $m = 0, 1, 2$, (II.76).
I_0, I_1, I_2	Current in r. m. s. amperes corresponding to three elementary dipoles in three mutually perpendicular directions, (II.76).
k	Propagation constant, $k = 2\pi/\lambda$, (II.34).
l	Used as a subscript to indicate a load, for example, $z_{l\nu}$ represents the impedance of a load at a radio frequency ν , (II.1).
l_{erv}, L_{erv}	The effective loss factor for a receiving antenna at a frequency ν hertz (II.6), $L_{erv} = 10 \log l_{erv}$ db, (II.8).
l_{etv}, L_{etv}	The effective loss factor for a transmitting antenna at a radio frequency ν hertz, (II.7), $L_{etv} = 10 \log l_{etv}$ db, (II.9).
l_{mv}	A mismatch loss factor defined by (II.4).
L_{fr}, L_{ft}	The decibel ratio of the resistance component of antenna input impedance to the free space antenna radiation resistance for the receiving and transmitting antennas, respectively, (II.11).
L_{rr}, L_{rt}	The ratio of the actual radiation resistance of the receiving or transmitting antenna to its radiation resistance in free space, (II.12), (II.13).
L_p	Propagation loss, (II.14).
L_{pb}	Basic propagation loss, (II.15). Basic propagation loss in free space is the same as basic transmission loss in free space.
\hat{p}, \hat{p}_n	Unit complex polarization vector for the incident wave, (II.54), and (II.68).
\hat{p}_r, \hat{p}_{rn}	Unit complex polarization vector associated with a receiving pattern, (II.51) and with the receiving pattern of the n^{th} incident wave, (II.68).
$\hat{p}_{r1}, \hat{p}_{r2}$	The complex receiving antenna polarization vectors \hat{p}_r for each of two ray paths between transmitter and receiver, (II.116).
r	Resistance of an antenna, (II.1).
r	Magnitude of the vector $\vec{r} = r \hat{r}$ in the direction $\hat{r}(\theta, \phi)$, and a coordinate of the polar coordinate system r, θ, ϕ , section II.3.1.
r_{fr}, r_{ft}	Antenna radiation resistance in free space for the receiving and transmitting antennas, respectively, (II.11), (II.12) and (II.13).
$r_{l\nu}$	Resistance of a load, (II.1).
r_r, r_t	Antenna radiation resistance of the receiving and transmitting antennas, respectively, (II.10).
r'_r, r'_t	Resistance component of antenna input impedance for the receiving and transmitting antennas, respectively, (II.10).
r_ν	Resistance of an equivalent loss-free antenna, (II.1c).
r'_ν	Resistance of an actual antenna in its actual environment, (II.1b).
\vec{r}	The vector distance between two points, $\vec{r} = r \hat{r}$, (II.80).

\hat{r}	A unit vector, (II.35)
$\hat{r}, \hat{e}_\theta, \hat{e}_\phi$	A cartesian unit vector coordinate system, (II.35) and (II.36).
s	Total mean power flux density, (II.58).
s_c, s_p	Mean power flux densities associated with cross-polarization, and principal polarization components, (II.56).
s_e	The fraction of the total flux density that contributes to the available power, (II.75).
s_l, s_r	Mean power flux densities associated with left-handed, and right-handed polarization, respectively, (II.61).
s_o	Free space field intensity in watts per square kilometer, (II.16).
$\langle s_e \rangle$	The statistical "expected value of s_e ", (II.76).
$s_c(\vec{r}), s_p(\vec{r})$	Mean power flux densities associated with the cross and principal polarization components of \vec{e} in the direction \vec{r} , (II.17).
v_n	Complex open-circuit r.m.s. signal voltage for coherently phased multipath components, (II.65).
v_v	The open-circuit r.m.s. voltage for an equivalent loss-free antenna at a frequency ν , (II.5).
v'_ν	The actual open-circuit r.m.s. voltage at the antenna terminals at a frequency ν , (II.2).
w_{ab}	The available power corresponding to propagation between hypothetical isotropic antennas, (II.72).
$w_{a\nu}$	Available power at the terminals of an equivalent loss-free receiving antenna at a radio frequency ν , (II.5).
$w'_{a\nu}$	Available power at the terminals of the actual receiving antenna at a radio frequency ν , (II.3).
$w_{l\nu}$	Power delivered to the receiving antenna load, at a radio frequency ν , (II.2).
$w_{t\nu}$	Total power radiated at a frequency ν , (II.7).
$w'_{t\nu}$	Total power delivered to the transmitting antenna at a frequency ν , (II.7).
$x_{l\nu}, x'_{\nu}, x_{\nu}$	Reactance of a load, an actual lossy antenna, and an equivalent loss-free antenna, respectively, (II.1).
\hat{x}_m	One of three mutually perpendicular directions, $m=0, 1, 2$, section II.3.7.
$\hat{x}_0, \hat{x}_1, \hat{x}_2$	Axes of a cartesian unit vector coordinate system, (II.35) figure II.1.
$z_{l\nu}$	Impedance of a load, (II.1).
z_{ν}	Impedance of an equivalent loss-free antenna (II.1).
z'_{ν}	Impedance of an actual lossy antenna, (II.1).
$z_{\nu}^{!*}$	The conjugate of z'_{ν} , following (II.2).

ϵ	A small increment used in (II. 97) and (II. 98).
η_0	Characteristic impedance of free space, $\eta_0 = 4\pi c \cdot 10^{-7}$, (II. 38).
θ	A polar coordinate, (II. 35).
ν	Radio frequency in hertz (cycles per second), section II. 1.
ν_l, ν_m	Limits of integration (II. 8), (II. 9).
τ	The time-varying phase $\tau = k(ct - r)$, where c is the free space velocity of radio-waves, t is the time at the radio source, and r is the length of the radio ray, (II. 34).
τ_a	Time element defined by (II. 103).
τ_{a1}, τ_{a2}	The time element τ_a corresponding to direct and ground-reflected waves at the receiving antenna, (II. 112).
τ_i	A time-independent phase which is a function of \vec{r} , (II. 42), (II. 64).
τ_{in}	The time-independent phase for the n^{th} component of an incident wave, section II. 3. 6.
τ_{i1}, τ_{i2}	The time-independent phase for two components of an incident wave, (II. 118).
$\tau_m, \tau_0, \tau_1, \tau_2$	Initial phase of the current supported by one of m elementary dipoles, where $m = 0, 1, 2$, (II. 79).
τ_p	A function of the ray path, including allowances for path length differences and diffraction or reflection phase shifts, (II. 64).
$\tau_{pn}, \tau_{p1}, \tau_{p2}$	The phase function τ_p for the n^{th} , first, and second plane wave incident on an antenna from a single source, (II. 65) and (II. 118).
τ_r	Antenna phase response for the receiving antenna, (II. 49).
$\tau_{rn}, \tau_{r1}, \tau_{r2}$	The antenna phase response, τ_r , for the n^{th} , first, and second plane wave incident on the receiving antenna, (II. 65) and section II. 3. 7.
τ_t	Antenna phase response for a transmitting antenna, (II. 64).
$\tau_{tn}, \tau_{t1}, \tau_{t2}$	The antenna phase response τ_t for the n^{th} , first, and second plane wave, (II. 65) and (II. 118).
τ_θ, τ_ϕ	Phases associated with the electrical field components $\vec{e}_\theta, \vec{e}_\phi$, (II. 40).
ϕ	One of the polar coordinates, r, θ, ϕ , (II. 89) and figure II.
ψ_{p1}, ψ_{p2}	The acute angle, ψ_p , for each of two waves, (II. 118).

Annex III

SUPPLEMENTARY INFORMATION AND FORMULAS USEFUL FOR PROGRAMMING

The material of this annex is organized into the following sections:

1. Line-of-sight
2. Diffraction over a single isolated obstacle
3. Diffraction over a single isolated obstacle with ground reflections
4. Diffraction over irregular terrain
5. Forward scatter
6. Forward scatter with antennas elevated
7. Long-term variability
8. List of special symbols used in annex III

Section 1 lists geometric optics formulas for computing transmission loss over a smooth earth, for determining the magnitude and phase of the reflection coefficient, and for computing a first Fresnel zone along a great circle path. Graphs of the magnitude R and phase c of the reflection coefficient are included. Section 2 gives mathematical expressions that approximate the curves $A(v, 0)$, $A(0, \rho)$ and $U(v\rho)$ for convenience in using a digital computer. Section 3 lists geometric optics formulas used to compute diffraction attenuation when several components of the received field are affected by reflection from the earth's surface. Section 4 defines the parameters K and b for both horizontally and vertically polarized radio waves. Section 5 shows the function $F(\theta d)$ for $N_g = 250, 301, 350, \text{ and } 400$, and for values of s from 0.01 to 1. Curve fits to the function $F(\theta d)$ and equations for computing $H_o(\eta_g = 0)$ are included. Section 6 suggests modifications of the prediction methods for use when antenna beams are elevated or directed out of the great circle plane. Section 7 shows diurnal and seasonal changes in long-term variability. Mathematical expressions used to compute predicted distributions are shown and a method of mixing distributions is described. Section 8 is a list of special symbols used in this annex.

Section I. 3 of annex I explains an easily programmed method for obtaining reference values of attenuation relative to free space A_{CR} for a wide range of applications. These reference values may be converted to estimates of transmission loss exceeded for $100 p = 100(1 - q)$ percent of the time by subtracting the quantities $V(0.5)$ and $Y(q)$ defined by (10.4) and (10.5) of volume 1 and discussed also in section 7 of this annex.

III.1 Line-of-Sight

Simple formulas for line-of-sight propagation which suffice for most applications, are given in section 5 of the report. Formulas for geometry over a smooth earth and for determining the magnitude and phase of the reflection coefficient are given here. These formulas may be used when the great circle path terrain visible to both antennas will support a substantial amount of reflection, and it is reasonable to fit a smooth convex curve of radius a to this portion of the terrain.

Figure 5.1b illustrates the geometry appropriate for reflection of a single ray by a smooth earth of effective radius a . In the figure, ψ is the grazing angle at the geometrical reflection point located at a distance d_1 from an antenna of height h_1 and at a distance d_2 from an antenna of height h_2 . The total path distance $d = d_1 + d_2$ is measured along an arc of radius a . The difference, Δr , between the reflected ray path length $r_1 + r_2$ and the length of the direct ray, r_0 , is calculated to find the phase of a radio field which is the sum of ground-reflected and free space fields. If Δr is less than 0.06λ , these ray optics formulas are not applicable. For almost all cases of interest the angle ψ is small and the straight line distances r_1 , r_2 and r_0 are very nearly equal to the mean sea level arc distances d_1 , d_2 and d . The geometric optics formulas given below usually require double-precision arithmetic,

$$\tan \psi = \cot(d_1/a) - (1 + h_1/a)^{-1} \csc(d_1/a) \cong \frac{h_1}{d_1} - \frac{d_1}{2a} \quad (\text{III. 1})$$

$$\tan \psi = \cot(d_2/a) - (1 + h_2/a)^{-1} \csc(d_2/a) \cong \frac{h_2}{d_2} - \frac{d_2}{2a} \quad (\text{III. 2})$$

$$r_0 = a \left\{ (h_1/a)^2 + (h_2/a)^2 - 2(h_1/a)(h_2/a) + 2[1 + h_1/a + h_2/a + (h_1/a)(h_2/a)][1 - \cos(d/a)] \right\}^{1/2} \quad (\text{III. 3})$$

$$r_1 = \left[(a \sin \psi)^2 + h_1(2a + h_1) \right]^{1/2} - a \sin \psi \quad (\text{III. 4})$$

$$r_2 = \left[(a \sin \psi)^2 + h_2(2a + h_2) \right]^{1/2} - a \sin \psi \quad (\text{III. 5})$$

$$\Delta r = r_1 + r_2 - r_0 = 4 r_1 r_2 \sin^2 \psi / (r_1 + r_2 + r_0) \quad (\text{III. 6})$$

Equating (III. 1) and (III. 2) and substituting $d - d_1$ for d_2 in (III. 2), the distance d_1 may be determined graphically or by trial and error, and $\tan \psi$ is then calculated using (III. 1).

Using double precision arithmetic, (III. 1) through (III. 6) give an accurate estimate of the path difference Δr for reflection of a single ray from a smooth earth. This value is then used in (5.4) or (5.5) of section 5 to compute the attenuation relative to free space.

If either h_1 or h_2 greatly exceeds one kilometer, and if it is considered worthwhile to trace rays through the atmosphere in order to determine ψ more accurately, values of d_1 or d_2 , tabulated by Bean and Thayer [1959], may be used. Given h_1 , h_2 , and the surface refractivity, N_s , select trial values for ψ , calculate d_1 and d_2 , and continue until $d_1 + d_2 = d$. Then (III.1) and (III.2) must be solved for new values of h_1 and h_2 if (III.3), (III.4), and (III.5) are used to obtain the path difference,

$$\Delta r = r_1 + r_2 - r_0.$$

The symbols R in (5.1) and c in (5.4) represent the magnitude and the phase angle relative to π , respectively, of the theoretical coefficient $R \exp[-i(\pi-c)]$ for reflection of a plane wave from a smooth plane surface of a given conductivity σ and relative dielectric constant ϵ . Values of R and c as a function of the grazing angle ψ are shown in figures III.1 to III.8 for vertical and horizontal polarization over good, average, and poor ground, and over sea water. The magnitude R of the smooth plane earth reflection coefficient is designated R_v or R_h for vertical or horizontal polarization respectively, and is read on the left-hand ordinate scale using the solid curves. The phase angle relative to π , is designated c_v or c_h for vertical or horizontal polarization respectively, and is read in radians on the right-hand scale using the dashed curves. As seen from these figures in most cases when the angle ψ is small, R is very nearly unity and c may be set equal to zero. A notable exception occurs in the case of propagation over sea water using vertical polarization.

In preparing figures III.1 to III.8, the following general expressions for the magnitudes R_v and R_h and lags $(\pi - c_v)$ and $(\pi - c_h)$ were used. In these equations, ϵ is the ratio of the surface dielectric constant to that of air, σ is the surface conductivity in mhos per meter, f is the radio frequency in megacycles per second, and ψ is the grazing angle in radians.

$$x = 1.80 \times 10^4 \sigma / f, \quad q = x / (2p) \tag{III. 7}$$

$$2p^2 = \left[(\epsilon - \cos^2 \psi)^2 + x^2 \right]^{1/2} + (\epsilon - \cos^2 \psi) \tag{III. 8}$$

$$b_v = \frac{\epsilon^2 + x^2}{p^2 + q^2}, \quad b_h = \frac{1}{p^2 + q^2} \tag{III. 9}$$

$$m_v = \frac{2(p\epsilon + qx)}{p^2 + q^2}, \quad m_h = \frac{2p}{p^2 + q^2} \tag{III. 10}$$

$$R_v^2 = \left[1 + b_v \sin^2 \psi - m_v \sin \psi \right] \left[1 + b_v \sin^2 \psi + m_v \sin \psi \right]^{-1} \quad (\text{III. 11})$$

$$R_h^2 = \left[1 + b_h \sin^2 \psi - m_h \sin \psi \right] \left[1 + b_h \sin^2 \psi + m_h \sin \psi \right]^{-1} \quad (\text{III. 12})$$

$$\pi - c_v = \tan^{-1} \left(\frac{x \sin \psi - q}{\epsilon \sin \psi - p} \right) - \tan^{-1} \left(\frac{x \sin \psi + q}{\epsilon \sin \psi + p} \right) \quad (\text{III. 13})$$

$$\pi - c_h = \tan^{-1} \left(\frac{-q}{\sin \psi - p} \right) - \tan^{-1} \left(\frac{q}{\sin \psi + p} \right) \quad (\text{III. 14})$$

The angle c_v is always positive and less than π , and c_h is always negative with an absolute magnitude less than π . The pseudo Brewster angle, where c_v suddenly changes from near zero to $\pi/2$, and where R_v is a minimum, is $\sin^{-1} \sqrt{1/b_v}$.

For grazing angles less than 0.1 radian, for overland propagation, and for frequencies above 30 Mc/s, excellent approximations to (III.11) and (III.12) are provided by the following formulas:

$$R_v = \exp(-m_v \psi) \quad (\text{III. 15})$$

$$R_h = \exp(-m_h \psi) \quad (\text{III. 16})$$

The assumption of a discrete reflection point with equal angles of incidence and reflection as shown in figure 5.1 is an oversimplification. Actually, reflection occurs from all points of the surface. For irregular terrain, this is taken into account by a terrain roughness factor σ_h , (subsection 5.1), which is the r.m.s. deviation of terrain relative to a smooth curve computed within the limits of a first Fresnel zone in a horizontal plane. The outline of such a Fresnel ellipse is determined by the condition that the length of a ray path, $r_{11} + r_{21}$, corresponding to scattering from a point on the edge of the ellipse is half a wavelength longer than the geometrical ray path, $r_1 + r_2$, where the angles of incidence and reflection are equal.

The first Fresnel ellipse cuts the great circle plane at two points, x_a and x_b kilometers from the transmitter. The distances x_a and x_b are defined by the relation

$$\sqrt{r_1^2 \sin^2 \psi + x^2} + \sqrt{r_2^2 \sin^2 \psi + [(r_1 + r_2) \cos \psi - x]^2} = r_1 + r_2 + \lambda/2 \quad (\text{III. 17})$$

The exact solution for x is

$$2x_{a,b}(1+\delta) = [(r_1+r_2)(1+\delta) + (r_1-r_2)] \cos \psi \pm (r_1+r_2 + \lambda/2) \delta \sqrt{1 + 4r_1r_2/[(r_1+r_2)^2 \delta]} \quad (\text{III. 18})$$

where

$$r_1^2 = h_1'^2 + d_1^2, \quad r_2^2 = h_2'^2 + d_2^2, \quad (r_1+r_2)^2 = (h_1'+h_2')^2 + d^2$$

$$\cos \psi = d_1/r_1 = d_2/r_2, \quad \sin \psi = h_1'/r_1 = h_2'/r_2$$

$$\delta = \left[\frac{\lambda^2}{4(r_1+r_2)^2} + \frac{\lambda}{r_1+r_2} \right] / \sin^2 \psi$$

d_1, d_2 are defined by (5.7), and λ is the radio wavelength in kilometers.

As an alternative method, the points x_a and x_b may be computed in terms of path distance, the heights h_1' and h_2' , and the radio frequency. In this method, the distance x_0 to the center of the first Fresnel zone is first computed, then the distance x_1 from the center to the margin of the zone is subtracted from x_0 to give x_a , and added to give x_b .

$$x_0 = d/2 \left[1 + B f(h_1'^2 - h_2'^2) \right] \text{ km} \quad (\text{III. 19})$$

where

$$B = \left[0.3d(1 + 2h_1'h_2'/d^2) + f(h_1'+h_2')^2 \right]^{-1} \quad (\text{III. 20})$$

$$x_1 = 0.548 B d^2 \left\{ \left[f h_1'h_2'/d + 0.075(1 + 2h_1'h_2'/d^2) \right] \left[\frac{1 + (h_1'+h_2')^2/d^2}{1 + 2h_1'h_2'/d^2} \right] \right\}^{1/2} \quad (\text{III. 21})$$

$$x_a = x_0 - x_1 \text{ km}, \quad x_b = x_0 + x_1 \text{ km}.$$

The method given in (III.19) to (III.21) is applicable whenever $d \gg \lambda$. If in addition, $h_1' h_2' \ll d^2$, the computation of B , and x_1 may be simplified as follows:

$$B = \left[0.3d + f(h_1' + h_2')^2 \right]^{-1} \quad (\text{III. 22})$$

$$x_1 = 0.548 B d^2 \left\{ \left[f h_1' h_2' / d + 0.075 \right] \left[1 + (h_1' + h_2')^2 / d^2 \right] \right\}^{1/2} \quad (\text{III. 23})$$

THE COMPLEX REFLECTION COEFFICIENT $Re^{-i(\pi-c)}$

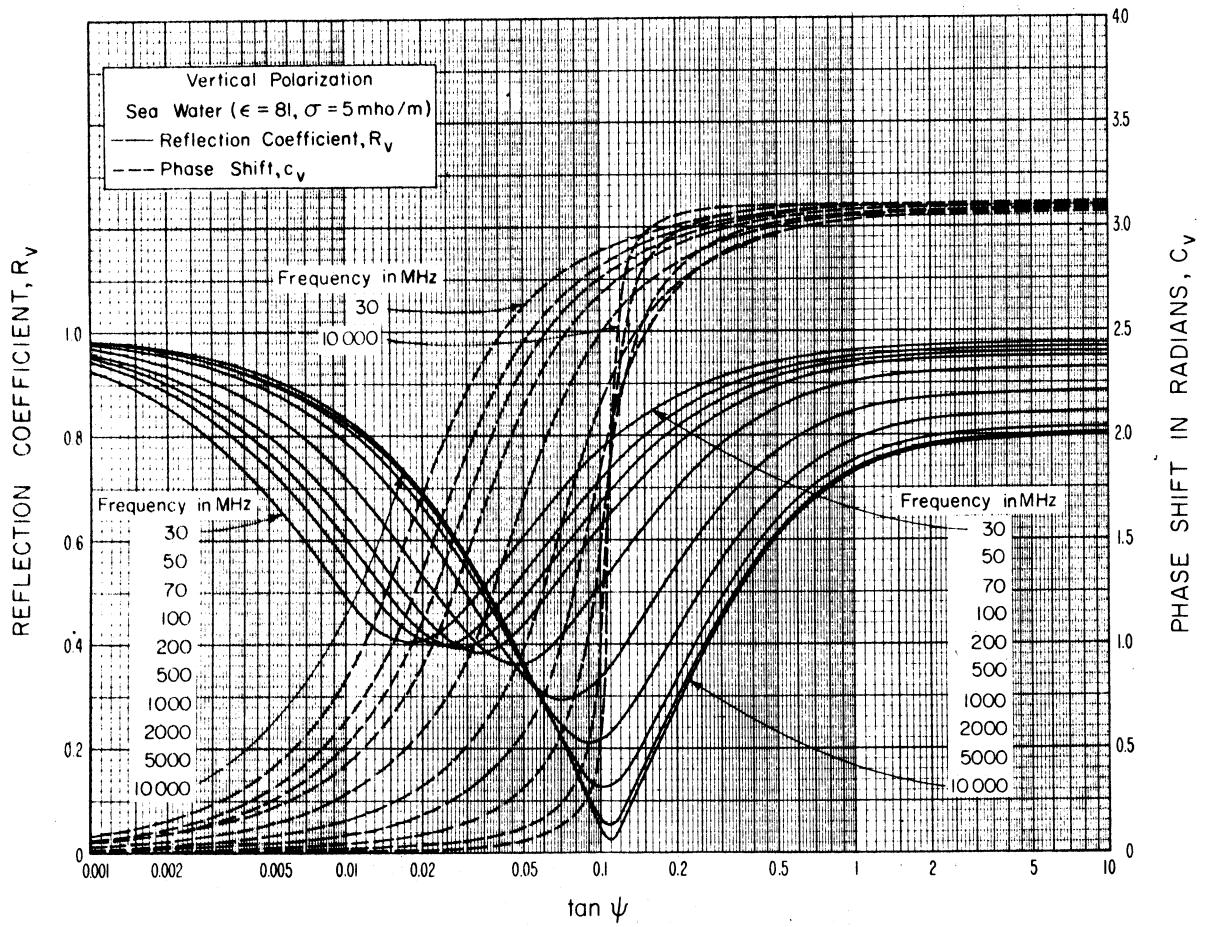


Figure III.1

THE COMPLEX REFLECTION COEFFICIENT $R_e^{i(\pi-c)}$

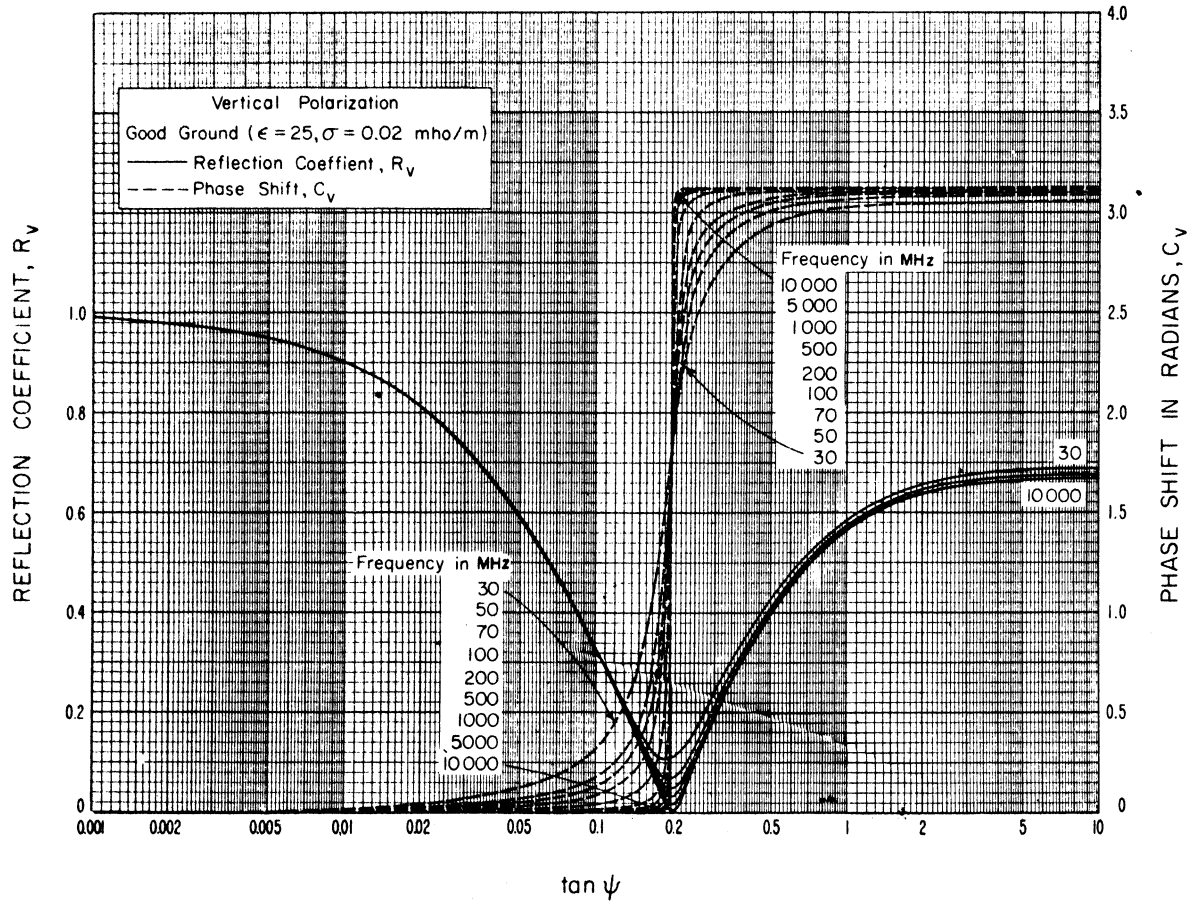


Figure III.2

THE COMPLEX REFLECTION COEFFICIENT $Re^{i(\pi-c)}$

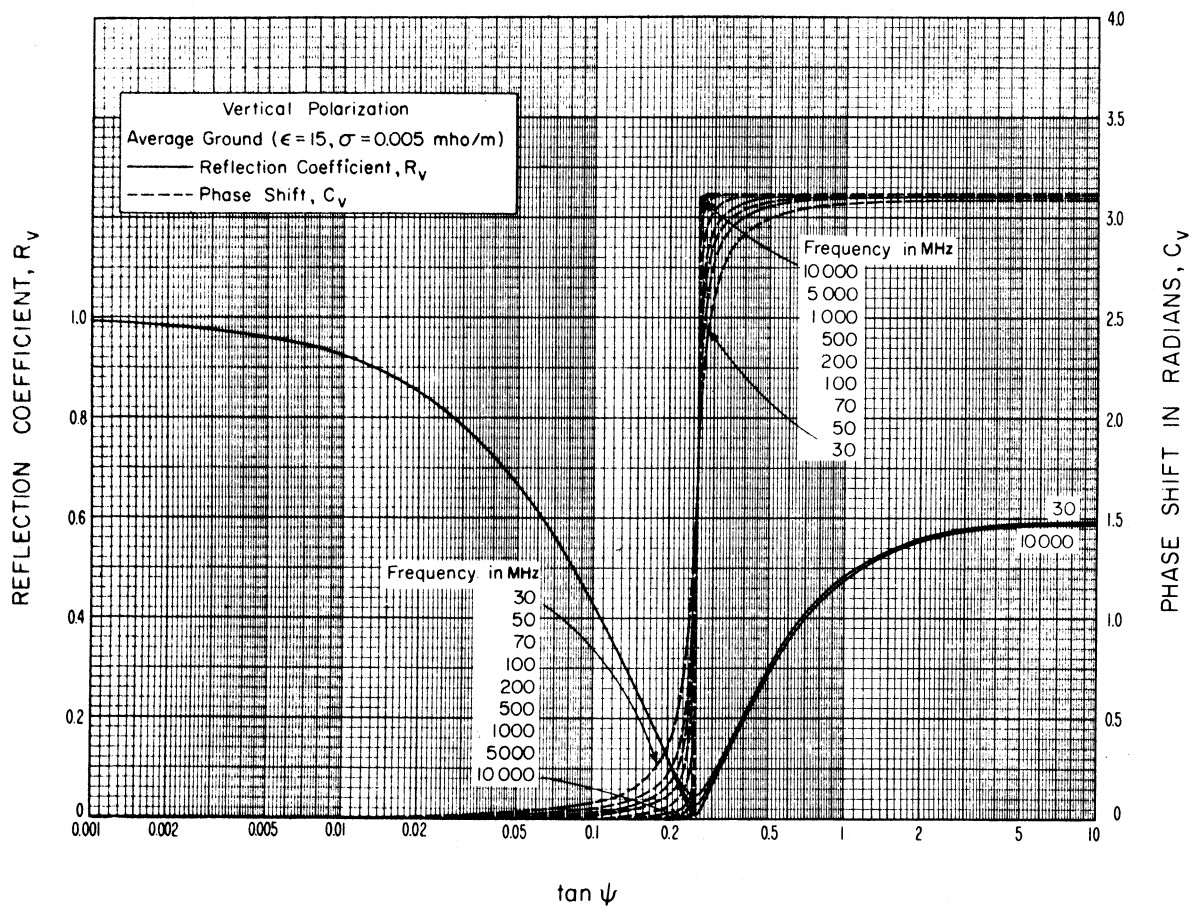


Figure III.3

THE COMPLEX REFLECTION COEFFICIENT $Re^{-i(\pi-c)}$

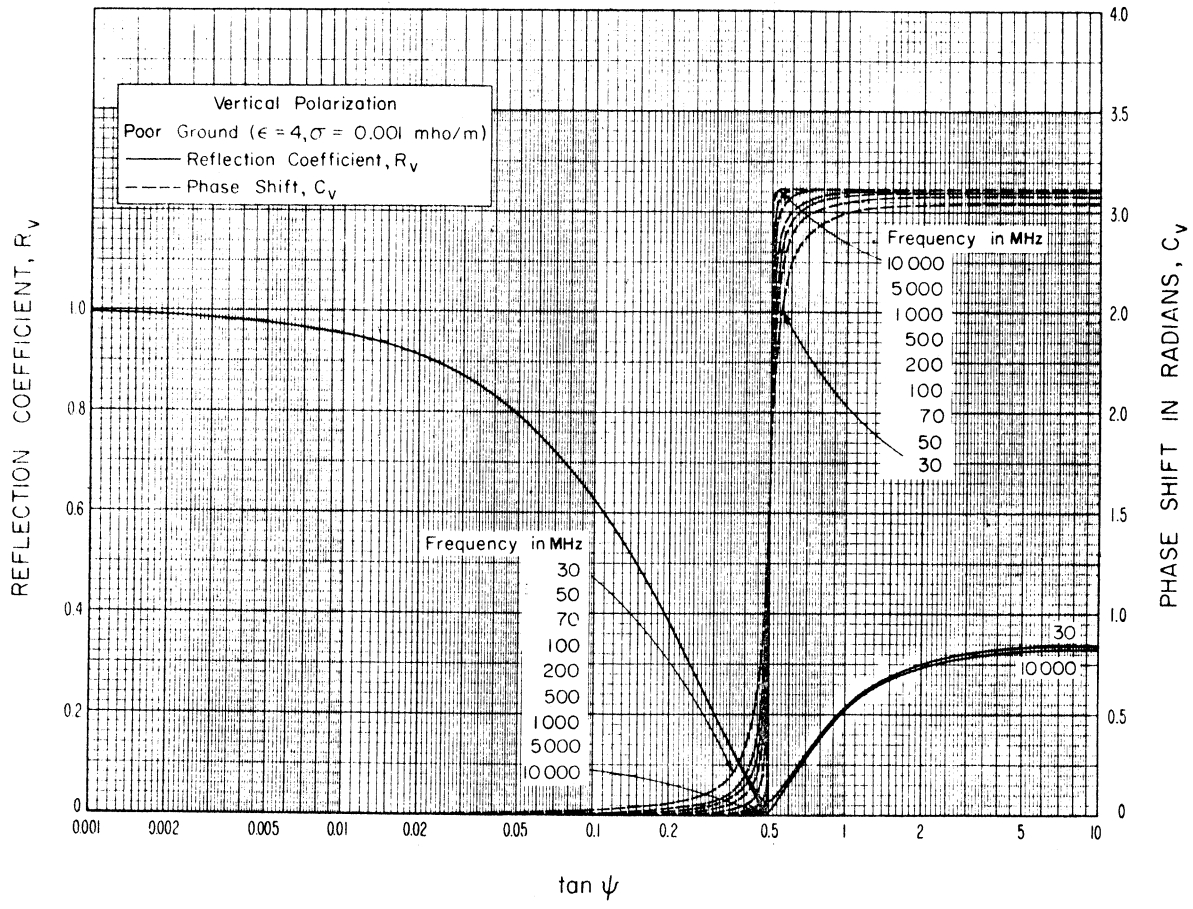


Figure III 4

THE COMPLEX REFLECTION COEFFICIENT $Re^{-i(\pi-c)}$

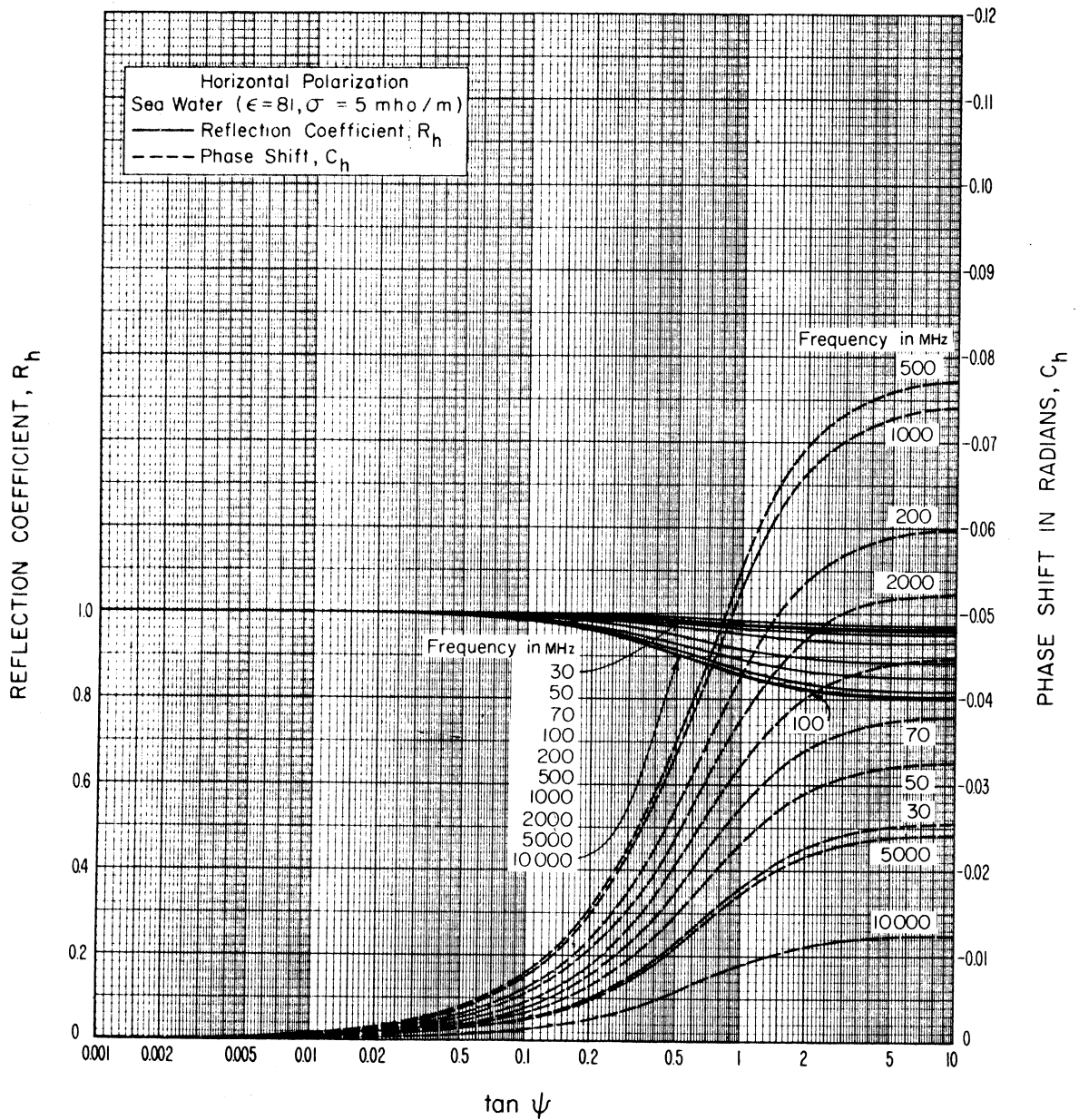


Figure III.5

THE COMPLEX REFLECTION COEFFICIENT $Re^{-i(\pi-c)}$

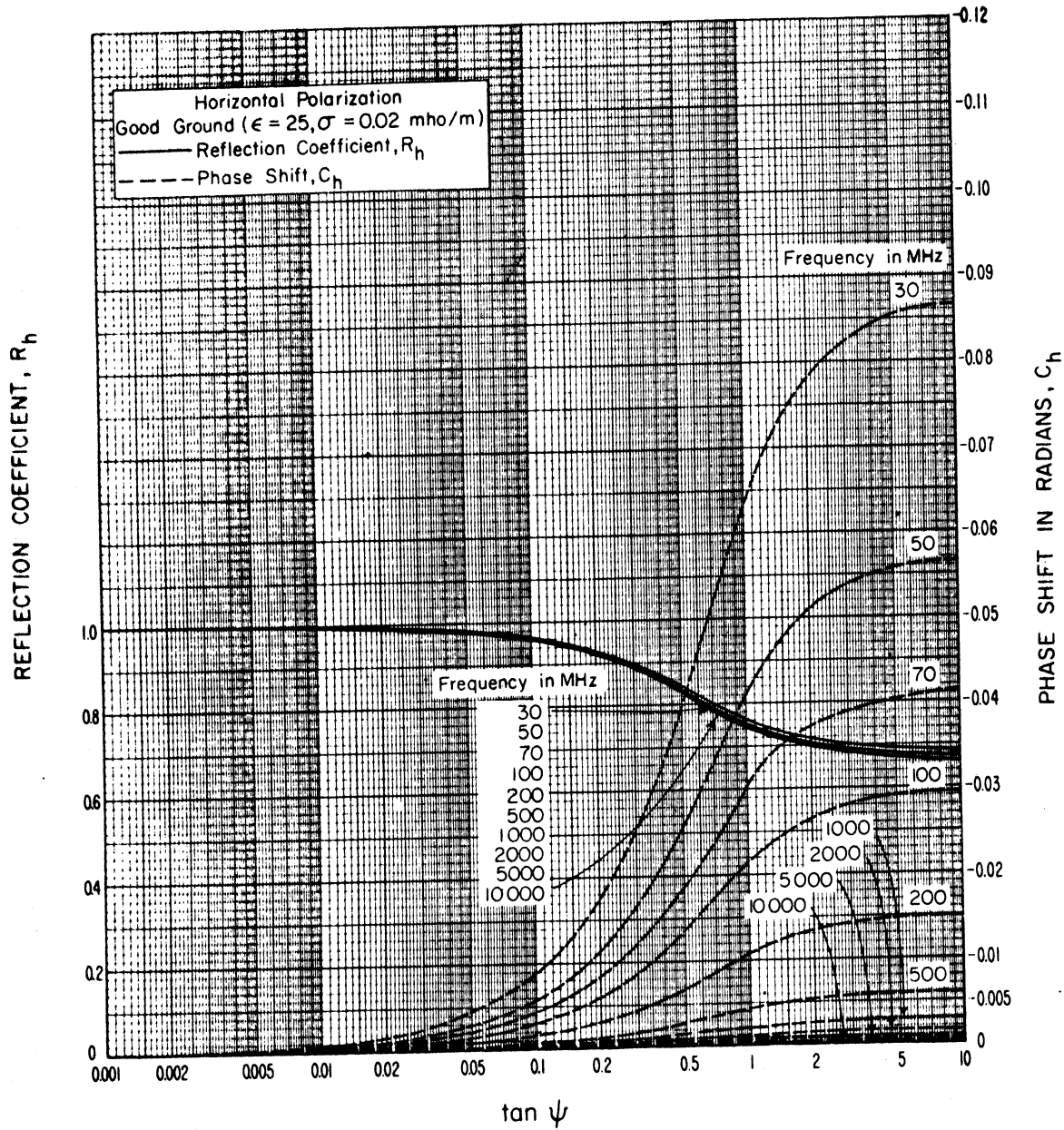


Figure III.6

THE COMPLEX REFLECTION COEFFICIENT $Re^{-i(\pi - c)}$

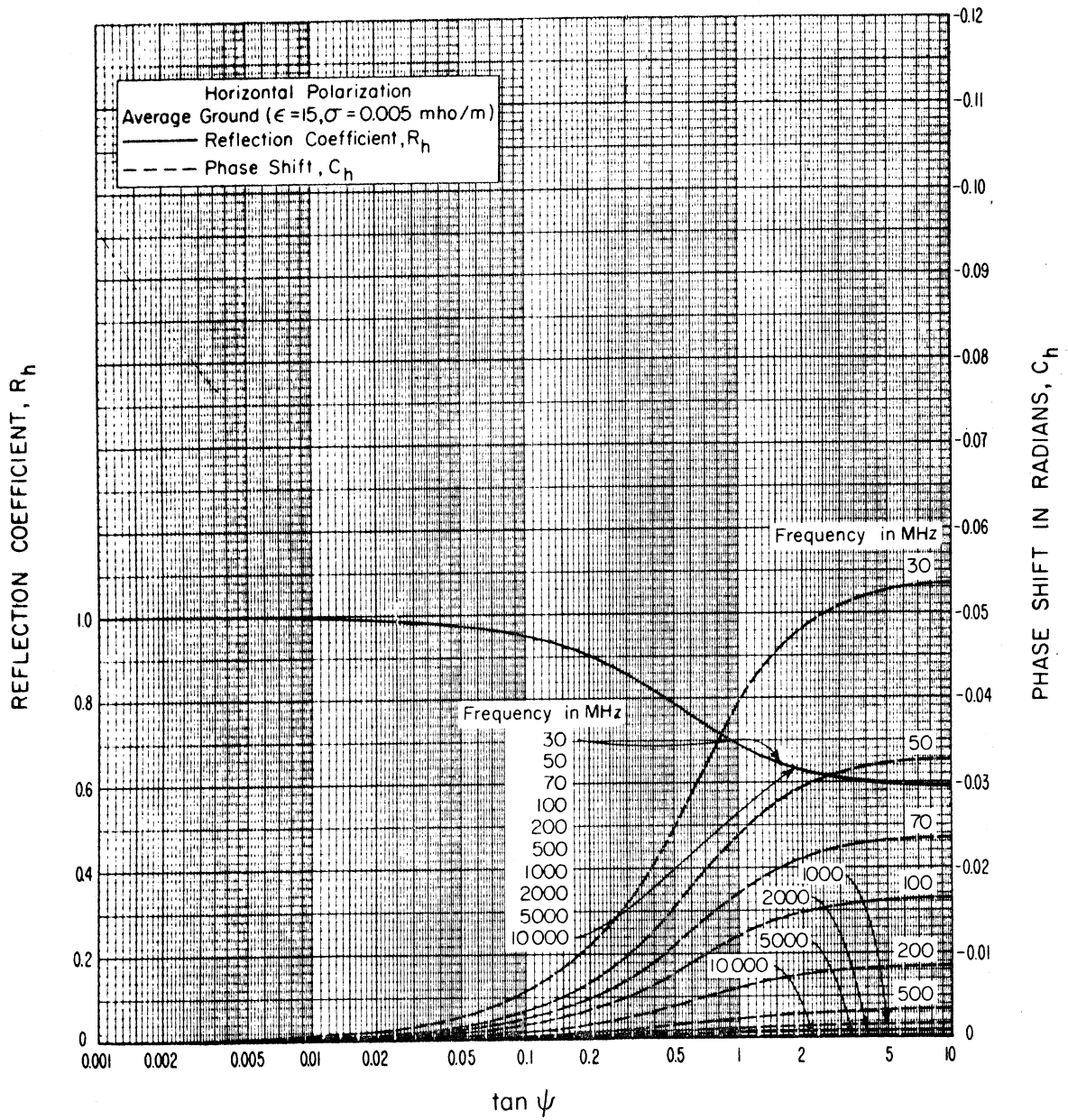


Figure III.7

THE COMPLEX REFLECTION COEFFICIENT $Re^{-i(\pi-c)}$

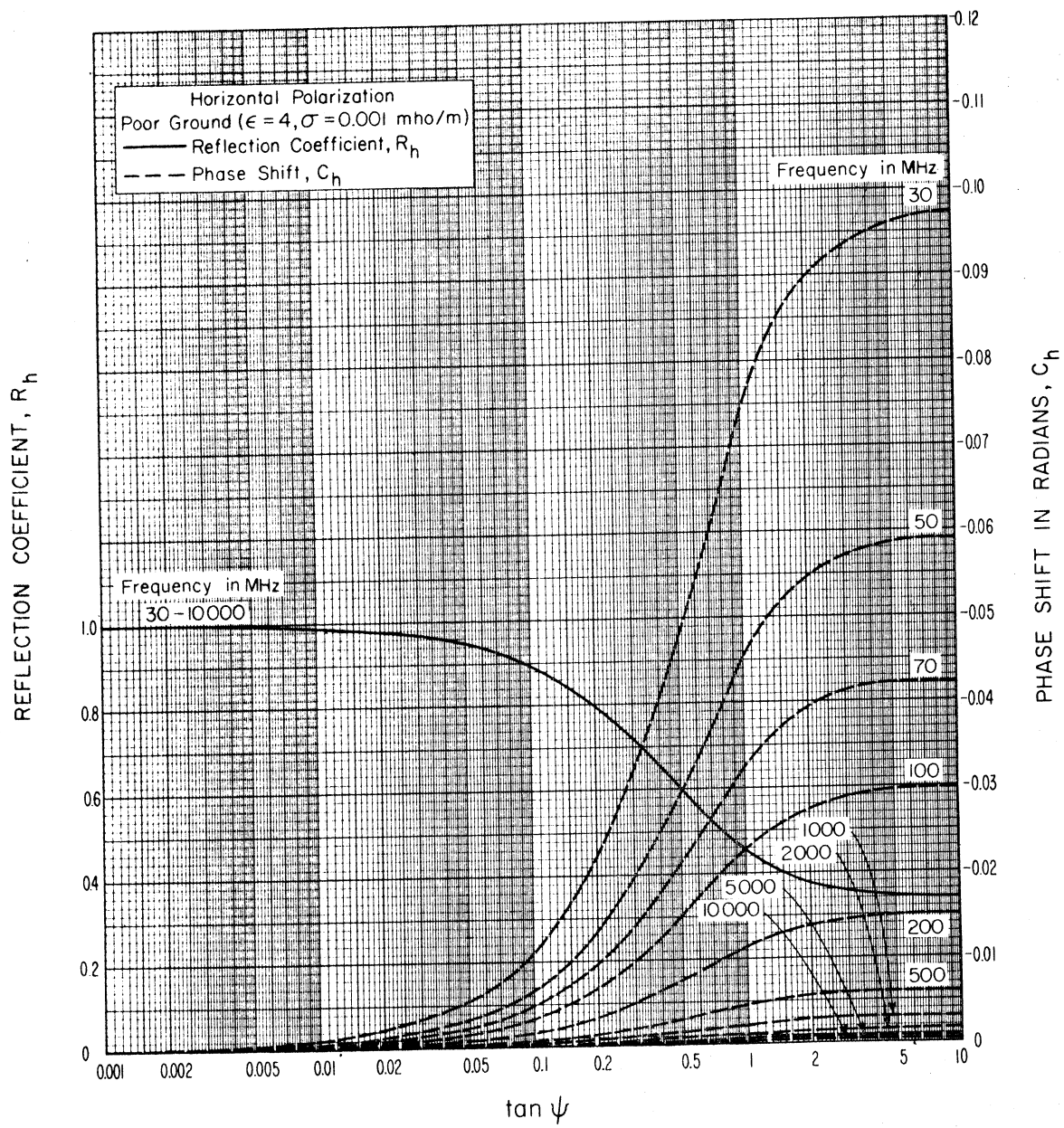


Figure III.8

III.2 Diffraction over a Single Isolated Obstacle.

The theoretical diffraction loss curves on figures 7.1 to 7.4 have been fitted by arbitrary mathematical expressions for convenience in using a digital computer.

The diffraction loss for an isolated rounded obstacle and irregular terrain is given in section 7 as:

$$A(v, \rho) = A(v, 0) + A(0, \rho) + U(v\rho) \text{ db} \quad (7.7)$$

where the parameter v is defined as

$$v = \pm 2\sqrt{\Delta r/\lambda} \cong \pm \sqrt{2d\alpha_o\beta_o/\lambda} \quad (7.1a)$$

or

$$v = \pm 2.5830\sqrt{fd_1d_2/d} \quad (7.1b)$$

and ρ an index of curvature of the rounded obstacles is defined as:

$$\rho = 0.676 r^{1/3} f^{-1/6} [d/r_1r_2]^{1/2} \quad (7.8)$$

For an ideal knife edge, ($\rho = 0$), the diffraction loss is $A(v, 0)$ and is shown on figure 7.1. For values of v from -0.8 to large positive values, this curve may be approximated using the following mathematical expressions:

For $-0.8 \leq v \leq 0$,

$$A(v, 0) = 6.02 + 9.0v + 1.65v^2 \text{ db.} \quad (\text{III. 24a})$$

For $0 \leq v \leq 2.4$,

$$A(v, 0) = 6.02 + 9.11v - 1.27v^2 \quad (\text{III. 24b})$$

For $v > 2.4$,

$$A(v, 0) = 12.953 + 20 \log v \text{ db.} \quad (\text{III. 24c})$$

The theoretical curve for $A(0, \rho)$ is approximated by:

$$A(0, \rho) = 6.02 + 5.556\rho + 3.418\rho^2 + 0.256\rho^3 \text{ db,} \quad (\text{III. 25})$$

and the curve $U(v\rho)$ is approximated as follows:

$$\text{For } v\rho \leq 3: \quad U(v\rho) = 11.45 v\rho + 2.19 (v\rho)^2 - 0.206 (v\rho)^3 - 6.02 \text{ db.} \quad (\text{III. 26a})$$

$$\text{For } 3 < v\rho \leq 5: \quad U(v\rho) = 13.47 v\rho + 1.058 (v\rho)^2 - 0.048 (v\rho)^3 - 6.02 \text{ db.} \quad (\text{III. 26b})$$

$$\text{For } v\rho < 5: \quad U(v\rho) = 20 v\rho - 18.2 \text{ db.} \quad (\text{III. 26c})$$

An average allowance for terrain foreground effects may be made by adding a term $10 \exp(-2.3 \rho)$ to $A(0, \rho)$. This term gives a correction which ranges from 10 db for $\rho = 0$ to 1 db for $\rho = 1$.

When reflections from terrain on either or both sides of the obstacle should be considered, the method given in the following section may be used. This method considers the diffraction loss and phase lag over the diffracting obstacle, and the path length differences and reflection coefficients of the reflected waves.

III. 3 Diffraction over a Single Isolated Obstacle with Ground Reflections

Diffraction over an isolated obstacle is discussed in section 7, where ways of approximating the effects of reflection and diffraction from foreground terrain are indicated. Where the effects of reflection are expected to be of great importance, such as in the case of propagation over a large body of water, the following geometric optics method may be used.

Figure III. 9 illustrates four distinct ray paths over a knife edge (which may be rounded); the first ray is not reflected from the ground, the second and third are each reflected once, and the fourth ray is reflected once on each side of the obstacle. Each ray is subject to a diffraction loss $f_j(v, \rho)$ and a phase lag $\Phi_j(v, \rho) - 90 v_j^2$ at the knife edge, where $j = 1, 2, 3, 4$. Both $f_j(v, \rho)$ and $\Phi_j(v, \rho)$ depend on the parameters v and ρ given in section III. 2. When the isolated obstacle is an ideal knife edge, the diffraction loss depends only on the parameter v , which may be written:

$$v_j = \pm 2\sqrt{\Delta_j/\lambda} \cong \pm \sqrt{2d \alpha_{oj} \beta_{oj}/\lambda} \quad (\text{III. 27})$$

where Δ_j , by figure III. 9, is

$$\begin{aligned} \Delta_1 &= r_{10} + r_{20} - r_{00}, & \Delta_2 &= r_{11} + r_{12} + r_{20} - r_{02} \\ \Delta_3 &= r_{10} + r_{21} + r_{22} - r_{03}, & \Delta_4 &= r_{11} + r_{12} + r_{21} + r_{22} - r_{04} \end{aligned} \quad (\text{III. 28})$$

Path differences Δ_j used to calculate v_j in (III. 27) are closely approximated by the following formulas:

$$\begin{aligned} \Delta_j &= d_r \theta_j^2, \quad d_r = d_1 d_2 / (2d), \quad \theta_j = \theta + \theta_{jr} \\ \theta_{1r} &= 0, \quad \theta_{2r} = 2d_{11} \psi_1 / d_1, \quad \theta_{3r} = 2d_{22} \psi_2 / d_2, \quad \theta_{4r} = \theta_{2r} + \theta_{3r} \end{aligned} \quad (\text{III. 29})$$

The total phase lag for an isolated rounded obstacle path relative to a reference free-space path of length $\Delta_j + r_{0j}$ is given by

$$\Phi_j(v, \rho) - 90 v_j^2 = \phi(v_j, 0) + \phi(0, \rho_j) + \phi(v_j \rho_j) \text{ degrees} \quad (\text{III. 30a})$$

where the functions $\phi(v, 0)$, $\phi(0, \rho)$, and $\phi(v\rho)$ are plotted as dashed curves on figures 7. 1, 7. 4, and 7. 5. For an ideal knife edge, where the radius of curvature of the crest is zero, $\rho = 0$, and (III. 30a) reduces to

$$\text{for } v > 0 \quad \Phi_j(v, 0) - 90 v_j^2 = \phi(v_j, 0) \text{ degrees} \quad (\text{III. 30b})$$

$$\text{for } v \leq 0 \quad \Phi_j(v, 0) - 90 v_j^2 = \phi(v_j, 0) - 90 v_j^2 \text{ degrees} \quad (\text{III. 30c})$$

The three components of the received field which are affected by reflection from the earth's surface depend also upon effective ground reflection coefficients $R_{e2} \exp[-i(\pi - c_2)]$ and $R_{e3} \exp[-i(\pi - c_3)]$, defined in section 5, and upon ray path differences Δ_{2r} and Δ_{3r} :

$$\begin{aligned}\Delta_{2r} &= r_{11} + r_{12} - r_{10} \approx 2 \psi_1^2 d_{11} d_{12}/d_1 \\ \Delta_{3r} &= r_{21} + r_{22} - r_{20} \approx 2 \psi_2^2 d_{21} d_{22}/d_2.\end{aligned}\quad (\text{III. 31})$$

Usually, it may be assumed that $c_2 = c_3 = 0$ so that the reflection coefficients are $-R_{e2}$ and $-R_{e3}$.

Introducing the propagation constant $k = 2\pi/\lambda$ rad/meter = 360/ λ degrees/meter and expressing the ray path differences $k \Delta_{2r}$ and $k \Delta_{3r}$ in electrical degrees, the attenuation relative to free space is then

$$\begin{aligned}A = -20 \log \left\{ \left| f_1 \exp[-i(\Phi_1 - 90 v_1^2)] - R_{e2} f_2 \exp[-i(\Phi_2 - 90 v_2^2 + k \Delta_{2r})] \right. \right. \\ \left. \left. - R_{e3} f_3 \exp[-i(\Phi_3 - 90 v_3^2 + k \Delta_{3r})] + R_{e2} R_{e3} f_4 \exp[-i(\Phi_4 - 90 v_4^2 + k \Delta_{2r} + k \Delta_{3r})] \right| \right\} \text{ db}\end{aligned}\quad (\text{III. 32})$$

For the general case of a rounded knife-edge, the magnitudes $f_j \equiv f_j(v, \rho)$ are determined from

$$\log f_j(v, \rho) = -A_j(v, \rho)/20, \quad (\text{III. 33})$$

where $A(v, \rho)$ is defined in (7.7) and shown graphically on figure 7.3. The total phase lag $\Phi_j \equiv \Phi_j(v, \rho)$ relative to a reference free space path of length r_{0j} is defined in (7.13a) and (III.30a). Components for $A(v, \rho)$ and $\Phi(v, \rho)$ are shown graphically in figures 7.1, 7.4 and 7.5. Approximate expressions for the components of $A(v, \rho)$ are given in section III.2.

For the ideal knife-edge, $\rho = 0$, and the f_j and Φ_j may be calculated from:

$$\begin{aligned}f_j = +\frac{1}{2} \sqrt{(1 - C_j - S_j)^2 + (C_j - S_j)^2}, \quad \tan \Phi_j = \frac{C_j - S_j}{1 - C_j - S_j} \\ C_j = \int_0^{v_j} \cos\left(\frac{\pi t^2}{2}\right) dt, \quad S_j = \int_0^{v_j} \sin\left(\frac{\pi t^2}{2}\right) dt.\end{aligned}\quad (\text{III. 34})$$

Pearcey [1956], and the NBS AMS 55 Handbook of Mathematical Functions [1964] give complete tables, series expansions, and asymptotic expressions for the Fresnel integrals C_j and S_j . Furthermore, if v is larger than 3;

$$f_j \approx 0.22508/v_j, \quad \Phi_j - 90 v_j^2 \approx 45 \text{ degrees} \quad (\text{III. 35})$$

Figure III. 10 is a nomogram which may be used in the determination of $f(v_j)$ and $\bar{f}(v_j)$ for both positive and negative values of v . This nomogram is based on the representation of Fresnel integrals by the Cornu spiral.

After θ , d , d_1 , d_2 , d_{11} , d_{12} , d_{21} , d_{22} , ψ_1 , and ψ_2 , as shown in figure III. 9 have been determined, the following procedure may be used.

1. Calculate θ_j and Δ_j for $j = 1, 2, 3, 4$, using (III. 29).
2. Calculate v_j , C_j , S_j , f_j , and $\bar{f}_j - 90 v_j^2$ using (III. 27), (III. 34), (III. 30) and figures in section 7 or equivalent mathematical approximations.
3. Calculate Δ_{2r} and Δ_{3r} from (III. 31).
4. Calculate R_{e2} and R_{e3} from (5. 1), or assume that $R_{e2} = R_{e3} = 1$.
5. Substitute these values in (III. 32).

To check the calculation of each v_j , the approximation given in (III. 27) may be used, with the following formulas for $\alpha_{oj} = d_2 \theta_j/d$ and $\beta_{oj} = d_1 \theta_j/d$:

$$\begin{aligned}
 \alpha_{01} &= d_2 \theta/d & \beta_{01} &= d_1 \theta/d \\
 \alpha_{02} &= \alpha_{01} + 2 d_{11} \psi_1 d_2 / (d_1 d) & \beta_{02} &= \beta_{01} + 2 d_{11} \psi_1 / d \\
 \alpha_{03} &= \alpha_{01} + 2 d_{22} \psi_2 / d & \beta_{03} &= \beta_{01} + 2 d_{22} \psi_2 d_1 / (d_2 d) \\
 \alpha_{04} &= \alpha_{02} + \alpha_{03} - \alpha_{01} & \beta_{04} &= \beta_{02} + \beta_{03} - \beta_{01} \quad (\text{III. 36})
 \end{aligned}$$

A special case will be described for which (III. 29) and (III. 31) may be simplified. Assume that each reflecting surface may be considered a plane. Let h_t and h_{tm} be the heights of the transmitting antenna and the knife edge above the first plane, and let h_{rm} and h_r be the heights of the knife edge and the receiving antenna above the second reflecting plane. Assume that Δr is very small for every Δ . In terms of the heights h_t , h_{tm} , h_{rm} , h_r , the parameters θ , d_1 , and d_2 and the parameter $d_r \equiv d_1 d_2 / (2d)$:

$$\begin{aligned}
 \Delta_{2r} &= 2 h_t h_{tm} / d_1, \quad \Delta_{3r} = 2 h_r h_{rm} / d_2 \\
 \Delta_1 &= d_r \theta^2, \quad \Delta_2 = d_r (0 + h_{tm} \Delta_{2r})^2 \\
 \Delta_3 &= d_r (0 + h_{rm} \Delta_{3r})^2, \quad \Delta_4 = d_r (0 + h_{tm} \Delta_{2r} + h_{rm} \Delta_{3r})^2. \quad (\text{III. 37})
 \end{aligned}$$

~~$$\Delta_{2r} = h_t \left[\sqrt{\theta_{ht}^2 + 4h_t/(3a) + \theta_{ht}} \right], \quad \Delta_{3r} = h_r \left[\sqrt{\theta_{hr}^2 + 4h_r/(3a) + \theta_{hr}} \right] \quad \text{(III. 38)}$$~~

~~For this special case, the formulas (III.29) for Δ_j may be simplified by writing~~

~~$$\theta_{2r} = \Delta_{2r}^2 d_1 / (2h_t), \quad \theta_{3r} = \Delta_{3r}^2 d_2 / (2h_r). \quad \text{(III. 39)}$$~~

BEYOND-HORIZON KNIFE-EDGE DIFFRACTION WITH GROUND REFLECTIONS

(KNIFE-EDGE NORMAL TO RAY PATH)

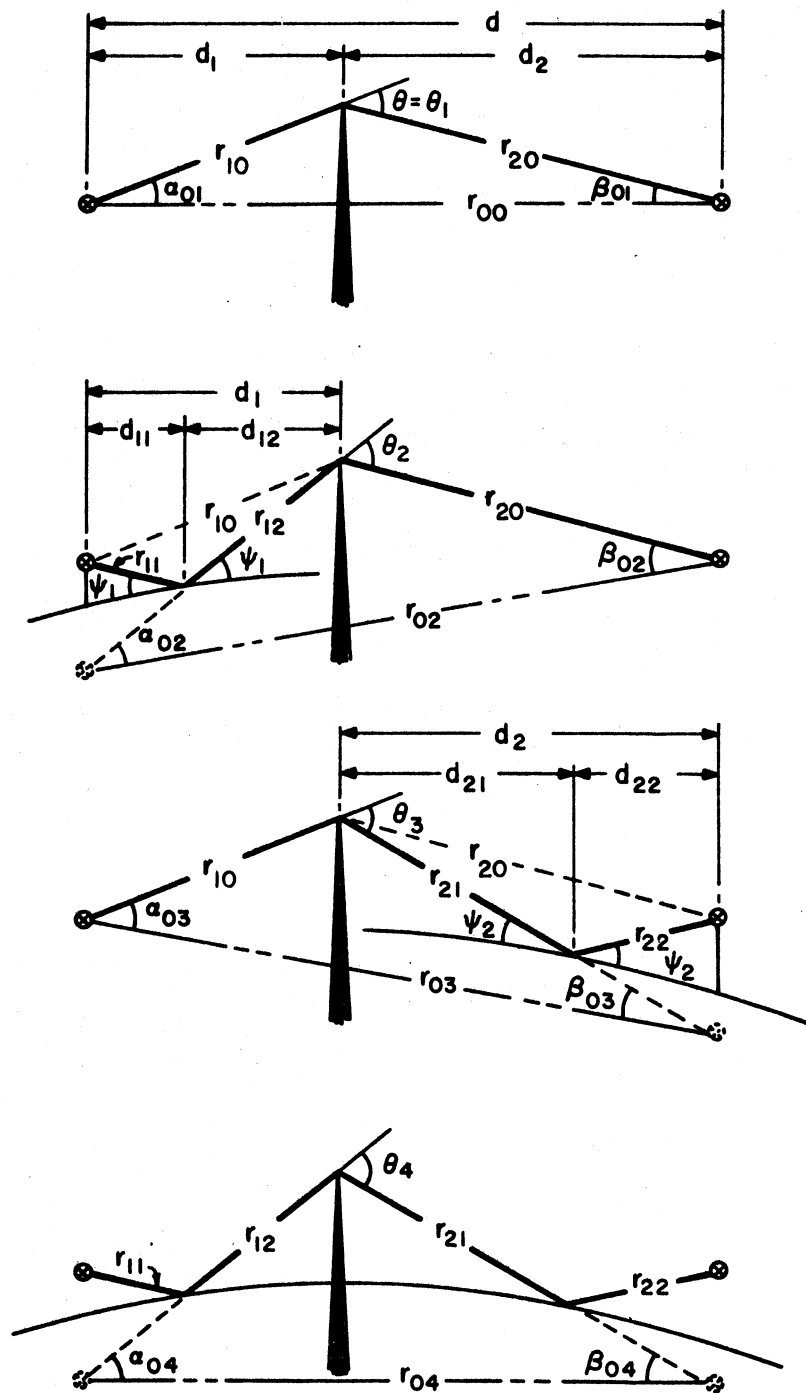


Figure III.9

CORNU'S SPIRAL

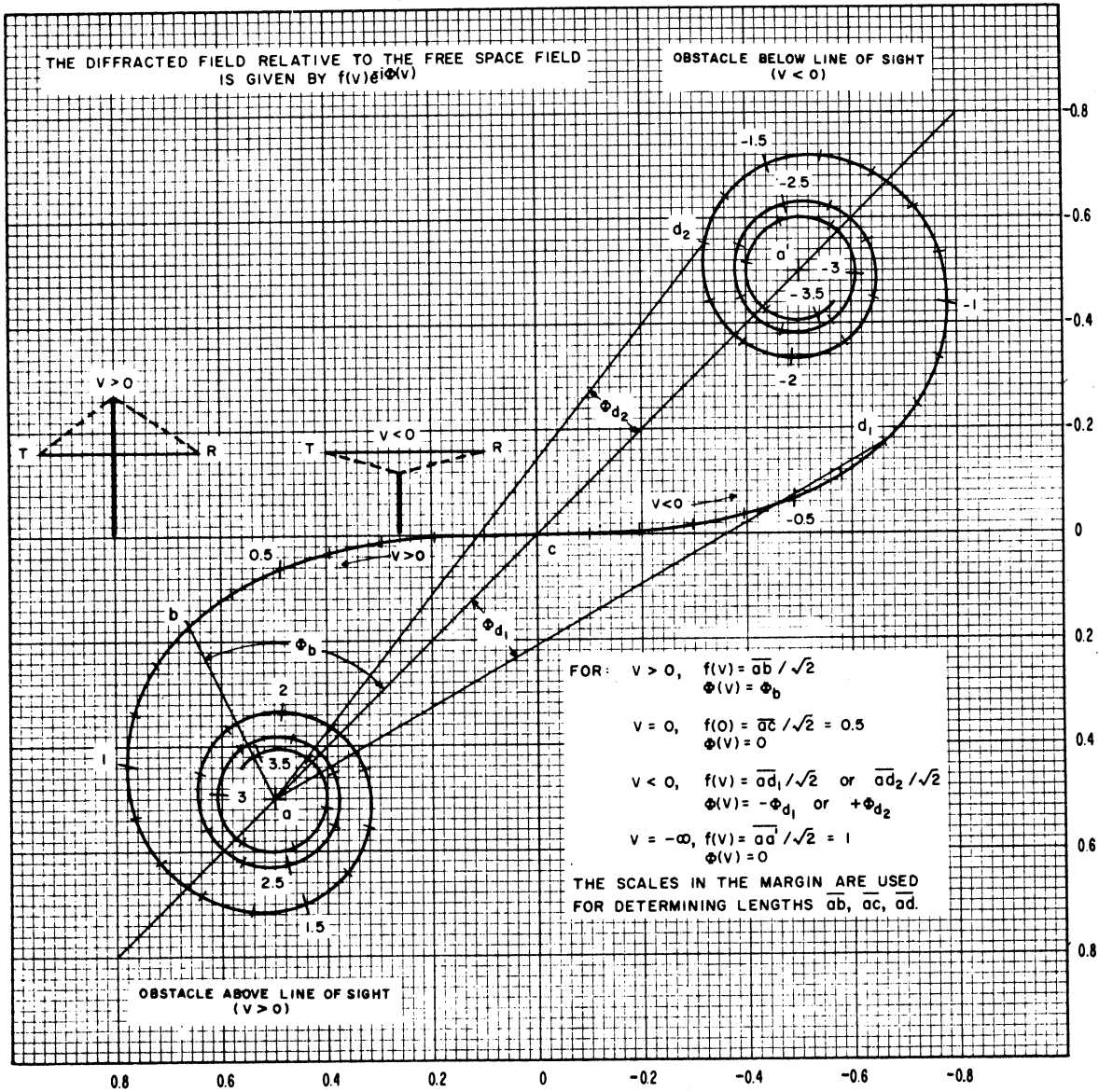


Figure III.10

III.4 Parameters K and b° for Smooth Earth Diffraction

In section 8, the parameters K and b° are shown on figures 8.1 and 8.2 for horizontally and vertically polarized waves for poor, average, and good ground, and for sea water.

Assume a homogeneous ground in which the relative dielectric constant ϵ and conductivity σ of the ground are everywhere constant. K and b° are defined as follows:

For horizontal polarization,

$$K_h = 1.7778 \times 10^{-2} C_o f^{-\frac{1}{3}} [(\epsilon-1)^2 + x^2]^{-\frac{1}{4}} \quad (\text{III. 40a})$$

$$b_h = 180^\circ - \tan^{-1} \left(\frac{\epsilon-1}{x} \right) \text{ degrees.} \quad (\text{III. 40b})$$

For vertical polarization,

$$K_v = (\epsilon^2 + x^2)^{\frac{1}{2}} K_h \quad (\text{III. 41a})$$

$$b_v = 2 \tan^{-1} (\epsilon/x) - \tan^{-1} \left(\frac{\epsilon-1}{x} \right) \text{ degrees} \quad (\text{III. 41b})$$

where x depends on the ground conductivity σ , in mhos per meter, and the radio frequency f , in megacycles per second, and has been defined by (III. 7) as

$$x = 1.8 \times 10^4 \sigma / f$$

C_o is defined in section 8 as

$$C_o = (8497/a)^{\frac{1}{3}}$$

where a is the effective earth's radius in kilometers.

When $\sigma/f \gg (\epsilon/2) \times 10^{-4}$, the parameters K and b° may be written as

$$K_h \approx 1.325 \times 10^{-4} C_o f^{1/6} \sigma^{-1/2}, \quad b_h \approx 180^\circ \quad (\text{III. 42})$$

$$K_v \approx 2.385 C_o \sigma^{1/2} f^{-5/6}, \quad b_v \approx 0^\circ \quad (\text{III. 43})$$

and when $\sigma/f \ll (\epsilon/2) \times 10^{-4}$, the parameters K and b° may be written as

$$K_h \approx 1.7778 \times 10^{-2} C_o f^{-\frac{1}{3}} (\epsilon-1)^{-\frac{1}{2}}, \quad b_h \approx 90^\circ \quad (\text{III. 44})$$

$$K_v \approx \epsilon K_h, \quad b_v \approx 90^\circ \quad (\text{III. 45})$$

III.5 Forward Scatter

The attenuation function $F(\theta d)$ for $N_s = 250, 301, 350,$ and 400 , shown in figure 9.1, may be used for most land-based scatter links. When a path is highly asymmetrical, the attenuation for a given value of θd is less than it would be for a symmetrical path.

Figures III.11 to III.14 show the function $F(\theta d)$ for values of s from 0.01 to 1, and for $N_s = 250, 301, 350$ and 400 . For values of $\theta d \leq 10$, the effect of asymmetry is negligible, but increases with increasing θd , particularly when $s < 0.5$.

For values of s between 0.7 and 1, the function $F(\theta d)$ for $N_s = 301$ may be computed as follows:

$$\text{for } 0.01 \leq \theta d \leq 10, \quad F(\theta d) = 135.82 + 0.33 \theta d + 30 \log(\theta d) \quad (\text{III.46})$$

$$\text{for } 10 \leq \theta d \leq 70, \quad F(\theta d) = 129.5 + 0.212 \theta d + 37.5 \log(\theta d) \quad (\text{III.47})$$

$$\text{for } \theta d \geq 70, \quad F(\theta d) = 119.2 + 0.157 \theta d + 45 \log(\theta d). \quad (\text{III.48})$$

The function $F(\theta d)$ may be obtained for any value of N_s , by modifying the value computed for $N_s = 301$:

$$F(\theta d, N_s) = F(\theta d, N_s = 301) - \left[0.1(N_s - 301) e^{-\theta d/40} \right].$$

The frequency gain function, H_o , for the special case $h_{te} = h_{re}$ frequently used in systems design, is shown as a function of r on figures III.15 to III.19 for $\eta_s = 1, 2, 3, 4, 5$, and for $s = 1, 0.5, 0.25$ and 0.1 . In this case, no correction factor ΔH_o is required.

The function H_o for $\eta_s = 0$, shown on figure 9.5 corresponds to the assumption of a constant atmospheric refractive index. Except for the special case where $h_{te} = h_{re}$ this function may be computed as follows:

$$H_o(\eta_s = 0) = 10 \log \left\{ \frac{2(1 - h_{re}^2/h_{te}^2)}{r_2^2 [h(r_1) - h(r_2)]} \right\} \quad (\text{III.49})$$

where $r_1 = 4\pi\theta h_{te}/\lambda$, $r_2 = 4\pi\theta h_{re}/\lambda$,

$$h(r_1) = r_1 f(r_1), \quad f(r_1) = \text{Ci}(r_1) \sin r_1 + [\pi/2 - \text{Si}(r_1)] \cos r_1 \quad (\text{III. 50})$$

and

$$h(r_2) = r_2 f(r_2), \quad f(r_2) = \text{Ci}(r_2) \sin r_2 + [\pi/2 - \text{Si}(r_2)] \cos r_2$$

$$\text{Ci}(r) = \int_{\infty}^r \frac{\cos t}{t} dt, \quad \text{Si}(r) = \int_0^r \frac{\sin t}{t} dt. \quad (\text{III. 51})$$

Values of the sine integral $\text{Si}(r)$ and the cosine integral $\text{Ci}(r)$ for arguments from 10 to 100 are tabulated in volume 32 of the U. S. NBS Applied Math Series [1954]. See also [NBS AMS 1964]. The function $h(r)$ is shown graphically in figures III.20 and III.21.

For the special case of equal effective antenna heights, $h_{te} = h_{re}$, equation (III.49) is not applicable. In this case $H_o(\eta_s = 0)$ is computed as:

$$H_o(\eta_s = 0) = 10 \log \left\{ \frac{4}{r^2 [h(r) - r g(r)]} \right\} \quad (\text{III. 52})$$

where

$$g(r) = \text{Ci}(r) \cos r - [\pi/2 - \text{Si}(r)] \sin r \quad (\text{III. 53})$$

When the effective height of one antenna is very much greater than that of the other, the computation may be simplified as follows:

$$\text{For } r_2 \ll r_1, \quad H_o(\eta_s = 0) = 10 \log \left\{ \frac{2}{r_2^2 [1 - h(r_2)]} \right\} \quad (\text{III. 54a})$$

$$\text{For } r_2 \gg r_1, \quad H_o(\eta_s = 0) = 10 \log \left\{ \frac{2}{r_1^2 [1 - h(r_1)]} \right\}. \quad (\text{III. 54b})$$

THE FUNCTION $F(\theta d)$ FOR $N_s = 250$

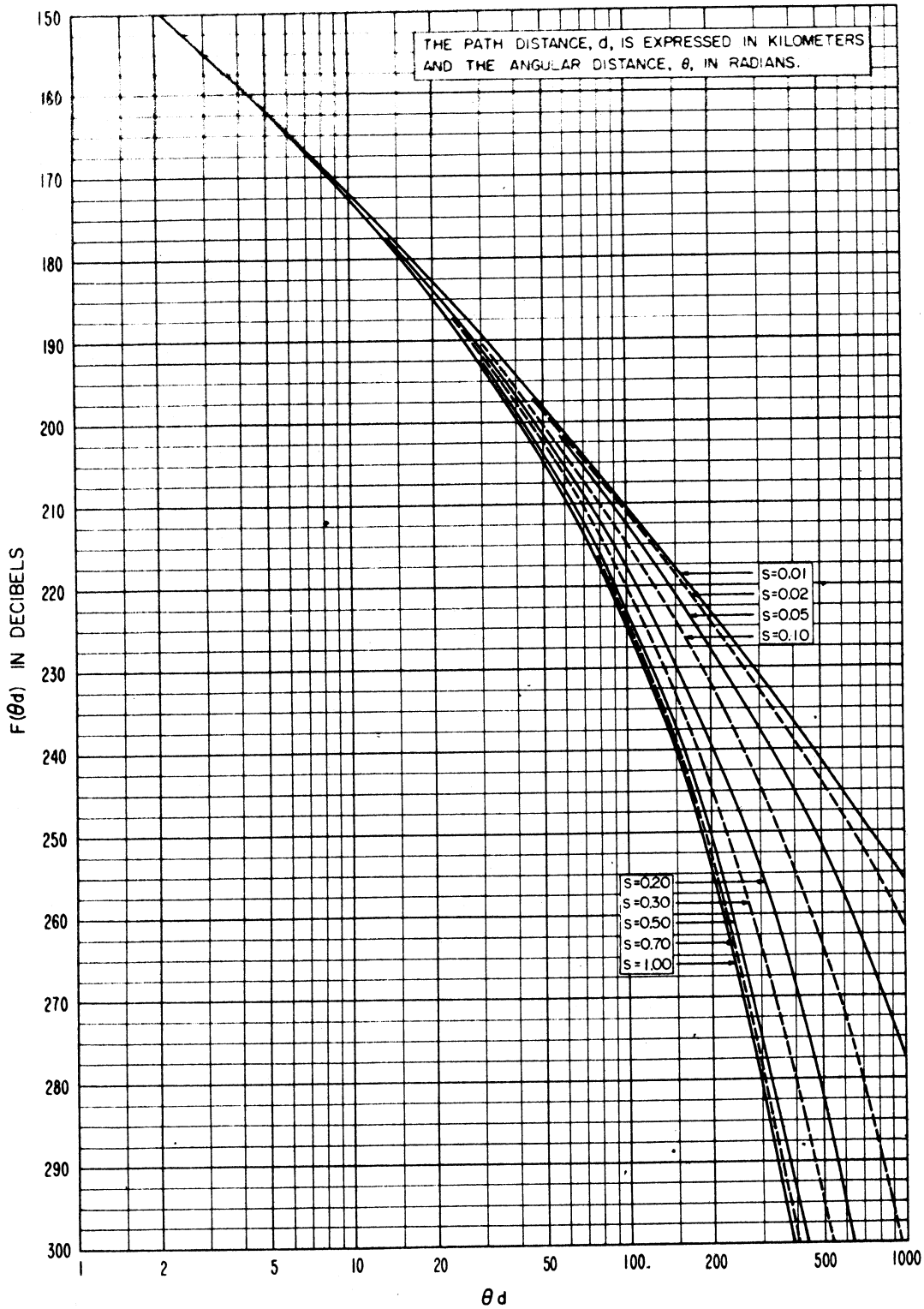


Figure III.11

THE FUNCTION $F(\theta d)$ FOR $N_s = 301$

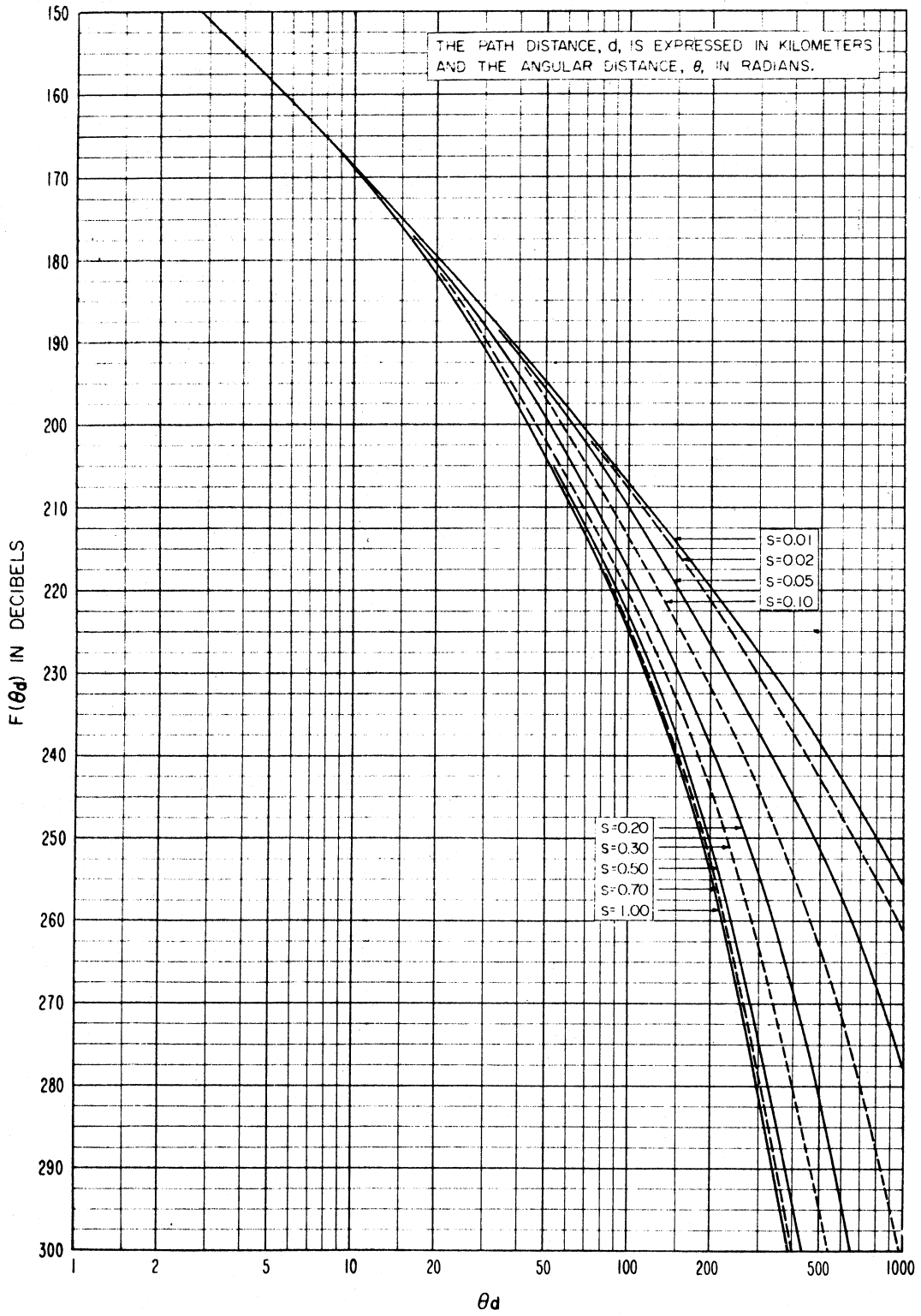


Figure III.12

THE FUNCTION $F(\theta_d)$ FOR $N_s = 350$

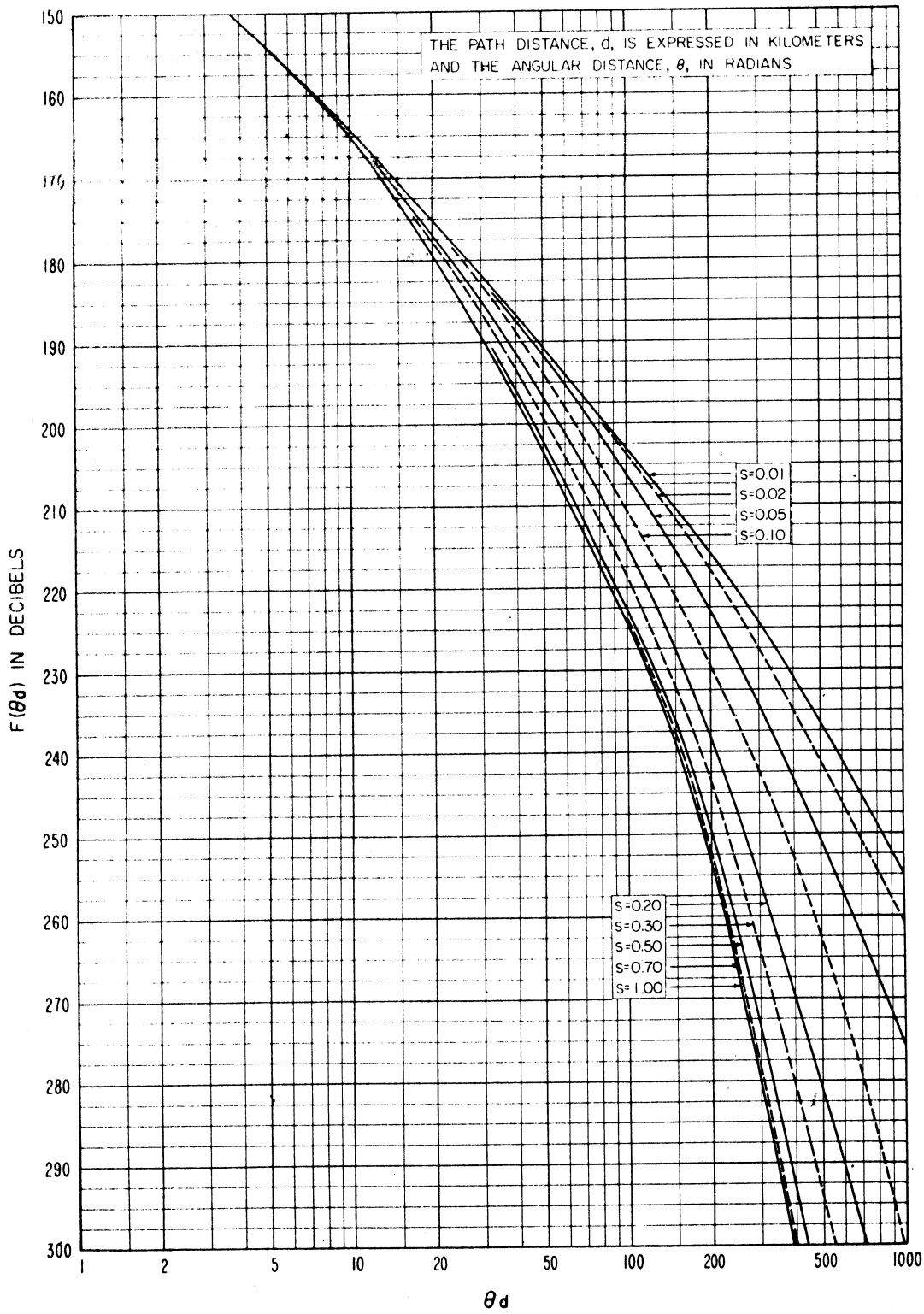


Figure III.13

THE FUNCTION $F(\theta_d)$ FOR $N_s = 400$

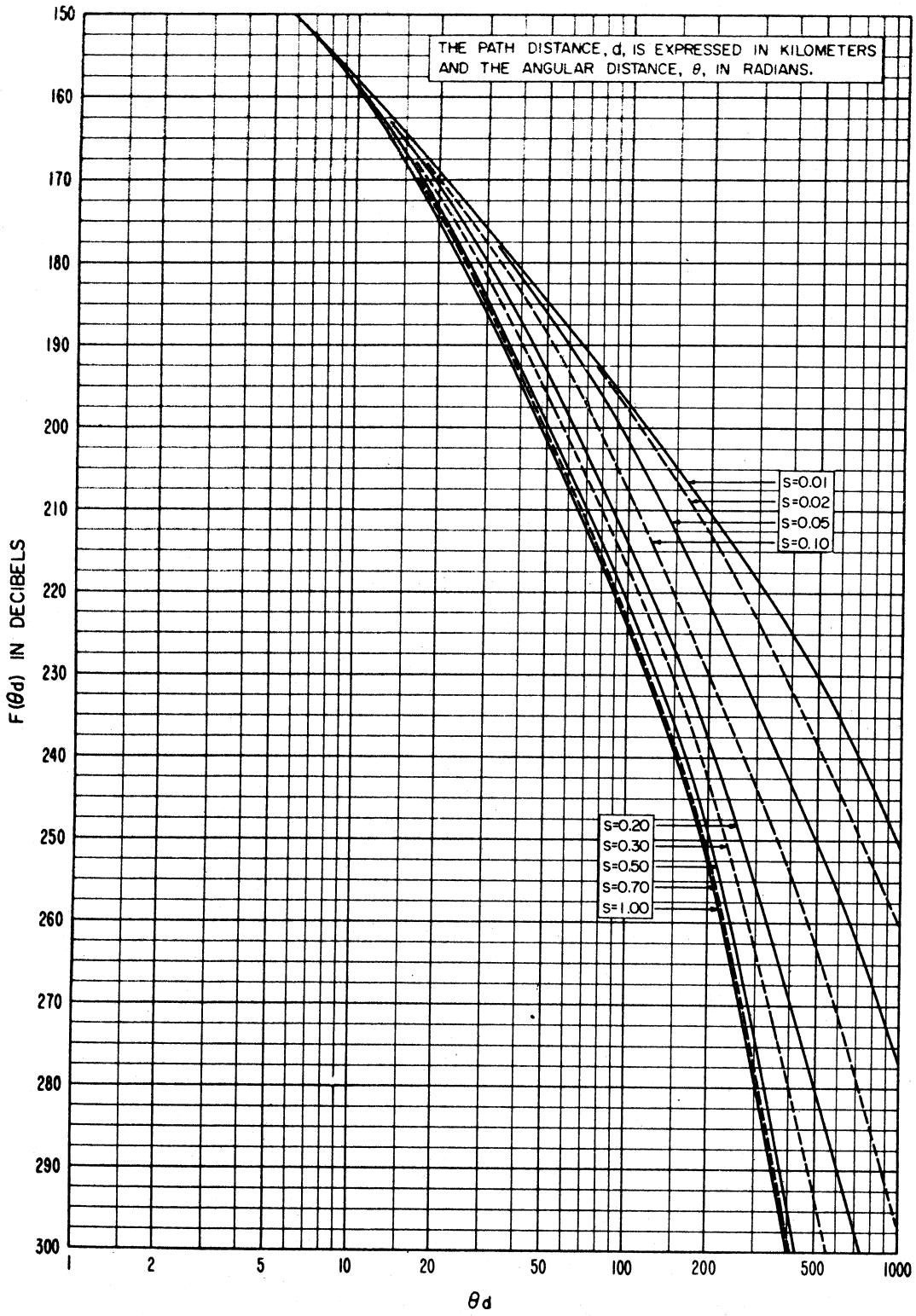


Figure III.14

THE FREQUENCY GAIN FUNCTION, H_0
 $h_{te} = h_{re}$

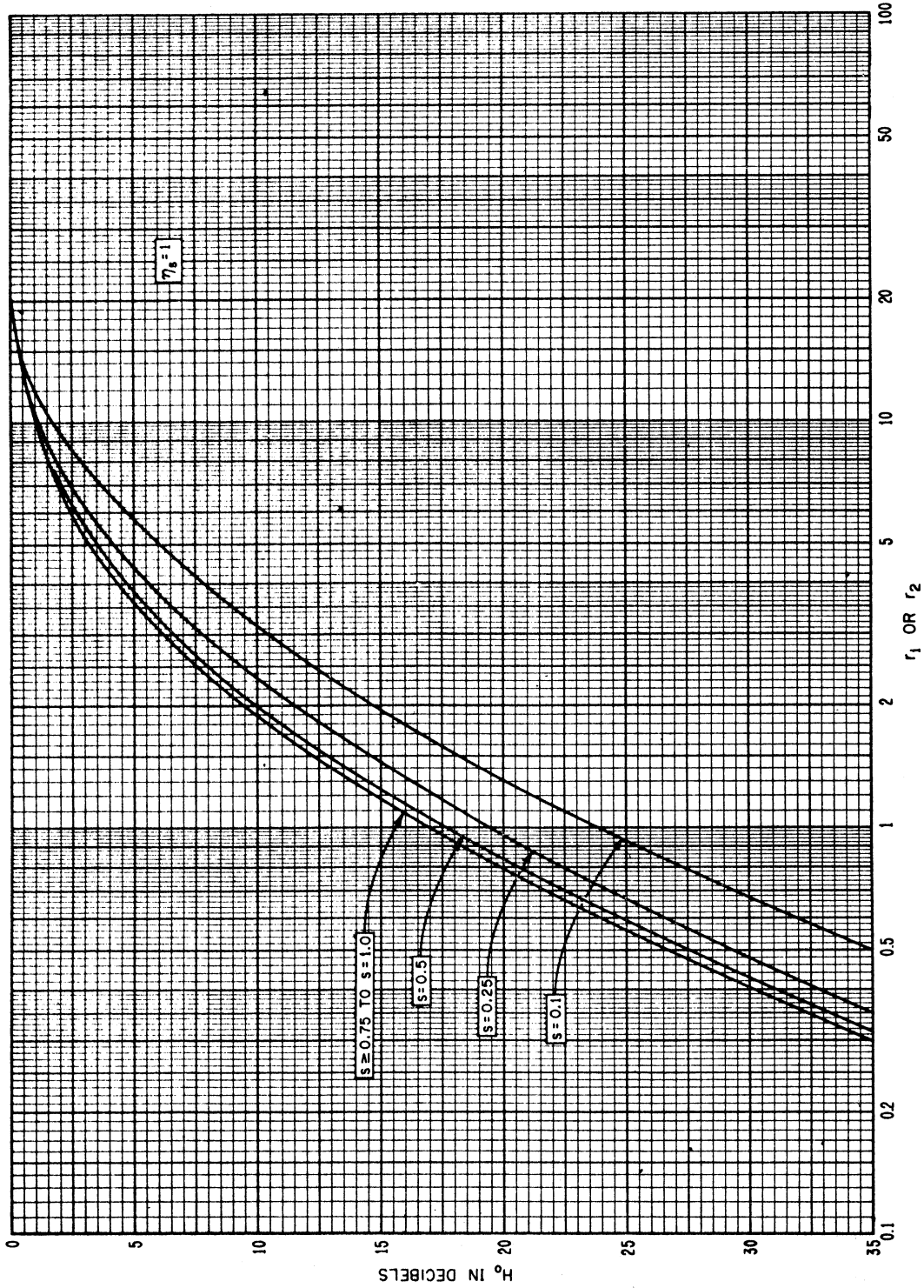


Figure III.15

THE FREQUENCY GAIN FUNCTION, H_o
 $h_{te} = h_{re}$

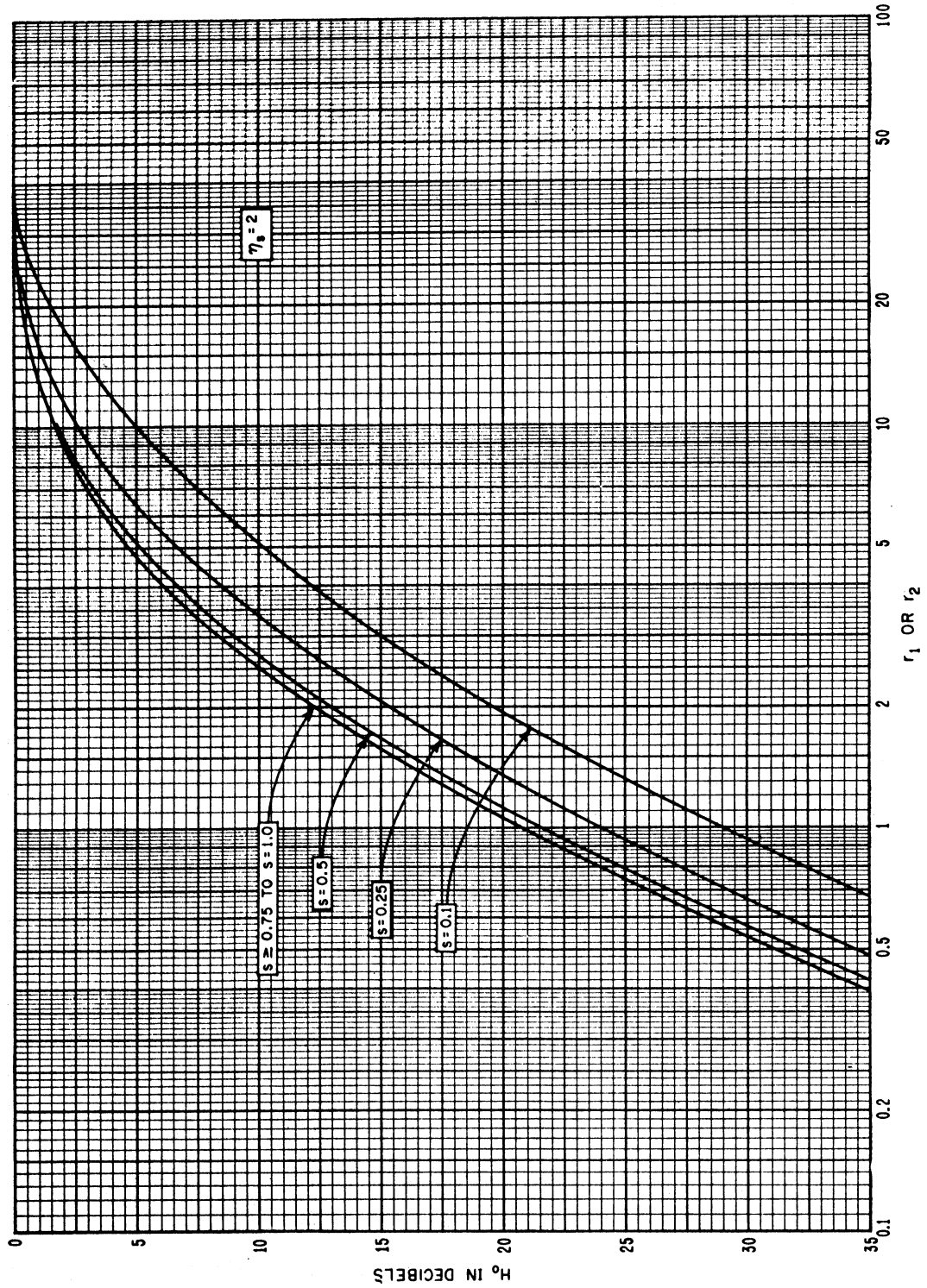


Figure III .16

THE FREQUENCY GAIN FUNCTION, H_0
 $h_{te} = h_{re}$

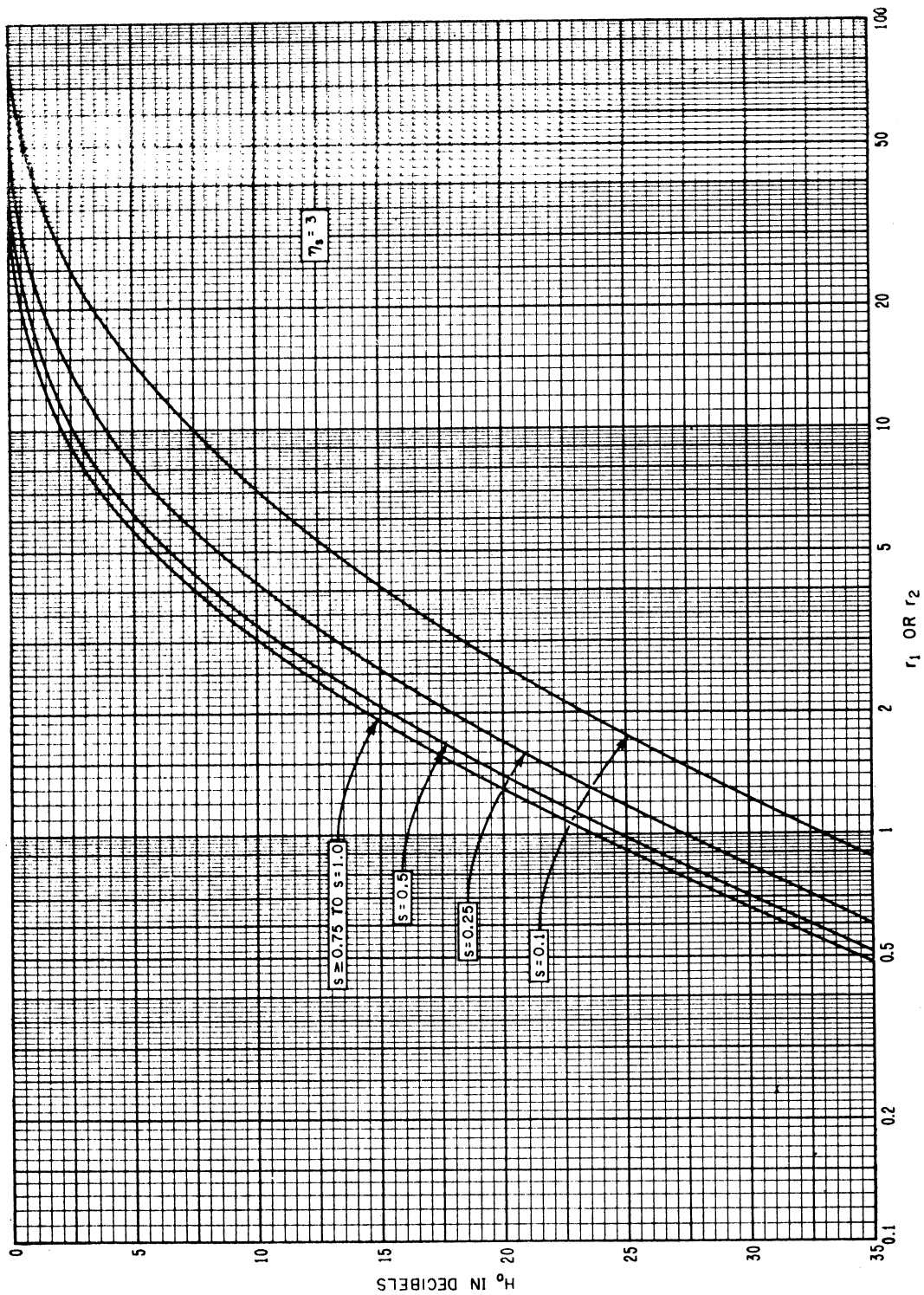


Figure III.17

THE FREQUENCY GAIN FUNCTION, H_0
 $h_{te} = h_{re}$

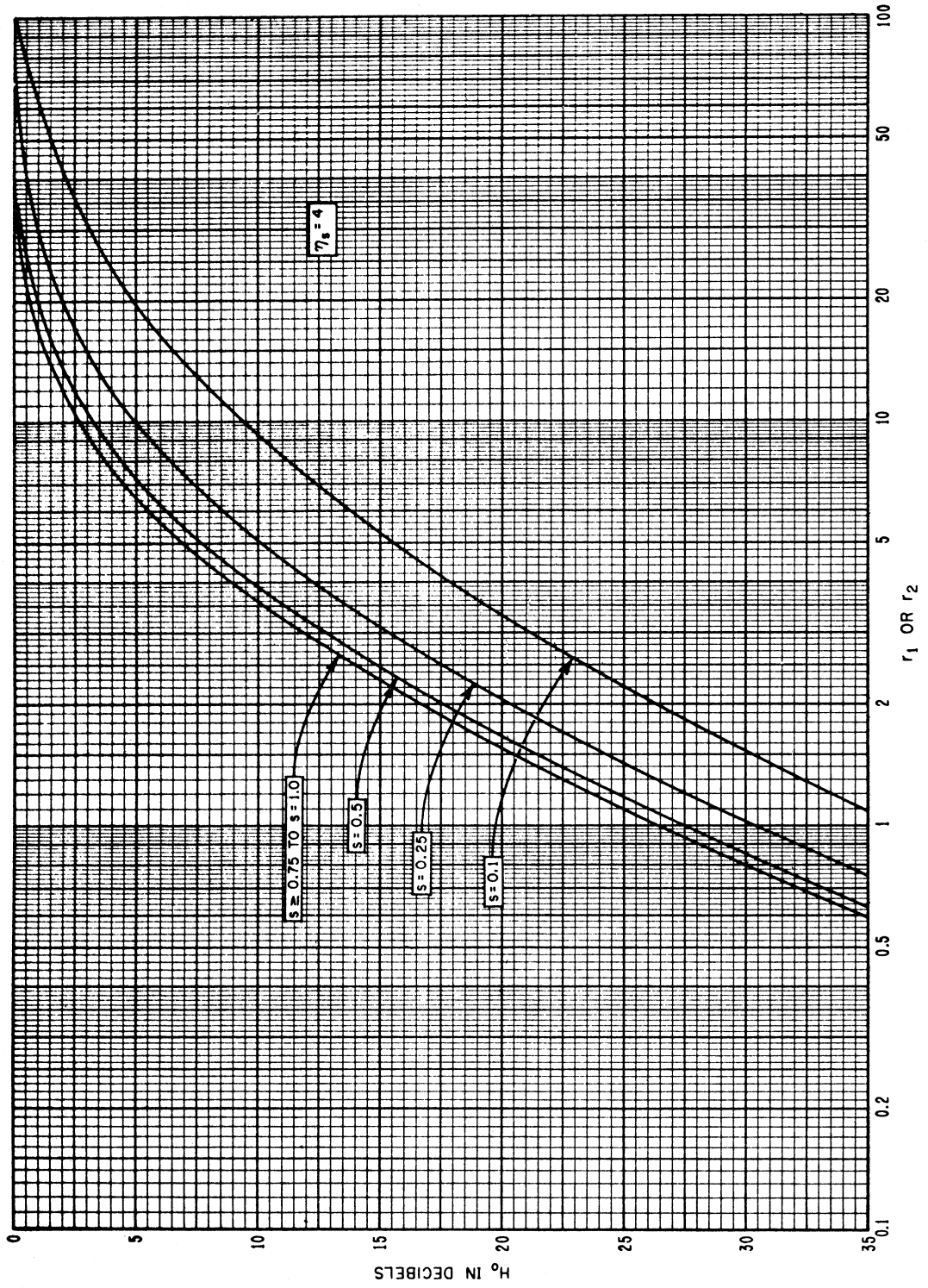


Figure III.18

THE FREQUENCY GAIN FUNCTION, H_0
 $h_{te} = h_{re}$

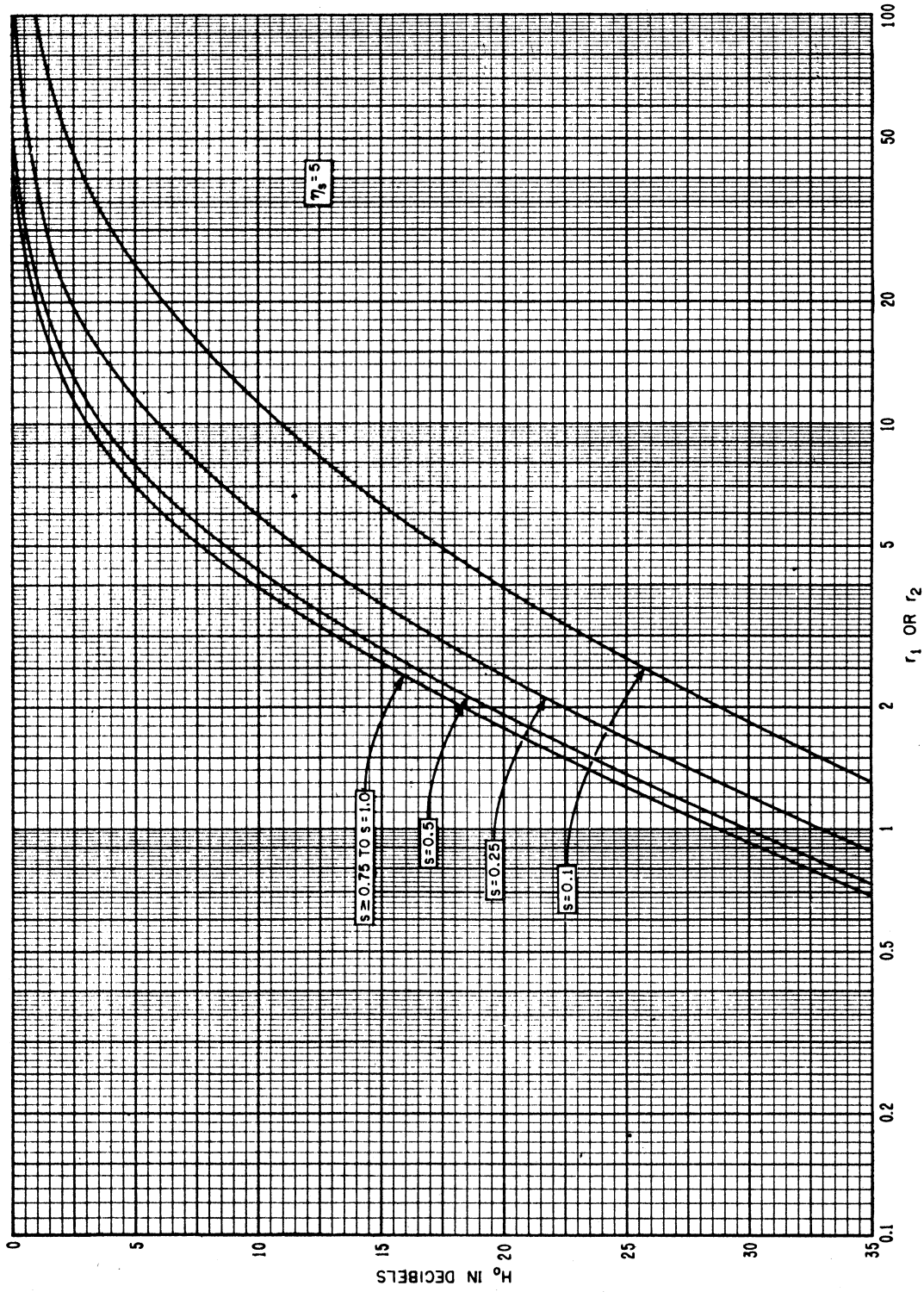
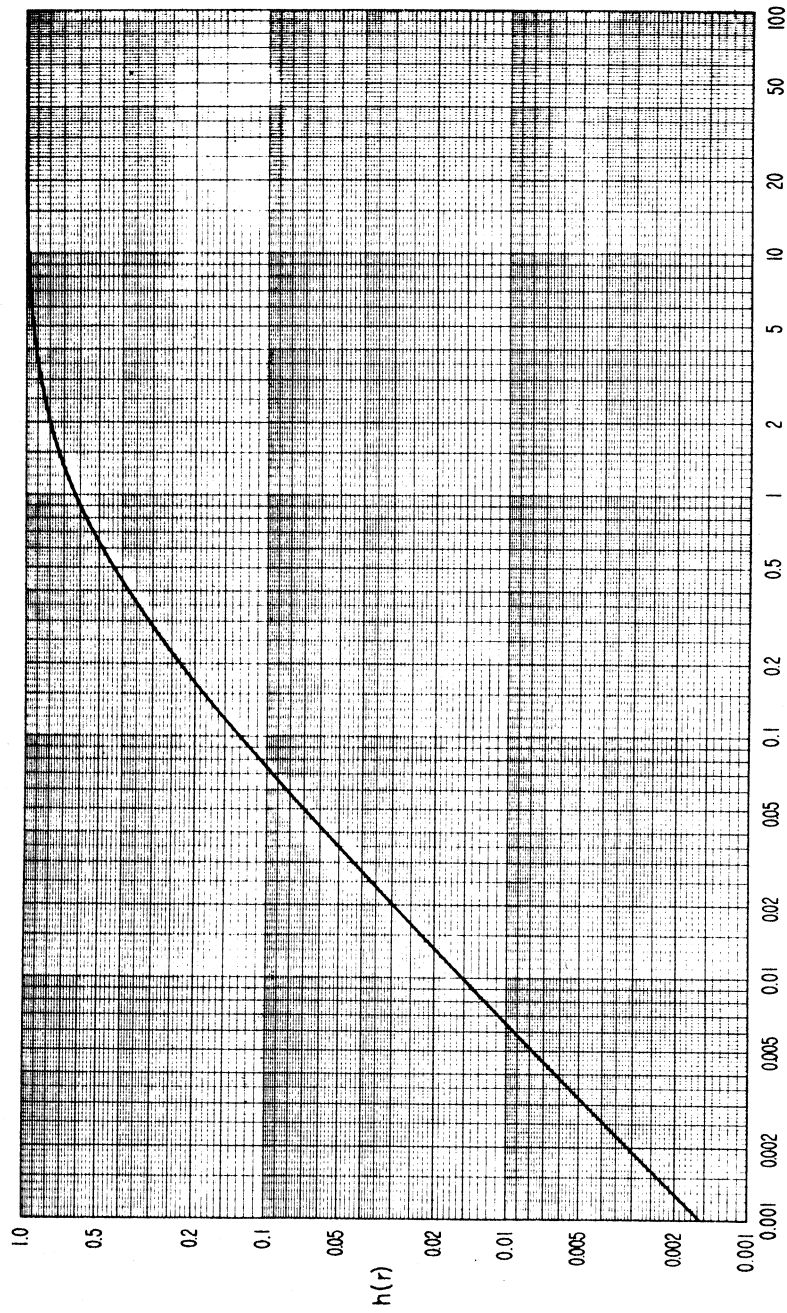


Figure III.19

THE FUNCTION $h(r)$



r

Figure III.20

THE FUNCTION $h(r)$

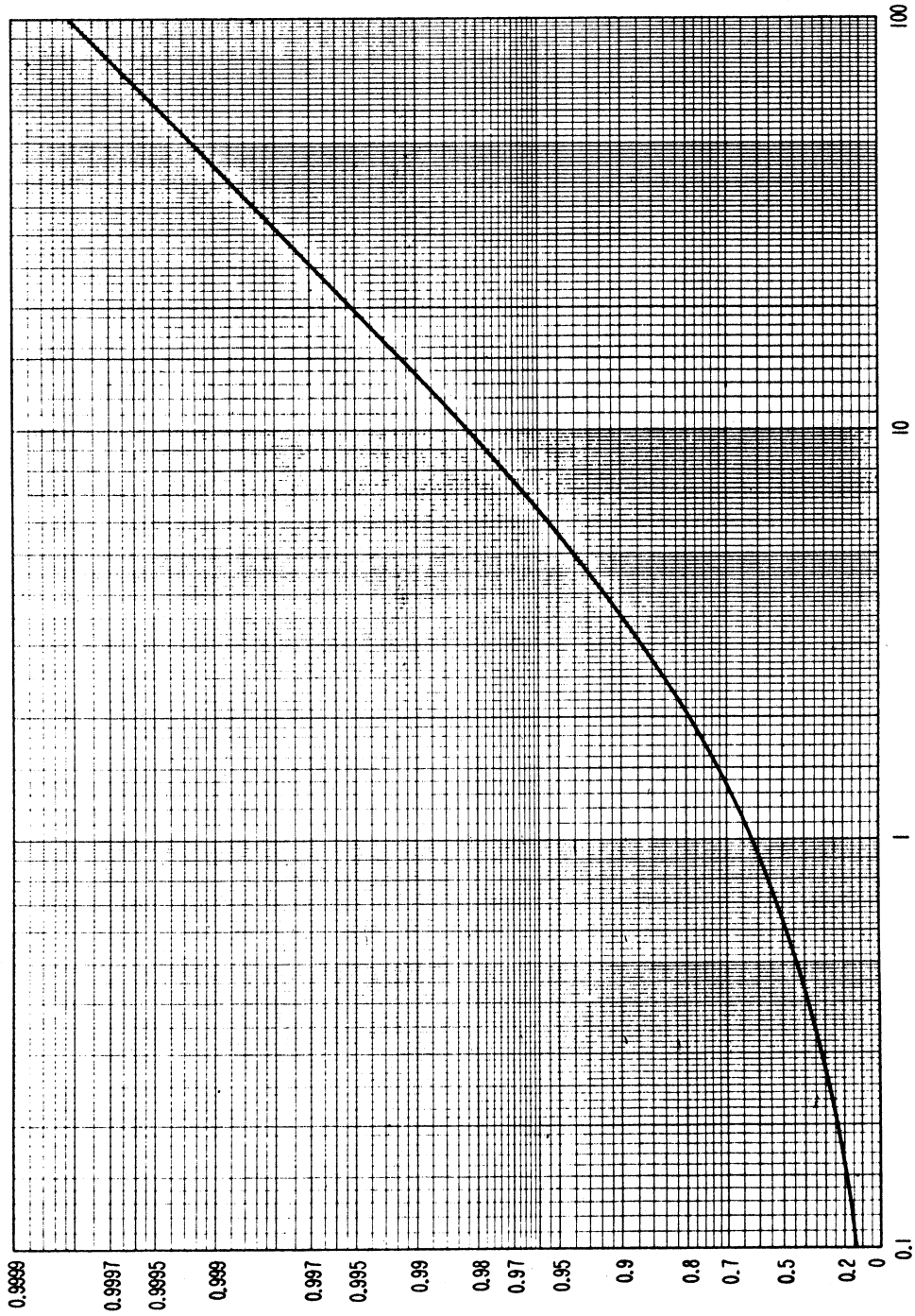


Figure III.21

(1)4

III.6 Transmission Loss with Antenna Beams Elevated or Directed Out of the Great Circle Plane

The methods of section 9 may be modified to calculate a reference value of long-term median transmission loss when antenna beams are either elevated or directed away from the great circle path between antennas. For many applications, the average transmission loss between antennas with random relative orientation is about 10 db more than the basic transmission loss, which assumes zero db antenna gains.

Figure III.22 shows scattering subvolumes at intersections of antenna main beams and side lobes. A "scatter" theory assumes that the total power available at a receiver is the sum of the powers available from many scattering subvolumes. For high gain antennas, the intersection of main beams defines the only important scattering volume. In general, all power contributions that are within 10 db of the largest one should be added.

For a total radiated power w_t :

$$w_a/w_t = 10^{-0.1 L_{sr}}, \quad w_{ai}/w_t = 10^{-0.1 L_i} \quad (\text{III. 55})$$

where L_{sr} is the transmission loss and L_i is the loss associated with the i th power contribution, w_{ai} :

$$L_{sr} = -10 \log (w_a/w_t) = -10 \log \sum_i 10^{-0.1 L_i} \quad (\text{III. 56})$$

$$L_i = 30 \log f - 20 \log (d^2/r_o) + F(\theta_{ei}d) - F_{oi} + H_{oi} + A_a - G_{ti} - G_{ri} + L_{gi} \quad (\text{III. 57})$$

In (III.57) f , d , and A_a are defined as in (9.1) and the other terms are related to similar terms in (9.1). If the effective scattering angle θ_{ei} for the i th intersection is equal to the minimum scattering angle θ , then $F(\theta_{ei}d)$, F_{oi} , H_{oi} are equal to $F(\theta d)$, F_o , and H_o , and $G_{ti} + G_{ri} - L_{gi} = G_p$. Note that a term $20 \log (r_o/d)$ has been added in (III.57) to provide for situations where the straight line distance r_o between antennas is much greater than the sea-level arc distance d . Such differences occur in satellite communication.

Scattering planes, defined by the directions of incident and scattered energy, may or may not coincide with the plane of the great circle path. Each "scattering plane" is determined by the line between antenna locations and the axis of the stronger of the two intersecting beams, making an angle ζ with the great circle plane.

The free space directive gain patterns of the antennas are replaced by equivalent values for ease in computation. For an idealized pencil-beam antenna with a half-power beamwidth 2δ and a circular beam cross-section, the directive gain g is $4/\delta^2$, assuming that all of the power is radiated through the main beam and between the half-power points. An equivalent beam pattern with a square cross-section and a semi-beamwidth δ_0 has a gain of π/δ_0^2 , thus $\delta_0 = \delta\sqrt{\pi/4}$, and the maximum free space gains are

$$G_t = 10 \log g_{t0} = 4.97 - 10 \log \delta_{t_{wo}} \delta_{t_{zo}} \quad \text{db} \quad (\text{III. 58a})$$

$$G_r = 10 \log g_{r0} = 4.97 - 10 \log \delta_{r_{wo}} \delta_{r_{zo}} \quad \text{db} \quad (\text{III. 58b})$$

where the subscripts w and z refer to azimuthal and vertical angles. In most cases, δ_{wo} and δ_{zo} may be replaced by their geometric mean, $\delta_0 = (\delta_{wo} \delta_{zo})^{1/2}$. The free space directive gain of a main beam may be measured or approximated as $g_0 \approx \pi/(2 \delta_{wo} \delta_{zo})$. Gains for side lobes are determined from g_0 and the ratios g_1/g_0 , g_2/g_0 , ..., which may be measured or calculated. The average gain g_b for other directions depends on the fraction of power radiated in those directions. For instance, if half the total power of a transmitter is radiated in these directions, and if the polarization coupling loss, L_{cp} , is 3 db, then

$$G_{bt} - L_{cp} = -6 \text{ db}$$

since the definition of the directive gain, G_{bt} , assumes for every direction the receiving antenna polarization appropriate for maximum power transfer.

Figure III.23 shows an antenna power pattern in several different ways, including a Mercator projection of the surface of a unit sphere.

The plane that determines the "bottom" of a beam is perpendicular to the great circle plane and forms an angle ψ_i with a horizon plane:

$$\psi_{ti} = \theta_{bti} - \theta_{et}, \quad \psi_{ri} = \theta_{bri} - \theta_{er} \quad (\text{III. 59})$$

where θ_b is the angle of elevation of the lower half-power point of a beam above the horizontal, and θ_{et} is defined in section 6. If an antenna beam is elevated sufficiently so that ray bending may be neglected, the angles α_e and β_e are denoted α_{e0} and β_{e0} :

$$\alpha_{e0} = (\alpha_{o0} + \psi_t) \sec \zeta, \quad \beta_{e0} = (\beta_{o0} + \psi_r) \sec \zeta \quad (\text{III. 60})$$

where ζ is the angle away from the great circle plane. The angles α_{o0} and β_{o0} are defined as in section 6 using the actual radius, $a_0 \approx 6370$ km, instead of an effective radius a .

When ray bending must be considered, the equations for α_e and β_e are

$$\alpha_e = \alpha_{e0} + \tau\left(\theta_{bt}, \frac{d_{Lt} \sec \zeta}{2}, N_s\right) - \tau\left(\theta_{bt}, \frac{d \sec \zeta}{2}, N_s\right) \quad (\text{III. 61a})$$

$$\beta_e = \beta_{e0} + \tau\left(\theta_{br}, \frac{d_{Lr} \sec \zeta}{2}, N_s\right) - \tau\left(\theta_{br}, \frac{d \sec \zeta}{2}, N_s\right) \quad (\text{III. 61b})$$

where $\tau(\theta_b, d, N_s)$ is the bending of a radio ray which takes off at an angle θ_b above the horizontal and travels d kilometers through an atmosphere characterized by a surface refractivity N_s . The ray bending τ may be determined using methods and tables furnished by Bean and Thayer [1959]. For short distances, d , or large angles, θ_b , τ is negligible. If θ_b is less than 0.1 radians, the effective earth's radius approximation is adequate for determining τ ,

$$\tau\left(\theta_b, \frac{d \sec \zeta}{2}, N_s\right) = \frac{d}{a_o} [1 - a_o/a(N_s)] \quad (\text{III. 62})$$

The reference value of long-term median transmission loss L_{sr} is computed using (III.56) where the losses associated with several scattering subvolumes are computed using (III.57). The attenuation function $F(d\theta_{ei})$ is read from figure 9.1 or figures III.11 - III.14 as a function of θ_{ei} .

The generalized scattering efficiency term F_{oi} is

$$F_{oi} = 1.086(\eta_{se}/h_e)(2h_o - h_l - h_e - h_{Lt} - h_{Lr}) \quad \text{db} \quad (\text{III. 63})$$

where

$$\theta_e = \alpha_e + \beta_e, \quad s_e = \alpha_e/\beta_e, \quad h_e = s_e d \theta_e / (1 + s_e)^2, \quad \eta_{se} = \eta_s(h_e, N_s) \quad (\text{III. 64})$$

and the other terms are defined in section 9. In computing the frequency gain function H_{oi} , if $\alpha_e > \alpha_o$ use $r_1 = \infty$, if $\beta_e > \beta_o$ use $r_2 = \infty$; then $H_{oi} = H_o + 3$ db. If both antennas are elevated above the horizon rays, $H_{oi} = 6$ db. Atmospheric absorption A_a is discussed in section 3. The gains G_{ti} and G_{ri} are the free space directive gains defined by (III.58), and the loss in gain L_{gi} is computed as shown in section 9 replacing η_s , s , δ , and θ by η_{se} , s_e , δ_e , and θ_e .

In computing long-term variability of transmission loss for beams elevated above the horizon plane, the estimates of V and Y given in section 10 should be reduced by the factor $f(\theta_h)$ shown in figure III.24, with $\theta_h = \theta_b$:

$$V_e(0.5, d_e) = V(0.5, d_e) f(\theta_h) \quad (\text{III.65a})$$

$$Y_e(q, d_e) = Y(q, d_e) f(\theta_h) \quad (\text{III.65b})$$

The angle θ_h used in (III.65) should be the elevation above the horizontal of the scattering subvolume corresponding to the minimum value of L_i .

SCATTERING SUBVOLUMES IN A SCATTERING PLANE

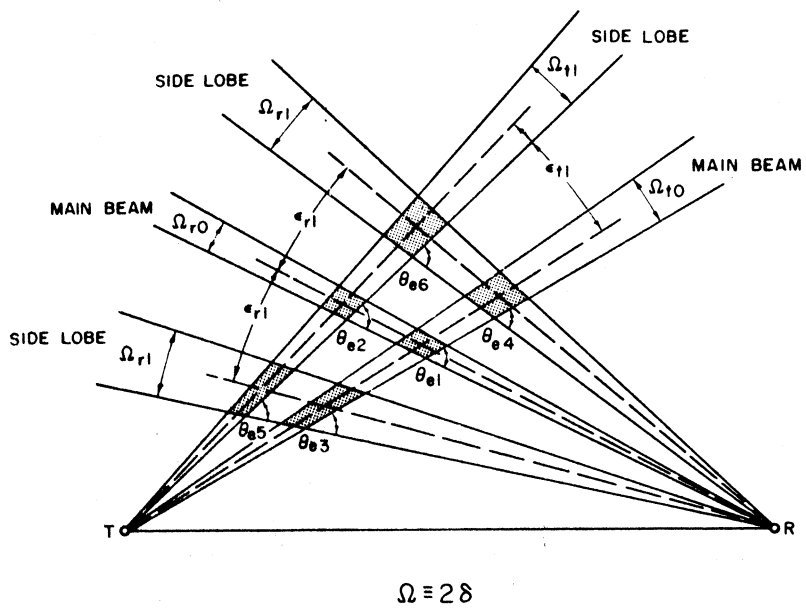


ILLUSTRATION OF A SCATTERING PLANE CONTAINING THE MAIN BEAM OF THE RECEIVING ANTENNA

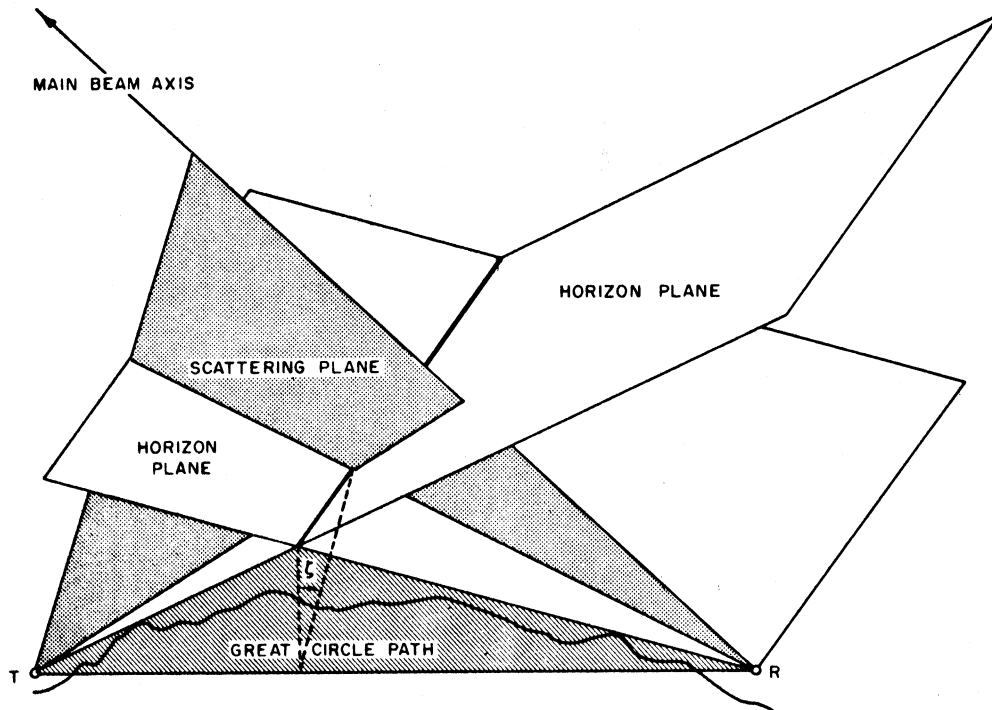
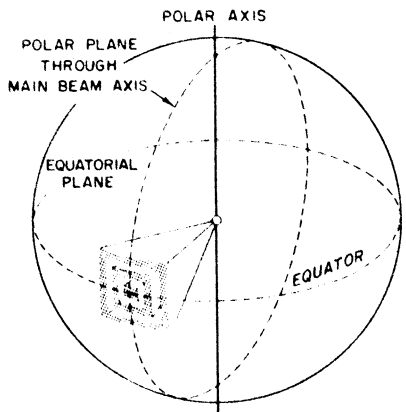


Figure III.22

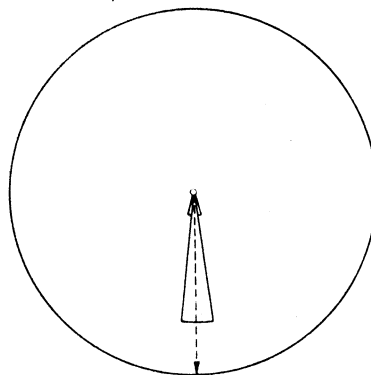
FREE SPACE ANTENNA PATTERN

INTERSECTION OF AN EQUIVALENT ANTENNA POWER PATTERN WITH THE SURFACE OF A UNIT SPHERE

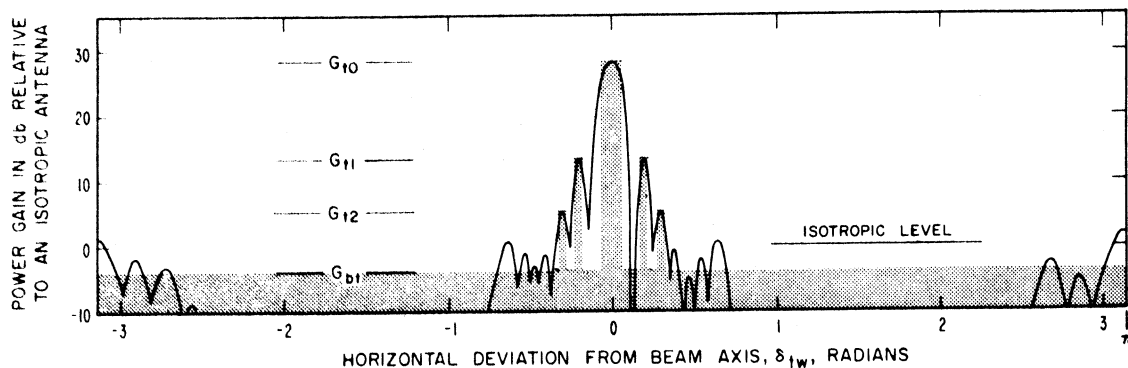


PATTERN PARAMETERS	
$\delta_{t0} = 0.04$	$\delta_{tw0} = 0.06$
$\delta_{tz1} = 0.02$	$\delta_{tw1} = 0.02$
$\delta_{tz2} = 0.02$	$\delta_{tw2} = 0.02$
$\epsilon_{tz1} = 0.12$	$\epsilon_{tw1} = 0.20$
$\epsilon_{tz2} = 0.22$	$\epsilon_{tw2} = 0.30$
$G_{t0} = 654.5$	$G_{t0} = 28.16 \text{ db}$
$G_{t1} = 20.7$	$G_{t1} = 13.16 \text{ db}$
$G_{t2} = 3.28$	$G_{t2} = 5.16 \text{ db}$
$G_{bt} = 0.395$	$G_{bt} = -4.04 \text{ db}$

ANTENNA VOLTAGE PATTERN. POLAR DIAGRAM IN THE EQUATORIAL PLANE



CARTESIAN DIAGRAM OF TRANSMITTING ANTENNA POWER PATTERN IN THE EQUATORIAL PLANE



MERCATOR PROJECTION OF THE INTERSECTION OF THE EQUIVALENT TRANSMITTING ANTENNA POWER PATTERN WITH THE SURFACE OF A UNIT SPHERE

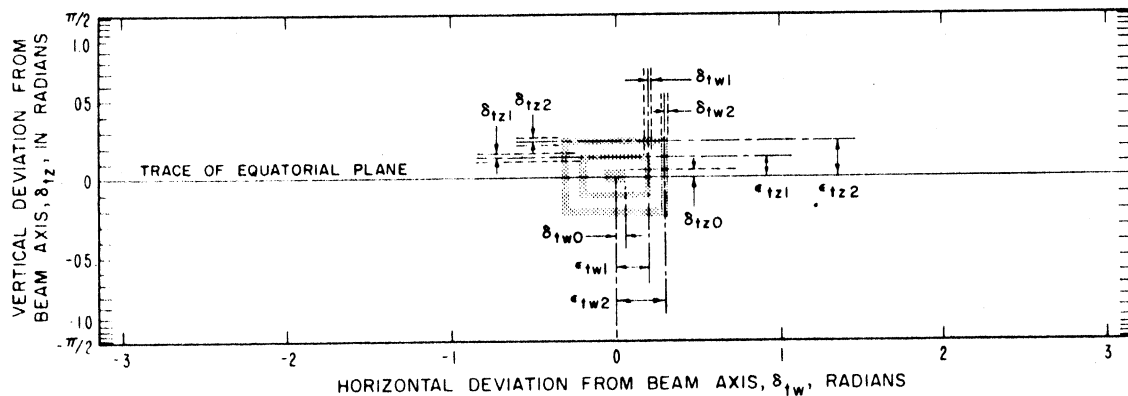


Figure III.23

THE ELEVATION ANGLE CORRECTION $f(\theta_h)$ FOR LINE-OF-SIGHT PATHS

FOR BEYOND-HORIZON PATHS, $f(\theta_h) = 1$

WITHIN THE HORIZON, $f(\theta_h) = \frac{1}{2} - \frac{1}{\pi} \tan^{-1} [20 \log(4\theta_h)]$

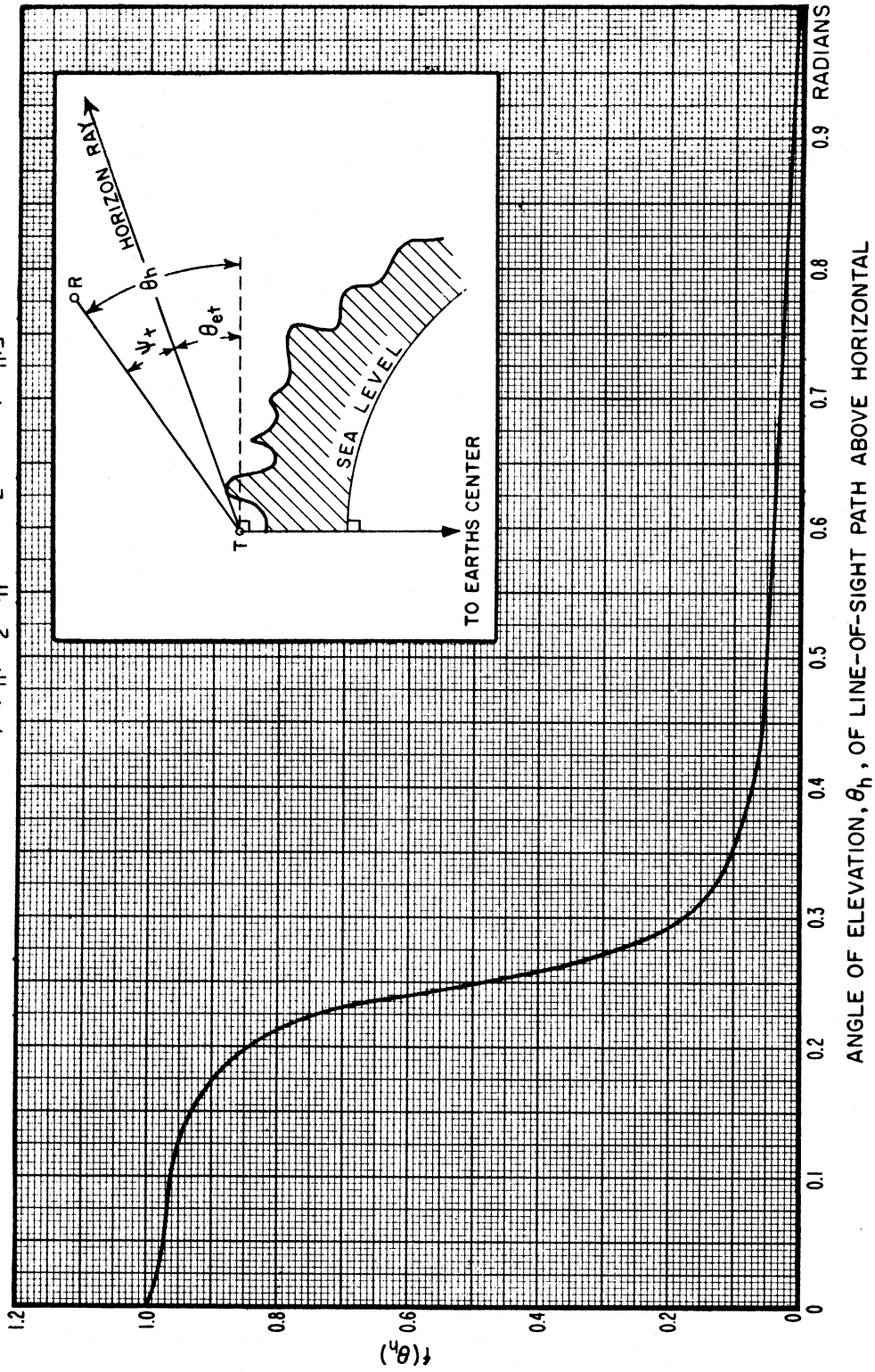


Figure III.24

III.7 Long-Term Power Fading

Long-term power fading is discussed in section 10. Figures 10.5 to 10.16 show empirical estimates of all-year variability for (1) continental temperate (2) maritime temperate overland and (3) maritime temperate oversea climates. The curves shown on these figures are based on a large amount of data. Estimates of variability in other climates are based on what is known about meteorological conditions and their effects on radio propagation, but have relatively few measurements to support them.

Figures III.25 to III.29 show curves of variability relative to the long-term median, prepared by the CCIR [1963 f] for the following climatic regions:

- (4) Maritime Subtropical, Overland.
- (5) Maritime Subtropical, Oversea.*
- (6) Desert.
- (7) Equatorial.
- (8) Continental Subtropical.

In some cases, random path differences have undoubtedly been attributed to climatic differences. Available data were normalized to a frequency of 1000 MHz, and the curves correspond to this frequency. They show all-year variability $Y(q, d_e, 1000 \text{ MHz})$ about the long-term median as a function of the effective distance d_e defined by (10.3). Variability estimates for other frequencies are obtained by using the appropriate correction factor $g(f)$ shown in figure III.30:

$$Y(q) = Y(q, d_e, 1000 \text{ MHz}) g(f). \quad (\text{III. 66})$$

The empirical curves $g(f)$ are not intended as an estimate of the dependence of long-term variability on frequency, but represent an average of many effects that are frequency-sensitive, as discussed in section 10.

Variability about the long-term median transmission loss $L(0.5)$ is related to the long-term reference median L_{cr} by means of the function $V(0.5, d_e)$ shown on figure 10.1. The predicted long-term median transmission loss is then:

$$L(0.5) = L_{cr} - V(0.5, d_e) \quad (\text{III. 67})$$

and the predicted value for any percentage of time is

$$L(q) = L(0.5) - Y(q). \quad (\text{III. 68})$$

* Curves for climate 5 have been deleted. They were based on a very small amount of data. For hot, moist tropical areas use climate 4, and for coastal areas where prevailing winds are from the ocean, use climate 3.

III. 7.1 Diurnal and Seasonal Variability in a Continental Temperate Climate

The curves shown in figures 10.5 to 10.16 and III.25 to III.29 represent variability about the long-term median for all hours of the day throughout the entire year. For certain applications, it is important to know something about the diurnal and seasonal changes that may be expected. Such changes have been studied in the continental United States, where a large amount of data is available. Measurement programs recorded VHF and UHF transmission loss over particular paths for at least a year to determine seasonal variations. Data were recorded over a number of paths for longer periods of time to study year-to-year variability.

As a general rule, transmission loss is less during the warm summer months than in winter, and diurnal trends are usually most pronounced in summer, with maximum transmission loss occurring in the afternoon. The diurnal range in signal level may be about 10 db for paths that extend just beyond the radio horizon, but is much less for very short or very long paths. Variation with season usually shows maximum losses in mid-winter, especially on winter afternoons, and high fields in summer, particularly during morning hours. Transmission loss is often much more variable over a particular path in summer than it is during the winter, especially when ducts and elevated layers are relatively common.

The data were divided into eight "time blocks" defined in table III.1. The data were assumed to be statistically homogeneous within each of the time blocks. With more and shorter time blocks, diurnal and seasonal trends would be more precisely defined, except that no data would be available in some of the time blocks over many propagation paths. Even with the division of the year into winter and summer and the day into four periods as in table III.1, it is difficult to find sufficient data to describe the statistical characteristics expected of transmission loss in Time Blocks 7 and 8.

Table III.1
Time Blocks

<u>No.</u>	<u>Months</u>	<u>Hours</u>
1	Nov. - Apr.	0600 - 1300
2	Nov. - Apr.	1300 - 1800
3	Nov. - Apr.	1800 - 2400
4	May - Oct.	0600 - 1300
5	May - Oct.	1300 - 1800
6	May - Oct.	1800 - 2400
7	May - Oct.	0000 - 0600
8	Nov. - Apr.	0000 - 0600

In some applications, it is convenient to combine certain time blocks into groups, for instance, some characteristics of long-term variability are significantly different for the winter group (Time Blocks 1, 2, 3, 8) than for the summer group (Time Blocks 4, 5, 6, 7).

In other climatic regions, if the annual range of monthly average values of N_s is less than 20 N units (figure III. 31), seasonal variations are expected to be negligible. One would also expect less diurnal change, for example, in a maritime temperate climate where changes in temperature during the day are less extreme. In climates where N_s changes considerably throughout the year, the consecutive 4-6 month period when N_s is lowest may be assumed to correspond to "winter", whatever months may be involved.

For the U.S. only, the parameter $V(0.5, d_e)$ for each of the eight time blocks and for "summer" and "winter" is shown in figure III. 32. Curves of the variability $Y(q, d_e, 100 \text{ MHz})$ about the long-term median for each of these times of day and seasons are shown in figures III. 33 to III. 42. These curves are drawn for a frequency of 100 MHz. Figures III. 33 and III. 34 show the range 0.01 to 0.99 of $Y(q, d_e, 100 \text{ MHz})$ for the winter time blocks, 1, 2, 3, 8 and the summer time blocks 4, 5, 6, 7. Each group of data was analyzed separately. Some of the differences shown between time blocks 1, 2, 3, and 8 are probably not statistically significant. Marked differences from one time block to another are observed during the summer months.

Figures III. 35 through III. 42 show data coded in the following frequency groups, 88-108, 108-250 and 400 to 1050 MHz as well as curves for $Y(q)$ drawn for 100 MHz. In general these figures show more variability in the two higher frequency groups especially during "summer" (time blocks 4, 5, 6 and 7). Because of the relatively small amount of data no attempt was made to derive a frequency factor $g(q, f)$ for individual time blocks.

The curves for summer, winter, and all hours shown in figures 10.13 through 10.22 represent a much larger data sample, since time block information was not available for some paths for which summer or winter distributions were available.

The smooth curves of $V(0.5, d_e)$ and $Y(q, d_e, 100 \text{ MHz})$ versus d_e shown in figures 10.13, 10.14, III.25 to III.29 and III.32 to III.42 may be represented by an analytic function of the general form:

$$\left. \begin{array}{l} V(0.5) \\ Y(0.1) \\ -Y(0.9) \end{array} \right\} = \left[c_1 d_e^{n_1} - f_2(d_e) \right] \exp(-c_3 d_e^{n_3}) + f_2(d_e) \quad (\text{III. 69})$$

where

$$f_2(d_e) = f_\infty + (f_m - f_\infty) \exp(-c_2 d_e^{n_2}) \quad (\text{III. 70})$$

The terms $c_1, c_2, c_3, n_1, n_2, n_3, f_m$, and f_∞ in (III. 69) and (III. 70) are constants for any given time block and value of q . The parameters f_m and f_∞ are maximum and asymptotic values, respectively. Tables III. 2 to III. 4 list values of the eight parameters required in (III. 69) to obtain $V(0.5, d_e)$, $Y(0.1, d_e, 100 \text{ MHz})$ and $-Y(0.9, d_e, 100 \text{ MHz})$ for the eight time blocks in table III. 1, and for summer, winter, and all hours. The constants given

in Tables III. 2 to III. 4 for summer, winter and all hours were determined using only radio paths for which time block information is available. They do not yield the curves shown in figures 10.13 and 10.14 of section 10, which represent a much larger data sample.

Tables III. 5 to III. 7 list values of the eight parameters in (III. 69) required to compute $V(0.5)$, $Y(0.1, d_e, f_{\text{MHz}})$ and $Y(0.9, d_e, f_{\text{MHz}})$ for each of the climatic regions discussed in section 10, Volume 1, and section III. 7 of this annex.

TABLE III. 2

Constants for Calculating $V(0.5, d_e)$

Time Block	c_1	$\frac{d_e \text{ in km.}}{c_2}$	c_3	n_1	n_2	n_3	f_m	f_∞
4	1.35^{-6}	5.02^{-18}	1.32^{-7}	2.80	6.74	3.08	5.2	4.0
5	1.05^{-6}	5.02^{-18}	4.14^{-9}	2.70	6.74	3.70	2.4	1.8
6	2.04^{-4}	6.61^{-18}	2.82^{-9}	1.87	6.67	3.76	5.2	4.2
7	8.00^{-4}	3.91^{-16}	1.20^{-5}	1.68	5.94	2.25	7.1	5.6
S*	1.18^{-5}	6.72^{-17}	1.65^{-6}	2.40	6.32	2.61	5.1	4.0
1	2.11^{-4}	3.44^{-17}	1.73^{-4}	1.67	6.52	1.82	1.2	0.5
3	3.47^{-4}	3.76^{-14}	5.42^{-4}	1.60	5.30	1.58	1.3	0.6
8	3.63^{-4}	1.80^{-23}	1.55^{-5}	1.65	8.91	2.36	1.95	0.8
W*	1.40^{-3}	1.79^{-34}	1.05^{-5}	1.27	13.23	2.51	1.05	0.5
A*	1.63^{-4}	1.81^{-25}	8.12^{-6}	1.80	9.59	2.32	3.0	1.9

* Time Blocks "S", "W", and "A" are all hours summer, all hours winter, and all hours all year respectively. See Table III. 1 for definitions of the other time blocks. Small digits represent the exponent of the number, for example $2.33^{-2} = 2.33 \times 10^{-2}$.

TABLE III. 3
 Constants for Calculating $Y(0.1, d_e, 100 \text{ MHz})$

Time Block	d_e in km.		c_3	n_1	n_2	n_3	f_m	f_∞
	c_1	c_2						
4	1.22^{-2}	9.81^{-6}	1.09^{-8}	1.36	2.00	3.58	10.8	5.5
5	2.58^{-4}	3.41^{-6}	2.01^{-11}	2.05	2.25	4.78	8.0	4.0
6	3.84^{-3}	4.22^{-5}	7.76^{-9}	1.57	1.76	3.66	9.6	5.2
7	7.95^{-3}	3.76^{-5}	3.19^{-8}	1.47	1.76	3.40	11.2	5.5
S*	4.47^{-3}	1.66^{-5}	2.06^{-8}	1.55	1.90	3.48	9.98	5.1
1	1.09^{-4}	1.21^{-6}	8.29^{-8}	2.28	2.29	3.26	9.6	2.8
2	1.04^{-5}	4.28^{-8}	3.51^{-8}	2.71	2.91	3.41	9.15	2.8
3	2.02^{-4}	1.45^{-6}	4.27^{-8}	2.15	2.28	3.37	9.4	2.8
8	1.70^{-4}	7.93^{-7}	1.29^{-7}	2.19	2.37	3.18	9.5	3.0
W*	2.46^{-4}	1.74^{-7}	1.27^{-8}	2.11	2.64	3.62	9.37	2.8
A*	5.25^{-4}	1.57^{-6}	4.70^{-7}	1.97	2.31	2.90	10.0	5.4

* Time Blocks "S", "W", and "A" are all hours summer, all hours winter, and all hours all year, respectively. See Table III.1 for definitions of the other time blocks.
 Small digits represent the exponent of the number, for example $2.33^{-2} = 2.33 \times 10^{-2}$.

TABLE III. 4

Constants for Calculating - $Y(0.9, d_e, 100 \text{ MHz})$

Time Block	d_e in km.			n_1	n_2	n_3	f_m	f_∞
	c_1	c_2	c_3					
4	1.84^{-4}	2.22^{-6}	3.65^{-16}	2.09	2.29	6.82	8.0	4.0
5	3.80^{-4}	4.76^{-6}	8.39^{-17}	1.92	2.19	7.10	6.6	3.3
6	1.81^{-3}	5.82^{-6}	6.37^{-13}	1.67	2.15	5.38	8.4	4.1
7	3.19^{-3}	2.51^{-6}	5.03^{-9}	1.60	2.27	3.69	10.0	4.4
S*	7.42^{-4}	5.55^{-5}	4.37^{-8}	1.84	1.69	3.28	8.25	4.0
1	1.72^{-4}	6.39^{-8}	2.93^{-10}	2.10	2.79	4.24	8.2	2.4
2	1.05^{-5}	7.00^{-13}	7.64^{-9}	2.59	4.80	3.68	7.05	2.8
3	3.64^{-5}	3.74^{-9}	3.53^{-7}	2.40	3.28	2.94	7.8	2.2
8	1.64^{-6}	1.43^{-7}	3.14^{-7}	3.08	2.66	3.03	8.6	2.6
W*	3.45^{-6}	1.25^{-8}	7.50^{-7}	2.87	3.07	2.82	7.92	2.45
A*	2.93^{-4}	3.78^{-8}	1.02^{-7}	2.00	2.88	3.15	8.2	3.2

* Time Blocks "S", "W", and "A" are all hours summer, all hours winter, and all hours all year, respectively. See Table III.1 for definitions of other time blocks. Small digits represent the exponent of the number, for example, $4.97^{-4} = 4.97 \times 10^{-4}$.

TABLE III.5
 Constants for Calculating $V(0.5, d_e)$ for Several Climatic Regions

Climate	d_e in km							
	c_1	c_2	c_3	n_1	n_2	n_3	f_m	f_∞
1. Continental Temperate	1.59^{-5}	1.56^{-11}	2.77^{-8}	2.32	4.08	3.25	3.9	0
2. Maritime Temperate Overland	1.12^{-4}	1.26^{-20}	1.17^{-11}	1.68	7.30	4.41	1.7	0
3. Maritime Temperate Oversea	1.18^{-4}	3.33^{-13}	3.82^{-9}	2.06	4.60	3.75	7.0	3.2
4. Maritime Subtropical Overland	1.09^{-4}	5.89^{-18}	2.21^{-7}	2.06	6.81	2.97	5.8	2.2
5. Maritime Subtropical Oversea (deleted)								
6. Desert (Sahara) (Computes - $V(0.5)$)	8.85^{-7}	2.76^{-14}	2.25^{-12}	2.80	4.82	4.78	8.4	8.2
7. Equatorial	3.45^{-7}	3.74^{-12}	6.97^{-8}	2.97	4.43	3.14	1.2	-8.4
8. Continental Subtropical	1.59^{-5}	1.56^{-11}	2.77^{-8}	2.32	4.08	3.25	3.9	0

Note - Corresponding curves of $V(0.5, d_e)$ are drawn on figure 10.13, section 10, Volume 1.

TABLE III. 6

Constants for Calculating $Y(0.1, d_e, f, \text{MHz})$ for Several Climatic Regions

Climatic Region	Figure	c_1	c_2	c_3	n_1	n_2	n_3	f_m	f_∞
1. Continental Temperate All hours and Summer Winter	10.14	3.56 ⁻² 3.56 ⁻²	9.85 ⁻⁸ 3.76 ⁻⁸	1.50 ⁻¹¹ 2.05 ⁻¹¹	1.13 1.13	2.80 2.92	4.85 4.78	10.5 10.5	5.4 2.9
2. Maritime Temperate Overland Bands I & II (40-100 MHz) Band III (150-250 MHz) Bands IV & V (450-1000 MHz)	10.23 10.25 10.27	6.96 ⁻³ 3.60 ⁻² 6.28 ⁻⁴	1.57 ⁻⁷ 3.19 ⁻⁸ 3.19 ⁻⁸	1.15 ⁻¹¹ 6.91 ⁻¹⁸ 6.06 ⁻¹²	1.52 1.11 1.92	2.83 2.96 2.96	5.04 7.14 5.05	13.5 12.5 13.0	11.0 11.0 12.5
3. Maritime Temperate Oversea Bands I & II (40-100 MHz) Band III (150-250 MHz) Bands IV & V (450-1000 MHz)	10.24 10.26 10.28	1.37 ⁻² 2.67 ⁻³ 1.82 ⁻²	1.04 ⁻¹¹ 5.88 ⁻¹ 2.40	1.42 ⁻⁵ 8.25 ⁻⁸ 6.92 ⁻¹⁵	1.38 1.79 1.29	4.42 0 0	2.27 3.27 5.78	16.0 18.5 19.0	13.0 16.5 14.0
4. Maritime Subtropical Overland	III.25	4.33 ⁻²	7.13 ⁻¹¹	1.19 ⁻¹²	1.09	3.89	4.93	17.5	13.6
5. Maritime Subtropical Oversea (deleted)									
6. Desert (Sahara)	III.27	6.09 ⁻²	1.36 ⁻⁵	3.18 ⁻¹¹	1.08	1.84	4.60	15.1	6.0
7. Equatorial	III.28	5.22 ⁻³	1.57 ⁻⁴	5.22 ⁻¹⁷	1.39	1.46	6.78	8.5	3.2
8. Continental Subtropical	III.29	1.01 ⁻²	2.26 ⁻⁷	3.90 ⁻⁹	1.46	2.67	3.78	16.0	9.1

Note - Corresponding curves of $Y(0.1, d_e)$ are drawn on the figures listed above.

TABLE III.7
 Constants for Calculating $-Y(0.9, d_e, f, \text{MHz})$ for Several Climatic Regions

Climate	Figure	c_1	c_2	c_3	n_1	n_2	n_3	f_m	f_∞
1. Continental Temperate	10.14								
All Hours		9.48 ⁻³	5.70 ⁻¹¹	5.56 ⁻⁶	1.33	3.96	2.44	8.2	3.0
Summer		9.48	1.81 ⁻¹¹	7.00 ⁻⁶	1.33	4.23	2.40	8.2	4.3
Winter		9.48 ⁻³	1.14 ⁻¹¹	7.36 ⁻⁶	1.33	4.22	2.39	8.2	2.1
2. Maritime Temperate Overland									
Bands I & II (40-100 MHz)	10.23	1.45 ⁻³	1.68 ⁻¹²	8.07 ⁻⁶	1.70	4.61	2.36	9.0	3.5
Band III (150-250 MHz)	10.25	9.32 ⁻⁴	2.68 ⁻¹⁴	1.02 ⁻¹⁶	1.74	5.29	6.82	10.5	3.5
Bands IV & V (450-1000 MHz)	10.27	1.29 ⁻⁴	1.93 ⁻¹⁵	2.81 ⁻⁴	2.14	5.80	1.65	10.0	4.5
3. Maritime Temperate Oversea									
Bands I & II (40-100 MHz)	10.24	4.52 ⁻²	8.69 ⁻¹⁶	1.28 ⁻³	1.13	5.95	1.14	13.5	3.5
Band III (150-250 MHz)	10.26	1.14 ⁻³	5.72 ⁻⁹	1.29 ⁻⁸	1.90	3.27	3.67	14.5	4.0
Bands IV & V (450-1000 MHz)	10.28	1.25 ⁻³	6.57 ⁻¹⁶	1.49 ⁻⁹	1.72	5.96	3.84	12.0	4.0
4. Maritime Subtropical Overland	III.25	7.24 ⁻³	4.26 ⁻¹⁵	1.12 ⁻⁶	1.35	5.41	2.56	12.7	8.4
5. Maritime Subtropical Oversea	(deleted)								
6. Desert (Sahara)	III.27	3.19 ⁻²	5.66 ⁻⁸	7.39 ⁻¹¹	1.14	2.76	4.40	11.4	3.3
7. Equatorial	III.28	6.51 ⁻³	2.53 ⁻⁴	2.61 ⁻¹⁶	1.36	1.36	6.55	8.4	2.7
8. Continental Subtropical	III.29	3.49 ⁻³	1.08 ⁻⁹	9.15 ⁻¹¹	1.55	3.49	4.48	10.1	3.5

Note - These constants will yield positive values, i.e., $-Y(0.9, d_e)$. Corresponding curves of $Y(0.9, d_e)$ are drawn on the figures listed above.

III. 7. 2 To Mix Distributions

When a prediction is required for a period of time not shown on the figures or listed in the tables, it may sometimes be obtained by mixing the known distributions. For example, the distributions for time blocks 5 and 6 would be mixed if one wished to predict a cumulative distribution of transmission loss for summer afternoon and evening hours. In mixing distributions, it is important to average fractions of time rather than levels of transmission loss. Distributions of data for time blocks may also be mixed to provide distributions for other periods of time. For example, data distributions for time blocks 1, 2, 3, and 8 were mixed to provide distributions of data for "winter". When averages are properly weighted, such mixed distributions are practically identical to direct cumulative distributions of the total amount of data available for the longer period.

The cumulative distribution of N observed hourly median values is obtained as follows: (1) the values are arranged in order from smallest to largest, $L_1, L_2, L_3, \dots, L_n, \dots, L_N$, (2) the fraction q of hourly median values less than L_n is computed:

$$q(n) = \frac{n}{N} - \frac{1}{2N};$$

(3) a plot of L_n versus $q(n)$ for values of q from $1/(2N)$ to $1 - 1/(2N)$ is the observed cumulative distribution.

To mix two distributions, the following procedure is used: (1) choose ten to fifteen levels of transmission loss L_1, \dots, L_n , covering the entire range of $L(q)$ for both distributions, (2) at each of these levels, read the value q for each distribution and average these values, (3) plot each selected level of transmission loss at the corresponding average fraction of time to obtain the "mixed" distribution. In this way, any number of distributions may be combined, if each of them represents the same number of hours. If the number of hours is not the same, a weighted average value q should be computed, using as weights the number of hours represented by each distribution.

CLIMATE 4, MARITIME SUBTROPICAL OVERLAND

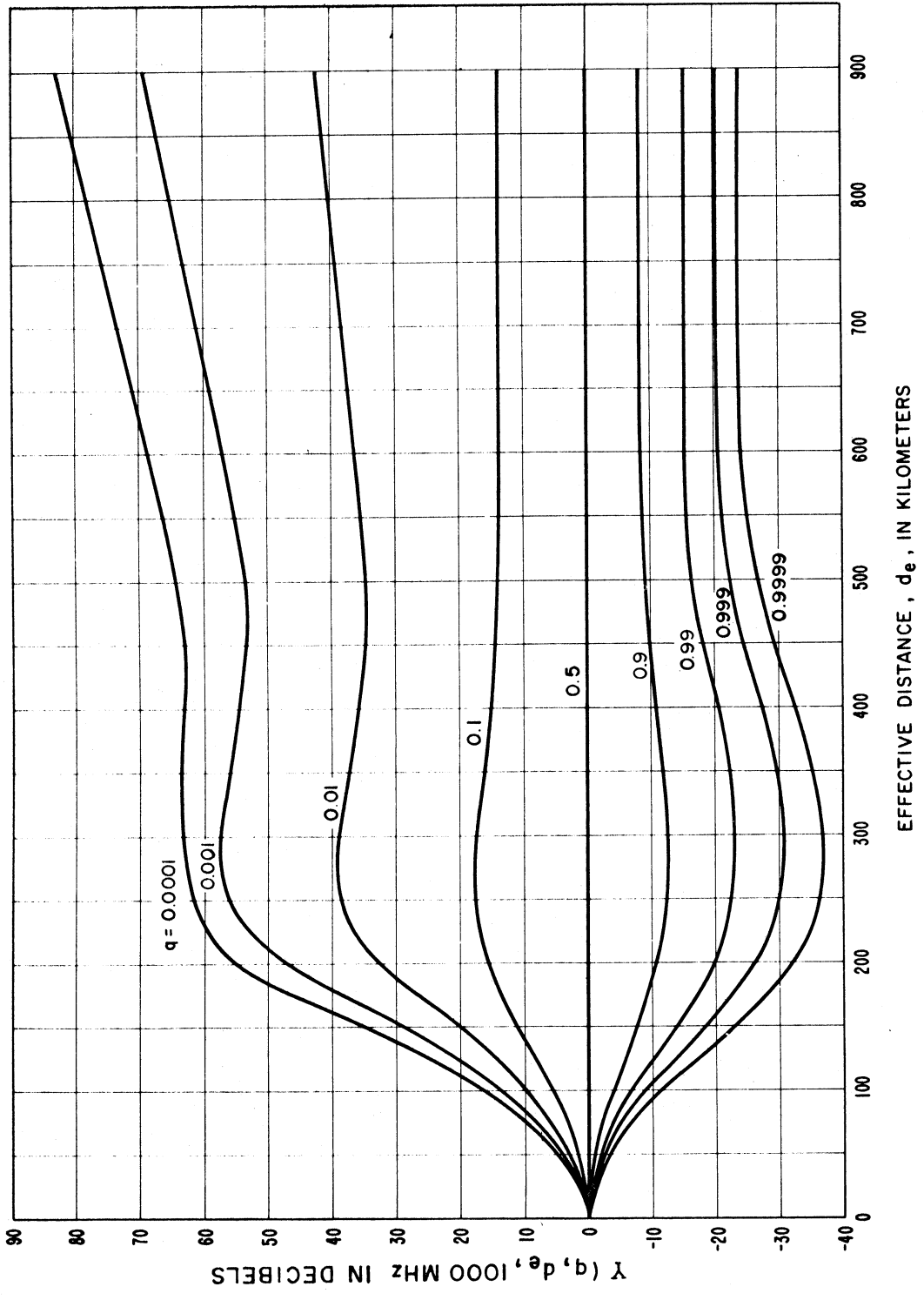


Figure III.25

The curves for climate 5, Maritime Subtropical Oversea, have been deleted. These were based on a very small amount of data. Data obtained since the preparation of these curves indicate that the following give good estimates:

Climate 4, Maritime Subtropical Overland, for hot moist tropical areas or climate 3, Maritime Temperate Oversea, for coastal areas where the prevailing winds are from the ocean.

CLIMATE 6, DESERT, SAHARA

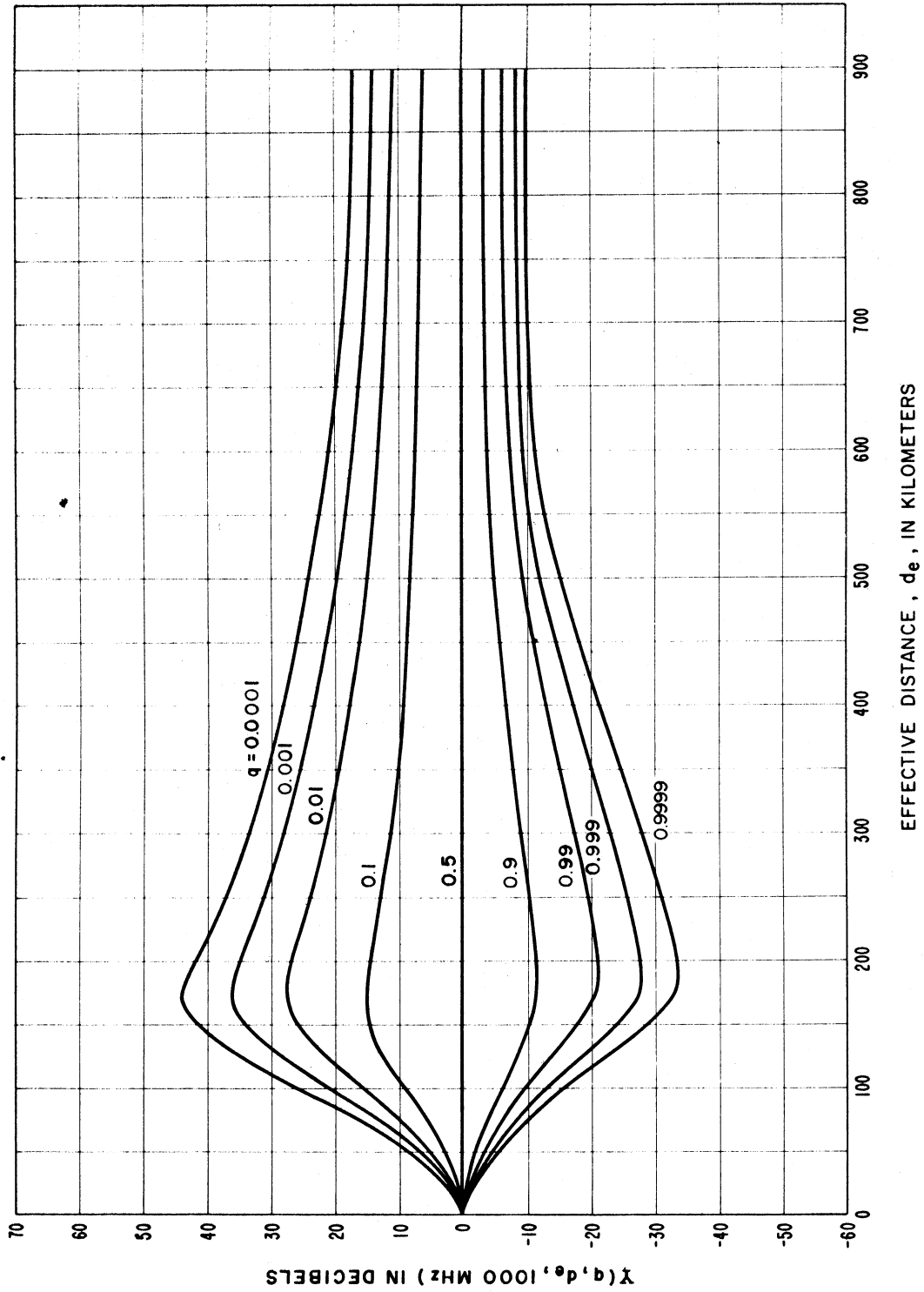


Figure III.27

CLIMATE 7, EQUATORIAL

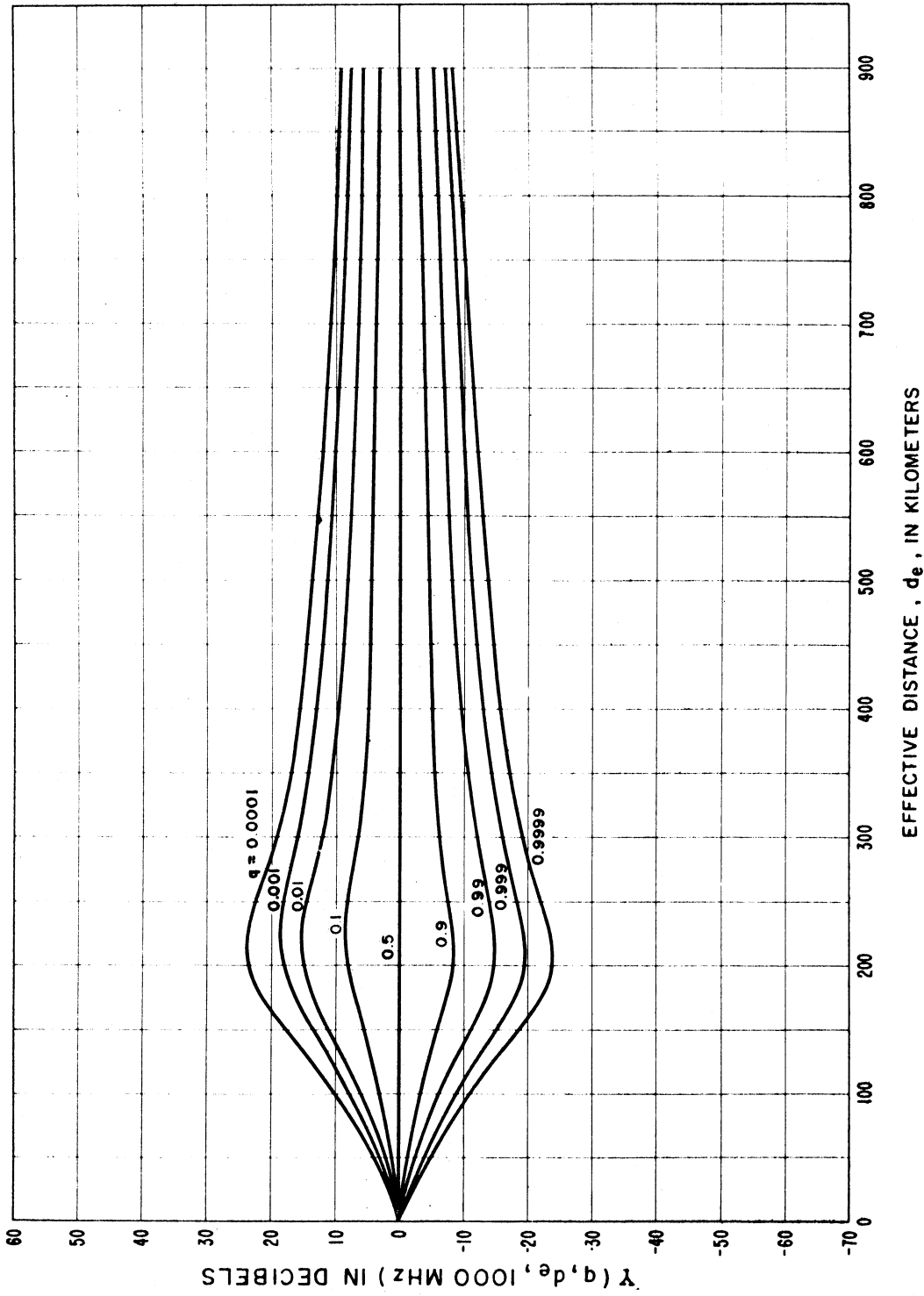
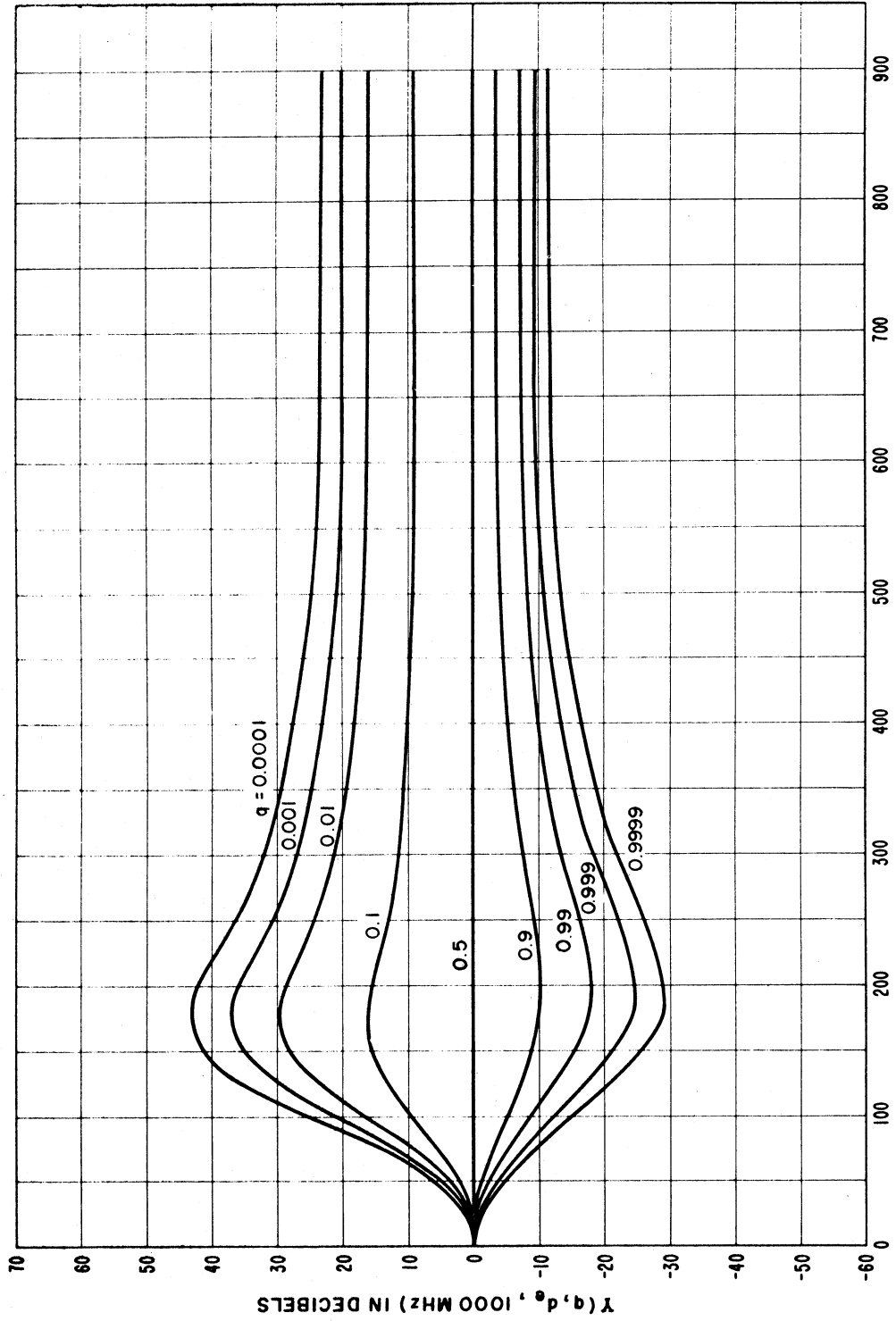


Figure III.28

CLIMATE 8, CONTINENTAL SUBTROPICAL



EFFECTIVE DISTANCE, d_e , IN KILOMETERS

Figure III.29

THE FACTOR $g(f)$
 $g(f) = 1$ FOR CLIMATES 4, 5, AND 7.

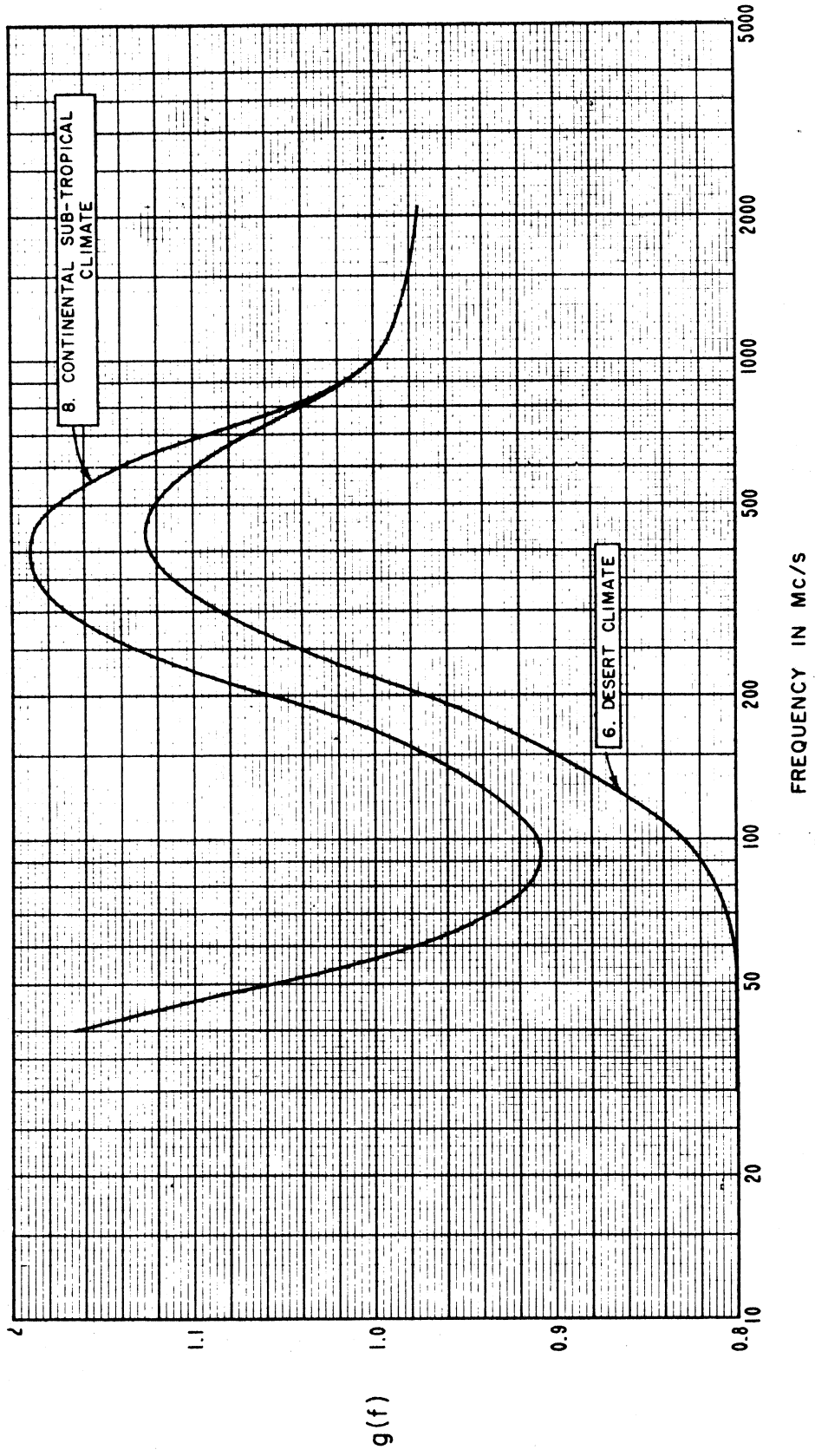


Figure III.30

ANNUAL RANGE OF MONTHLY MEAN N_g

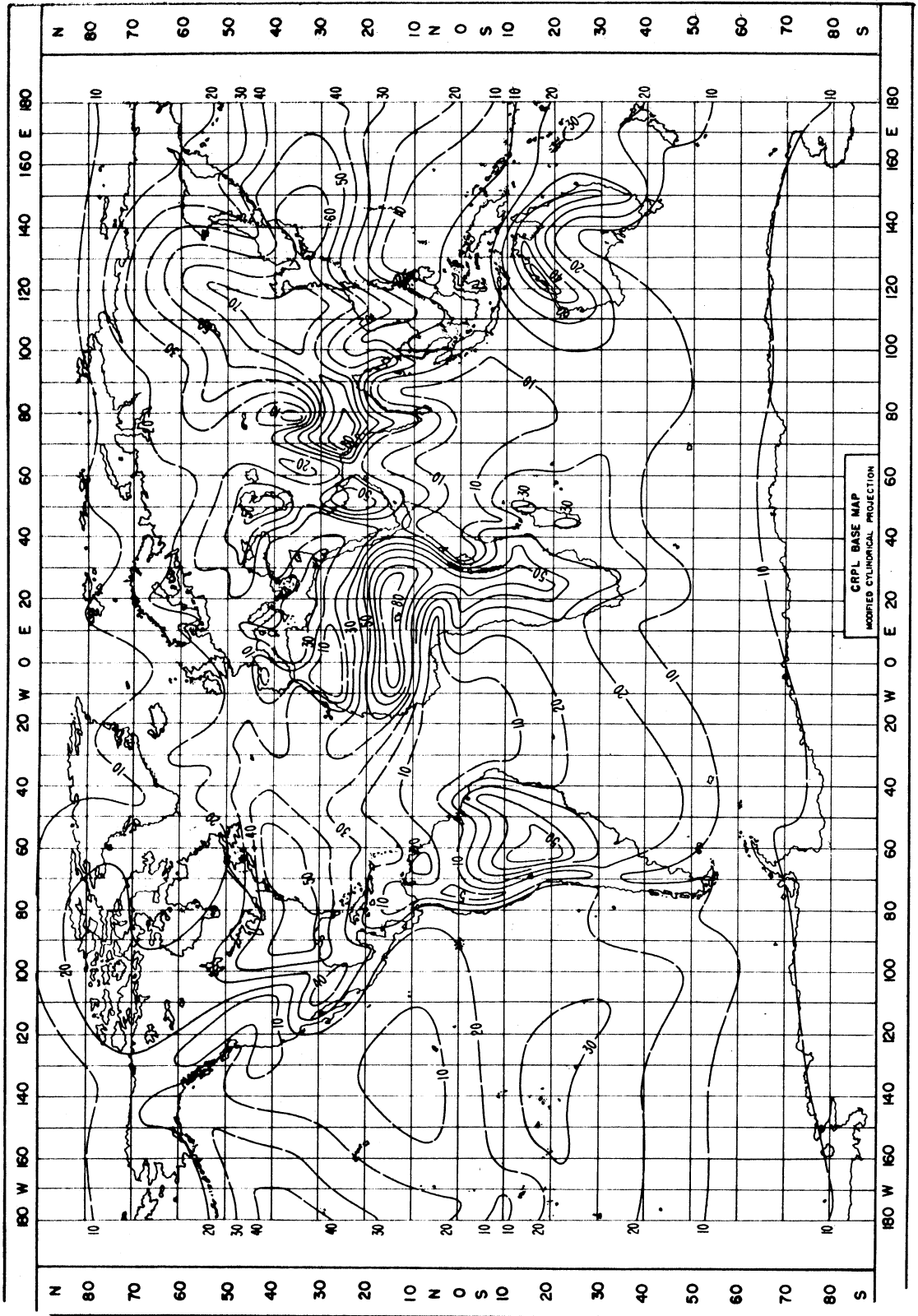


Figure III.31

THE FUNCTION $V(0.5, d_e)$ FOR VARIOUS PERIODS OF TIME IN THE U.S.A.

$$L(0.5) = L_{cr} - V(0.5, d_e) \text{ db}$$

TIME BLOCK	
WINTER	SUMMER
1. NOV.-APR. 0600-1300	4. MAY-OCT. 0600-1300
2. NOV.-APR. 1300-1800	5. MAY-OCT. 1300-1800
3. NOV.-APR. 1800-2400	6. MAY-OCT. 1800-2400
8. NOV.-APR. 0000-0600	7. MAY-OCT. 0000-0600

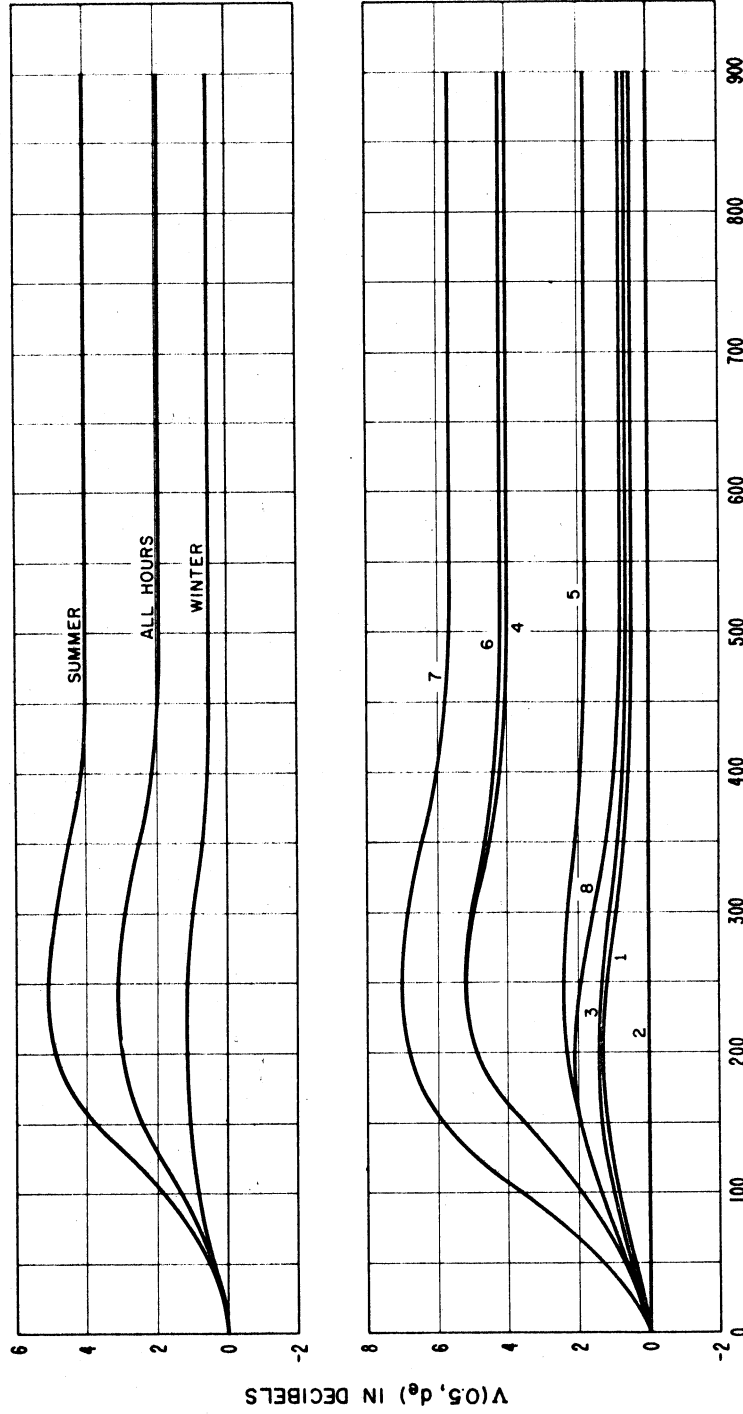


Figure III.32

WINTER TIME BLOCKS, NOV. - APRIL, U. S. A.
 CURVES FOR 88-108 MHz

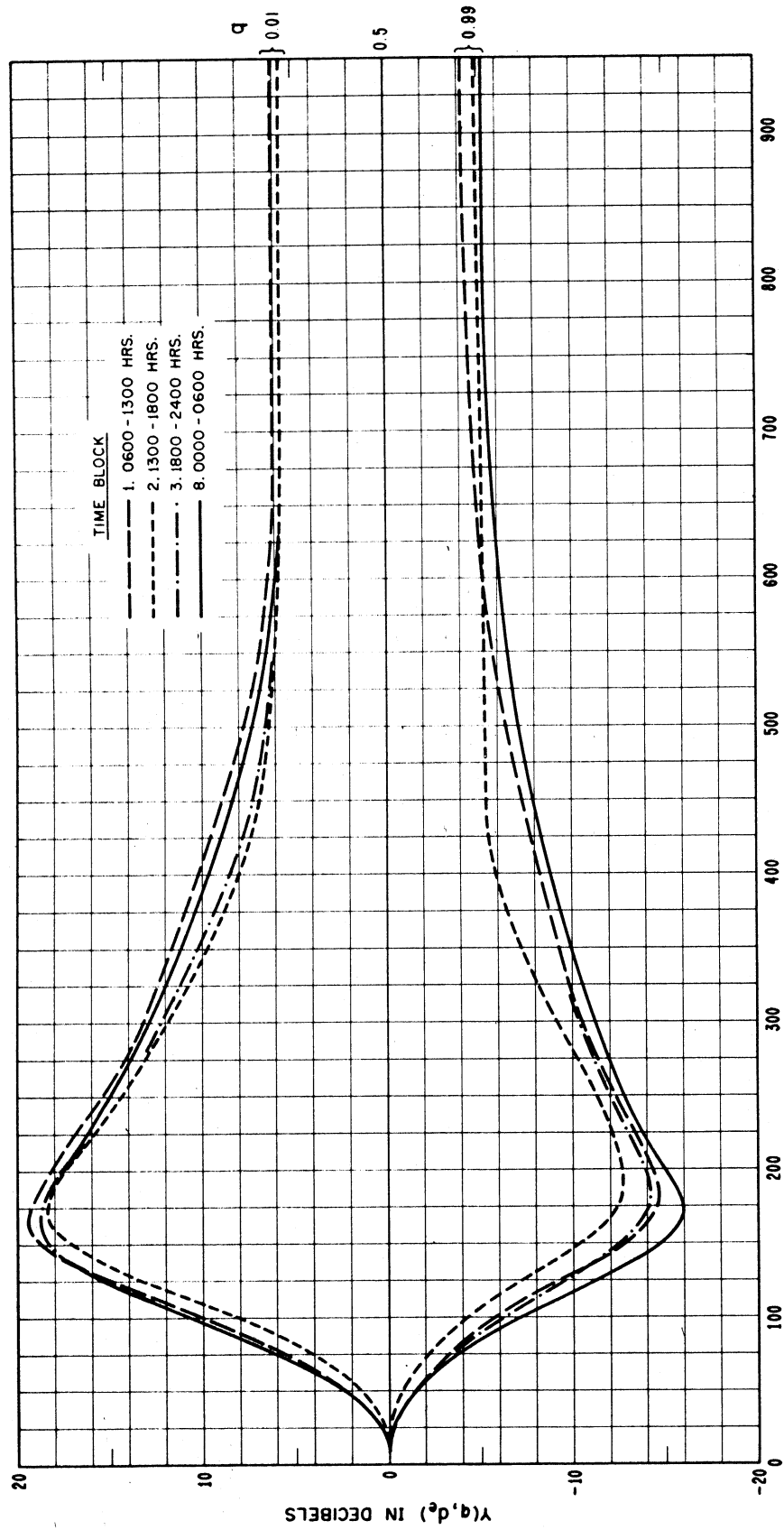
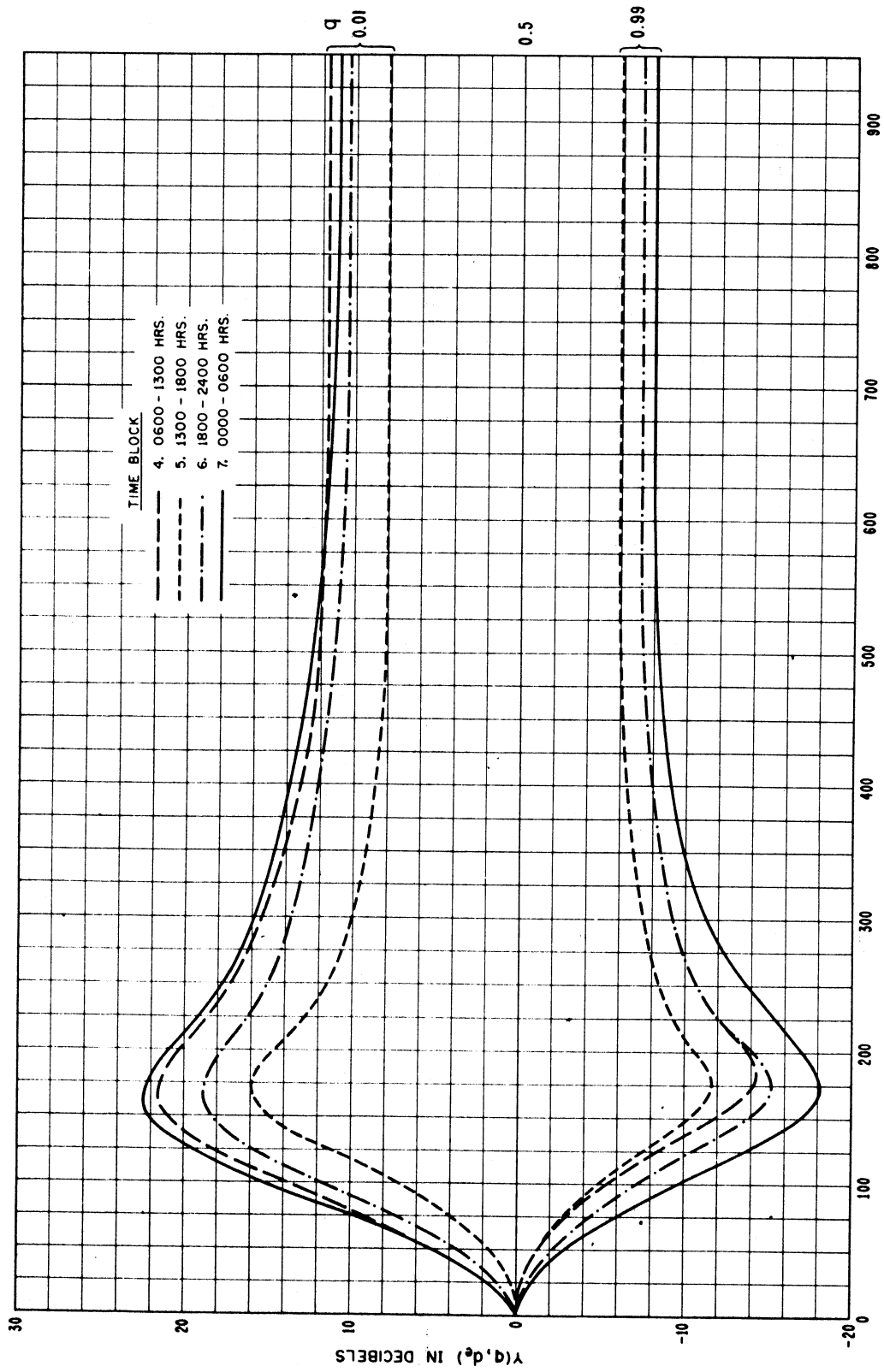


Figure III.33

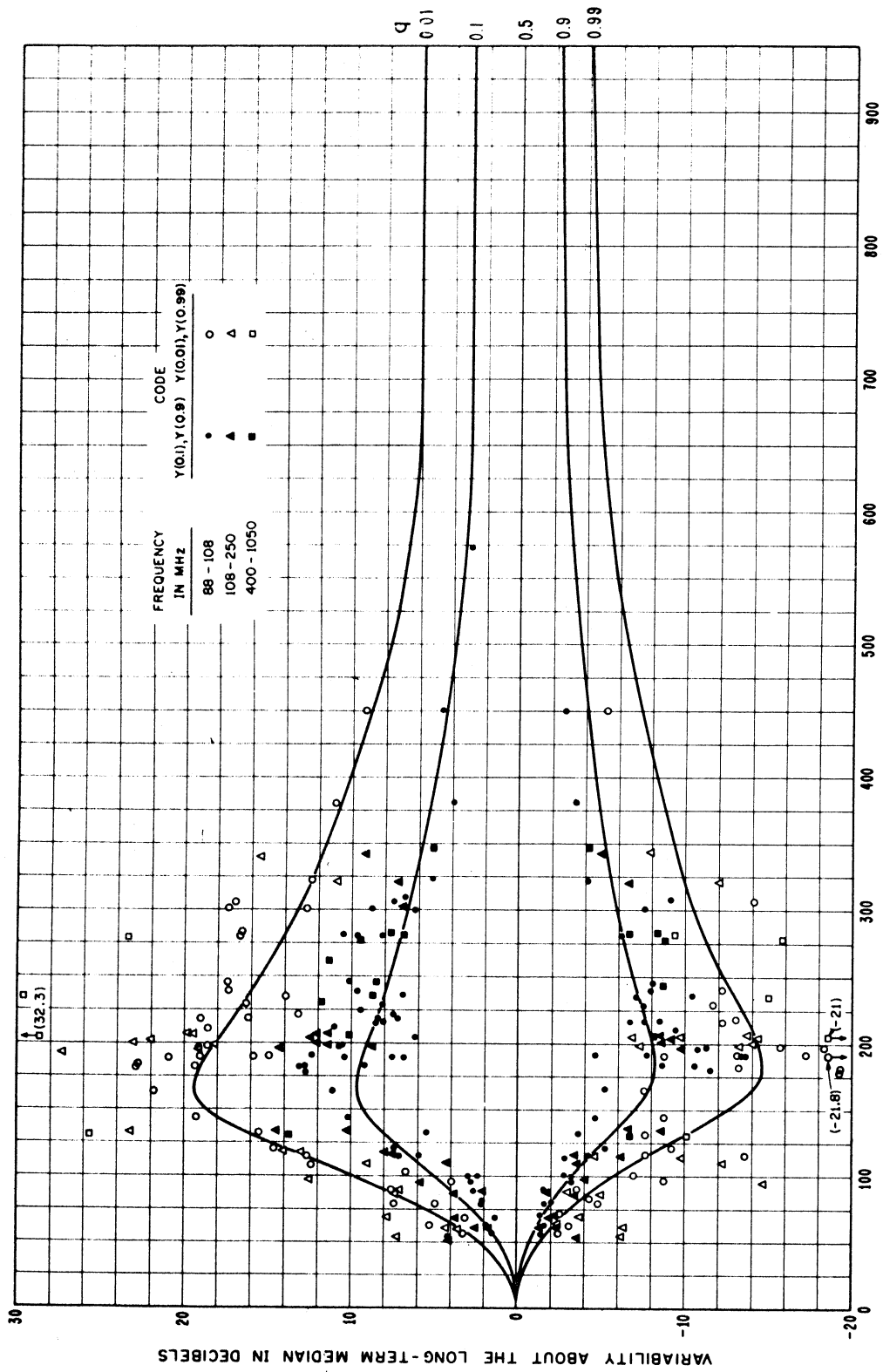
SUMMER TIME BLOCKS, MAY - OCT., U. S. A.
 CURVES FOR 88-108 MHz



EFFECTIVE DISTANCE, d_e , IN KILOMETERS

Figure III.34

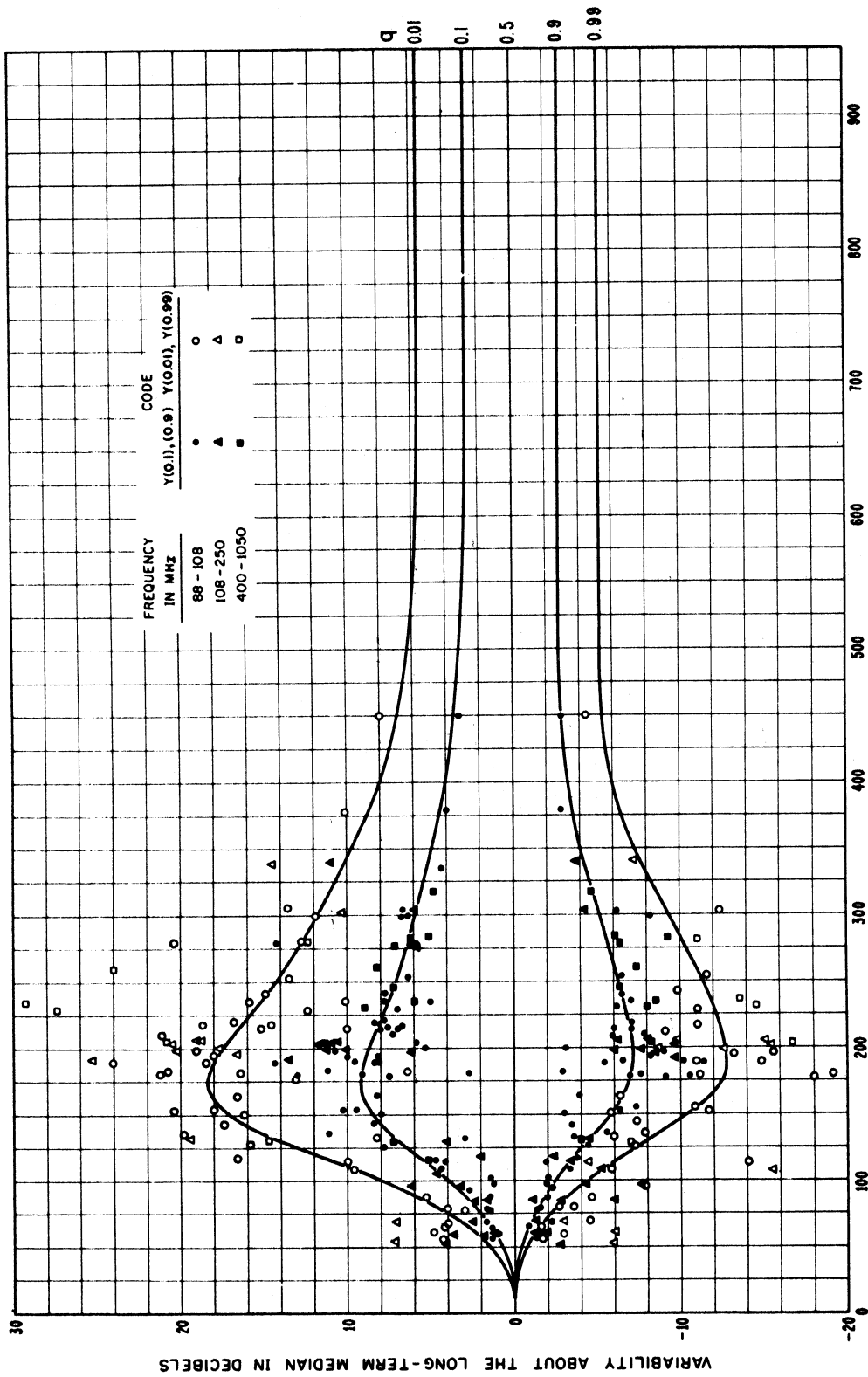
TIME BLOCK 1, NOV. - APRIL, 0600 - 1300 HRS., U. S. A.
 CURVES SHOW $Y(q, d_e)$ FOR THE FREQUENCY RANGE 88 - 108 MHz



EFFECTIVE DISTANCE, d_e , IN KILOMETERS

Figure III.35

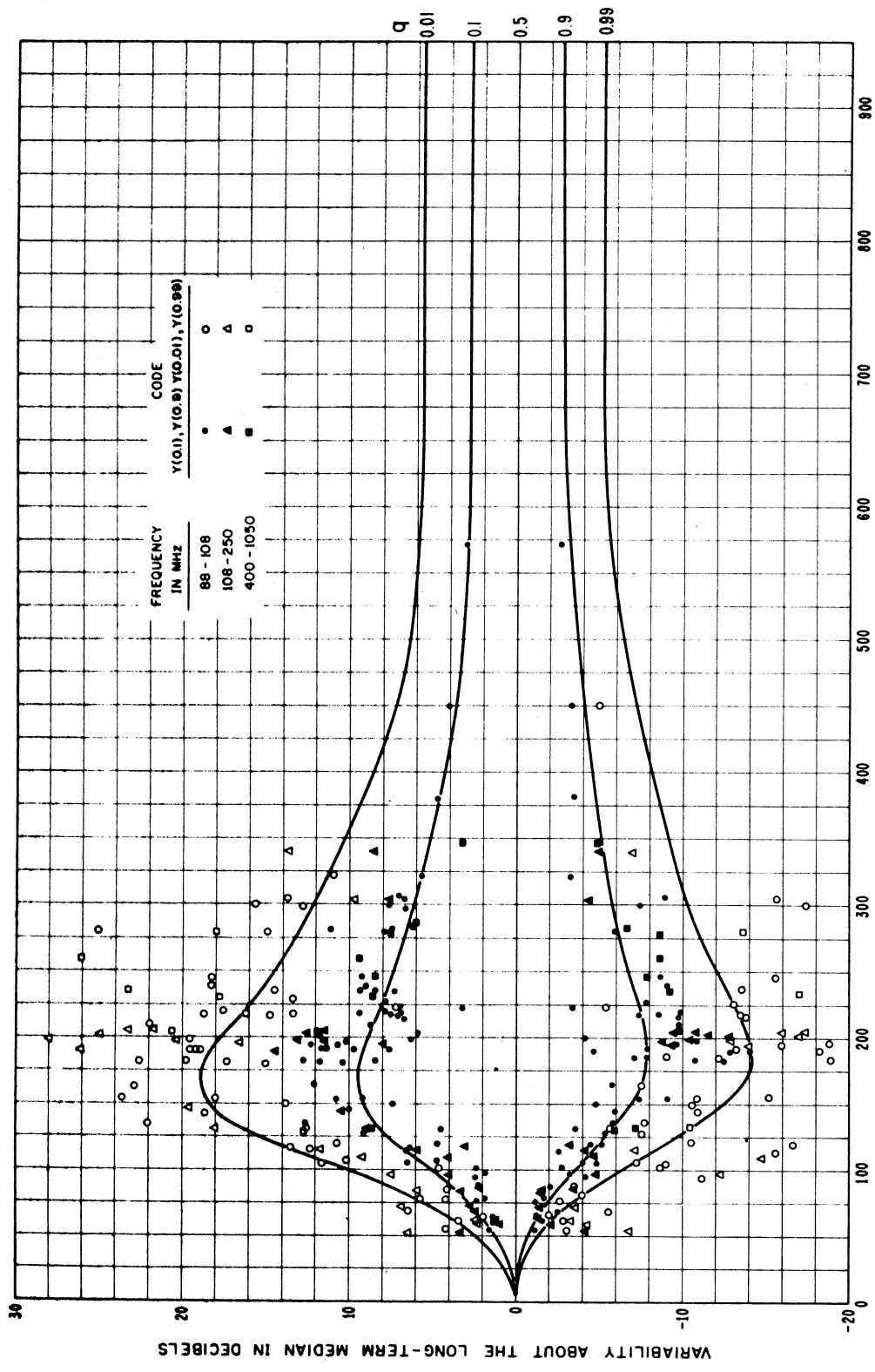
TIME BLOCK 2, NOV. - APRIL, 1300 - 1800 HRS., U. S. A.
 CURVES SHOW $Y(q, d_e)$ FOR THE FREQUENCY RANGE 88 - 108 MHz



EFFECTIVE DISTANCE, d_e , IN KILOMETERS

Figure III.36

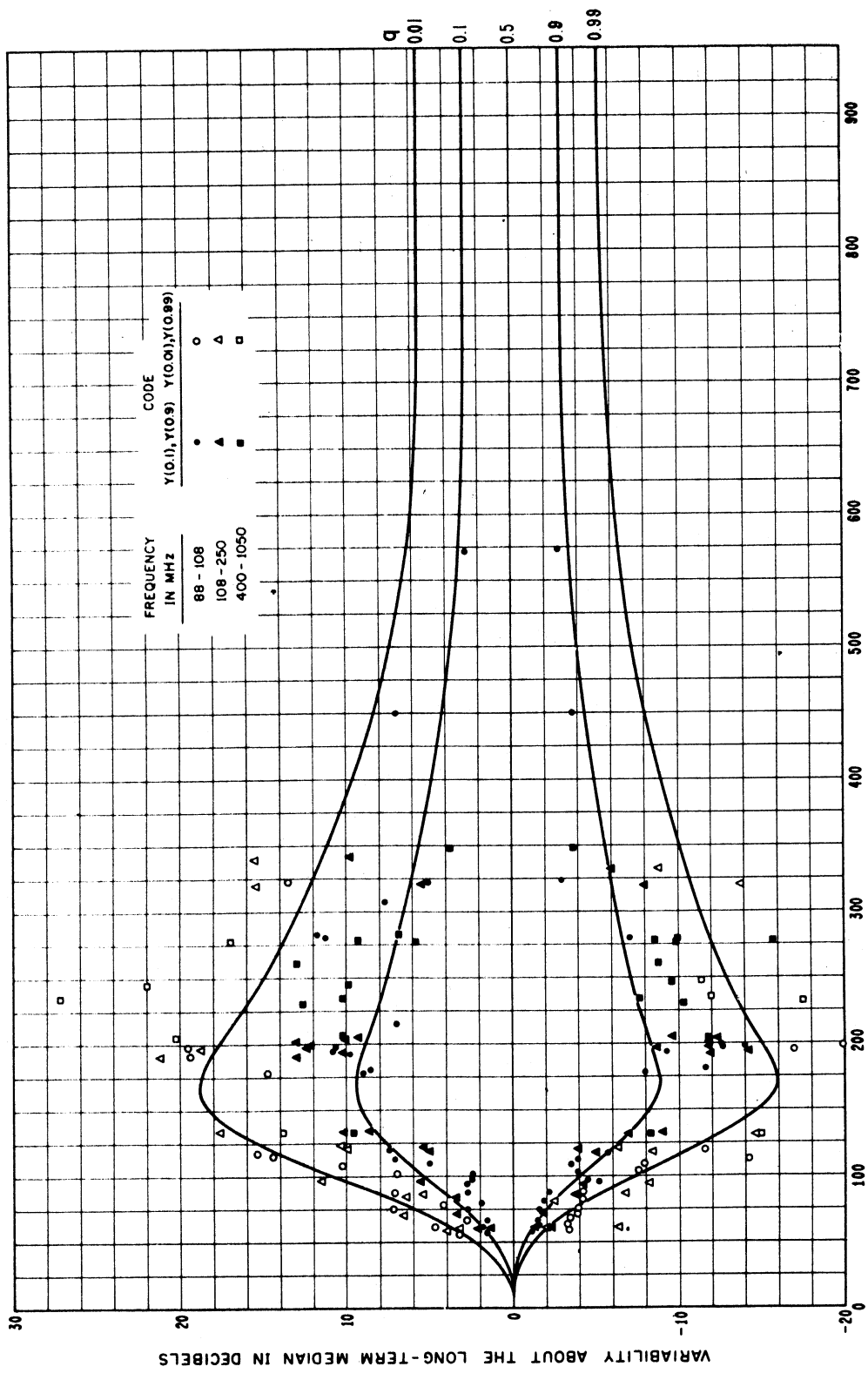
TIME BLOCK 3, NOV. - APRIL, 1800 - 2400 HRS., U.S.A.
 CURVES SHOW $Y(q, d_e)$ FOR THE FREQUENCY RANGE 88 - 108 MHz



EFFECTIVE DISTANCE, d_e , IN KILOMETERS

Figure III.37

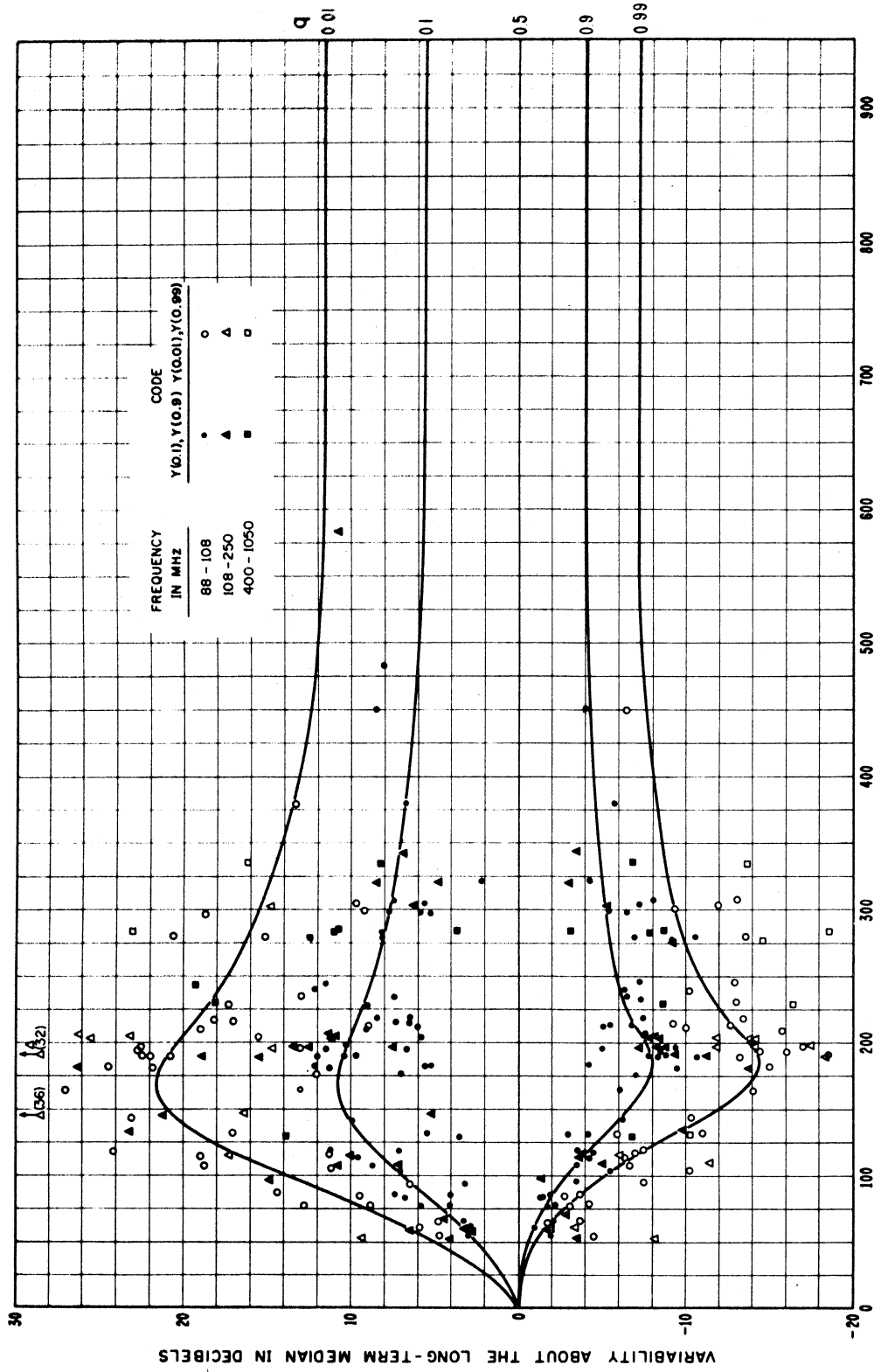
TIME BLOCK 8, NOV. - APRIL, 0000-0600 HRS., U. S. A.
 CURVES SHOW $Y(q, d_e)$ FOR THE FREQUENCY RANGE 88 - 108 MHz



EFFECTIVE DISTANCE, d_e , IN KILOMETERS

Figure III.38

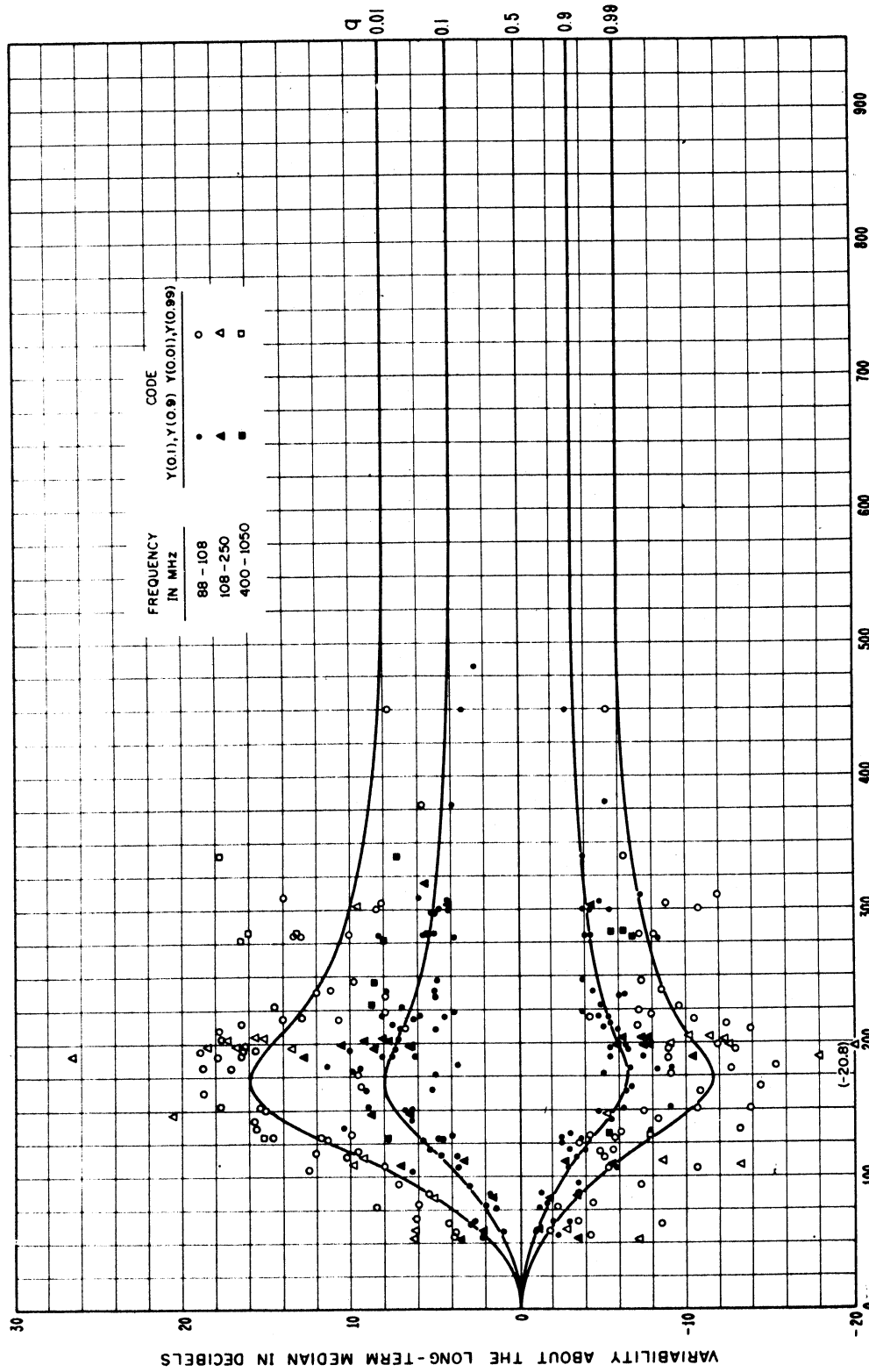
TIME BLOCK 4, MAY - OCT., 0600-1300 HRS., U.S.A.
 CURVES SHOW $Y(q, d_e)$ FOR THE FREQUENCY RANGE 88 - 108 MHz



EFFECTIVE DISTANCE, d_e , IN KILOMETERS

Figure III.39

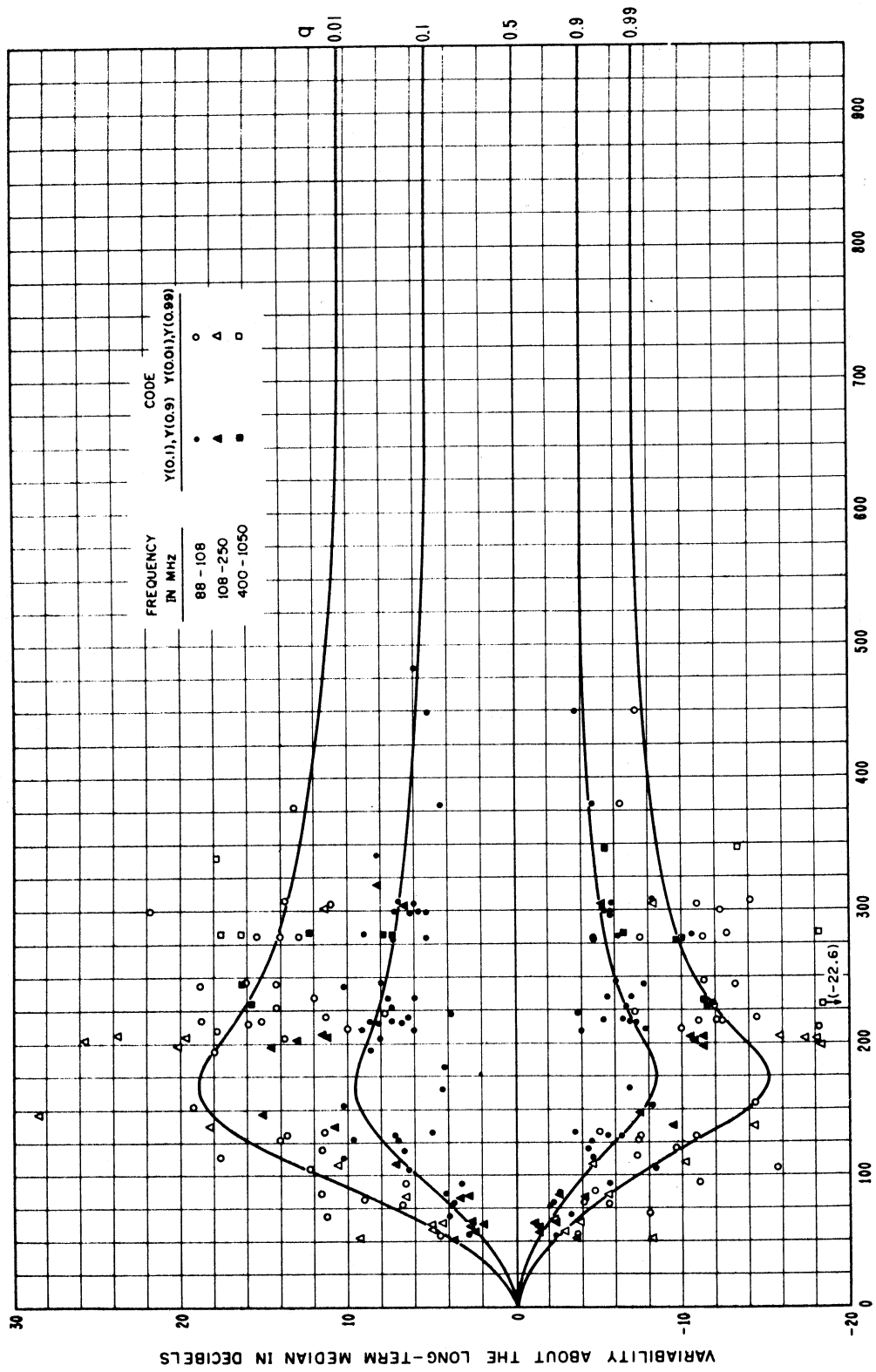
TIME BLOCK 5, MAY - OCT., 1300 - 1800 HRS., U. S. A.
 CURVES SHOW $Y(q, d_e)$ FOR THE FREQUENCY RANGE 88 - 108 MHZ



EFFECTIVE DISTANCE, d_e , IN KILOMETERS

Figure III.40

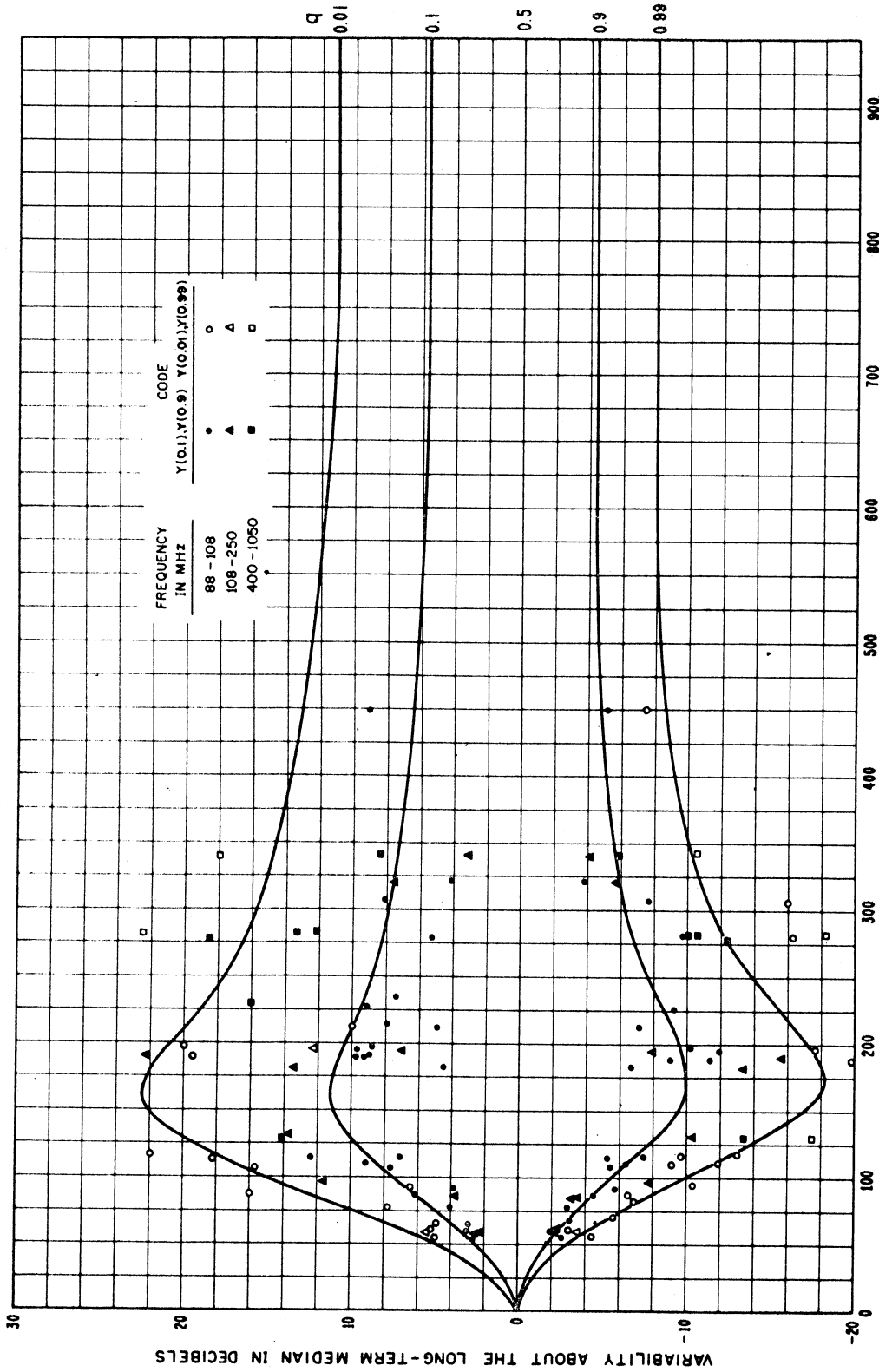
TIME BLOCK 6, MAY - OCT., 1800 - 2400 HRS., U.S.A.
 CURVES SHOW $Y(q, d_e)$ FOR THE FREQUENCY RANGE 88 - 108 MHz



EFFECTIVE DISTANCE, d_e , IN KILOMETERS

Figure III.41

TIME BLOCK 7, MAY - OCT., 0000-0600 HRS., U.S.A.
 CURVES SHOW $Y(q, d_e)$ FOR THE FREQUENCY RANGE 88-108 MHz



EFFECTIVE DISTANCE, d_e , IN KILOMETERS

Figure III.42

III.8 List of Special Symbols Used in Annex III

$A(v_j)$	Attenuation relative to free space for each of several rays as a function of the parameter v_j , where $j = 1, 2, 3, 4$, (III. 34).
b	The parameter b , a function of ground constants, carrier frequency, and polarization, expressed in degrees, figure 8.2, and equations (III. 40) and (III. 41).
b_h	The parameter b for horizontal polarization defined by (III. 40).
b_v	The parameter b for vertical polarization, (III. 41).
c	A parameter showing the phase change associated with the complex plane wave reflection coefficient $R \exp[-i(\pi-c)]$ corresponding to reflection from an infinite smooth plane surface, (5.4) figures III. 1 through III. 8.
c_h, c_v	Values of c for horizontal and vertical polarization, respectively, (III. 13) and (III. 14) figures III. 1 through III. 8.
C_j	Fresnel integral, (III. 33), where $j = 1, 2, 3, 4$.
$Ci(r), Ci(r_1), Ci(r_2)$	Cosine integral as a function of r , (III. 51), r_1 and r_2 (III. 50).
d_r	Distance used in calculating ground reflections in knife edge diffraction; d_r is defined by (III. 29).
$d_{11}, d_{12}, d_{21}, d_{22}$	Distances used in computing diffraction attenuation with ground reflections, (III. 31) figure III. 9.
f_j	Diffraction loss for each of several distinct rays over an isolated obstacle, where $j = 1, 2, 3, 4$, (III. 32-III. 35).
f_1, f_2, f_3, f_4	Diffraction loss for each of four distinct rays over an isolated obstacle, (III. 32).
$f(r_1), f(r_2)$	Functions of the normalized antenna heights r_1 and r_2 , (III. 50).
$f(v_j)$	A function identically equal to f_j for $v = v_j$, (III. 33) figure III. 10.
$f(\theta_h)$	A factor used to reduce estimates of variability for antenna beams elevated above the horizon plane, (III. 65) figure III. 22. See θ_h and θ_b .
F_{oi}	Scattering efficiency correction term for the i^{th} lobe of an antenna pattern, (III. 63).
$F(\theta_{ei}, d)$	This function is the same as $F(\theta d)$ with the effective angular distance θ_{ei} substituted for the angular distance, θ , annex III, (III. 57).
g_b, g_{bt}	A high gain antenna radiates g_b watts per unit area in every direction not accounted for by the main beam or by one of the side lobes of an antenna. The gain g_b for a transmitting antenna is g_{bt} , section III. 6.
$g(f)$	A frequency correction factor shown in figure III. 30, (III. 66).
G_b, G_{bt}	Decibel equivalent of g_b , $G_b = 10 \log g_b$, and of g_{bt} , annex III section III. 6.
G_{ri}, G_{ti}	Gains of the i^{th} lobe of receiving and transmitting antennas, respectively, (III. 57).
h_e	A height, using elevated beams, that is equivalent to h_o for horizon rays, (III. 63).
h_{rm}, h_{tm}	Height of a knife edge above a reflecting plane on the receiver or transmitter side of the knife edge, (III. 37).

$h(r)$ A function of r shown in figures III. 20 and III. 21.

$h(r_1), h(r_2)$ A function of r_1 or r_2 defined by (III. 50) and shown on figures III. 20 and III. 21.

H_{oi} The frequency gain function for the i^{th} beam intersection in a scattering plane (III. 57).

j Represents a series of subscripts 1, 2, 3, 4, as used in equations (III. 27) to (III. 35).

K_h The diffraction parameter K for horizontal polarization, section III. 4.

K_v The diffraction parameter K for vertical polarization, section III. 4.

L_{gi} Loss in antenna gain for the i^{th} scattering subvolume, (III. 57).

L_i Transmission loss associated with the i^{th} power contribution, (III. 55) and (III. 57).

$L_1, L_2 \dots L_n \dots L_N$ A series of hourly median values of transmission loss arranged in order from the smallest to the largest value, section III. 7.

$L(q)$ Transmission loss exceeded a fraction q of the time, (III. 68).

m_h, m_v Parameters used in computing the magnitudes R_h and R_v of the smooth plane earth reflection coefficient R , (III. 10).

$mho.$ A unit of conductance, the reciprocal of resistance which is measured in ohms, figures III. 1 to III. 8.

p A function of the dielectric constant and grazing angle used in computing the plane wave reflection coefficient, (III. 8).

q A parameter used in calculating a plane wave reflection coefficient, (III. 7) to (III. 14).

$r_{11}, r_{12}, r_{21}, r_{22}$ Distances to and from the bounce point of reflected rays, (III. 28) figure III. 9.

R_h Plane earth reflection coefficient R for horizontal polarization, (III. 12) and figures III. 1 to III. 8.

R_v Plane earth reflection coefficient R for vertical polarization, (III. 12) figures III. 1 to III. 8.

s_e Path asymmetry factor for beams elevated above the horizon, $s_e = \alpha_e / \beta_e$, (III. 64).

$Si(r)$ Sine integral as a function of r , (III. 51).

S_j Fresnel integral, (III. 33).

v_j The parameter v for each of j paths over an isolated obstacle, (III. 27).

w_{ai} Contribution to the total available power from the i^{th} scattering subvolume, (III. 55) and (IV. 11).

x_a, x_b Points at which a first Fresnel ellipse cuts the great circle plane, III. 18 to III. 23.

α_e, β_e The angles between the "bottoms" of transmitting or receiving antenna beams or side lobes and a line joining the antennas, (III. 61).

α_{ei}, β_{ei}	Angles α_e and β_e for the i^{th} lobe of an antenna pattern.
α_{eo}, β_{eo}	When beams are elevated sufficiently that there is no bending of the ray due to atmospheric refraction $\alpha_e = \alpha_{eo}$, $\beta_e = \beta_{eo}$, (III. 60); when ray bending must be considered α_e and β_e are computed using (III. 61).
α_{oj}, β_{oj}	The angles α_o , β_o made by each of j rays, over an isolated obstacle, (III. 36).
$\alpha_{o1}, \alpha_{o2}, \beta_{o1}, \beta_{o2}$	The angles α_o and β_o for each of four rays over an isolated obstacle, (III. 36).
δ	A parameter used in computing the first Fresnel zone in a reflecting plane, (III. 18).
δ	The effective half-power semi-beamwidth of an antenna, section III. 6.
δ_e	The effective half-power semi-beamwidth of an antenna that is elevated or directed out of the great circle plane, section III. 6.
δ_o	The semi-beamwidth of an equivalent beam pattern with a square cross-section $\delta_o = \delta\sqrt{\pi/4}$, section III. 6.
$\delta_{rwo}, \delta_{two}$	Azimuthal equivalent semi-beamwidths with square cross-section, (III. 58) figure III. 23.
$\delta_{rzo}, \delta_{tzo}$	Vertical angle equivalent semi-beamwidths with square cross-section, (III. 58) figure III. 23.
δ_{wo}	Azimuthal equivalent semi-beamwidth with square cross-section, section III. 6.
δ_{zo}	Vertical angle equivalent semi-beamwidth, section III. 6.
Δ_j	The j^{th} value of Δr , where $\Delta r = r_1 + r_2 - r_o$, (III. 27) and (III. 29).
$\Delta_1, \Delta_2, \Delta_3, \Delta_4$	Ray path differences between a direct ray and a ray path over a single isolated obstacle with ground reflections, (III. 28) figure (III. 9).
$\Delta_{1r}, \Delta_{2r}, \Delta_{3r}, \Delta_{4r}$	Ray path difference between straight and ground reflected rays on either side of an isolated obstacle, (III. 31), (III. 37).
ϵ	Ratio of the dielectric constant of the earth's surface to the dielectric constant of air, figures 8.1 and 8.2, annex III. 4.
$\epsilon_{r1}, \epsilon_{t1}$	Angle between the axis of the main beam and the axis of the first side lobe of an antenna pattern, figure III. 22.
$\epsilon_{tw1}, \epsilon_{tw2}$	Azimuth angles of the first and second lobes of a transmitting antenna relative to the main beam axis, figure III. 23.
$\epsilon_{ts1}, \epsilon_{ts2}$	Elevation angles of the first and second lobes of a transmitting antenna relative to the main beam axis, figure III. 23.
ζ	The angle that a scattering plane makes with the great circle plane, (III. 60), (III. 61), and figure III. 22.
η_{se}	A function of h_e and N_s used in computing F_{oi} and H_{oi} for scattering from antenna beams directed above the horizon or away from the great circle plane, (III. 64).
θ_b	Angle of elevation of the lower half power point of an antenna beam above the horizontal, (III. 62). See θ_h and $f(\theta_h)$.

θ_{br}, θ_{bt}	Values of θ_b for the receiving and transmitting antennas, respectively, (III. 61).
$\theta_{bri}, \theta_{bti}$	Values of θ_b for the i^{th} beam intersection, (III. 59).
θ_e	The angle between radio rays elevated above the horizon and/or away from the great circle plane, (III. 64).
θ_{ei}	The angle θ_e at the i^{th} intersection of radio rays elevated above the horizon and/or away from the great circle plane, (III. 57).
$\theta_{e1}, \theta_{e2}, \dots, \theta_{en}$	The angle θ_e for the first, second, ... n^{th} intersection of radio rays, figure III. 22.
θ_{hr}, θ_{ht}	Angle of elevation of a knife edge relative to the horizontal at the receiving or transmitting antenna, (III. 38).
θ_j	Angle between direct and/or reflected ray over a knife-edge, where $j = 1, 2, 3, 4$ as shown in figure III. 9.
θ_{jr}	Angles defined in (III. 29), where $j = 1, 2, 3, 4$, which are added to θ to determine $\theta_j = \theta + \theta_{jr}$.
$\theta_{1r}, \theta_{2r}, \theta_{3r}, \theta_{4r}$	Values of θ_{jr} for $j = 1, 2, 3, 4$, (III. 29).
$\theta_1, \theta_2, \theta_3, \theta_4$	The angle between rays from the transmitting and receiving antennas over an isolated obstacle with ground reflections, figure III. 9.
σ	Surface conductivity in mhos per meter, figures 8.1 and 8.2, section III. 4.
τ	The amount a radio ray bends in the atmosphere, (III. 62).
$\tau(\theta_b, d, N_s)$	Bending of a radio ray that takes off at an initial angle θ_b and travels d kilometers through an atmosphere characterized by a surface refractivity N_s , (III. 61).
$\phi(v, 0)$	Component of phase lag due to diffraction over an idealized knife edge, (7.13) figure 7.1, and (III. 30).
$\phi(v\rho)$	Component of phase lag due to diffraction over an isolated perfectly-conducting rounded obstacle, (7.13) figure 7.5 and (III. 30).
$\phi(0, \rho)$	The component of the phase lag of the diffracted field over an isolated perfectly-conducting rounded obstacle for $v = 0$, (7.13) figure 7.4 and (III. 30).
Φ_j	The phase lag of the diffracted field for the j^{th} ray over an isolated perfectly-conducting rounded obstacle (III. 30a), where $j = 1, 2, 3, 4$.
$\Phi_j(v, \rho)$	The phase lag of the diffracted ray over an isolated rounded obstacle for the j^{th} ray, $\Phi_j(v, \rho) \equiv \Phi_j$, (III. 30).
$\Phi_j(v, 0)$	The phase lag over an ideal knife edge for the j^{th} ray, (III. 30).
$\Phi_1, \Phi_2, \Phi_3, \Phi_4$	The phase lag $\Phi_j(v, \rho)$ for values of $j = 1, 2, 3, 4$, (III. 32).
ψ_r, ψ_t	The angle between the plane of the lower half-power point of an antenna beam and the receiver or transmitter horizon plane, (III. 60).
ψ_{ri}, ψ_{ti}	The angle ψ_r or ψ_t for the i^{th} lobe of an antenna pattern, (III. 59).
ψ_1, ψ_2	Angle of reflection at the ground of a reflected ray that passes over a knife-edge, (III. 36) figure III. 9.

Ω The half-power beamwidth, $\Omega = 2\delta$, (9.10) and figure III.22.

$\Omega_{ro}, \Omega_{rl}, \Omega_{to}, \Omega_{tl}$ Half-power beamwidths corresponding to $2\delta_o, 2\delta_l$ for the receiving and transmitting antenna patterns, respectively, figure III.22.

Annex IV
FORWARD SCATTER

IV.1 General Discussion

This annex discusses some of the similarities and differences between forward scatter from refractive index turbulence and forward scatter or incoherent reflections from tropospheric layers.

To scatter is to spread at random over a surface or through a space or substance. Scattering which tends to be coherent is more properly called forward scatter, reflection, refraction, focusing, diffraction, or all of these, depending on the circumstances. Modes of scattering as well as mechanisms of propagation bear these names. For example, we may speak of the reflection, refraction, diffraction, focusing, scattering, and absorption of a radio wave by a single spherical hailstone, and all of these modes can be identified in the formal solutions of Maxwell's equations for this problem.

The large volume of beyond-the-horizon radio transmission loss data available in the frequency range 40 to 4000 MHz and corresponding to scattering angles between one and three degrees indicates that the ratio $10^{-A}/10$ corresponding to the transmission loss, A, relative to free space is approximately proportional to the wavelength, λ , or inversely proportional to the radio frequency, f, [Norton, 1960], so that the ratio $10^{-L_b}/10$ corresponding to the forward scatter basic transmission loss is approximately proportional to λ^3 or to f^{-3} . This circumstance is more readily explained in terms of forward scatter from layers [Friis, Crawford, and Hogg, 1957] or in terms of glancing or glinting from brilliant points on randomly disposed "feuilletts", [duCastel, Misme, Spizzichino, and Voge, 1962], than in terms of forward scatter from the type of turbulence characterized by the modern Obukhov-Kolmogorov theory [Obukhov, 1941, 1953; Batchelor, 1947, 1953]. There is recent evidence [Norton and Barrows, 1964] that the wavenumber spectrum of refractivity turbulence in a vertical direction has the same form as the more adequately studied spectrum of variations in space in a horizontal direction. Some mechanism other than scatter from refractivity turbulence must be dominant most of the time to explain the observed transmission loss values over a majority of the transhorizon tropospheric paths for which data are available. Scattering from refractivity turbulence and scattering from sharp gradients are mechanisms which coexist at all times in any large scattering volume. Sharp gradients always exist somewhere, and the atmosphere between them is always somewhat turbulent. Power scattered by these mechanisms is occasionally supplemented by diffraction, specular reflection from strong extended layers, and/or ducting.

A tropospheric duct exists, either ground-based or elevated, if a substantial amount of energy is focused toward or defocused away from a receiver as super-refractive gradients of N exceed a critical value called a "ducting gradient." This gradient is about -157 N-units per kilometer at sea level for horizontally launched radio waves. The duct thickness must

exceed about $5062 f^{-\frac{2}{3}}$ meters with f in MHz [Kerr, 1964] for a duct to completely trap such radio waves. A few useful references in this connection are cited at the end of section 4, Volume 1.

A more or less horizontally homogeneous "kink" in a refractive index profile may indicate the possibility of ducting for very short wavelengths, the presence of a refracting layer for some of the longer waves, and merely a slight and random perturbation of average atmospheric conditions for other frequencies, antenna locations, or antenna beam patterns and elevation angles. The layer that presents a sharp discontinuity for radio frequencies from 30 to 100 MHz ($\lambda = 10$ to 3 meters) may represent a relatively gradual change of refractive index at 300 MHz ($\lambda = 1$ meter) and higher frequencies. A tropospheric layer or "feuillet" requires a sufficiently abrupt change in refractive index, usually associated with fine weather conditions, to reflect a substantial amount of radio energy at the grazing angles and frequencies of interest. These may be horizontal changes, in thermals, for instance, as well as changes of refractivity, N , with height.

Almost specular reflection from tropospheric layers is often observed between 30 MHz and 200 MHz. At higher frequencies, where focusing, defocusing, and ducting are common, and where extensive layers are not sufficiently abrupt or sufficiently numerous to provide strong reflections, a number of small and randomly oriented surfaces come into play. A recent summary of the role of the layer structure of the troposphere in explaining tropospheric propagation [Saxton, Lane, Meadows, and Matthews, 1964] includes an extensive list of references. Also useful are general discussions of tropospheric propagation by Bullington [1955], du Castel [1960], Crawford, Hogg, and Kummer [1959], Fengler [1964], Fengler, Jeske, and Stilke [1964], Kirby, Rice, and Maloney [1961], Johnson [1958], Rice and Herbstreit [1964], Shkarofsky [1958], and Vvedenskii and Arenberg [1957].

There are at least three distinguishing features in most theories of forward scatter from clouds, precipitation, refractive index turbulence, layers, or feuillets. A calculation is first made of the expected or average forward scattering pattern, reradiation pattern, or diffraction pattern of a scatterer or a group of scatterers, usually located in free space, and usually assuming an incident plane wave and a distant receiver. Second, a decision is made that the relative phases of waves scattered from individual raindrops or subvolumes of refractivity turbulence or feuillets are random, so that we may simply add the power contributions from these elements and ignore the phases. This is an essential feature of a random scatter theory. And third, some way is found to relate the actual terrain, atmosphere, and antenna parameters to the theoretical model so that a comparison may be made between data and theory.

IV.2 Models for Forward Scattering

The mechanisms of scattering from refractivity turbulence, reflection from elevated layers, and ducting are much more sensitive to vertical refractivity gradients than to the

horizontal gradients commonly observed. The forward scatter theory used to develop the prediction methods of section 9 assumes that only vertical scales of turbulence or layer thicknesses are important. The radio wave scattered forward by all the scattering subvolumes visible to both antennas or by all the layers of feuillets visible to both antennas is most affected by a particular range of "eddy sizes", l , or by layers of an average thickness $l/2$. A stack of eddies of size l must satisfy the Bragg condition that reradiation by adjacent eddies shall add in phase. Reflections from the exterior and interior boundaries of a layer will add in phase if the ray traversing the interior of the layer is an odd number of wavelengths longer than the ray reflected from the exterior boundary. Either the mechanism of forward scatter from refractivity turbulence or the mechanism of reflection from layers or feuillets selects a wavenumber direction \hat{k} that satisfies the specular reflection condition corresponding to Snell's law that angles of incidence and reflection, ψ , are equal. Mathematically, these conditions are represented by the following relations:

$$l = \frac{\lambda}{2 \sin(\theta/2)} \cong \frac{\lambda}{\theta}, \quad \hat{k} = \frac{\hat{R}_o + \hat{R}}{|\hat{R}_o + \hat{R}|} \quad (\text{IV. 1})$$

where \hat{R}_o and \hat{R} are unit vectors from the centers of radiation of the transmitting and receiving antenna, respectively, towards an elementary scattering volume, or towards the point of geometrical reflection from a layer. The angle between \hat{R} and \hat{R}_o is the scattering angle θ illustrated in figure IV-1 and is thus twice the grazing angle ψ for reflection from a layer:

$$\theta = 2\psi = \cos^{-1}(-\hat{R} \cdot \hat{R}_o) \text{ radians.} \quad (\text{IV. 2})$$

The plane wave Fresnel reflection coefficient q_o for an infinitely extended plane boundary between homogeneous media with refractive indices n_1 and n_2 and for horizontal polarization [Wait, 1962] is

$$q_o = \frac{\sin \psi - \left[\frac{2(n_1 - n_2) + (n_1 - n_2)^2 + \sin^2 \psi}{2(n_1 - n_2) + (n_1 - n_2)^2 + \sin^2 \psi} \right]}{\sin \psi + \left[\frac{2(n_1 - n_2) + (n_1 - n_2)^2 + \sin^2 \psi}{2(n_1 - n_2) + (n_1 - n_2)^2 + \sin^2 \psi} \right]} \quad (\text{IV. 3})$$

The following approximation, valid for $(n_1 - n_2)^2 < \sin^2 \psi < 1$ is also good for vertical polarization:

$$q_o \cong \frac{n_2 - n_1}{2\psi^2} \exp \left[- (n_2 - n_1)^2 / (2\psi^2) \right] \cong \frac{n_2 - n_1}{2\psi^2} = \frac{2(n_2 - n_1)}{\theta^2} \quad (\text{IV. 4})$$

A differential amplitude reflection coefficient dq for a tropospheric layer is next defined as proportional to the difference between two gradients of refractive index, m and m_0 , where m is the average refractive index gradient dn/dz across the layer, and m_0 is the average refractive index gradient for the region in which the layer is embedded. Let the layer extend in depth from $z = 0$ to $z = z_0$ in the wavenumber direction \hat{k} defined by (IV. 1), and write the differential reflection coefficient as

$$dq = dz (m - m_0) / (2\psi^2). \quad (\text{IV. 5})$$

A phasor $\exp[-iz(4\pi\psi/\lambda)]$ is associated with dq , and the power reflection coefficient q^2 for a tropospheric layer of thickness z_0 is approximated as

$$q^2 = \left| \int_{z=0}^{z=z_0} dq \exp[-iz(4\pi\psi/\lambda)] \right|^2 = (4\pi)^2 \lambda^2 \psi^{-6} M \quad (\text{IV. 6a})$$

$$M = (m - m_0)^2 [1 - \cos(4\pi\psi z_0/\lambda)] / (4\pi)^4. \quad (\text{IV. 6b})$$

If M is assumed continuous at $z = 0$ and $z = z_0$, somewhat smaller values of q^2 and m will result [Wait, 1962].

Friis, Crawford, and Hogg [1957] point out that the power received by reflection from a finite layer can be approximated as the diffracted power through an absorbing screen with the dimensions of the layer projection normal to the direction of propagation. They then consider layers of large, small, and medium size compared to

$$2x = 2(\lambda R_0 R/d)^{1/2}, \quad d \cong R_0 + R \quad (\text{IV. 7})$$

which is the width of a first Fresnel zone. Let b represent the dimensions of a layer or feuillet in any direction perpendicular to \hat{k} . Since \hat{k} is usually nearly vertical, b is usually a horizontal dimension. Adopting a notation which conforms to that used elsewhere in this report, the available power w_a at a receiver at a distance d from a transmitting antenna radiating w_t watts is

$$w_a = \frac{4 w_t g_t g_r \lambda^2 q^2}{(4\pi d)^2} [C^2(u) + S^2(u)] [C^2(v) + S^2(v)] \quad (\text{IV. 8})$$

in terms of Fresnel integrals given by (III. 33), where

$$u = b\sqrt{2}/x, \quad v = b\psi\sqrt{2}/x \quad (\text{IV. 9})$$

and g_t and g_r are antenna directive gains. For large u and v ,

$$C^2(u) = S^2(u) = C^2(v) = S^2(v) = 1/4,$$

and for small u and v , $C^2(u) = u^2$, $C^2(v) = v^2$, and $S^2(u) = S^2(v) = 0$.

For large layers, where $b \gg 2x$:

$$w_a = w_t g_t g_r \lambda^4 \psi^{-6} d^{-2} M. \quad (\text{IV.10a})$$

For intermediate layers, where $b \cong 2x$:

$$w_a = w_t g_t g_r \lambda^3 \psi^{-4} (RR_o d)^{-1} b^2 M. \quad (\text{IV.10b})$$

For small layers, where $b \ll 2x$:

$$w_a = w_t g_t g_r \lambda^2 \psi^{-4} (RR_o)^{-2} b^4 M. \quad (\text{IV.10c})$$

Forward scatter from layers depends on the statistics of sharp refractive index gradients in the directions $\hat{\kappa}$ defined by (IV.1). The determination of these statistics from radio and meteorological measurements is only gradually becoming practical. A study of likely statistical averages of the meteorological parameters M , $b^2 M$, and $b^4 M$ indicates that these expected values should depend only slightly on the wavelength λ and the grazing angle ψ , as was assumed by Friis, et al. [1957]. The expected value of

$$[1 - \cos(4\pi \psi z_o / \lambda)]$$

can vary only between 0 and 2 and is not likely to be either 0 or 2 for any reasonable assumptions about the statistics of z_o .

Available long-term median radio transmission loss data usually show the frequency law given by (IV.10b) for medium-size layers. Long-term cumulative distributions of short-term available power ratios on spaced frequencies rarely show a wavelength law outside the range from λ^2 to λ^4 [Crawford, Hogg, and Kummer, 1959; Norton 1960]. An unreported analysis of 8978 hours of matched simultaneous recordings at 159.5, 599, and 2120 MHz over a 310-km path in Japan shows that this wavelength exponent for transmission loss w_a/w_t is within the range from 2 to 4 ninety-eight percent of the time. This corresponds to a wavelength exponent range from 0 to 2 or a frequency exponent range from 0 to -2 for attenuation relative to free space values, and to corresponding ranges λ^2 to λ^4 or f^{-2} to f^{-4} for values of basic transmission loss, L_b .

Figures IV.1(a) and IV.1(b) illustrate forward scattering from a single small layer and from refractivity turbulence in a single small scattering subvolume of the volume V of space visible to two antennas. Figures IV.1(c) and IV.1(d) illustrate models for the addition of power contributions from large parallel layers, and from scattering or reflection subvolumes, respectively. Contributions from diffraction or ducting are ignored, as well as returns from well-developed layers for which a geometrical reflection point is not visible to both antennas. Combinations of these mechanisms, though sometimes important, are also not considered here.

For each of the cases shown in figure IV.1, coherently scattered or reflected power w_{ai} from the neighborhood of a point \vec{R}_{oi} is conveniently associated with a scattering subvolume $d^3R_o = dv = v_i(\vec{R}_{oi})$, so that the total available forward scattered power at a receiver is

$$w_a = \sum_{i=1}^{N_v} w_{ai} = \sum_{i=1}^{N_v} v_i w_{vi} \cong \int_V d^3R_o w_v(\vec{R}_o, \vec{R}) \text{ watts} \quad (\text{IV. 11})$$

where

$$w_{vi} = w_{ai}/v_i = w_v(\vec{R}_o, \vec{R}) \quad (\text{IV. 12})$$

is the available power per unit scattering volume for the i^{th} scattering subvolume, feuillet, or layer, and it is assumed that only N_v such contributions to w_a are important.

Each of the power contributions w_{ai} is governed by the bistatic radar equation. Omitting the subscript i , this equation may be written as

$$w_a = \left(\frac{w_t g_t}{4\pi R_o^2} \right) \left(\frac{a_s c_p}{4\pi R^2} \right) \left(\frac{\lambda^2 g_r}{4\pi} \right) \text{ watts ,} \quad (\text{IV. 13})$$

where $a_s c_p$ is the effective scattering cross-section of a single scatterer or group of scatterers, including the polarization efficiency c_p of the power transfer from transmitter to receiver. The first set of parentheses in (IV.13) represents the field strength in watts per square kilometer at the point \vec{R}_o , the second factor enclosed in parentheses shows what fraction of this field strength is available at the receiver, and $\lambda^2 g_r / (4\pi)$ is the absorbing area of the receiving antenna.

The key to an understanding of scattering from spacecraft, aircraft, rain, hail, snow, refractivity turbulence, or inhomogeneities such as layers or feuillets is the scattering cross-section $a_s c_p$ defined by (IV.13) or the corresponding scattering cross-section per unit volume a_v , defined from (IV.12) and (IV.13) as

$$a_v = (4\pi)^3 (R_o R)^2 w_v / (w_t g_t g_r \lambda^2) \quad \text{per km} \cdot \quad (\text{IV. 14})$$

This quantity is usually estimated by isolating a small volume of scatterers in free space at large vector distances \vec{R}_o and \vec{R} , respectively, from the transmitter and receiver. If both antennas are at the same place, (IV. 13) becomes the monostatic radar equation, corresponding to backscatter instead of to forward scatter.

The scattering cross-sections per unit volume for large, medium, and small layers, assuming a density of N_ℓ layers per unit volume, may be obtained by substituting (IV. 10a) to (IV. 10c) in (IV. 14):

For large layers, where $b \gg 2x$:

$$a_{v1} = x^4 \psi^{-6} M N_\ell = \lambda^2 \psi^{-6} (R_o R/d)^2 M N_\ell \cdot \quad (\text{IV. 15})$$

For intermediate layers, where $b \cong 2x$:

$$a_{v2} = x^2 \psi^{-4} b^2 M N_\ell = \lambda \psi^{-4} (R_o R/d) b^2 M N_\ell \cdot \quad (\text{IV. 16})$$

For small layers, where $b \ll 2x$:

$$a_{v3} = \psi^{-4} b^2 M N_\ell = \lambda^0 \psi^{-4} b^2 M N_\ell \cdot \quad (\text{IV. 17})$$

The modern Obukhov-Kolmogorov theory of homogeneous turbulence in a horizontal direction, when extended to apply to the wavenumber spectrum of instantaneous variations of refractive index in a vertical direction, predicts a $\lambda^{-1/3}$ or $f^{1/3}$ law for the variation with wavelength λ or carrier frequency f of either a_v or attenuation relative to free space, or a $\lambda^{5/3}$ or $f^{-5/3}$ law for variations of the transmission loss w_a/w_t . Theoretical studies of multiple scattering by Beckmann [1961a], Bugnolo [1958], Vysokovskii [1957, 1958], and others suggest that single scattering adequately explains observed phenomena. Descriptions of atmospheric turbulence are given by Batchelor [1947, 1953], de Jager [1952], Heisenberg [1948], Kolmogoroff [1941], Merkulov [1957], Norton [1960], Obukhov [1941, 1953], Rice and Herbstreit [1964], Sutton [1955], Taylor [1922], and Wheelon [1957, 1959].

The observed wavelength exponent for the Japanese transmission loss data previously noted was below 5/3 less than two tenths of one percent of the time, and an examination of other data also leads to the conclusion that forward scatter from Obukhov-Kolmogorov turbulence can rarely explain what is observed with frequencies from 40 to 4000 MHz and scattering angles from one to three degrees.

Early recognition of this fact by Norton, Rice, and Vogler [1955] led to the proposal of a mathematical form for the vertical wavenumber spectrum which would achieve agreement between radio data and the theory of forward scatter from refractivity turbulence [Norton, 1960]. Radio data were used to determine the following empirical form for a_v , upon which the predictions of section 9 are based:

$$a_v = \lambda \psi^{-5} M \quad (\text{IV. 18})$$

$$M = 3 \langle (\Delta n)^2 \rangle / (32 l_0^2) \quad (\text{IV. 19})$$

where

$$\Delta n = n - \langle \Delta n \rangle \quad (\text{IV. 20})$$

is the deviation of refractive index from its expected value $\langle \Delta n \rangle$, and l_0 is a "scale of turbulence" [Rice and Herbstreit, 1964].

Values of the variance $\langle (\Delta n)^2 \rangle$ of refractivity fluctuations and scales of turbulence l_0 obtained from meteorological data lead to good agreement between (IV.18) and radio data when an exponential dependence of M on height is assumed, substituting the corresponding value of w_v in (IV.11). It is not yet clear how the estimates of m , m_0 , z_0 , b , and N_l required by the theory of forward scatter from layers of a given type can be obtained from direct meteorological measurements, nor how these parameters will vary throughout the large volume of space visible to both antennas over a long scatter path. It does seem clear that this needs to be done.

Data from elevated narrow-beam antennas that avoid some of the complex phenomena due to reflection and diffraction by terrain, and which select small scattering volumes, suggest that for scattering angles exceeding ten degrees, reflections from large layers can hardly be dominant over reflection from intermediate and small layers or from refractivity turbulence. Preliminary results indicate that field strengths decrease more slowly at a fixed distance and with scattering angles θ increasing up to fifteen degrees than would be possible with the θ^{-6} dependence of a_v given by (IV.15) added to a probable exponential decay with height of the expected value of the meteorological parameter MN_l for large layers.

The wavelength and angle dependence of forward scatter characterized by the Obukhov-Kolmogorov turbulence theory is nearly the same as that for small layers, given by (IV.17). For scattering from refractivity turbulence:

$$a_{v0} = \lambda^{-1/3} \psi^{-11/3} M_0 \quad (\text{IV. 21})$$

$$M_0 = \frac{\Gamma(11/6) \langle (\Delta n)^2 \rangle}{4(2\pi)^{13/3} \Gamma(1/3) l_0^{2/3}} \quad (\text{IV. 22})$$

Although most of the propagation paths which have been studied rarely show this frequency dependence, some occasionally do agree with (IV.21). In general, the radiowave scattering cross-section per unit volume a_v is a weighted average of scattering from all kinds of layers or feuillets and the turbulence between them.

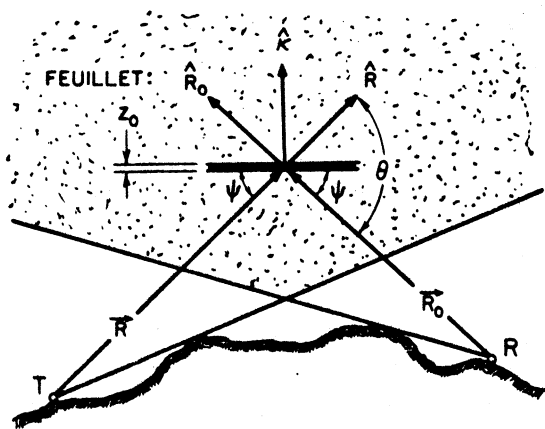
Summarizing the argument:

$$a_v = a_{v0} + a_{v1} + a_{v2} + a_{v3} \cong \lambda \psi^{-5} M \quad (\text{IV.23})$$

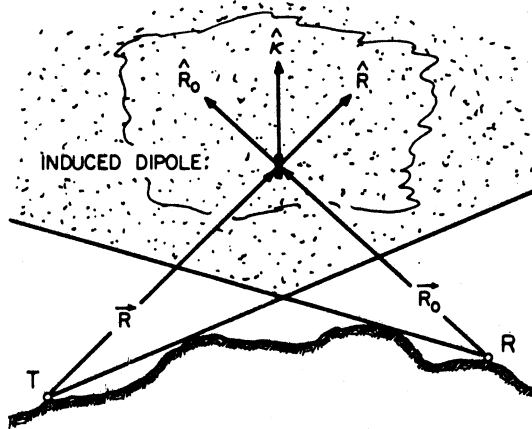
for $10^{-4} < \lambda < 10^{-2}$ km, $0.01 < \psi < 0.03$ radians, where M has been determined from radio data, subject to the assumption that M decreases exponentially with height above the earth's surface. Equation (IV.23) is intended to indicate the present state of the twin arts of formulating theories of tropospheric forward scatter and comparing these theories with available long-term median transmission loss data. A great deal of available data is not forward scatter data, and it is for this reason that estimates of long-term variability as given in section 10 and annex III are almost entirely empirical.

Also, for this reason, estimates of L_{gp} as given in section 9 are restricted to long-term median forward scatter transmission loss. Available measurements of differences in path antenna gain agree within the limits of experimental error with the values predicted by the method of section 9 whenever the dominant propagation mechanism is forward scatter.

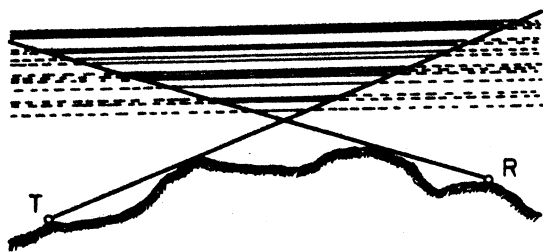
GEOMETRY FOR FORWARD SCATTER



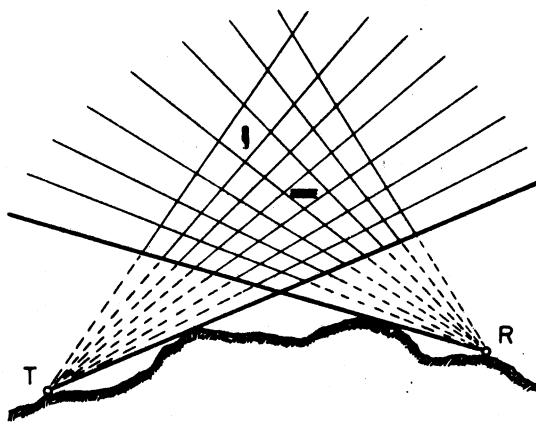
(a)



(b)



(c)



(d)

Figure IV.1

IV. 3 List of Special Symbols Used in Annex IV

a_s	Radiowave scattering cross-section of a single scatterer or group of scatterers, (IV. 13).
a_v	Radiowave scattering cross-section per unit volume, (IV. 14).
a_{v_0}	Radiowave scattering cross-section from refractivity turbulence, (IV. 21).
$a_{v_1}, a_{v_2}, a_{v_3}$	Radiowave scattering cross-sections per unit volume for large, medium, and small layers, (IV. 15) to (IV. 17).
b	The dimensions of an atmospheric layer or feuillet in any direction perpendicular to \hat{k} , (IV. 9).
c_p	Polarization efficiency of the power transfer from transmitter to receiver, (IV. 13).
$C(u), C(v)$	Fresnel cosine integrals, (IV. 8).
l	A range of eddy sizes or layers; the radio wave scattered forward is most affected by a particular range of "eddy sizes," l , or by layers of an average thickness $l/2$, that are visible to both antennas, (IV. 1).
l_0	Scale of turbulence, (IV. 19).
m	Average refractive index gradient, dn/dz , across a layer, (IV. 5).
m_0	Average refractive index gradient for the region in which a layer is imbedded, (IV. 5).
M	A term defined by (IV. 6) used in the power reflection coefficient q^2 .
M_0	A term defined by (IV. 22) used in defining a_{v_0} , the scattering cross-section from refractivity turbulence.
n_1, n_2	Refractive indices of adjacent layers of homogeneous media, (IV. 3).
N_l	The number of layers per unit volume of a scattering cross-section, (IV. 15) to (IV. 17).
N_v	The number of scattering subvolumes that make an appreciable contribution to the total available power, (IV. 11).
q	The power reflection coefficient, q^2 , for a tropospheric layer is approximated by (IV. 6).
q_0	The plane wave Fresnel reflection coefficient for an infinitely extended plane boundary, (IV. 3).
\vec{R}, \vec{R}_0	Vector distances from transmitter and receiver, respectively, to a point \vec{R}_0 .
\hat{R}, \hat{R}_0	Unit vectors from the centers of radiation of the receiving and transmitting antennas, respectively, (IV. 1).
\vec{R}_{oi}	A point from which power is coherently scattered or reflected, (IV. 11).
$S(u), S(v)$	Fresnel sine integrals, (IV. 8).
u	A parameter defined by (IV. 9).
v	A parameter defined by (IV. 9).
v_i	The i^{th} scattering subvolume, (IV. 11).

w_v	Available power per unit scattering volume, (IV.11).
w_{vi}	Available power per unit scattering volume for the i^{th} scattering subvolume, (IV.12)
x	Half the width of a first Fresnel zone, (IV.7).
z	Thickness of a tropospheric layer, (IV.6).
z_0	The thickness of a tropospheric layer, (IV.6).
Δn	The deviation of refractive index from its expected value, (IV.20).
$\langle \Delta n \rangle$	The expected value of refractive index, (IV.20).
$\langle (\Delta n)^2 \rangle$	The variance of fluctuations in refractive index, (IV.19).
\hat{k}	A wave number direction defined by (IV.1).
ψ	The grazing angle for reflection from a layer, (IV.2).

Annex V

PHASE INTERFERENCE FADING AND SERVICE PROBABILITY

As a general rule, adequate service over a radio path requires protection against noise when propagation conditions are poor, and requires protection against interference from cochannel or adjacent channel signals when propagation conditions are good. Optimum use of the radio spectrum requires systems so designed that the reception of wanted signals is protected to the greatest degree practicable from interference by unwanted radio signals and by noise.

The short-term fading of the instantaneous received power within periods of time ranging from a few minutes up to one hour or more is largely associated with random fluctuations in the relative phasing between component waves. These waves arrive at the receiving antenna after propagation via a multiplicity of propagation paths having electrical lengths that vary from second to second and from minute to minute over a range of a few wavelengths. A small part of this short-term fading and usually all of the long-term variations arise from minute-to-minute changes in the root-sum-square value of the amplitudes of the component waves, i. e., in short-term changes in the mean power available from the receiving antenna. In the analysis of short-term fading, it is convenient to consider the effects of these phase and root-sum-square amplitude changes as being two separate components of the instantaneous fading. Multipath or "phase interference fading" among simultaneously occurring modes of propagation usually determines the statistical character of short-term variability.

Over most transhorizon paths, long-term variability is dominated by "power fading", due to slow changes in average atmospheric refraction, in the intensity of refractive index turbulence, or in the degree of atmospheric stratification. The distinction between phase interference fading and power fading is somewhat arbitrary, but is nevertheless extremely useful. Economic considerations, as contrasted to the requirements for spectrum conservation, indicate that radio receiving systems should be designed so that the minimum practicable transmitter power is required for satisfactory reception of wanted signals in the presence of noise. Fading expected within an hour or other convenient "short" period of time is allowed for by comparing the median wanted signal power w_m available at the receiver with the median wanted signal power w_{mr} which is required for satisfactory reception in the presence of noise. This operating sensitivity w_{mr} assumes a specified type of fading signal and a specified type of noise, but does not allow for other unwanted signals.

In the presence of a specified unwanted signal, but in the absence of other unwanted signals or appreciable noise, the fidelity of information delivered to a receiver output will increase as the ratio r_u of wanted-to-unwanted signal power increases. The degree of fidelity of the received information may be measured in various ways. For example, voice signals are often measured in terms of their intelligibility, television pictures by subjective

observation, and teletype signals by the percentage of correctly interpreted received characters. A specified grade of service provided by a given wanted signal will guarantee a corresponding degree of fidelity of the information delivered to the receiver output. For example, a Grade A teletype service could be defined as one providing 99.99 percent error-free characters, while a Grade B service could be defined as one providing 99.9 percent error-free characters.

The protection ratio r_{ur} required for a given grade of service will depend upon the nature of the wanted and unwanted signals; i. e., their degree of modulation, their location in the spectrum relative to the principal and spurious response bands of the receiving system, and their phase interference fading characteristics. The use of receiving systems having the smallest values of r_{ur} for the kinds of unwanted signals likely to be encountered will permit the same portions of the spectrum to be used simultaneously by the maximum number of users. For instance, FM with feedback achieves a reduction in r_{ur} for a cochannel unwanted signal by occupying a larger portion of the spectrum. But optimum use of the spectrum requires a careful balance between reductions in r_{ur} on the same channel and on adjacent channels, taking account of other system isolation factors such as separation between channels, geographical separation, antenna directivity, and cross-polarization.

Note that the operating sensitivity w_{mr} is a measure of the required magnitude of the median wanted signal power but r_{ur} involves only the ratio of wanted to unwanted signal powers. For optimum use of the spectrum by the maximum number of simultaneous users, the transmitting and receiving systems of the individual links should be designed with the primary objective of ensuring that the various values of r_u exceed r_{ur} for a large percentage of the time during the intended periods of operation. Then sufficiently high transmitter powers should be used so that the median wanted signal power w_m exceeds w_{mr} for a large percentage of the time during the intended period of reception at each receiving location. This approach to frequency assignment problems will be unrealistic in a few cases, such as the cleared channels required for radio astronomy, but these rare exceptions merely serve to test the otherwise general rule [Norton, 1950, 1962 and Norton and Fine 1949] that optimum use of the spectrum can be achieved only when interference from other signals rather than from noise provides the ineluctable limit to satisfactory reception.

This annex discusses the requirements for service of a given grade g , how to estimate the expected time availability q of acceptable service, and, finally, how to calculate the service probability Q for a given time availability.

V.1 Two Components of Fading

Both the wanted and the unwanted signal power available to a receiving system will usually vary from minute to minute in a random or unpredictable fashion. It is convenient to divide the "instantaneous received signal power" $W_{\pi} = 10 \log w_{\pi}$ into two or three additive components where w_{π} is defined as the average power for a single cycle of the radio frequency, so as to eliminate the variance of power associated with the time factor $\cos^2(\omega t)$:

$$W_{\pi} = W_m + Y_{\pi} = W_m(0.5) + Y + Y_{\pi} \text{ dbw} \quad (\text{V.1})$$

W_m is that component of W_{π} which is not affected by the usually rapid phase interference fading and is most often identified as the short-term median of the available power W_{π} at the receiving antenna. $W_m(0.5)$ is the median of all such values of W_m , and is most often identified as the long-term median of W_{π} . In terms of the long-term median transmission loss $L_m(0.5)$ and the total power W_t radiated from the transmitting antenna:

$$W_m(0.5) = W_t - L_m(0.5) \text{ dbw} \quad (\text{V.2})$$

The characteristics of long-term fading and phase interference fading, respectively, are described in terms of the two fading components Y and Y_{π} in (V.1):

$$Y = W_m - W_m(0.5), \quad Y_{\pi} = W_{\pi} - W_m \quad (\text{V.3})$$

The long term for which the median power, $W_m(0.5)$, is defined may be as short as one hour or as long as several years but will, in general, consist of the hours within a specified period of time. For most continuously operating services it is convenient to consider $W_m(0.5)$ as the median power over a long period of time, including all hours of the day and all seasons of the year. Observations of long-term variability, summarized in section 10 and in annex III, show that W_m is a very nearly normally distributed random variable characterized by a standard deviation that may range from one decibel within an hour up to ten decibels for periods of the order of several years. These values of standard deviation are representative only of typical beyond-the-horizon propagation paths and vary widely for other propagation conditions.

For periods as short as an hour, the variance of Y_{π} is generally greater than the variance of W_m . The long-term variability of W_m is identified in section 10 with the variability of hourly medians, expressed in terms of $Y(q)$:

$$Y(q) = W_m(q) - W_m(0.5) = L_m(0.5) - L_m(q) \quad (\text{V.4})$$

where $W_m(q)$ is the hourly median signal power exceeded for a fraction q of all hours, and $L_m(q)$ is the corresponding transmission loss not exceeded for a fraction q of all hours.

Often, data for a path are available in terms of the long-term cumulative distribution of instantaneous power, W_{π} ; that is, we know $W_{\pi}(q)$ versus q , but not $W_m(q)$ versus q . An approximation to the cumulative distribution function $L_o(q)$ versus q is given by

$$L_o(q) \approx L_m(0.5) \pm [Y^2(q) + Y_{\pi}^2(q)]^{\frac{1}{2}}. \quad (V.5)$$

The plus sign in (V.5) is used for $q > 50$ percent, and the minus sign for $q < 50$ percent.

V.2 The Nakagami-Rice Distribution

For studies of the operating sensitivity w_{mr} of a receiver in the presence of a rapidly fading wanted signal, and for studies of the median wanted signal to unwanted signal ratio $R_{ur}(g)$ required for a grade g service, it is helpful to consider a particular statistical model which may be used to describe phase interference fading. Minoru Nakagami [1940] describes a model which depends upon the addition of a constant signal and a Rayleigh-distributed random signal [Rayleigh 1880; Rice, 1945; Norton, Vogler, Mansfield and Short, 1955; Beckmann, 1961a, 1964]. In this model, the root-sum-square value of the amplitudes of the Rayleigh components is K decibels relative to the amplitude of the constant component. $K = +\infty$ corresponds to a constant received signal. For a Rayleigh distribution, $K = -\infty$ and the probability q that the instantaneous power, w_{π} , will exceed $w_{\pi}(q)$ for a given value of the short-term median power, w_m , may be expressed:

$$q [w_{\pi} > w_{\pi}(q) \mid w_m] = \exp \left[- \frac{w_{\pi}(q) \log_e 2}{w_m} \right], \quad [K = -\infty] \quad (V.6a)$$

Alternatively, the above may be expressed in the following forms:

$$q [Y_{\pi} > Y_{\pi}(q)] = \exp [- y_{\pi}(q) \log_e 2], \quad [K = -\infty] \quad (V.6b)$$

$$Y_{\pi}(q) = 5.21390 + 10 \log \{ \log (1/q) \}, \quad [K = -\infty] \quad (V.6c)$$

Figures V.1-V.3 and table V.1 show how the Nakagami-Rice phase interference fading distribution $Y_{\pi}(q)$ depends on q , K , and the average \bar{Y}_{π} and standard deviation σ_Y of Y_{π} . It is evident from figure V.1 that the distribution of phase interference fading depends only on K . The utility of this distribution for describing phase interference fading in ionospheric propagation is discussed in CCIR report [1963k] and for tropospheric propagation is demonstrated in papers by Norton, Rice and Vogler [1955], Janes and Wells [1955], and Norton, Rice, Janes and Barsis [1955]. Bremmer [1959] and Beckmann [1961a] discuss a somewhat more general fading model.

For within-the-horizon tropospheric paths, including either short point-to-point terrestrial paths or paths from an earth station to a satellite, K will tend to have a large positive value throughout the day for all seasons of the year. As the length of the terrestrial propagation path is increased, or the elevation angle of a satellite is decreased, so that the path has less than first Fresnel zone clearance, the expected values of K will decrease until, for some hours of the day, K will be less than zero and the phase interference fading for signals propagated over the path at these times will tend to be closely represented

by a Rayleigh distribution. For most beyond-the-horizon paths K will be less than zero most of the time. For knife-edge diffraction paths K is often much greater than zero. When signals arrive at the receiving antenna via ducts or elevated layers, the values of K may increase to values much greater than zero even for transhorizon propagation paths. For a given beyond-the-horizon path, K will tend to be positively correlated with the median power level W_m ; i.e., large values of K are expected with large values of W_m . For some within-the-horizon paths, K and W_m tend to be negatively correlated.

It is assumed that a particular value of K may be associated with any time availability q , however, few data analyses of this kind are presently available. A program of data analysis is clearly desirable to provide empirical estimates of K versus q for particular climates, seasons, times of day, lengths of recording, frequencies, and propagation path characteristics. It should be noted that K versus q expresses an assumed functional relationship.

An analysis of data for a single day's recording at 1046 MHz over a 364-kilometer path is presented here to illustrate how a relationship between K and q may be established. Figure V.4 shows for a single day the observed interdecile range $W_\pi(0.1) - W_\pi(0.9)$ $L_\pi(0.9) - L_\pi(0.1)$ for each five-minute period plotted against the median transmission loss L_m for the five-minute period. Figure V.1 associates a value of K with each value of $L_\pi(0.9) - L_\pi(0.1)$, and the cumulative distribution of L_m associates a time availability q with each value of L_m . In figure V.4, K appears to increase with increasing L_m for the hours 0000 - 1700, although the usual tendency over long periods is for K to decrease with L_m . The straight line in the figure is drawn through medians for the periods 0000 - 1700 and 1700 - 2400 hours, with linear scales for K and L_m , as shown by the inset for figure V.4. The corresponding curve of K versus q is compared with the data in the main figure.

Figure V.5 shows for $f = 2$ GHz and 30-meter antenna heights over a smooth earth a possible estimate of K versus distance and time availability. These crude and quite speculative estimates are given here only to provide the example in the lower part of figure V.5 which shows how such information with (V.6) may be used to obtain curves of $L_\pi(q)$ versus q . The solid curves in the lower part of figure V.5 show how $L_\pi(q)$ varies with distance for $q = 0.0001, 0.01, 0.5, 0.99$ and 0.9999 , where L_π is the transmission loss associated with the instantaneous power, W_π .

Table V.1 Characteristics of the Nakagami-Rice
Phase Interference Fading Distribution $Y_{\pi}(q)$
 $Y_{\pi} > Y_{\pi}(q)$ with Probability q ; $Y_{\pi}(0.5) \cong 0$

K	\bar{Y}_{π} db	$\sigma_{Y_{\pi}}$ db	$Y_{\pi}(0.005)$		$Y_{\pi}(0.01)$		$Y_{\pi}(0.02)$		$Y_{\pi}(0.05)$		$Y_{\pi}(0.1)$		$Y_{\pi}(0.9)$		$Y_{\pi}(0.95)$		$Y_{\pi}(0.98)$		$Y_{\pi}(0.99)$		$Y_{\pi}(0.995)$		$Y_{\pi}(0.1) - Y_{\pi}(0.9)$ db	
			db	db	db	db	db	db	db	db	db	db	db	db	db	db	db	db	db	db	db	db	db	db
40	-0.0002	0.061	0.1568	0.1417	0.1252	0.1004	0.0784	-0.0790	-0.1016	-0.1270	-0.1440	-0.1596	0.1574											
35	-0.0007	0.109	0.2768	0.2504	0.2214	0.1778	0.1352	-0.1411	-0.1815	-0.2272	-0.2579	-0.2860	0.2763											
30	-0.0022	0.194	0.4862	0.4403	0.3898	0.3136	0.2453	-0.2525	-0.3254	-0.4082	-0.4638	-0.5151	0.4978											
25	-0.0069	0.346	0.8460	0.7676	0.6811	0.5496	0.4312	-0.4538	-0.5868	-0.7391	-0.8421	-0.9374	0.8850											
20	-0.0217	0.616	1.4486	1.3184	1.1738	0.9524	0.7508	-0.8218	-1.0696	-1.3572	-1.5544	-1.7389	1.5726											
18	-0.0343	0.776	1.7840	1.6264	1.4508	1.1846	0.9332	-1.0453	-1.3660	-1.7416	-2.0014	-2.2461	1.9785											
16	-0.0543	0.980	2.1856	1.9963	1.7847	1.4573	1.1558	-1.3326	-1.7506	-2.2463	-2.5931	-2.9231	2.4884											
14	-0.0859	1.238	2.6605	2.4355	2.1829	1.7896	1.4247	-1.7028	-2.2526	-2.9156	-3.3872	-3.8422	3.1275											
12	-0.136	1.569	3.2136	2.9491	2.6507	2.1831	1.7455	-2.1808	-2.9119	-3.8143	-4.4715	-5.1188	3.9263											
10	-0.214	1.999	3.8453	3.5384	3.1902	2.6408	2.1218	-2.7975	-3.7820	-5.0372	-5.9833	-6.9452	4.9193											
8	-0.334	2.565	4.5493	4.1980	3.7975	3.1602	2.528	-3.5861	-4.9287	-6.7171	-8.1418	-9.6386	6.1389											
6	-0.507	3.279	5.3093	4.9132	4.4591	3.7313	3.0307	-4.5714	-6.4059	-8.9732	-11.0972	-13.4194	7.6021											
4	-0.706	4.036	6.0955	5.6559	5.1494	4.3315	3.5366	-5.7101	-8.1216	-11.5185	-14.2546	-17.1017	9.2467											
2	-0.866	4.667	6.8613	6.3811	5.8252	4.9219	4.0366	-6.7874	-9.6278	-13.4690	-16.4258	-19.4073	10.8240											
0	-0.941	5.094	7.5411	7.0246	6.4248	5.4449	4.4782	-7.5267	-10.5553	-14.5401	-17.5512	-20.5618	12.0049											
-2	-0.953	5.340	8.0697	7.5228	6.8861	5.8423	4.8088	-8.0074	-11.0005	-15.0271	-18.0527	-21.0706	12.8162											
-4	-0.942	5.465	8.4231	7.8525	7.1873	6.0956	5.0137	-8.0732	-11.1876	-15.2273	-18.2573	-21.2774	13.0869											
-6	-0.929	5.525	8.6309	8.0435	7.3588	6.2354	5.1233	-8.1386	-11.2606	-15.3046	-18.3361	-21.3565	13.2619											
-8	-0.922	5.551	8.7394	8.1417	7.4451	6.3034	5.1749	-8.1646	-11.2893	-15.3349	-18.3669	-21.3880	13.3395											
-10	-0.918	5.562	8.7918	8.1881	7.4857	6.3341	5.1976	-8.1753	-11.3005	-15.3466	-18.3788	-21.4000	13.3729											
-12	-0.916	5.567	8.8155	8.2090	7.5031	6.3474	5.2071	-8.1792	-11.3048	-15.3512	-18.3834	-21.4046	13.3863											
-14	-0.916	5.569	8.8258	8.2179	7.5106	6.3531	5.2112	-8.1804	-11.3065	-15.3529	-18.3852	-21.4064	13.3916											
-16	-0.915	5.570	8.8301	8.2216	7.5136	6.3552	5.2128	-8.1811	-11.3072	-15.3537	-18.3860	-21.4072	13.3929											
-18	-0.915	5.570	8.8319	8.2232	7.5149	6.3561	5.2135	-8.1813	-11.3075	-15.3540	-18.3863	-21.4075	13.3948											
-20	-0.915	5.570	8.8326	8.2238	7.5154	6.3565	5.2137	-8.1814	-11.3076	-15.3541	-18.3864	-21.4076	13.3951											
-∞	-0.915	5.570	8.8331	8.2242	7.5158	6.3567	5.2139	-8.1815	-11.3077	-15.3542	-18.3865	-21.4077	13.3954											

THE NAKAGAMI-RICE PROBABILITY DISTRIBUTION OF THE INSTANTANEOUS FADING ASSOCIATED WITH PHASE INTERFERENCE

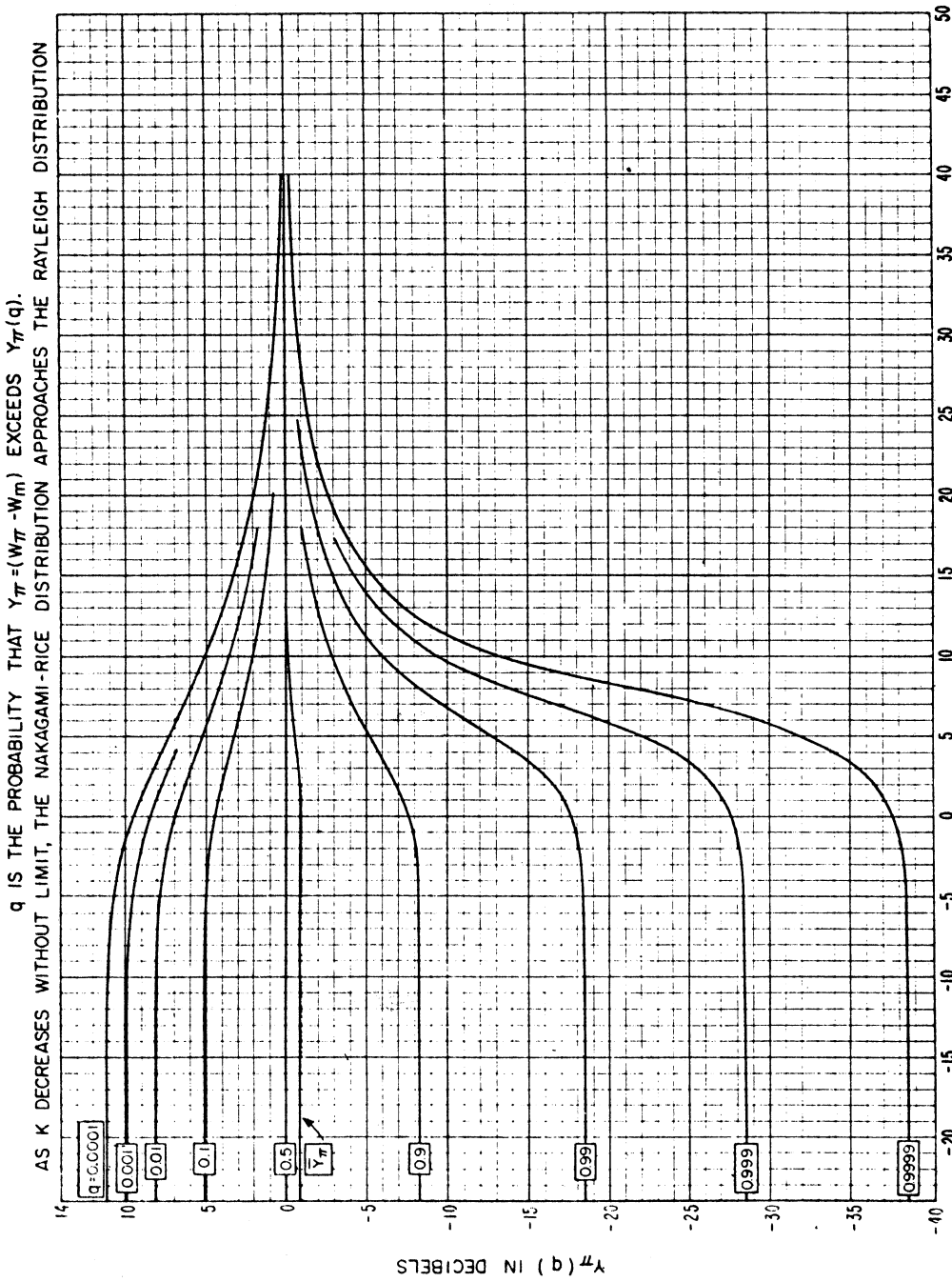
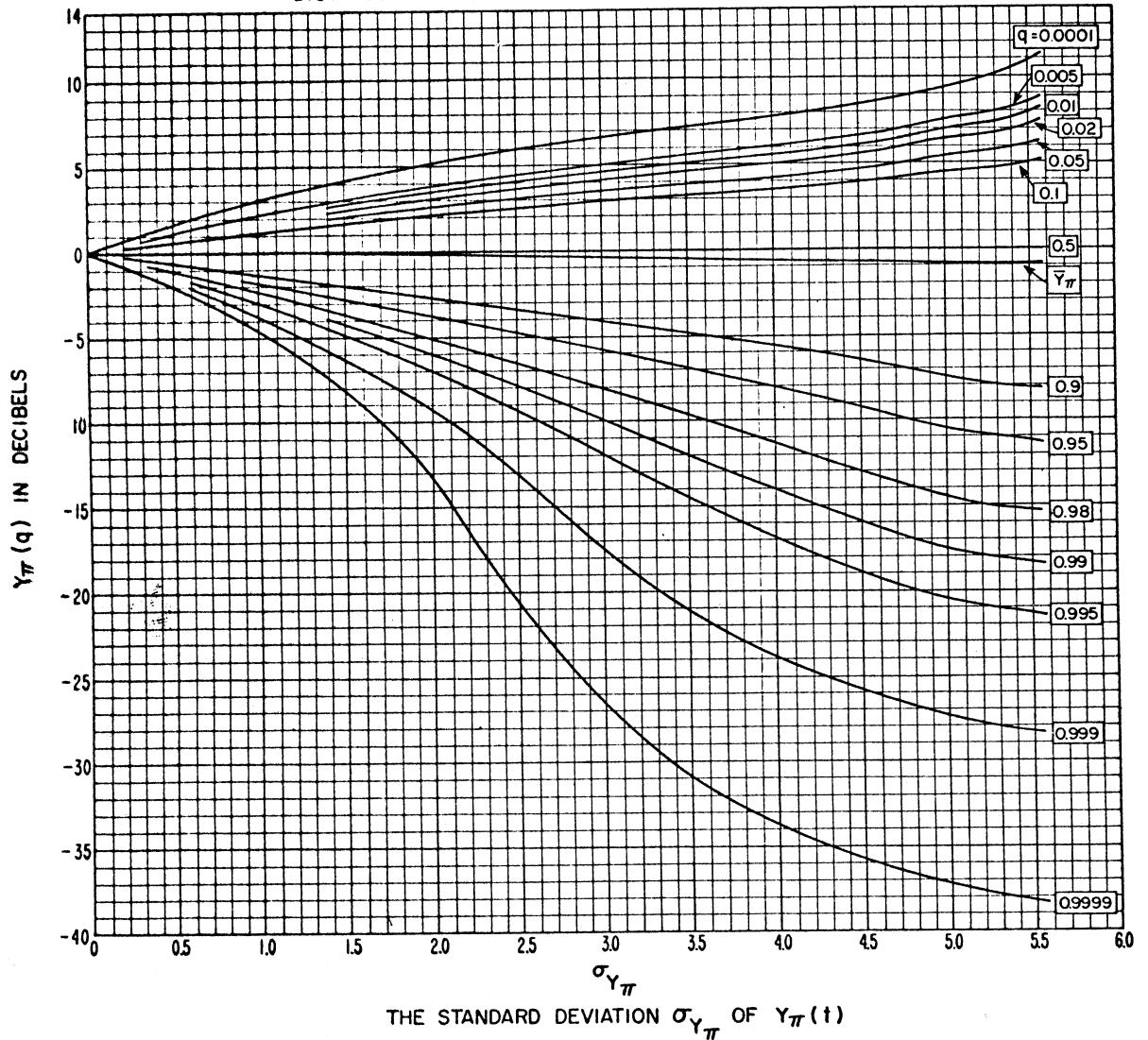


Figure 5.1

THE NAKAGAMI-RICE PROBABILITY DISTRIBUTION OF THE INSTANTANEOUS FADING ASSOCIATED WITH PHASE INTERFERENCE

q IS THE PROBABILITY THAT $Y_{\pi} = (W_{\pi} - W_m)$ EXCEEDS $Y_{\pi}(q)$.

AS K DECREASES WITHOUT LIMIT, THE NAKAGAMI-RICE DISTRIBUTION APPROACHES THE RAYLEIGH DISTRIBUTION



K = RATIO IN DECIBELS BETWEEN THE STEADY COMPONENT OF THE RECEIVED POWER AND THE RAYLEIGH FADING COMPONENT

Figure V.2

STANDARD DEVIATION $\sigma_{Y_{\pi}}$ AND MEAN \bar{Y}_{π} FOR
THE NAKAGAMI-RICE PHASE INTERFERENCE DISTRIBUTION

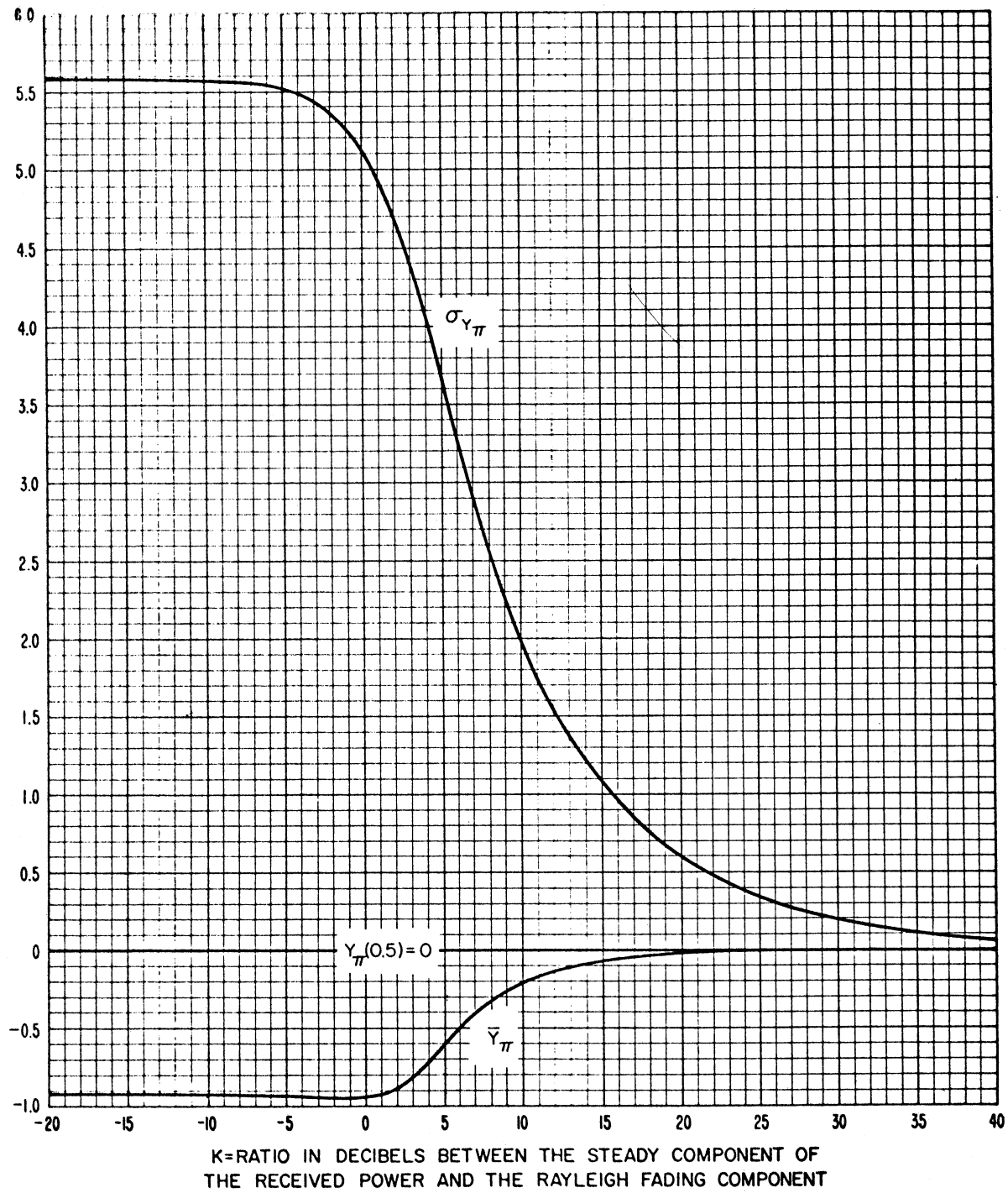


Figure V.3

CHEYENNE MOUNTAIN, COLORADO TO GARDEN CITY, KANSAS
 24 FEBRUARY 1953
 1046 MHz d = 364.5 km

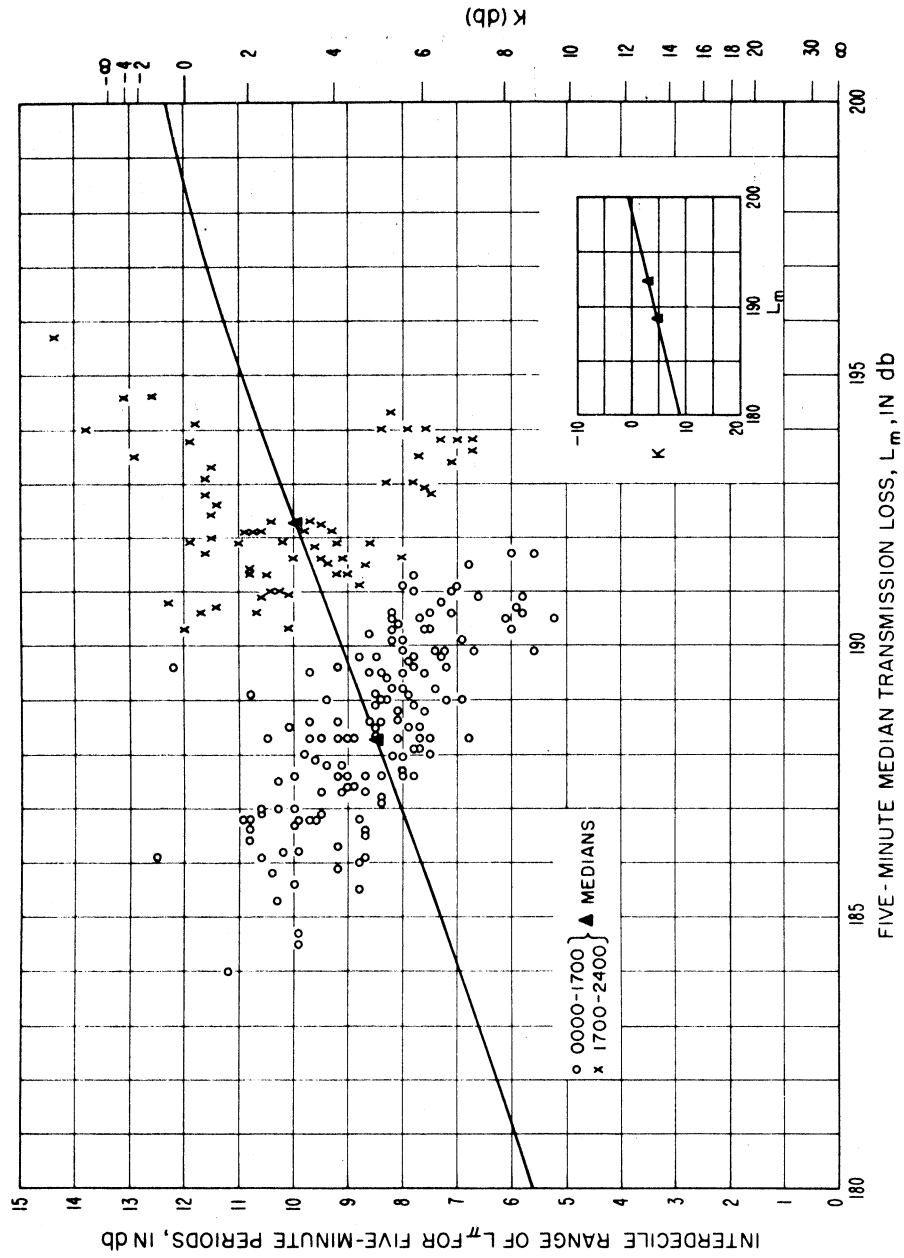
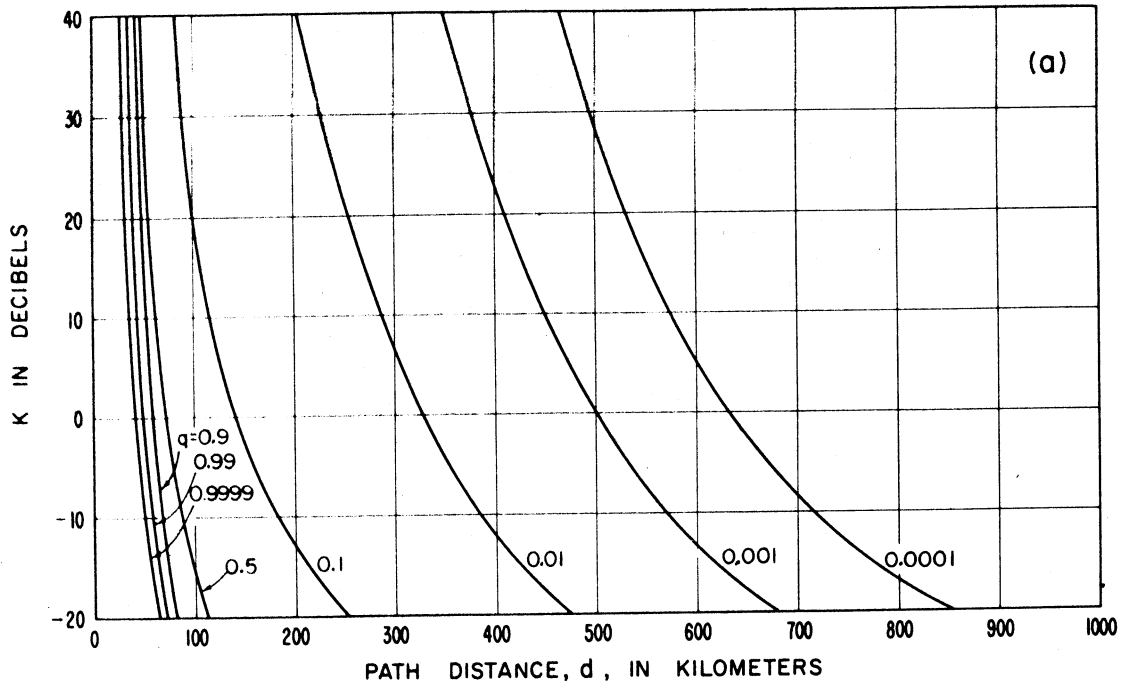


Figure V.4

TENTATIVE ESTIMATE OF K VERSUS q AND d



CUMULATIVE DISTRIBUTIONS OF INSTANTANEOUS TRANSMISSION LOSS
 FREQUENCY = 2 MHz , $h_{te} = h_{re} = 30$ METERS

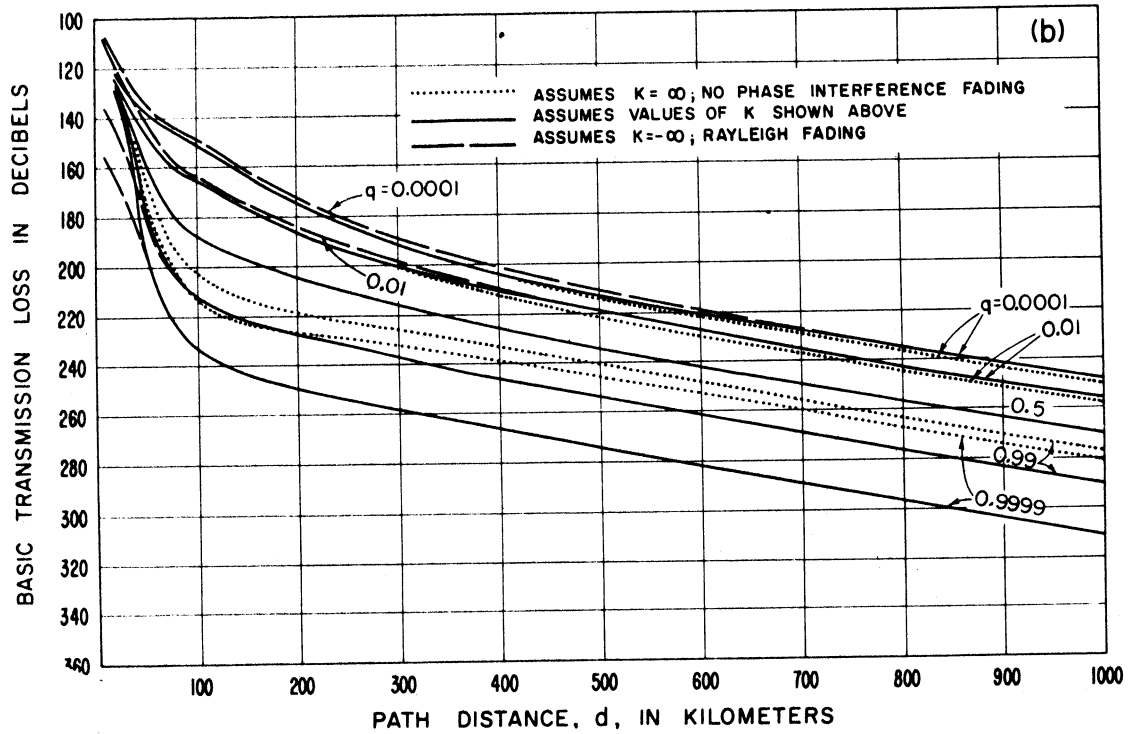


Figure X.5

V.3 Noise-Limited Service

A detailed discussion of the effective noise bandwidth, the operating noise factor, and the operating sensitivity of a receiving system is presented in a recent report, "Optimum Use of the Radio Frequency Spectrum," prepared under Resolution 1 of the CCIR [Geneva, 1963c].

The median value of the total noise power w_{mn} watts in a bandwidth b cycles per second at the output load of the linear portion of a receiving system includes external noise accepted by the antenna as well as noise generated within the receiving system, including both principal and spurious responses of the antenna and transmission line as well as the receiver itself. This total noise power delivered to the pre-detection receiver output may be referred to the terminals of an equivalent loss-free antenna (as if there were only external noise sources) by dividing w_{mn} by g_o , the maximum value of the operating gain of the pre-detection receiving system.

The operating noise factor of the pre-detection receiving system, f_{op} , may be expressed as the ratio of the "equivalent available noise power" w_{mn}/g_o to the Johnson noise power $kT_o b$ that would be available in the band b from a resistance at a reference absolute temperature $T_o = 288.37$ degrees Kelvin, where $k = 1.38054 \times 10^{-23}$ joules per degree is Boltzmann's constant:

$$f_{op} = \frac{w_{mn}/g_o}{k T_o b} \quad (V.7)$$

or in decibels :

$$F_{op} = (W_{mn} - G_o) - (B - 204) \text{ db} . \quad (V.8)$$

The constant 204 in (V.8) is $-10 \log (k T_o)$.

Note that the available power from the antenna as defined in annex II has the desired property of being independent of the receiver input load impedance, making this concept especially useful for the definition and measurement of the operating noise factor f_{op} as defined under CCIR Resolution 1 [Geneva, 1963c].

At frequencies above 100 MHz, where receiver noise rather than external noise usually limits reception, f_{op} is essentially independent of external noise. In general, f_{op} is proportional to the total noise w_{mn} delivered to the pre-detection receiver output and so measures the degree to which the entire system, including the antenna, is able to discriminate against both external noise and receiver noise.

Let W_m represent the median available wanted signal power associated with phase interference fading at the terminals of an equivalent loss-free receiving antenna, and let the "operating threshold" $W_{mr}(g)$ represent the minimum value of W_m which will provide a grade g service in the presence of noise alone. The operating threshold W_{mr} assumes a specified type of wanted signal and a specified type of noise, but does not allow for other unwanted signals. Compared to the total range of their long-term variability, it is assumed that W_m and $W_{mr}(g)$ are hourly median values; i. e., that long-term power fading is negligible over such a short period of time. Let G_{ms} represent the hourly median operating signal gain of a pre-detection receiving system, expressed in db so that $W_m + G_{ms}$ very closely approximates the hourly median value of that component of available wanted signal power delivered to the pre-detection receiver output and associated with phase interference fading. The median wanted signal to median noise ratio available at the pre-detection receiver output is then

$$R_m = [W_m + G_{ms}] - W_{mn} \text{ db} \quad (\text{V. 9a})$$

and the minimum value of R_m which will provide a desired grade of service in the presence of noise alone is

$$R_{mr}(g) = [W_{mr}(g) + G_{ms}] - W_{mn} \text{ db.} \quad (\text{V. 9b})$$

V.4 Interference-Limited Service

Separation of the total fading into a phase interference component Y_{π} and the more slowly varying component Y as described in Section V.1 appears to be desirable for several reasons: (1) variations of Y_{π} associated with phase interference may be expected to occur completely independently for the wanted and unwanted signals, and this facilitates making a more precise determination of the required wanted-to-unwanted signal ratio, $R_{ur}(g)$, (2) the random variable Y_{π} follows the Nakagami-Rice distribution, as illustrated on figure V.1, while variations with time of Y are approximately normally distributed, (3) the variations with time of the median wanted and unwanted signal powers W_m and W_{um} tend to be correlated for most wanted and unwanted propagation paths, and an accurate allowance for this correlation is facilitated by separating the instantaneous fading into the two additive components Y and Y_{π} and (4) most of the contribution to the variance of W_m with time occurs at low fluctuation frequencies ranging from one cycle per year to about one cycle per hour, whereas most of the contribution to the variance of Y_{π} occurs at higher fluctuation frequencies, greater than one cycle per hour. Only the short-term variations of the wanted signal power w_{π} and the unwanted signal power $w_{u\pi}$ associated with phase interference fading are used in determining $r_{ur}(g)$; the ratio of the median wanted signal power w_m to the median unwanted signal power w_{um} required to provide a specified grade of service g . Let $R_{u\pi}$ denote the ratio between the instantaneous wanted signal power $W_m + Y_{\pi}$ and the instantaneous unwanted signal power $W_{um} + Y_{u\pi}$.

$$R_{u\pi} = \frac{W_m + Y_{\pi}}{W_{um} + Y_{u\pi}} = R_u + Z_{\pi} \quad (V.10)$$

where

$$Z_{\pi} \equiv \frac{Y_{\pi}}{W_{um} + Y_{u\pi}} \text{ and } R_u = \frac{W_m}{W_{um}} \quad (V.11)$$

Note that the cumulative distribution function $Y_{\pi}(q, K)$ for Y_{π} will usually be different from the cumulative distribution function $Y_{u\pi}(q, K_u)$ for $Y_{u\pi}$ since the wanted signal propagation path will differ from the propagation path for the unwanted signal. Let $Z_{\pi} > Z_{\pi}(q, K, K_u)$ with probability q ; then the approximate cumulative distribution function of Z_{π} is given by:

$$Z_{\pi a}(q, K, K_u) = \pm \sqrt{Y_{\pi}^2(q, K) + Y_{u\pi}^2(1-q, K_u)} \quad (V.12)$$

In the above, the plus sign is to be used when $q < 0.5$ and the minus sign when $q > 0.5$; note that $-Z_{\pi a}(1-q, K, K_u) = Z_{\pi a}(q, K, K_u)$. This method of approximation is suggested by two observations: (1) service may be limited for a fraction q of a short period of time either by downfades of the wanted signal corresponding to a level exceeded with a probability q or by

upfades of an unwanted signal corresponding to a level exceeded with a probability $1-q$, and (2) the standard deviation of the difference of two uncorrelated random variables Y_{π} and $Y_{u\pi}$ equals the square root of the sum of their variances, and under fairly general conditions $Z_{\pi}^2(q)$ is very nearly equal to $Y_{\pi}^2(q) + Y_{u\pi}^2(1-q)$. Equation (V.11) is based on the reasonable assumption that Y_{π} and $Y_{u\pi}$ are independent random variables and, for this case, (V.11) would be exact if Y_{π} and $Y_{u\pi}$ were normally distributed. The departure from normality of the distribution of Y_{π} is greatest in the limiting case of a Rayleigh distribution, and for this special case, the following exact expression is available [Siddiqui, 1962]:

$$Z_{\pi}(q, \infty, \infty) = 10 \log \left(\frac{1}{q} - 1 \right) \quad (V.13)$$

Table V.2 compares the above exact expression $Z_{\pi}(q, \infty, \infty)$ with the approximate expression $Z_{\pi a}(q, \infty, \infty)$. Note that the two expressions differ by less than 0.2 dB for any value of q and, since this difference may be expected to be even smaller for finite values of K , it appears that (V.12) should be a satisfactory approximation for most applications and for any values of K and q .

Table V.2

The Cumulative Distribution Function $Z_{\pi}(q, \infty, \infty)$ for the Special Case of the Ratio of Two Rayleigh-Distributed Variables

q	$Z_{\pi}(q, \infty, \infty)$	$Z_{\pi a}(q, \infty, \infty)$	$Z_{\pi} - Z_{\pi a}$
	db	db	db
0.0001	39.99957	40.0178	-0.01823
0.0002	36.98883	37.0362	-0.04737
0.0005	33.00813	33.0757	-0.06757
0.001	29.99566	30.1099	-0.11424
0.002	26.98101	27.1216	-0.14059
0.005	22.98853	23.1584	-0.16987
0.01	19.95635	20.1420	-0.18565
0.02	16.90196	17.0949	-0.19294
0.05	12.78754	12.9719	-0.18436
0.1	9.54243	9.7016	-0.15917
0.2	6.02060	6.1331	-0.11250
0.5	0	0	0

Let $R_{uro}(g)$ denote the required value of R_u for non-fading wanted and unwanted signals and it follows from (V.10) that the instantaneous ratio for fading signals will exceed $R_{uro}(g)$ with a probability at least equal to q provided that:

$$R_u > R_{ur}(g, q, K, K_u) = R_{uro}(g) - Z_{\pi}(q, K, K_u) \quad (V.14)$$

The use of (V.14) to determine an allowance for phase interference fading will almost always provide a larger allowance than will actually be necessary since (V.14) was derived on the assumption that $R_{uro}(g)$ is constant. For most services, $R_{uro}(g)$ will not have a fixed value for non-fading signals but will instead have either a probability distribution or a grade of service distribution; in such cases $R_{ur}(g)$ should be determined for a given q by a convolution of the distributions of $R_{uro}(g)$ and $-Z_{\pi}$. In still other cases the mean duration of the fading below the level $Z_{\pi}(q, K, K_u)$ will be comparable to the mean duration of the individual message elements and a different allowance should then be made. In some cases it may be practical to determine R_{ur} as a function of $g, q, K,$ and K_u in the laboratory by generating wanted and unwanted signals that vary with time the same as Y_{π} and $Y_{u\pi}$. This latter procedure will be successful only to the extent that the fading signal generators properly simulate natural phase interference fading both as regards their amplitude distributions and their fading duration distributions. As this annex is intended to deal only with general definitions and procedures, functions applicable to particular kinds of wanted and unwanted signals which include an appropriate phase interference fading allowance are not developed here.

The ratio R_u defined as an hourly median value equal to the difference between $W_m(0.5) + Y$ and $W_{um}(0.5) + Y_u$ will also vary with time:

$$R_u \equiv W_m - W_{um} = W_m(0.5) - W_{um}(0.5) + Z \quad (V.15)$$

$$Z \equiv Y - Y_u \quad (V.16)$$

The random variables Y and Y_u tend to be approximately normally distributed with a positive correlation coefficient ρ which will vary considerably with the propagation paths

and the particular time block involved. For the usual period of all hours of the day for several years preliminary analyses of data indicate that ρ will usually exceed 0.4 even for propagation paths in opposite directions from the receiving point. Z will exceed a value $Z_a(q)$ for a fraction of time q where the approximate cumulative distribution function $Z_a(q)$ of Z is given by

$$Z_a(q) = \pm \sqrt{Y^2(q) + Y_u^2(1-q) + 2\rho Y(q) Y_u(1-q)} \quad (V.17)$$

where the plus sign is to be used for $q < 0.5$ and the minus sign for $q > 0.5$ while $Z_a(0.5) \equiv 0$. It follows from (V.15) and (V.17) that R_u will exceed $R_{ur}(g)$ for at least a fraction of time q provided that

$$W_m(0.5) - W_{um}(0.5) > R_{ur}(g) - Z_a(q) \quad (V.18)$$

In some cases it may be considered impractical to determine the function $R_{ur}(g)$ by adding an appropriate phase interference fading allowance to $R_{uro}(g)$; in such cases it may be useful to use the following approximate relation which will ensure that the instantaneous ratio $R_{u\pi} > R_{uro}(g)$ for at least a fraction of time q :

$$W_m(0.5) - W_{um}(0.5) > R_{uro}(g) \pm \sqrt{Z_a^2(q) + Z_{\pi}^2(q, K, K_u)} \quad (V.19)$$

In the above, the minus sign is to be used for $q < 0.5$ and the plus sign for $q > 0.5$. Although (V.19), or its equivalent, has often been used in past allocation studies, this usage is deprecated since it does not provide a solution which is as well adapted to the actual nature of the problem as the separation of the fading into its two components Y_{π} and Y , and the separate use of (V.14) and (V.18). Note that (V.19) provides a fading allowance which is too small compared with that estimated using (V.14) and (V.18) separately. The latter formulas are recommended. They make more appropriate allowance for the fact that communications at particular times of the day or for particular seasons of the year are especially difficult.

V.5 The Joint Effect of Several Sources of Interference Present Simultaneously

The effects of interference from unwanted signals and from noise have so far been considered in this report as though each affected the fidelity of reception of the wanted signal independently. Let $w_{mr}(g)$ and $r_{ur}(g)w_{um}$ denote power levels which the wanted median signal power w_m must exceed in order to achieve a specified grade of service when each source of interference is present alone. To the extent that the various sources of interference have a character approximating that of white noise, this same grade of service may be expected from a wanted signal with median level

$$w_m = w_{mr}(g) + \sum r_{ur}(g)w_{um}$$

when these sources are present simultaneously.

An approximate method has been developed [Norton, Staras, and Blum, 1952] for determining for a broadcasting service the distribution with time and receiving location of the ratio

$$w_m / \left[w_{mr}(g) + \sum r_{ur}(g)w_{um} \right]$$

Although this approach to the problem of adding the effects of interference will probably always provide a good upper bound to the interference, this assumption that the interference power is additive is often not strictly valid. For example, when intelligible cross-talk from another channel is present in the receiver output circuit, the addition of some white noise will actually reduce the nuisance value of this cross-talk.

Frequently, however, both $w_{mr}(g)$ and w_{um} will be found to vary more or less independently over wide ranges with time and a good approximation to the percentage of time that objectionable interference is present at a particular receiving location may then be obtained [Barsis, et al, 1961] by adding the percentage of time that w_m is less than $w_{mr}(g)$ to the percentages of time that w_m is less than each of the values of $r_{ur}(g)w_{um}$. When this total time of interference is small, say less than 10%, this will represent a satisfactory estimate of the joint influence of several sources of interference which are present simultaneously. Thus, when the fading ranges of the various sources of interference are sufficiently large so that this latter method of analysis is applicable, the various values of $w_{mr}(g)$ and of $r_{ur}(g)w_{um}$ will have comparable magnitudes for negligible percentages of the time so that one may, in effect, assume that the various sources of interference occur essentially independently in time.

Minimum acceptable wanted-to-unwanted signal ratios r_{ur} may sometimes be a function of r_m , the available wanted signal-to-noise ratio. When r_{ur} is within 3 db of r_{mr} , an unwanted signal may be treated the same as external noise, and, in a similar fashion, long-term distributions of available wanted-to-unwanted signal ratios may be determined for each class of unwanted signals for which r_{ur} is nearly the same.

V.6 The System Equation for Noise-Limited Service

Essential elements of a noise-limited communication circuit are summarized in the following system equation. The transmitter output W_{lt} dbw which will provide W_t dbw of total radiated power in the presence of transmission line and matching network losses L_{lt} db, and which will provide a median delivered signal at the pre-detection receiver output which is R_m db above the median noise power W_{mn} delivered to the pre-detection receiver output is given by

$$W_{lt} = L_{lt} + L_m + R_m + (W_{mn} - G_{ms}) \text{ dbw} \quad (\text{V.20})$$

in the presence of a median transmission loss L_m and a median operating receiving system signal gain G_{ms} . The operating signal gain is the ratio of the power delivered to the pre-detection receiver output to the power available at the terminals of an equivalent loss-free antenna. Let G_o be the maximum of all values of operating signal gain in the receiver pass band, and G_{ms} the median value for all signal frequencies in the pass band. $(W_{mn} - G_{ms})$ in (V.20) is the equivalent median noise power at the antenna terminals, as defined in section V.3.

It is appropriate to express the system equation (V.20) in terms of the operating noise factor F_{op} defined by (V.8), rather than in terms of W_{mn} or $(W_{mn} - G_{ms})$ in order to separate studies of receiving system characteristics from studies of propagation. For this reason all predicted power levels are referred to the terminals of an equivalent loss-free antenna, and receiving system characteristics such as F_{op} , G_o , G_{ms} , and $B = 10 \log b$ are separated from transmission loss and available power in the formulas.

Rearranging terms of (V.8), the equivalent median noise power $(W_{mn} - G_{ms})$ delivered to the antenna terminals may be expressed as

$$W_{mn} - G_{ms} = F_{op} + (G_o - G_{ms}) + (B - 204) \quad (\text{V.21})$$

where G_o and G_{ms} are usually nearly equal. Assuming that L_{lt} , G_o , G_{ms} , and B are constant, it is convenient to combine these parameters into an arbitrary constant K_o :

$$K_o = L_{lt} + G_o - G_{ms} + B - 204 \text{ dbw} \quad (\text{V.22})$$

and rewrite the system equation as:

$$W_{lt} = K_o + L_m + R_m + F_{op} \text{ dbw} \quad (\text{V.23})$$

In general, if unwanted signals other than noise may be disregarded, service exists whenever $R_m(q)$ exceeds $R_{mr}(g)$, where $R_m(q)$ is the value of R_m exceeded a fraction q of all hours. With G_{ms} and W_{mn} assumed constant, so that

$$R_m(q) = W_m(q) + G_{ms} - W_{mn} \quad (\text{V.24})$$

service exists whenever $W_m(q)$ exceeds W_{mr} , or whenever $L_m(q)$ is less than the maximum allowable transmission loss $L_{mo}(g)$. An equivalent statement may be made in terms of the system equation. The transmitter power $W_{lt}(q)$ which will provide for a fraction q of all hours at least the grade g service defined by the required signal-to-noise ratio $R_{mr}(g)$ is

$$W_{lt}(q) = K_o + L_m(q) + F_{op} + R_{mr}(g) \quad (V.25)$$

where $L_m(q)$ is the hourly median transmission loss not exceeded for a fraction q of all hours.

For a fixed transmitter power W_o dbw, the signal-to-noise ratio exceeded q percent of all hours is

$$R_m(q) = W_o - K_o - F_{op} - L_m(q) \quad \text{db} \quad (V.26)$$

for a "median" propagation path for which the service probability, Q , is by definition equal to 0.5.

The maximum allowable transmission loss

$$L_{mo}(g) = W_o - K_o - F_{op} - R_{mr}(g) \quad (V.27)$$

is set equal to the loss $L_m(q, Q)$ exceeded during a fraction $(1 - q)$ of all hours with a probability Q . This value is fixed when P_o , K_o , and $R_{mr}(g)$ have been determined, and for each time availability q there is a corresponding service probability, $Q(q)$. Section V.9 will explain how to calculate $Q(q)$.

When external noise is both variable and not negligible, the long-term variability of F_{op} must be considered, and the following relationships may be used to satisfy the condition

$$R_m(q) > R_{mr}(g) \quad (V.28)$$

$$R_m(q) \cong R_m(0.5) + Y_m(q) \quad (V.29)$$

$$R_m(0.5) \cong W_o - K_o - F_{op}(0.5) - L_m(0.5) \quad (V.30)$$

$$Y_m^2(q) \cong Y^2(q) + Y_n^2(1 - q) - 2\rho_{tn} Y(q) Y_n(1 - q) \quad (V.31)$$

$$Y(q) \cong L_m(0.5) - L_m(q), \quad Y_n(q) \cong F_{op}(q) - F_{op}(0.5) \quad (V.32)$$

where ρ_{tn} is the long-term correlation between W_m and F_{op} . Though ρ_{tn} could theoretically have any value between -1 and 1, it is usually zero.

V.7 The Time Availability of Interference-Limited Service

Let ρ_{tu} denote the long-term correlation between W_m and W_{um} , the power expected to be available at least q percent of all hours at the terminals of an equivalent loss-free receiving antenna from wanted and unwanted stations radiating w_o and w_u watts, respectively:

$$W_m(q) = W_o - L_m(q) \text{ dbw}, \quad W_{um}(q) = W_u - L_{um}(q) \text{ dbw} \quad (V.33)$$

$$W_o = 10 \log w_o \text{ dbw}, \quad W_u = 10 \log w_u \text{ dbw} \quad (V.34)$$

The criterion for service of at least grade g in the presence of a single unwanted signal and in the absence of other unwanted signals or appreciable noise is

$$R_u(q) > R_{ur}(g, q) \quad (V.35)$$

where

$$R_u(q) = R_u(0.5) + Y_R(q) \quad (V.36)$$

$$R_u(0.5) \cong W_m(0.5) - W_{um}(0.5) \quad (V.37)$$

$$Y_R^2(q) \cong Y^2(q) + Y_u^2(1-q) - 2\rho_{tu} Y(q) Y_u(1-q) \quad (V.38)$$

$$Y_u(q) = W_{um}(q) - W_{um}(0.5) = L_{um}(0.5) - L_{um}(q) \quad (V.39)$$

If W_m , W_{um} , and F_{op} were exactly normally distributed, (V.31) and (V.38) would be exact; they represent excellent approximations in practice.

V.8 The Estimation of Prediction Errors

Consider the calculation of the power $W_m(q)$ available at the terminals of an equivalent loss-free receiving antenna during a fraction q of all hours. $W_m(q)$ refers to hourly median values expressed in dbw. For a specific propagation path it is calculated in accordance with the methods given in sections 2-10 using a given set of path parameters (d, f, θ, h_{te} , etc.). Denote by $W_{mo}(q)$ observations made over a large number of randomly different propagation paths, which, however, can all be characterized by the same set of prediction parameters. Values of $W_{mo}(q)$ will be very nearly normally distributed with a mean (and median) equal to $W_m(q)$, and a variance denoted by $\sigma_c^2(q)$. This path-to-path variability is illustrated in Fig. V.6 for a hypothetical situation which assumes a random distribution of all parameters which are not taken into account in the prediction method.

The variance σ_c^2 of deviations of observation from prediction depends on available data and the prediction method itself. The most sophisticated of the methods given in this report for predicting transmission loss as a function of carrier frequency, climate, time block, antenna gains, and path geometry have been adjusted to show no bias, on the average, for the data discussed in section 10 and in annex I.

Most of these data are concentrated in the 40-1000 MHz frequency range, and were obtained primarily for transhorizon paths in climates 1, 2, and 3. Normally, one antenna was on the order of 10 meters above ground and the other one was higher, near 200 meters. Even the low receiving antennas were located on high ground or in clear areas well removed from hills and terrain clutter. Few of the data were obtained with narrow-beam antennas. An attempt has been made to estimate cumulative distributions of hourly transmission loss medians for accurately specified time blocks, including estimates of year-to-year variability.

A prediction for some situation that is adequately characterized by the prediction parameters chosen here requires only interpolation between values of these parameters for which data are available. In such a case, $\sigma_c(q)$ represents the standard error of prediction. The mean square error of prediction, referred to a situation for which data are not available, is $\sigma_c^2(q)$ plus the square of the bias of the prediction method relative to the new situation.

Based on an analysis of presently available transhorizon transmission loss data, the variance $\sigma_c^2(q)$ is estimated as

$$\sigma_c^2(q) = 12.73 + 0.12 Y^2(q) \quad \text{db}^2 \quad (\text{V.40})$$

where $Y(q)$ is defined in section 10. Since $Y(0.5) \equiv 0$, the variance $\sigma_c^2(0.5)$ of the difference between observed and predicted long-term medians is 12.73 db^2 , with a corresponding standard deviation $\sigma_c(0.5) = 3.57 \text{ db}$.

It is occasionally very difficult to estimate the prediction error $\sigma_c(q)$ and the service probability Q . Where only a small amount of data is available there is no adequate way of estimating the bias of a prediction. One may, however, assign weights to the curves of $V(0.5, d_e)$ in figure 10.13 for climates 1-7 based on the amount of supporting data available:

Climate Number	Weight
1	300
2	120
3	60
4	2
5	(deleted)
6	5
7	5

As an example, for $d_e = 600$ km, the average $V(0.5, d_e)$ weighted in accordance with the above is 0.1 db, and the corresponding climate-to-climate variance of $V(0.5)$ is 3.1 db^2 . If a random sampling of these climates is desired the predicted median value $L(0.5)$ is $L_{cr} - V(0.5) = L_{cr} - 0.1$ db, with a standard error of prediction equal to $(12.7 + 3.1)^{\frac{1}{2}} = 4$ db, where 12.7 db^2 is the variance of $V(0.5)$ within any given climate.

If there is doubt as to which of two particular climates i and j should be chosen, the best prediction of $L_b(q)$ might depend on the average of $V_i(0.5, d_e)$ and $V_j(0.5, d_e)$ and the root-mean square of $Y_i(q, d_e)$ and $Y_j(q, d_e)$:

$$L(q) = L_{cr} - 0.5 \left[V_i(0.5, d_e) + V_j(0.5, d_e) \right] - Y_{ij}(q, d_e) \text{ db}, \quad (\text{V. 41})$$

$$Y_{ij}(q, d_e) = \left[0.5 Y_i^2(q, d_e) + 0.5 Y_j^2(q, d_e) \right]^{\frac{1}{2}} \text{ db} \quad (\text{V. 42})$$

The bias of this prediction may be as large as $\left[0.5 V_i(0.5, d_e) - V_j(0.5, d_e) \right]$ db. The root-mean square prediction error may therefore be estimated as the square root of the sum of the variance, $\sigma_c^2(0.5)$ and the square of the bias, or

$$\left\{ 12.73 + 0.12 Y_{ij}^2(q, d_e) + 0.25 \left[V_i(0.5, d_e) - V_j(0.5, d_e) \right]^2 \right\}^{\frac{1}{2}} \text{ db}.$$

According to figure 10.13, $V(0.5, d_e)$ is expected to be the same for climates 1 and 8. This conclusion and the estimate for $Y(q, d_e)$ shown in figure III. 29 for climate 8 are based solely on meteorological data. In order to obtain these estimates, the percentages of time for which surface-based ducts existed in the two regions were matched with the same value of $Y(q, d_e)$ for both climates. In this way, $Y_8(q, d_e)$ was derived from $Y_1(q, d_e)$ by relating q_8 to q_1 for a given Y instead of relating Y_8 to Y_1 for a given q .

V.9 The Calculation of Service Probability Q for a Given Time Availability q

For noise-limited service of at least grade g and time availability q , the service probability Q is the probability that

$$L_{mo}(g) - L_m(q) > 0 \quad (V.43)$$

if external noise is negligible. $L_{mo}(g)$ is defined by (V.27). The criterion for service limited by variable external noise is

$$R_m(q) - R_{mr}(g) > 0 \quad (\text{from equation V.28})$$

For service limited only by interference from a single unwanted signal,

$$R_u(q) - R_{ur}(g, q) > 0 \quad (\text{from equation V.35})$$

Combining (V.22) and (V.27), (V.43) may be rewritten as

$$W_o - L_{lt} - G_o + G_{ms} - B + 204 - F_{op} - R_{mr}(g) - L_m(q) > 0 \quad (V.44)$$

where the terms are defined in (V.8) and section V.6. Assuming that the error of estimation of these terms from system to system is negligible except for the path-to-path variance $\sigma_c^2(q)$ of $L_m(q)$ it is convenient to represent the service probability Q as a function of the standard normal deviate z_{mo} :

$$z_{mo} = \frac{L_{mo} - L_m(q)}{\sigma_c(q)} \quad (V.45)$$

which has a mean of zero and a variance of unity. L_{mo} is identified as the transmission loss exceeded a fraction $(1-q)$ of the time with a probability Q , which is expressed in terms of the error function as

$$Q(z_{mo}) = \frac{1}{2} + \frac{1}{2} \operatorname{erf}(z_{mo} / \sqrt{2}) \quad (V.46)$$

Figure V.7 is a graph of Q versus z_{mo} .

For the method described here, the condition

$$0.12 Y(q) z_{mo}(Q) < -\sigma_c(q) \quad (V.47)$$

is sufficient to insure that the service probability Q increases as the time availability q is decreased. A less restrictive condition is

$$Y(q) [L_{mo} - L_m(0.5)] < 106 \text{ db}^2 \quad (V.48)$$

An example is shown in figure V.8, with q versus Q for radiated powers $W_o = 30$ dbw and $W_o = 40$ dbw, and $L_m(q, Q) = W_o + 140$ db. Here,

$$q = 0.5 + 0.5 \operatorname{erf} \left[\frac{L_m(q) - 140}{10\sqrt{2}} \right], \quad (\text{V. 49})$$

corresponding to a normal distribution with a mean $L_m(0.5) = 140$ db and a standard deviation $Y(0.158) = 10$ db. [Note that $L_m(q)$ versus q as estimated by the methods of section 10 is usually not normally distributed].

To obtain the time availability versus service probability curves on figure V.8, $L_m(q)$ was obtained from q , $Y(q)$ from (V.4), $\sigma_c^2(q)$ from (V.40), z_{mo} from (V.45), and Q from figure V.7. This same method of calculation may be used when there are additional sources of prediction error by adding variances to $\sigma_c^2(q)$. Examining possible trade-offs between time availability and service probability shown in figure V.8, note the increase from $q = 0.965$ to $q = 0.993$ for $Q = 0.95$, or the increase from $Q = 0.78$ to $Q = 0.97$ for $q = 0.99$, as the radiated power is increased from one to ten kilowatts.

For the case of service limited by external noise (V.28) to (V.30) may be rewritten as

$$W_o - K_o - F_{op}(0.5) - L_m(0.5) + Y_m(q) - R_{mr}(g) > 0. \quad (\text{V. 50})$$

One may ignore any error of estimation of W_o , K_o , and $R_{mr}(g)$ as negligible and assume no path-to-path correlation between $F_{op}(0.5)$ and $L_m(0.5)$. The variance $\sigma_{op}^2(q)$ of $F_{op}(0.5) + L_m(0.5) - Y_m(q)$ in (V.50) may then be written as a sum of component variances σ_F^2 and $\sigma_c^2(q)$:

$$\sigma_{op}^2(q) = \sigma_F^2 + 12.73 + 0.12 Y_m^2(q) \text{ db}^2. \quad (\text{V. 51})$$

Very little is known about values for the variance σ_F^2 of $F_{op}(0.5)$, but it is probably on the order of 20 db^2 .

The corresponding standard normal deviate z_{op} is:

$$z_{op} = \frac{R_m(q) - R_{mr}(g)}{\sigma_{op}(q)} \quad (\text{V. 52})$$

and the service probability $Q(q)$ is given by (V.46) with z_{mo} replaced by z_{op} . The restriction (V.47) still holds with z_{mo} and σ_c replaced by z_{op} and σ_{op} . A less restriction condition equivalent to (V.48) can be stated only if a specific value of σ_F is assumed.

For the case of service limited only by interference from a single unwanted radio signal (V. 35) to (V. 39) may be rewritten as

$$L_{um}(0.5) - L_m(0.5) + Y_R(q) - R_{ur}(g, q) > 0 \quad (V. 53)$$

Let ρ_{lu} denote the normalized correlation or covariance between path-to-path variations of $W_m(0.5)$ and $W_{um}(0.5)$. Then assuming a variance of $25.5(1 - \rho_{lu}^2) + 0.12 Y_R^2(q) \text{ db}^2$ for $R_u(q)$, given by the first three terms of (V. 53) and a variance σ_{ur}^2 for the estimate of $R_{ur}(g, q)$, the total variance $\sigma_{uc}^2(q)$ of any estimate of the service criterion given by (V. 53) may be written as

$$\sigma_{uc}^2(q) = 25.5(1 - \rho_{lu}^2) + 0.12 Y_R^2(q) + \sigma_{ur}^2 \quad (V. 54)$$

where $Y_R^2(q)$ is given by (V. 38). The corresponding standard normal deviate z_{uc} is:

$$z_{uc} = \frac{R_u(q) - R_{ur}(g, q)}{\sigma_{uc}(q)} \quad (V. 55)$$

and the service probability $Q(q)$ is given by (V. 46) with z_{mo} replaced by z_{uc} . The variance σ_{ur}^2 may range from 10 db^2 to very much higher values. The restrictions (V. 47) and (V. 48) apply with z_{mo} and σ_c replaced by z_{uc} and σ_{uc} and with 106 db in (V. 48) replaced by $(212 + \sigma_{ur}^2) \text{ db}^2$.

TYPICAL PATH - TO - PATH VARIATION OF INFINITE - TIME DISTRIBUTIONS
FOR A SINGLE SET OF VALUES OF THE PREDICTION PARAMETERS

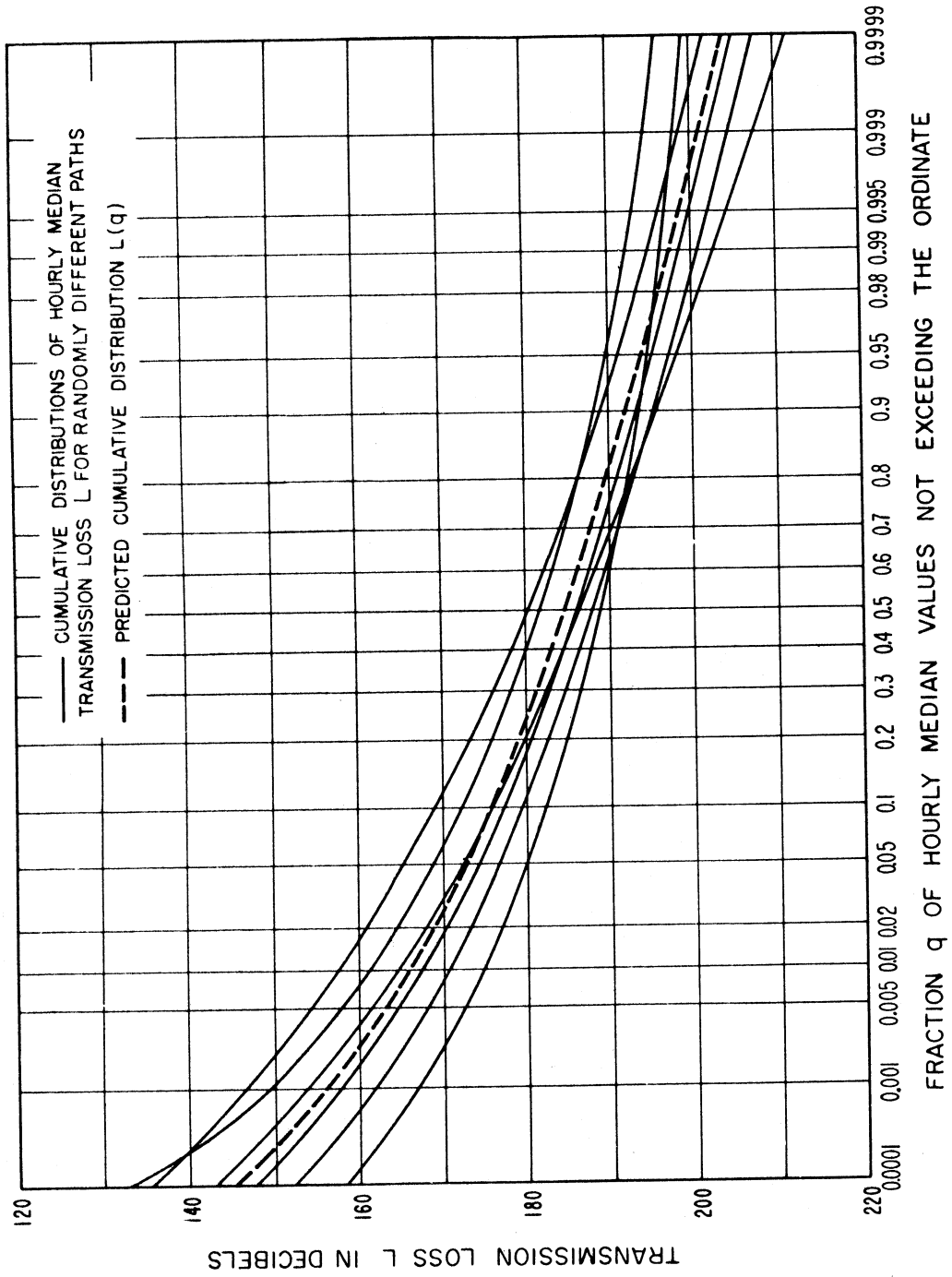


Figure V.6

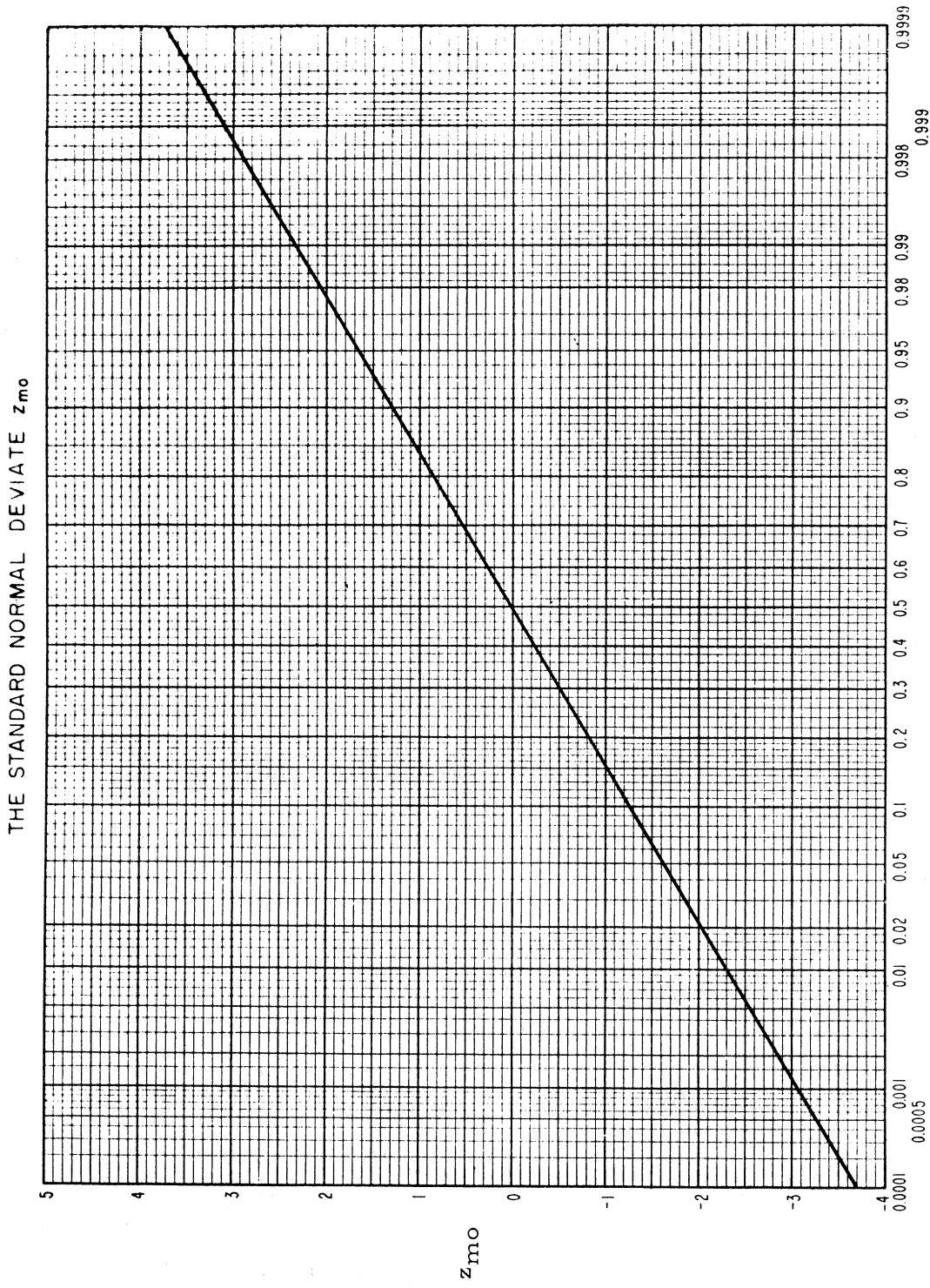
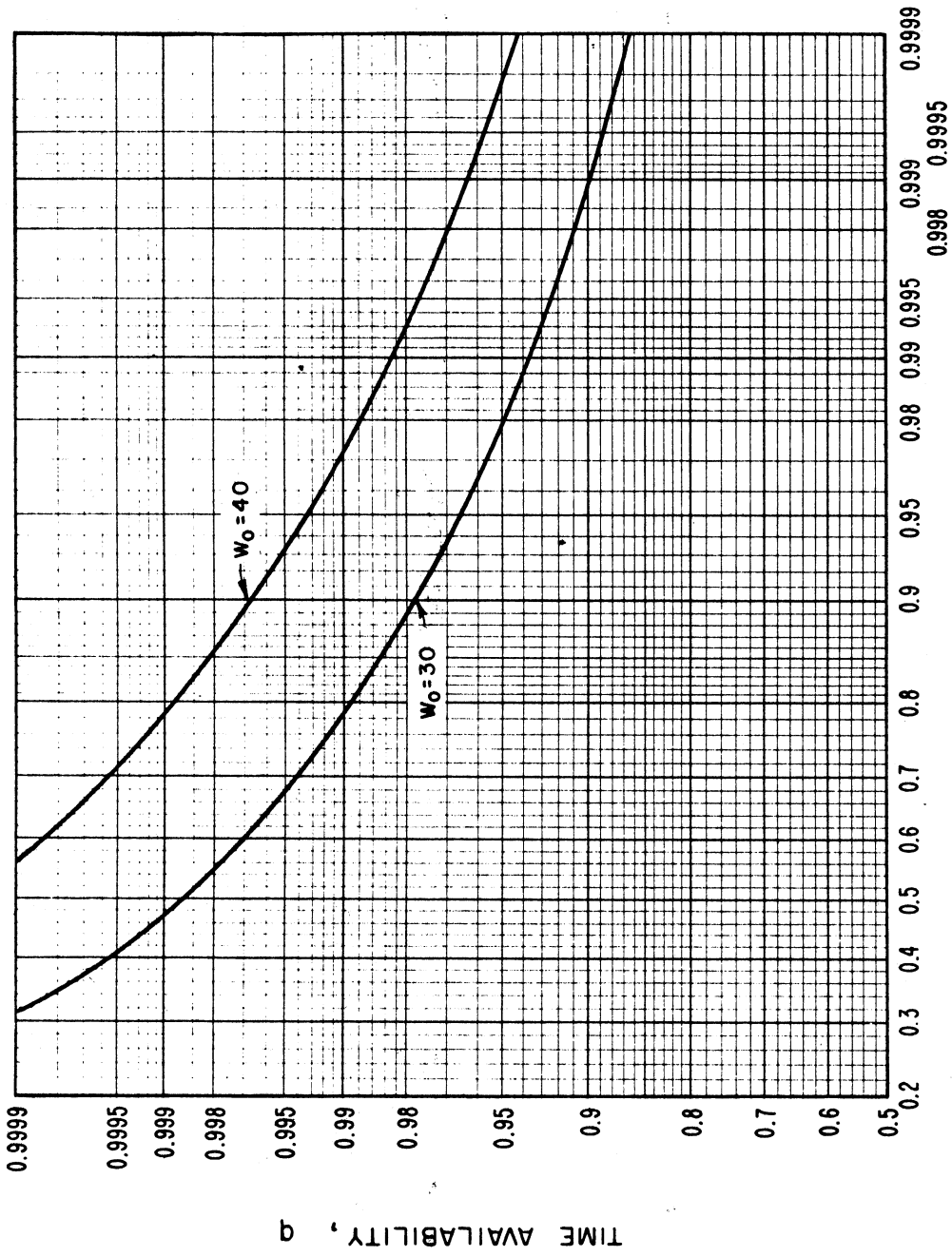


Figure V.7

TIME AVAILABILITY VERSUS SERVICE PROBABILITY



SERVICE PROBABILITY, Q

Figure V.8

V. 10 Optimum Use of the Radio Frequency Spectrum

The business of the telecommunications engineer is to develop efficient radio systems, and the principal tool for improving efficiency is to adjust the various parameters to their optimum values. For example, it is usually more economical to use lower effective radiated powers from the transmitting systems by reducing the operating sensitivities of the receiving systems. Receiving system sensitivities can be reduced by (a) reducing the level of internally generated noise, (b) using antenna directivity to reduce the effects of external noise, (c) reducing man-made noise levels by using suppressors on noise generators such as ignition systems, relays, power transmission systems, etc., and (d) using space or time diversity and coding. The use of more spectrum in a wide band FM system or in a frequency diversity system can also reduce the receiving system operating sensitivity as well as reduce the acceptance ratios against unwanted signals other than noise.

Unfortunately, unlike other natural resources such as land, minerals, oil, and water, there is currently no valid method for placing a monetary value on each hertz of the radio spectrum. Thus, in the absence of a common unit of exchange, these tradeoffs are often made unrealistically at the present time. It is now generally recognized that the use of large capacity computers is essential for optimizing the assignment of frequencies to various classes of service including the development of optimum channelization schemes. Typical inputs to such computers are:

1. Nominal frequency assignments.
2. Transmitting system locations, including the antenna heights.
3. Transmitting system signatures; i. e., the radiated emission spectrum characteristics including any spurious emission spectrums.
4. Transmitting antenna characteristics.
5. Receiving system locations, including the antenna heights.
6. Spurious emission spectrums of the receiving systems.
7. Operating sensitivities of the receiving systems in their actual environments which thus make appropriate allowance for the effects of both man-made and natural noise.
8. Required values of wanted-to-unwanted phase interference median signal powers for all unwanted signals which could potentially cause harmful interference to the wanted signal; these acceptance ratios include appropriate allowances for reductions in the effects of fading achieved by the use of diversity reception and coding.

9. Long-term median reference values of basic transmission loss and path antenna gain for the wanted path and all of the unwanted signal propagation paths; these path antenna gains include allowances for antenna orientation, polarization, and multipath phase mismatch coupling losses.
10. Distributions with time of the transmission loss for the wanted signal path and all of the unwanted signal paths.
11. Correlations between the transmission losses on the wanted and on each of the unwanted propagation paths.
12. Transmission line and antenna circuit losses.
13. The spurious emission spectrum of any unwanted signals arising from unlicensed sources such as diathermy machines, electronic heaters, welders, garage door openers, etc.
14. Assigned hours of operation of each wanted and each unwanted emission.

The output of the computer indicates simply the identity and nature of the cases of harmful interference encountered. Harmful interference is defined as a failure to achieve the specified grade of service for more than the required fraction of time during the assigned hours of operation. Changing some of the inputs to the computer, an iterative process can be defined which may lead to an assignment plan with no cases of harmful interference.

It is assumed that a given band of radio frequencies has been assigned to the kind of radio service under consideration and that the nature of the services occupying the adjacent frequency bands is also known. Furthermore, it is assumed that the geographical locations of each of the transmitting and receiving antennas are specified in advance, together with the relative values of the radiated powers from each transmitting antenna and the widths and spacings of the radio frequency channels. In the case of a broadcasting service the specification of the intended receiving locations can be in terms of proposed service areas. With this information given, use may be made of the following procedures in order to achieve optimum use of the spectrum by this particular service :

- (a) The system loss for each of the wanted signal propagation paths should be minimized and for each of the unwanted signal propagation paths should be maximized; this may be accomplished by maximizing the path antenna power gains for each of the wanted signal propagation paths, minimizing the path antenna gains for each of the unwanted propagation paths, and in exceptional cases, by appropriate antenna siting. The path antenna gains for the unwanted signal propagation paths may be minimized

by the use of high-gain transmitting and receiving antennas with optimum side lobe suppression and front-to-back ratios and, in some cases, by the use of alternate polarizations for geographically adjacent stations or by appropriate shielding.

(b) The required protection ratios $r_{ur}(g)$ should be minimized by (1) appropriate radio system design, (2) the use of stable transmitting and receiving oscillators, (3) the use of linear transmitting and receiving equipment, (4) the use of wanted and unwanted signal propagation paths having the minimum practicable phase interference fading ranges; from band 6 to band 9 (0.3 to 3000 MHz), minimum phase interference fading may be achieved by the use of the maximum practicable transmitting and receiving antenna heights, and (5) the use of space diversity, time diversity, and coding.

(c) Wanted signal propagation paths should be employed having the minimum practicable long-term power fading ranges. In bands 8 and 9, minimum fading may be achieved by the use of the maximum practicable transmitting and receiving antenna heights.

The above procedures should be carried out with various choices of transmitting and receiving locations, relative transmitter powers, and channel spacings until a plan is developed which provides the required service with a minimum total spectrum usage. After the unwanted signal interference has been suppressed to the maximum practicable extent by the above methods so that, at each receiving location each of the values of r_u exceeds the corresponding protection ratio $r_{ur}(g)$ for a sufficiently large percentage of the time, then the following additional procedures should be adopted in order to essentially eliminate interference from noise :

(d) The system loss on each of the wanted signal propagation paths should be minimized; this may be accomplished by (1) the use of the highest practicable transmitting and receiving antenna heights in bands 8 and 9, and (2) maximizing the path antenna power gains for each of the wanted signal propagation paths. The path antenna power gains of the wanted signal propagation paths may be maximized by using the maximum practicable transmitting and receiving antenna gains and by minimizing the antenna circuit and polarization coupling losses. The minimization of the system loss on each of the wanted signal propagation paths will already have been achieved to a large extent in connection with procedures (a), (b), and (c) above.

(e) In general, receiving systems should be employed which have the lowest practicable values of operating sensitivity $w_{mr}(g)$.

(f) Finally, sufficiently high transmitter powers should be used [keeping the relative powers at the optimum relative values determined by procedures (a), (b), and (c)] so that the wanted signal power w_m will exceed the operating sensitivity $w_{mr}(g)$ for a sufficiently large fraction of the time during the intended period of operation at every receiving location.

Although it might at first seem impracticable, serious consideration should be given to the use of auxiliary channels from wanted receivers to wanted transmitters. The provision of such channels might well be feasible in those cases where two-way transmissions are involved and might lead to important economies in both power and spectrum occupancy [Hitchcock and Morris, 1961].

Ultimately, when optimum use of the spectrum has been achieved, it will not be possible to find a single receiving location at which radio noise rather than either wanted or unwanted signals can be observed for a large percentage of the time throughout the usable portions of the radio spectrum not devoted to the study of radio noise sources, as is the radio astronomy service. Although everyone will agree that the attainment of this ideal goal of interference-free spectrum usage by the maximum number of simultaneous users can be achieved only over a very long period of time because of the large investments in radio systems currently in operation, nevertheless it seems desirable to have a clear statement of the procedures which should be employed in the future in order to move in the direction of meeting this ultimately desirable goal whenever appropriate opportunities arise.

V. II Supplementary List of Symbols for Annex V

b, B	Effective bandwidth, b , of a receiver in cycles per second, $B = 10 \log b$ decibels, (V. 7) and (V. 8).
f_{op}, F_{op}	Operating noise factor of the pre-detection receiving system, $F_{op} = 10 \log f_{op}$ db, (V. 7) and (V. 8)
g	Grade of service. A specified grade of service provided by a given signal will guarantee a corresponding degree of fidelity of the information delivered to the receiver output.
g_o, G_o	The maximum value of the operating gain of a pre-detection receiving system, $G_o = 10 \log g_o$ db, (V. 7) and (V. 8).
g_{ms}, G_{ms}	The hourly median operating signal gain of a pre-detection receiving system, $G_{ms} = 10 \log g_{ms}$ db, (V. 9).
k	Boltzmann's constant, $k = 1.38054 \times 10^{-23}$ joules per degree, (V. 7).
$k T_o b$	Johnson's noise power that would be available in the bandwidth b cycles per second at a reference absolute temperature $T_o = 288.37$ degrees Kelvin, (V. 7).
K	The decibel ratio of the amplitude of the constant or power-fading component of a received signal relative to the root-sum-square value of the amplitudes of the Rayleigh components, figure V. 1.
K_o	An arbitrary constant that combines several parameters in the systems equation, (V. 22).
L_{ft}	Transmission line and matching network losses at the transmitter, (V. 20).
L_m	Hourly median transmission loss, (V. 20).
$L_m(q)$	Hourly median transmission loss not exceeded for a fraction q of all hours, or exceeded $(1-q)$ of all hours, (V. 25).
$L_m(q, Q)$	Hourly median transmission loss exceeded for a fraction $(1-q)$ of all hours with a probability Q , section V. 6.
$L_m(0.5)$	Median value of $L_m(q)$, (V. 2).
$L_{mo}(g)$	Maximum allowable hourly median transmission loss for a grade g of service, (V. 27).
$L_o(q)$	Observed values of transmission loss not exceeded a fraction q of the recording period, (V. 5).
$L_{um}(q)$	Hourly median transmission loss of unwanted signal not exceeded for a fraction q of all hours, (V. 33).
$L_{um}(0.5)$	Long-term median value of $L_{um}(q)$, (V. 39).

L_{π}	Transmission loss associated with the "instantaneous" power W_{π} , (V.6) and figure V.2.
$L_{\pi}(q)$	Transmission loss L_{π} not exceeded a fraction q of the time.
$L_{\pi}(0.1)$	The interdecile range $L_{\pi}(0.9) - L_{\pi}(0.1)$ of values of transmission loss associated with the "instantaneous" power W_{π} , figure V.2.
q	Time availability.
q_1, q_8	Time availability in climates 1 and 8, section V.8.
Q	Service probability, discussed in section V.8.
$Q(q)$	The probability Q of obtaining satisfactory service for a fraction of time q , figure V.6.
$Q(z_{mo})$	Service probability Q expressed in terms of the error function of z_{mo} , (V.46), figure V.5.
r_m, R_m	Ratio of the hourly median wanted signal power to the hourly median operating noise power, $R_m = 10 \log r_m$ db, (V.9).
r_{mr}, R_{mr}	A specified value of r_m which must be exceeded for at least a specified fraction of time to provide satisfactory service in the presence of noise alone, $R_{mr} = 10 \log r_{mr}$ db, (V.9).
r_u, R_u	Ratio of hourly median wanted to unwanted signal power available at the receiver, $R_u = 10 \log r_u$ db, (V.14).
r_{ur}, R_{ur}	A specified value of r_u which must be exceeded for at least a specified fraction of time to provide satisfactory service in the presence of a single unwanted signal, $R_{ur} = 10 \log r_{ur}$ db, (V.14).
$r_{mr}(g), R_{mr}(g)$	The minimum acceptable signal to noise ratio which will provide service of a given grade g in the absence of unwanted signals other than noise, $R_{mr}(g) = 10 \log r_{mr}(g)$ db, (V.9).
$r_{ur}(g), R_{ur}(g)$	The protection ratio r_{ur} required to provide a specified grade of service g , $R_{ur}(g) = 10 \log r_{ur}(g)$ db, sections V.4 and V.5.
$R_m(q)$	The value of R_m exceeded at least a fraction q of the time, (V.24).
$R_m(0.5)$	The median value of R_m , (V.29).
$R_u(q)$	A specified value of R_u exceeded at least a fraction q of the time, (V.36).
$R_u(0.5)$	The median value of R_u , (V.36).
$R_{ur}(g, q)$	The required ratio R_{ur} to provide service of grade g for at least a fraction q of the time, (V.35).
$R_{uro}(g)$	The required ratio R_{ur} for non-fading wanted and unwanted signals, (V.14).
$R_{u\pi}$	The ratio between the instantaneous wanted and unwanted signal powers, (V.10).
T_o	Reference absolute temperature $T_o = 288.37$ degrees Kelvin, (V.7).
$V(0.5), d_e$	A parameter used to adjust the predicted reference median for various climatic regions or periods of time, section V.8 and section 10, volume 1.

$V_i(0.5, d_e)$, $V_j(0.5, d_e)$ The parameter $V(0.5, d_e)$ for each of two climates represented by the subscripts i and j , (V.41).

w_m , W_m The median wanted signal power available at a receiver, $W_m = 10 \log w_m$ dbw, (V.1).

w_{mn} , W_{mn} The median value of the total noise power is w_{mn} watts, $W_{mn} = 10 \log w_{mn}$ dbw, (V.7) and (V.8).

w_{mr} , W_{mr} Operating threshold, the median wanted signal power required for satisfactory service in the presence of noise, $W_{mr} = 10 \log w_{mr}$ dbw, (V.9).

w_o , W_o A fixed value of transmitter output power w_o in watts, $W_o = 10 \log w_o$ dbw, (V.26).

w_t , W_t Total radiated power in watts and in dbw, section V.6.

w_u , W_u Power radiated from an unwanted or interfering station, w_u watts, $W_u = 10 \log w_u$ dbw, (V.33).

w_{um} , W_{um} Median unwanted signal power w_{um} in watts, $W_{um} = 10 \log w_{um}$ dbw, (V.33) and (V.34).

$w_{u\pi}$, $W_{u\pi}$ Unwanted signal power associated with phase interference fading, $w_{u\pi}$ in watts, $W_{u\pi} = 10 \log w_{u\pi}$ dbw, section V.4.

w_π , W_π Wanted signal power associated with phase interference fading, w_π is defined as the average power for a single cycle of the radio frequency, $W_\pi = 10 \log w_\pi$ dbw, (V.1).

W_{ft} Transmitter output power, (V.20).

$W_{ft}(q)$ Transmitter power that will provide at least grade g service for a fraction q of all hours, (V.25).

$W_m(q)$ The hourly median wanted signal power exceeded for a fraction q of all hours, (V.24).

$W_m(0.5)$ Long-term median value of W_m , (V.2).

$W_{mo}(q)$ Observed values of $W_m(q)$ made over a large number of paths which can be characterized by the same set of prediction parameters, section V.8.

$W_{mr}(g)$ The operating threshold of a receiving system, defined as the minimum value of W_m required to provide a grade of service g in the presence of noise alone, (V.9).

$W_{um}(q)$ The hourly median unwanted signal power W_{um} expected to be available at least a fraction q of all hours, (V.33).

$W_{um}(0.5)$ The median value of $W_{um}(q)$, (V.37).

$W_\pi(q)$ The "instantaneous" power W_π exceeded for a fraction of time q , (V.6).

$W_\pi(0.1)$, $W_\pi(0.9)$ The interdecile range $W_\pi(0.1) - W_\pi(0.9)$ of the power $W_\pi(q)$, equivalent to the interdecile range of short term transmission loss shown on figure V.2.

Y A symbol used to describe long-term fading, (V.1) and (V.3).

Y_u Long-term fading of an unwanted signal, (V.16).

$Y_{u\pi}$	Phase interference component of the total fading of an unwanted signal, (V. 10).
Y_{π}	Phase interference fading component for a wanted signal, (V. 10).
$Y(q)$	Long-term variability Y for a given fraction of hourly medians q , defined by (V. 4).
$Y(0.5)$	The median value of Y , which by definition is zero.
$Y_i(q, d_e), Y_j(q, d_e)$	Values of Y for climates i and j , (V. 41) and (V. 42).
$Y_{ij}(q, d_e)$	The root-mean-square value of the variability for two climates, (V. 42).
$Y_m(q)$	Long-term variability in the presence of variable external noise, (V. 31).
$Y_n(q)$	Variability of the operating noise factor, F_{op} , (V. 31) and (V. 32).
$Y_R(q)$	Long-term variability of the wanted to unwanted signal ratio, (V. 38).
$Y_u(q)$	Long-term variability of an unwanted signal, (V. 39).
$Y_{u\pi}(q)$	The phase interference fading component of the total variability of an unwanted signal, section V. 4.
$Y_{\pi}(q)$	The phase interference fading component of the total variability of a wanted signal, section V. 4.
Y_1, Y_8	Values of Y for climates 1 and 8, section V. 9.
z_{mo}, z_{op}, z_{uc}	Standard normal deviates defined by (V. 45), (V. 52) and (V. 55).
Z	The decibel ratio of the long-term fading, Y , of a wanted signal and the long-term fading, Y_u , of an unwanted signal, (V. 16).
$Z_a(q)$	The approximate cumulative distribution function of the variable ratio Z , (V. 17).
$Z_a(0.5)$	Median value of the variable ratio Z , $Z_a(0.5) \equiv 0$.
Z_{π}	The decibel ratio of the phase interference fading component Y_{π} for a wanted signal and the phase interference fading component $Y_{u\pi}$ for an unwanted signal, (V. 11).
$Z_{\pi a}(q, K, K_u)$	The approximate cumulative distribution function of Z_{π} , (V. 12).
ρ_{fu}	The normalized correlation or covariance between path-to-path variations of $W_m(0.5)$ and $W_{um}(0.5)$, (V. 54).
ρ_{tn}	The long-term correlation between W_m and F_{op} , (V. 31).
ρ_{tu}	The long-term correlation between W_m and W_{um} , (V. 38).
σ_c^2	The path-to-path variance of deviations of observed from predicted transmission loss, section V. 8.
$\sigma_c^2(q)$	The path-to-path variance of the difference between observed and predicted values of transmission loss expected for a fraction q of all hours.
$\sigma_c^2(0.5)$	The path-to-path variance of the difference between observed and predicted long-term median values of transmission loss, (V. 40) and the following paragraph.
σ_F^2	The variance of the operating noise factor F_{op} , (V. 51).
$\sigma_{op}^2(q)$	Total variance of any estimate of the service criterion for service limited only by external noise, (V. 51).

$\sigma_{uc}^2(q)$

Total variance of any estimate of the service criterion for service limited only by interference from a single unwanted source, (V. 54).

σ_{ur}^2

Variance of the estimate of $R_{ur}(g, q)$, (V. 54).